Magnetic and Transport Properties of Spin Polarized Molecular Systems: A Theoretical Perspective

A Thesis submitted to the University of North Bengal

For the Award of
Doctor of Philosophy
in
Chemistry

By
Prodipta Sarbadhikary

Supervisor
Prof. Anirban Misra

Department of Chemistry
University of North Bengal
January-2021

DECLARATION

I declare that the thesis entitled "**Magnetic and Transport Properties of Spin Polarized Molecular Systems: A Theoretical Perspective**" has been prepared by me under the guidance of Prof. Anirban Misra, Department of Chemistry, University of North Bengal.

No part of this thesis has formed the basis for the award of any degree or fellowship previously.

Prodipta Sarbadhikary.

Prodipta Sarbadhikary

Department of Chemistry,
University of North Bengal,
Dist- Darjeeling,
West Bengal
Pin- 734013.

Date: 27.01.2021

ENLIGHTENMENT TO PERFECTION

UNIVERSITY OF NORTH BENGAL

Accredited by NAAC with Grade A

DEPARTMENT OF CHEMISTRY

P.O. NORTH BENGAL UNIVERSITY, Raja Rammohunpur, Dist. Darjeeling, West Bengal, India, PIN - 734013.
PHONE : (0353) 2776 381, Fax: (0353) 2699 001

Ref. No..... *Dated.....20.....*

CERTIFICATE

I certify that the thesis entitled "**Magnetic and Transport Properties of Spin Polarized Molecular Systems: A Theoretical Perspective**" has been prepared by **Prodipta Sarbadhikary**, for the award of Ph.D. degree of the University of North Bengal, under my guidance. She has carried out the work at the Department of Chemistry, University of North Bengal.

No part of this thesis has formed the basis for the award of any degree or fellowship previously.

27.1.2021

Professor
Department of Chemistry
University of North Bengal
Darjeeling - 734013, India

Dr. Anirban Misra,
Professor,
Department of Chemistry,
University of North Bengal,
Dist- Darjeeling,
West Bengal
India

URKUND

Urkund Analysis Result

Analysed Document:	Prodipta Sarbadhikary_Chemistry.pdf (D92096365)
Submitted:	1/14/2021 11:06:00 AM
Submitted By:	nbuplg@nbu.ac.in
Significance:	7 %

Sources included in the report:

08a79302-72b8-4d26-a098-571b81cb5038
871e4f71-3546-4152-b2e3-5861292bfaf7
900b11b1-02a2-4986-8b2a-35d15385138e
https://www.nature.com/articles/s41467-020-17303-4
https://pubs.rsc.org/en/content/articlehtml/2013/sc/c3sc52061g
https://pubs.rsc.org/en/content/articlehtml/2014/cs/c4cs00022f
https://pubs.rsc.org/en/content/articlelanding/2015/cp/c5cp03193a
https://www.ncbi.nlm.nih.gov/pmc/articles/PMC7180855/
https://www.researchgate.net/publication/261138208_Synthesis_and_properties_of_long_n_cumulenes_n_5
https://www.researchgate.net/publication/225701304_Intramolecular_ferromagnetic_coupling_in_bis-oxoverdazyl_and_bis-thioxoverdazyl_diradicals_with_polyacene_spacers
https://core.ac.uk/download/pdf/157813866.pdf
https://www.ncbi.nlm.nih.gov/pmc/articles/PMC6150729/
https://www.researchgate.net/publication/340224326_Pyrrole-25-Diyl-BisNitronyl_Nitroxide_andBisIminonitroxide_Specific_Features_of_the_Synthesis_Structure_and_Magnetic_Properties
https://www.nature.com/articles/srep07363
https://repository.lib.ncsu.edu/bitstream/handle/1840.16/4635/Coote.pdf?sequence=1&isAllowed=y
https://repository.lib.ncsu.edu/bitstream/handle/1840.16/3667/etd.pdf?sequence=2&isAllowed=y
https://www.neutron-sciences.org/articles/sfn/pdf/2011/01/sfn201112005.pdf
https://digitalcommons.usu.edu/cgi/viewcontent.cgi?article=1965&context=etd
https://d-nb.info/1154485773/34
https://www.ncbi.nlm.nih.gov/pmc/articles/PMC3089375/
https://digital.csic.es/bitstream/10261/76135/1/Spin%20Density.pdf
https://www.researchgate.net/publication/228674274_Spin_Exchange_Coupling_in_Dimethoxo-Bridged_Dichromium_III_Complexes_A_Density_Functional_Theory_Study

Instances where selected sources appear:

84

Prodipta Sarbadhikary
27.01.2021

Professor
Department of Chemistry
University of North Bengal
Darjeeling - 734013, India

ABSTRACT

The first chapter describes a brief history of magnetism and the origin of magnetism in different types of magnetic materials. Starting from the early paradigm of magnets which was first observed in a type of mineral magnetite, the discussion moves forward according to the requisite of novel kind of magnetic materials. This chapter also deals with the transport property of spin polarized molecular systems. Transport property of different types of metal complexes, Single Molecule Magnets (SMMs) and different organic radical systems coupled with electrodes are discussed here. A detailed analysis of literature along with the objectives of the thesis is stated in this chapter.

The second chapter depicts the theoretical background for the estimation of magnetic exchange coupling constant (J) of molecules. Among different variety of methodologies, the broken symmetry (BS) formalism in density functional theory (DFT) framework is found to come up with the optimal solution for the determination of J. The theoretical background for the estimation of transport property of molecules through green function-based technique in DFT framework has also been discussed here.

The crux of the third chapter is to study the effect of length of unsaturated organic molecular wires and radical substituted wires on the electrical transport properties. Extended π-conjugated systems are known to have interesting applications as memory devices, conducting nanowires, and diodes. In this chapter, the investigation of the transport property of two molecular wires of different length shows that the molecular wires of smaller length have higher transmission, i.e., higher conduction. The magnetic exchange coupling constant of the radical substituted molecular wires (substituting the molecular wire with two methylene radical centers at two different positions) depend only on the distance between the spin centers, not on the outsider substitution. The transmission characteristics of the radical substituted molecular wires (for ferromagnetically coupled diradicals) show similar observation as that of the wires without radical substitution. But for antiferromagnetically coupled diradical substituted molecular wires, there is a small variation in transmission characteristics.

In fourth chapter, the magnetic property of diradical-based organic molecules with allene and chiral cumulene couplers has been studied theoretically. Generally, for most of the diradicals, J value decreases with the increase in distance between radical centers. However, the designed diradicals show ferromagnetic interaction with conflicting behavior i.e., J value increases with the increase in distance between radical centers. Moreover, spin density within the coupler increases remarkably as

length of the coupler increases which is quite contradictory from the normal concept that spin density within the coupler decreases with the increase in length of the coupler. A large accumulation of spin density within the coupler overcomes the distance factor between radical centers that results higher magnetic exchange coupling for longer coupler in the designed diradicals. Moreover, addition of chiral centers within the coupler lowers the energy of lowest unoccupied molecular orbital (LUMO) and a smaller HOMO (highest occupied molecular orbital) - LUMO gap facilitates a stronger magnetic coupling. From natural orbital occupancies it is found that, with increasing chain length of chiral coupler the occupancy of LUMO increases. Therefore, a correlation between the LUMO occupation and magnetic exchange coupling constant is intuited. These designed molecules may be used as molecular building blocks for organic chiral magnetic solids.

The key issue of the fifth chapter is to investigate the magnetic and transport properties of diradicals attached by a range of linear conjugated and cumulene couplers focusing on the unusual π-interaction properties within the couplers. Generally, chains containing *sp*-hybridized carbon atoms are interesting for their unique linear structure and physical properties. On the other hand, linear chains of carbon atoms have been anticipated to have excellent properties for several transport related applications. In this chapter, it is observed that the spin density within the couplers, distance between radical centers, dihedral angles between the plane of the coupler and radical centers influence the strength of magnetic coupling for all the diradicals. It is established that the strength of magnetic interaction in cumulated and conjugated systems varies in a different way as the length of the coupler increases. Transport calculations show that with the increase in chain length, diradicals based on even cumulene couplers act as better conductor than odd cumulenes couplers. However, in conjugated coupler based diradicals, transmission does not vary in a sequential way.

The sixth chapter has embodied the study of magnetic property of heteroallene (>C=C=X−) and heterocumulene (>C=C=C=X−) based *tert*-butyl nitroxide diradicals (X is P/As) by density functional theory based methods. Different research works show that the presence of heteroatom in the exchange pathway significantly influences magnetic exchange coupling. Moreover, heteroallene and heterocumulene (with 4 atoms in backbone chain) containing double bonded heavy elements have attracted interest from a theoretical point of view because of their peculiar physicochemical properties. In this chapter a theoretical investigation on the potential effect of P/As atom substitution within the allene and cumulene couplers in mediating the exchange interaction between the two radical centers has been carried out. Calculation of magnetic exchange coupling constant (*J*) shows ferromagnetic interactions in heteroallene based diradicals. Interestingly, in heterocumulene based diradicals, tuning of *J* value from antiferromagnetic to ferromagnetic state is observed from *Z*- to *E*- isomer. The essence of all findings is further explored by the structural effects, spin density distributions and molecular orbital analysis. Delocalization of

spin density from *tert*-butyl nitroxide radical site to the coupler (in planar arrangement) is observed in the spin distribution analysis. Moreover, the shapes of singly occupied molecular orbitals (SOMOs) advocate the delocalization of spin from radical center to the coupler. The *J* value of all the diradicals strongly depends on the dihedral angle between the radical center and the coupler. Magneto-structural correlation shows that the change in dihedral angle tunes the magnetic property between ferromagnetic and antiferromagnetic states for both the *Z*- and *E*- isomers of heterocumulene based diradicals depending on the spin accumulation on two nearby magnetic centers. The energy gap between two consecutive SOMOs also supports this observation such that when this energy gap is low, ferromagnetic interaction is observed and for higher value of the energy gap antiferromagnetic situation arises in heterocumulene based diradicals.

A comprehensive remark, summarizing all the works done, is put in the seventh chapter.

PREFACE

The design of smart multifunctional material is essential for the rapidly developing technological world. Magnetic and transport properties are important characteristics to delve into. Since the magnetic status depends on the interaction between magnetic centers, it requires the mechanism of such interaction followed by quantification. On the other hand, transport property depends on how the system is connected to electrodes and the nature of the electrodes. To start with, a crisp discussion about the categories of magnetic materials and the transport property of different spin polarized molecular systems are made in first chapter. Theoretical constructs for the quantification of magnetic and transport properties are discussed in second chapter. It is well known that the extended π-conjugated systems have interesting applications as memory devices, conducting nanowires etc. The transport property of conjugated molecular wires of different length is studied in third chapter to show the effect of length on the electrical transport properties. In this context the magnetic and transport properties of these molecular wires substituted by two radical centers at two different positions are also studied. The fourth chapter deals with the magnetic property of diradicals based on allene and chiral cumulene couplers which contain *sp*-hybridized carbon atoms. Generally, the magnetic exchange coupling constant value decreases with the increase in distance between radical centers in conjugated systems. However, in this chapter we explored that the diradicals based on allene and cumulene coupler have opposite behavior compared to conjugated systems. It is found that spin density distribution within allene and cumulene systems and HOMO-LUMO energy gap has intimate correlation with magnetic property in such systems. These designed systems are ferromagnetic, chiral as well as organic and they may be used as molecular building blocks for organic chiral magnetic solids in future. In the fifth chapter we extend our study towards the magnetic and transport properties of diradicals attached by a range of conjugated coupler and chiral as well as achiral cumulene couplers (which are planar) focusing on the unusual π-interaction properties within the couplers. Transport calculations represent that diradicals based on even cumulene couplers act as better conductor than odd cumulenes couplers (with the increase in chain length of coupler). In the sixth chapter a potential effect of heteroatom substitution within the allene and cumulene couplers in mediating the exchange interaction between the two radical centers is investigated. Several research works show that the presence of heteroatom in the exchange pathway significantly influences magnetic exchange coupling. Interestingly, in heterocumulene based diradicals, tuning of magnetic exchange coupling constant value from antiferromagnetic to ferromagnetic state is observed from *Z*- to *E*- isomer and a unique type of spin delocalization is observed in these systems. In the last chapter, the essence and significance of previous chapters are surmised.

TABLE OF CONTENTS

Chapter 1. Magnetic and transport properties of spin polarized molecules 1-23

1.1 Introduction 2
1.2 Types of magnetism 2
1.3 Molecular magnet and single-molecule magnet 3
1.4 Organic radicals as magnetic molecules 5
1.5 Transport through spin polarized molecular systems 8
1.6 Objectives of the thesis 12
1.7 References 13

Chapter 2. Theoretical background 24-32

2.1 Introduction 25
2.2 Density Functional Theory 25
2.3 Spin Hamiltonian and magnetic exchange coupling constant (*J*) 27
2.4 Broken symmetry approach 28
2.5 Electron transport (Density functional method) 29
2.6 References 31

Chapter 3. Effect of length on the transport and magnetic properties of diradical substituted molecular wires 33-47

3.1 Introduction 34
3.2 Theoretical and computational methodology 35
3.3 Results and discussion 38
3.3.1 Transport properties of the molecular wires 38
3.3.2 Molecular orbitals 39
3.3.3 J values of the diradical substituted molecular wires 41
3.3.4 Spin density distribution between diradical centers 43
3.3.5 Transport property of the diradical substituted molecular wires 44
3.4 Conclusion 45
3.5 References 46

Chapter 4. A perspective on designing chiral organic magnetic molecules with unusual behavior in magnetic exchange coupling 48-67

4.1 Introduction 49
4.2 Theoretical background 50
4.3 Computational strategy 51
4.4 Results and discussion 51

4.4.1 Magnetic exchange coupling constant 53
4.4.2 Spin density distribution 54
4.4.3 Spin polarization 56
4.4.4 Molecular structures 58
4.4.5 Molecular orbital analysis 60
4.4.6 Mechanism of magnetic interaction 62
4.5 Conclusion 65
4.6 References 65

Chapter 5. Magnetic and transport properties of conjugated and cumulated molecules: the π-system enlightens part of the story **68-97**

5.1 Introduction 69
5.2 Theoretical background and computational strategy 70
5.3 Results and discussion 73
5.3.1 Magnetic exchange coupling constant 73
5.3.2 Coherent electron transport through diradicals 83
5.4 Conclusion 94
5.5 References 94

Chapter 6. Magnetic modulation in heteroallene and heterocumulene based *tert*-butyl nitroxide diradicals: spin delocalization and conformation play crucial roles **98-121**

6.1 Introduction 99
6.2 Theoretical background and computational strategy 101
6.3 Results and Discussion 102
6.3.1 Structural characters and effects 103
6.3.1.1 Distance between radical centers 104
6.3.1.2 Dihedral angle 104
6.3.2 Spin density distribution 106
6.3.3 Magneto-structural correlation 112
6.3.4 Molecular orbital analysis 113
6.4 Conclusion 118
6.5 References 118

Chapter 7. Conclusions **122-125**

Bibliography **126-147**

Index **148-149**

LIST OF TABLES

Table 3.1 Orbital coefficients of molecular wires	37
Table 3.2 Energy, $\langle S^2 \rangle$ and *J* values of the diradical based molecular wire 1	41
Table 3.3 Energy, $\langle S^2 \rangle$ and *J* values of the diradical based molecular wire 2	42
Table 4.1 Energy, $\langle S^2 \rangle$ and *J* for all diradicals	53
Table 4.2 Absolute energies of the diradicals and for mixed radical systems	54
Table 4.3 Spin density of diradicals	55
Table 4.4 Bond length of diradicals	58
Table 4.5 Bond angle	59
Table 4.6 Energy (in eV) of molecular orbitals	63
Table 4.7 Natural orbital occupation	64
Table 5.1 Energy, $\langle S^2 \rangle$ and *J* values of odd cumulene systems	75
Table 5.2 Energy, $\langle S^2 \rangle$ and *J* values of even cumulene systems	75
Table 5.3 Energy, $\langle S^2 \rangle$ and *J* values of conjugated systems	76
Table 5.4 Percent Net Weight of Triplet and Singlet Components (B3LYP	77
Table 5.5 Percent Net Weight of Triplet and Singlet Components (B3LYP-D)	77
Table 5.6 Percent Net Weight of Triplet and Singlet Components (CAM-B3LYP)	78
Table 5.7 Distance between radical centers	79
Table 5.8 Spin density distribution on even cumulene-based systems	81
Table 5.9 Spin density distribution on conjugated systems	81
Table 5.10 $HOMO_\alpha$–$LUMO_\alpha$ for odd cumulenes systems	88
Table 5.11 $HOMO_\alpha$–$LUMO_\alpha$ for even cumulenes and conjugated systems	89
Table 5.12 Distance between two leads	89
Table 6.1 Energy,$\langle S^2 \rangle$, and *J* values for all the diradicals (B3LYP)	102
Table 6.2 Energy,$\langle S^2 \rangle$, and *J* values for all the diradicals (M06)	102
Table 6.3 Energy,$\langle S^2 \rangle$, and *J* values for all the diradicals (CAM-B3LYP)	103
Table 6.4 Distance between radical centers	104
Table 6.5 Dihedral angles	105
Table 6.6 Spin density distribution on heterocumulene based diradicals	106
Table 6.7 Spin density distribution on heteroallene based diradicals	107
Table 6.8 Energy, $\langle S^2 \rangle$ and *J* values of all the nitronyl nitroxide diradicals	108
Table 6.9 Spin density distribution on P-substituted even cumulene based nitronyl nitroxide diradical	108
Table 6.10 Spin density distribution on P-substituted allene based nitronyl nitroxide diradical	108
Table 6.11 Dihedral angle, ΔE_{SS} and *J* values (in P-substituted cumulene systems)	117
Table 6.12 Molecular orbital energies of *Z*-isomer (P-substituted cumulene systems)	117
Table 6.13 Molecular orbital energies of *E*-isomer (P-substituted cumulene systems)	117

LIST OF FIGURES AND SCHEMES

Figure 1.1 Diethyldithiocarbamate-Fe (III) compounds	3
Figure 1.2 Mn_{12} (acetate) molecule	4
Figure 1.3 Examples of organic radicals	5
Figure 1.4 Examples of polyradicals	8
Figure 1.5 The Electrode–Molecule–Electrode transport structure	10
Figure 3.1 Molecular wires without radical substitution	35
Figure 3.2 Diradicals based on molecular wire 1	35
Figure 3.3 Diradicals based on molecular wire 2	35
Figure 3.4 Au-molecule-Au structures	36
Figure 3.5 Molecular wire1 and molecular wire 2	37
Figure 3.6 Transmission spectra of molecular wire without radical substitution	39
Figure 3.7 Molecular orbitals of the wire 1 under different electric fields	40
Figure 3.8 Molecular orbitals of the wire 2 under different electric fields	40
Figure 3.9 Plot of *J* vs. distance between the radical centers	42
Figure 3.10 Spin density distribution of radical substituted molecular wire 1	43
Figure 3.11 Spin density distribution of radical substituted molecular wire 2	43
Figure 3.12 Transmission spectra of diradical substituted molecular wire 1	44
Figure 3.13 Transmission spectra of diradical substituted molecular wire 2	45
Figure 4.1 Allene and cumulene based diradicals	50
Figure 4.2 *R* and *S* configuration of the diradicals	52
Figure 4.3 VCD spectra of two enantiomers of series 2	52
Figure 4.4 Spin density plot of all the diradicals	55
Figure 4.5 Spin density plot for the diradicals of series 1	56
Figure 4.6 Spin polarization of π electron within the coupler	57
Figure 4.7 Plot of *J* vs. distance between radical centers	57
Figure 4.8 Molecular orbitals of all the diradicals	60
Figure 4.9 Molecular orbitals of the diradicals with varying geometry	61
Figure 4.10 Molecular orbital of the diradicals in broken symmetry state	62
Figure 4.11 Allene and cumulenes based diradical with phases of HOMO-2	63
Figure 4.12 Plot of energy vs. distance between radical centers	64
Figure 5.1 Designed diradicals	70
Figure 5.2 Designed diradical for transport calculations	73
Figure 5.3 Plot of *J* vs. number of carbon atoms within the coupler	74
Figure 5.4 Regression analyses for odd cumulene series	78
Figure 5.5 Regression analyses for even cumulene series	79
Figure 5.6 Spin density plot for even cumulene systems	80
Figure 5.7 Spin density plot for conjugated systems	81
Figure 5.8 π-interaction of diradicals	82
Figure 5.9 Representation for the radical based systems	84
Figure 5.10 Transmission spectra (for α spin)	85
Figure 5.11 Transmission spectra (for β spin)	86
Figure 5.12 Representation for systems without radical centers	86
Figure 5.13 Transmission spectra of molecular wires without radical centers	87

Figure 5.14 Designed even cumulene based molecular wires	90
Figure 5.15 Designed even conjugated system based molecular wires	91
Figure 5.16 Designed odd cumulene based molecular wires	91
Figure 5.17 Spin polarization within the odd cumulene systems	92
Figure 5.18 Spin polarization within the even cumulene systems	92
Figure 5.19 Spin polarization within conjugated systems	93
Figure 6.1 Heteroallene and heterocumulene based diradicals	100
Figure 6.2 Dihedral angles in heterocumulene and heteroallene systems	105
Figure 6.3 Nitronyl nitroxide diradicals (with P-substitution)	107
Figure 6.4 Delocalization of unpaired electron in *Z*-isomer of heterocumulene based diradical	109
Figure 6.5 Spin density plot for the P-substituted allene and cumulene based *tert*-butyl nitroxide diradicals	110
Figure 6.6 Spin density plot for the As-substituted allene and cumulene based *tert*-butyl nitroxide diradicals	110
Figure 6.7 Delocalization of unpaired electron in heteroallene based diradicals	111
Figure 6.8 *J* values of P-substituted cumulene based diradicals at different dihedral angle	112
Figure 6.9 Spatial distribution of SOMOs of the P-substituted cumulene based diradicals	113
Figure 6.10 Spatial distribution of molecular orbitals of the P-substituted nitronyl nitroxide diradicals	114
Figure 6.11 Spatial distribution of molecular orbitals of the As-substituted *tert*-butyl nitroxide diradicals	115
Figure 6.12 Spatial distribution of SOMOs of the allene based diradicals with P-substitution	116

LIST OF APPENDICES

APPENDIX A: List of Publications

Published

1. Shil, S.; **Sarbadhikary, P**.; Misra, A. Effect of length on the transport and magnetic properties of diradical substituted molecular wires. *RSC Adv.* **2016**, *6*, 99467-99474.

2. Sarbadhikary, P.; Shil, S.; Misra, A. A Perspective on Designing Chiral Organic Magnetic Molecules with Unusual Behavior in Magnetic Exchange Coupling. *J. Org. Chem.* **2016**, *81*, 5623-5630.

3. Sarbadhikary, P.; Shil, S.; Misra, A. Magnetic and Transport Properties of Conjugated and Cumulated Molecules: the π-System Enlightens Part of the Story. *Phys. Chem. Chem. Phys.* **2018**, *20*, 9364-9375.

Communicated

4. Sarbadhikary, P.; Misra, A. Magnetic modulation in heteroallene and heterocumulene based *tert*-butyl nitroxidediradicals: spin delocalization and conformation play crucial roles, Communicated, **2021**.

APPENDIX B: Poster presentations

1. A Perspective on Designing Chiral Organic Magnetic Molecules with Unusual Behavior in Magnetic Exchange Coupling, **Prodipta Sarbadhikary** and Anirban Misra*, 19th CRSI National Symposium in Chemistry 2016,Organized by Department of Chemistry, University of North Bengal, Darjeeling, India.

2. Magnetic and Transport Properties of Conjugated and Cumulated Molecules: the π-System Enlightens Part of the Story, **Prodipta Sarbadhikary** and Anirban Misra*, 15th Indian Theoretical Chemistry Symposium 2016, Hyderabad.

APPENDIX C: Acknowledgements

Foremost, I would like to express my sincere gratitude to my supervisor Professor Anirban Misra for his inspirational leadership and for giving me the opportunity to do research. He provides me his sincere guidance during all stages of my PhD work. He taught me to think through the research problem and always inspired me to think independently. I learned a lot during the discussions with him which is very challenging.

I express my sincere thanks to all of my teachers in the Department of Chemistry. I am appreciative to all the research scholars and all the staff of the Department of Chemistry for their cooperation.

I am grateful to my co-authors Dr. Suranjan Shil and Dr. Anirban Panda for their active effort to my work. They were very helpful, and I had many useful discussions with them. I would also like to thank my labmates Debojitda, Satadalda, Manojda, Tamalda, Banitadi, Manoswita, Tanushree, Sudip and Soumik for their friendly cooperation and help during my Ph.D. tenure.

I am also thankful to Prof. Carmen Herrmann for giving the permission for using her transport code ARTAIOS.

DST and CSIR are thankfully acknowledged for financial support.

Last but not the least; I would like to thank my parents, sister and my husband, without their love, prayer and sacrifices this endeavor could not have been successful.

CHAPTER 1

Magnetic and transport properties of spin polarized molecules

A general introduction of magnetic and transport properties of different spin polarized molecules is presented in this chapter. A detailed review of literature along with the objectives of the thesis is systematically stated here.

1.1 Introduction

Magnetism has captivated the imagination of mankind from ancient times[1] and in the twentieth century, the development of magnetically active materials becomes essential for the progress of present high-tech civilization. Magnetism was first observed in a type of mineral magnetite called lodestone, which consists of iron oxides. Since then, research interests on magnetism and magnetic materials are growing in order to understand and exploit magnetic materials. Many organisms are found that have at least some kind of magnetite in them including homing pigeons, honeybees, whales, dolphins, green turtles etc. However, in order to deal with the requirements of technological world, the search for novel kind of materials is being carried out which will have a tunable magnetic property and can be synthesized and tailored in laboratory. Magnetic molecules of metal-based complexes and assemblies[2] are extensively studied as the early magnetic materials are of inorganic origin. However, in past few decades, the realm of magnetic materials is moved towards organic molecules[3] and become the most fascinating topics in this line of research.

1.2 Types of magnetism

Depending on the nature of the magnetic interactions and the magnetic moments within a system, several different forms of magnetism have been distinguished. Except diamagnetic substances containing spin paired electrons, all other types of magnetic interactions involve the existence of unpaired electrons. In the presence of an external field, the magnetic moments of the unpaired electrons of a paramagnetic material will be likely to align with the direction of the applied field and show spontaneous magnetization but in the absence of such field, there is no such interaction between unpaired electrons within the system. However, ferromagnetism, antiferromagnetism and ferrimagnetism all are typified by a magnetic ordering even though the external magnetic field is absent. In a ferromagnetic material, neighbouring magnetic moments align in parallel fashion and spontaneous coupling between them gives rise to permanent magnetization. Conversely, an antiferromagnetism arises when neighbouring magnetic moments anti-align with respect to their adjacent neighbours, avoiding spin pairing and leads to lowering of magnetism. In a ferrimagnetic material the adjacent magnetic moments will also be likely to orient in an anti-parallel pattern. However, an imbalance in the opposing magnetic moments in ferrimagnetic material arise as the neighbouring moments are of different magnitudes, that leads to spontaneous magnetization. All the different types of magnetism are adequately discussed in different articles.[4]

1.3 Molecular magnet and single-molecule magnet (SMM)

Traditional magnetic materials play a fundamental role in almost all corner of everyday life. The construction of most of the conventional inorganic magnetic materials are based on metals (Fe, Co, Ni, Gd, Nd, Sm) or metal oxides (e.g., CrO_2, Fe_3O_4, Co_3O_4) and the unpaired electrons which provide the net magnetic moment, are located only in *d*- or *f*-type orbitals on metal atoms. However in past decades, a rapid progress has been made on molecule-based magnetism and the rational design of molecular magnetic materials.[5,6] Molecule-based magnets are often soluble in organic solvents and dispersible with high flexibility and do not require any energy exhaustive metallurgical preparative methods.[7] Molecular magnetism cope with the magnetic properties of isolated molecules and their assemblies.[8] Therefore, in this case the unpaired electrons may reside in *d*- or *f*- orbitals of metal atoms and also may reside in *s*- and *p*- orbitals of the purely organic component. The history of molecule-based magnetism started early in the year 1951 with Cu (II) acetate monohydrate.[9] Research in the field of molecule-based magnet enhances with the synthesis of diethyldithiocarbamate-Fe (III) chloride compound (Figure 1.1) by Wickman and co-workers in the year of 1972.[10] After that a large number of molecular magnets have been developed in which the building units are either organic, inorganic or a combination of the both. In molecule-based magnetism, molecules may have one or more magnetic sites and in assemblies of the molecules in solid state, the magnetic interaction occurs between different magnetic units. Recently with the development of the science related to molecular magnetism, more emphasis is given on the discovery of new magnetic building blocks and the way to bring them together in the solid state. In this case the spin bearing entity is called the building block. The seminal work of Tamura et al. in 1991 discovered the first pure organic magnet, *β*-phase of the *p*-nitrophenyl nitronyl nitroxide with ferromagnetic ordering below 0.6K and a new era in molecule based magnetic materials has been arrived.[11]

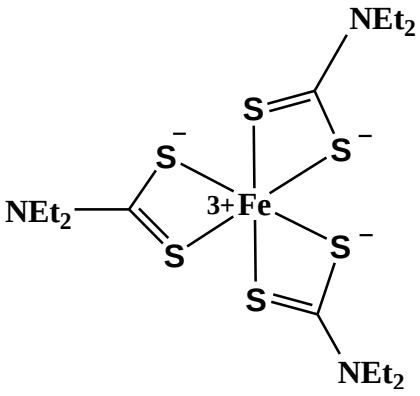

Figure 1.1 Diethyldithiocarbamate-Fe (III) compounds.

A very special category of magnetic materials, known as single-molecule magnets (SMM), has large value of total spin angular magnetic moment and can be magnetized individually as in such cases one molecular unit is capable of showing magnetic hysteresis.[12] These molecular materials have been the focus of multidisciplinary research in last few decades for their potential applications in molecule-based magnetic storage materials,[13] high-density data storage devices,[14] spintronic devices,[15] q-bits[15a,16] etc. SMMs are generally a class of metal-organic or metal-only skeleton. The superparamagnetic behavior is observed in SMMs below a certain blocking temperature where the magnetization can be arranged in a particular orientation for a long time. The first SMM was discovered by Sessoli et al.[12a] in 1993 is polymetallic manganese (Mn) complex called "Mn_{12}-acetate", shown in Figure 1.2,[12b] and since then much effort was put on constructing new SMM materials. Rumberger et al.[17] had reported the Mn_{12} based wheel. Next to manganese based SMMs, the most widely studied complex is based on iron clusters, as for example, the Fe_8 system, $[Fe_8O_2(OH)_{12}(tacn)_6]Br_8 \cdot 9H_2O$ (tacn = 1,4,7-triazacyclononane).[18] Other SMMs containing vanadium ions are also known.[19] Recently SMMs based on lanthanide ions becomes trendy for developing high performance SMMs.[20] There are a number of luminescent Ln based SMMs that have SMM behavior as well as optical property.[21] Zhang et al. have investigated that, by tuning of ligands on the coordination sites in some $Dy(III)_4$ SMMs, the intramolecular magnetic exchange can be switched from antiferromagnetic to ferromagnetic state.[22] Moreover some actinide SMMs have emerged and are already showing encouraging properties.[23] Gaggioli et al. have even investigated theoretically the Plutonium-based SMMs.[24]

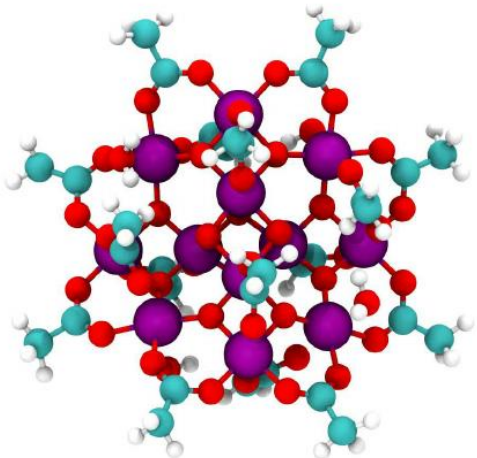

Figure 1.2 Structure of the Mn_{12} (acetate) molecule. Violet, red, sky and white colors signify Mn, O, C, and H respectively.

1.4 Organic radicals as magnetic molecules

After the discovery of triphenylmethyl radical in 1990 as a first example of open-shell system,[25] organic radicals have become a source of inspiration for research as a new building block of molecular magnets. However, to be an efficient building block of a magnetic molecule, the constituting radicals should be stable in air and moisture as well as isolated and characterized with ease at room temperature. Therefore, few organic radical classes are useful for this purpose as organic radicals are open-shell molecules with an unpaired electron in highest molecular orbital and are highly reactive. They can easily take part in reactions such as dimerization, recombination, hydrogen abstraction etc. to gain the close-shell character.[26] However, by screening the radical center with bulky substituent, it is possible to protect the radical from undesired reactions.[27] Besides these, the delocalization of the unpaired electron within a huge part of the atomic framework is another effective way to produce persistent radicals.[27d, 28]

Among various types of stable organic radical, the family of nitroxide radical undoubtedly play a prime role since long,[29] where the delocalization of unpaired electrons occurs between the nitrogen and oxygen atoms. The mostly studied nitroxide-based radicals are iminonitroxides (IN), nitronylnitroxides (NN) (Figure 1.3a and 1.3b) and *tert*-butyl nitroxides (Figure 1.3c). NN is assumed to be the most capable neutral radical to produce strong magnetism and has been studied actively.[30]

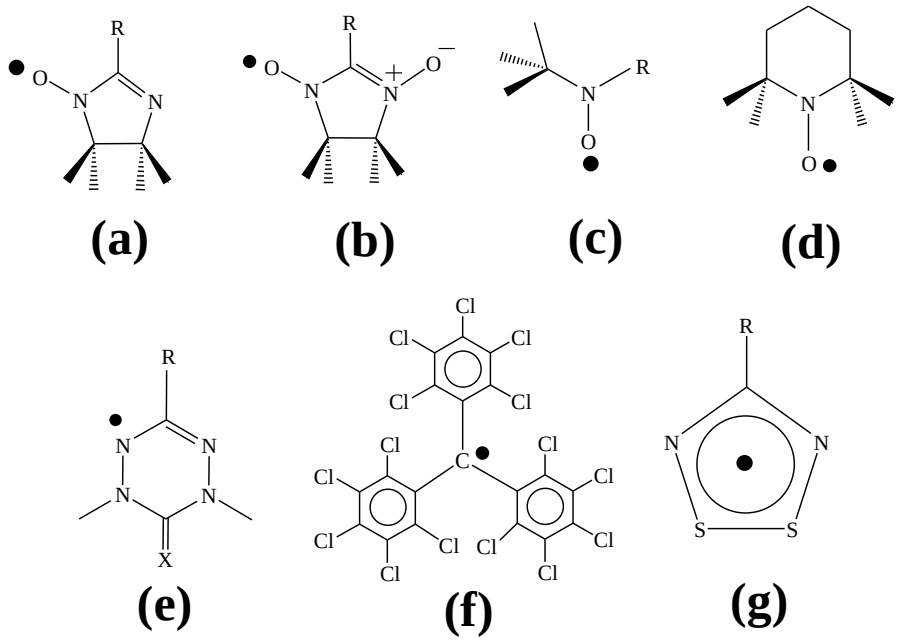

Figure 1.3 Structure of (a) iminonitroxide, (b) nitronylnitroxide, (c) *tert*-butyl nitroxide (d) TEMPO (e) verdazyl (f) Polychlorotriphenylmethyl and (g) dithiadiazolyl (DTDA) radicals. X on verdazyl represents O/ S.

The 2,2,6,6-Tetramethylpiperidin-N-oxyl (TEMPO)[31] radicals (Figure 1.3d) are stable enough to handle in air, contributes to the progress of the molecule-based magnetism as well as spin sciences. Verdazyl becomes one of the biggest families of stable radicals since it was first synthesized and characterized by Kuhn et al. in early 1960s.[32] Verdazyl radicals[33] (Figure 1.3e) are stabilized by delocalization of unpaired electrons over the four nitrogen atoms of the heterocyclic ring. Recently much efforts being given to synthesize and characterize the heteroverdazyl radicals where different heteroatoms are incorporated in the heterocyclic ring.[34] The most commonly known heteroverdazyls are thioverdazyl, oxoverdazyl, and phosphaverdazyl. The method of synthesizing the different types of verdazyl radicals have been established by different research groups.[34,35] Hicks et al. have synthesized and characterized Phosphaverdazyl radicals.[34] 6-oxo- and 6-thioxo-verdazyl radicals are known to be chemically stable and are isolated in pure crystalline form.[36] An extensive study has been made to determine the magnetic property of different derivatives of verdazyl radicals.[36a,37] Polychlorotriphenylmethyl radicals (Figure 1.3f) are also characterized by enormously high persistence and stability.[38] Another neutral radical, dithiadiazolyl (DTDA) (Figure 1.3g) is spotlighted due to its synthetic simplicity and remarkable stability and are well known as a building block for super-conducting materials[39] as well as organic magnets.[40] The DTDA radicals are sulfur-nitrogen-containing heterocyclic free radicals. The first synthesized DTDA radical is phenyl-1,2,3,5-dithiadiazolyl in 1980[41] and after that a variety of DTDA derivatives have been explored. The family of persistent radicals find applications in catalysis,[42] biochemistry,[43] and molecular magnetism.[44]

Based on the different radical centers, a large number of organic diradicals[45] have been extensively investigated experimentally as well as theoretically for several decades.[46] Ziessel et al.[47] have isolated and studied the diradical based on NN with ethylene coupler. Turek et al. have theoretically designed a series of diradicals based on *m*-phenylene couplers and investigated that the molecular conformation and the spin polarization controls the magnetic exchange coupling.[30b,48] Trindle et al.[49] have explained the spin density alternation rule which predicts the nature of exchange coupling interaction in a reliable way. The exchange coupling constant of a diradical generally depends on the distance between two radical centers as well as on the nature of the couplers.[50] The interaction may follow different mechanisms[51] such as super exchange, direct exchange, ligand mediated exchange and so on. Bhattacharya et al.[52] have studied the magnetic property of oxoverdazyl and thioxoverdazyl-radical coupled with polyacene spacers of different length. There are a number of studies where the switching of magnetic nature between ferromagnetic and antiferromagnetic states occurs.[53] The existence of heteroatom in the exchange pathway influences magnetic exchange coupling.[54] It is observed that when a heteroatom is involved in the exchange pathway, the magnetic interaction between radical centers becomes more complicated.[54a] The effect of spin leakage phenomenon of certain phosphoverdazyl systems on magnetic exchange coupling has been investigated.[54c,54d] Ali and Datta have studied the influence of nucleus independent chemical shift

(NICS) of aromatic ring couplers on the magnetic interaction.[55] Recently, the *J* values for few diradicals based on conjugated and their corresponding unconjugated systems have been estimated to understand the role of π-conjugation in such systems.[56] However, all the diradicals are not expected to have sustainable magnetism due to the less number of spins within it. Organic polyradicals (in Figure 1.4) are the potential candidate that are widely explored for organic ferromagnetic materials.[5b, 27b,57] Several di- and poly-radicals based on verdazyls have been made by attaching of verdazyl moieties at either the C_3 carbon or one of the nitrogen atoms.[3a] Presently chiral magnetic molecules have attracted interest to organic chemists and pharmaceutical chemists. Stable chiral magnets are important components for future data storage, spintronic devices and other applications for their interesting properties.[58]

In recent years, the study of magnetic property of polyradicals, particularly of organic origin has attracted extensive interest. Organic polyradicals have huge number of possible applications in magnetic nanomaterials,[59] spintronics,[60] conducting systems.[61] Polynitroxides is an organic ferromagnet that can work as contrast agents in MRI, radiation protectors in whole-brain radiotherapy.[62] Most of the polyradicals are contained within a dendritic structure.[63] Organic radicals are obtained to form 1-D polymers, 2-D networks as well as 3-D solids with required properties. Hansda et al. have investigated the magnetic properties of 1-D chain of silicon-substituted meta-xylylene polyradicals and predicted a ferromagnetic coupling with moderate transition temperature (~100K).[64] A theoretical study was done on the structural and magnetic properties of 1D-like polyradicals based on triarylmethyl radical derivatives where the helical folding induces the stabilization of these polyradicals.[65] Stable two dimensional polyradicals, with *p*-phenylenediamine-based cationic radicals have been prepared by Michinobu et al.[66] Kaneko et al. have investigated the through space magnetic interaction of folding-induced poly (1,3-phenyleneethynylene)-based polyradicals bearing galvinoxyl side groups.[67] Iwamura and co-workers have designed triradical containing nitroxyl group that shows ferromagnetic interactions with quartet ground state.[29h] A computational study is done on organic polyradicals stabilized by chromium atoms i.e., on $Cr(coronene\text{-}6O)_2$ which has the high multiplicity indicating a further way to organic magnets by organometallic sandwich compounds.[68] Tetrakis (dimethylamine) ethylene fullerene (TDAE-C_{60}) is also synthesized and characterized by different research groups.[69]

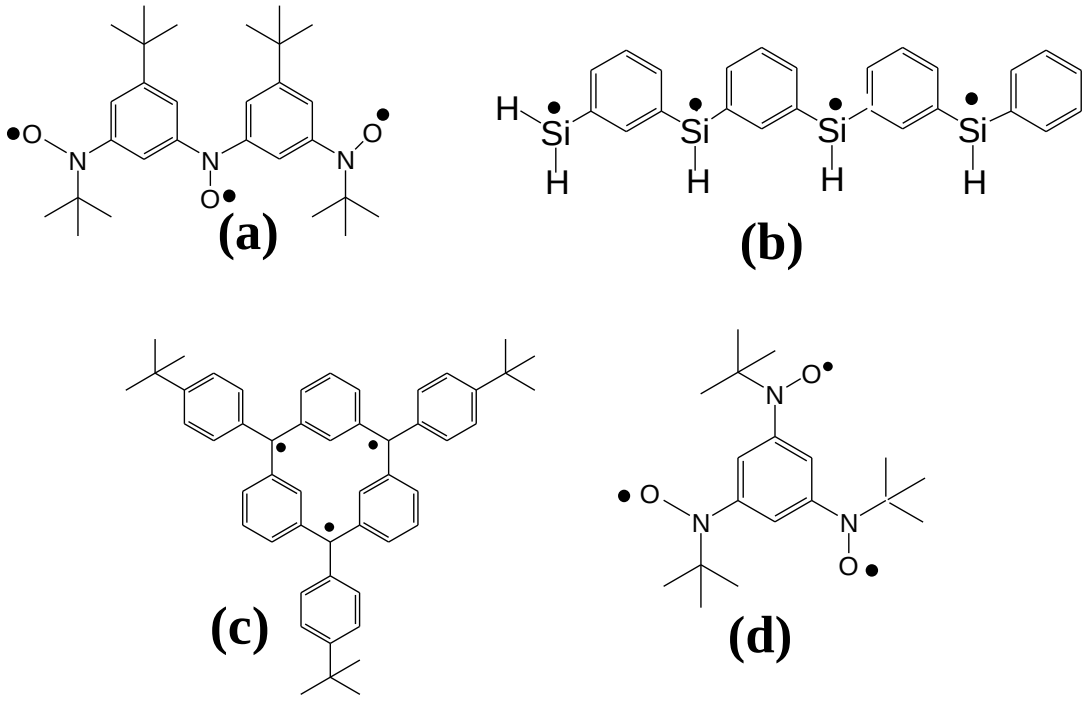

Figure 1.4 Examples of polyradicals.

Rajca and coworkers have designed organic branched chain π-conjugated ferromagnets with heptaradical (*S*=7/2) and decaradical (*S*=5).[70] They have also synthesized polyradicals of extended triarylmethyl systems with highest spin multiplicity (*S* = 13).[71] Meta-phenylene unit was studied both experimentally and theoretically as one of the best ferromagnetic couplers to form polyradicals.[72] In multi-Beryllium-expanded graphene-like molecules, a remarkable magnetic interaction was observed by Song et al. with distinct polyradical characters.[73] Yang et al. have synthesized two-dimensional organic magnetic polyradical nanosheets which show antiferromagnetic phase transition with a Neel temperature of 42.5 K.[74] For this distinctive property, they can act as building blocks in antiferromagnetic spintronic devices.[74]

1.5 Transport through spin polarized molecular systems

Molecular electronics concerns the incorporation of molecular elements into nanoelectronic devices where only the charge is in consideration. However, the research field that offers a novel device structure which utilizes the spin polarized electrons is named as "spintronics" where electron spin in addition to its charge is employed for information processing.[75] The main motivation behind the spintronic research is Moore's law which states that the computing power of microprocessor will doubles about every 18 months, as the chips become smaller.[76] But the devices experience some problems such as leakage and heat dissipation before they get too small.[77] On the other hand spintronic devices are more flexible and faster than the conventional electronic devices. Addition of spin degree of freedom offers new

capabilities as well as new functionality. With the discovery of giant magnetoresistance (GMR) in 1988 by using Fe/Cr multi-layers, spintronics was born and draw significant attention in research field.[78] After that similar GMR effects were found in Co/Cu multi-layers and so on.[79] GMR is a quantum mechanical magneto resistance effect based upon spin dependent scattering which is observed in thin film structures made up of alternating ferromagnetic and nonmagnetic layers. The discovery of GMR developed modern information storage and tiled a way for future spin-logic devices. The GMR effect using nonmagnetic metallic interlayers has been widely studied and potential applications as magnetic recording, electric switching etc. were proposed and employed.[80] In 1995, Miyazaki[81] and Moodera[82] separately observed the tunneling magnetoresistance (TMR) effect where insulating layers is inserted between two ferromagnetic layers. Spin polarized coherent transport was found in different inorganic materials.[83] However there are some limitations on application of all-metallic spintronic devices as they are not suitable for coherent spin manipulation and are characterized by small spin relaxation times (~picosecond).[80] To overcome these problems, the attention is moved towards hybrid devices with semiconductor materials sandwiched between ferromagnetic layers.[84] Spintronics using inorganic semiconductors such as GaAs, Si are vigorously investigated.[85] Organic semiconductors have employed as a spacer for spintronic devices for just about a decade. Several devices based on spintronics are non-volatile magnetic random access memory (MRAM), magnetic-field sensors, racetrack memories etc.[80,86] This field has been exploited on the marketplace, such as it is at the base of each hard disk read head and also has potential applications in quantum computing.[80b] Though spintronics is exclusively based on conventional inorganic metals and semiconductors, the door of molecular spintronics was unlocked in 1999 by the first report on the spin-dependent transport through multi-walled carbon nanotubes (MWNT).[87] The main motivation in molecular spintronics is that, it is placed at the crossover of molecular magnetism and spintronics with molecular electronics. Molecular spintronics attracts much attention as a molecule has a relatively smaller spin-orbit interaction. Another important reason is the structural, chemical and electronic versatility in molecular world. Besides, the spin-relaxation times of magnetic molecules are remarkably long i.e., between a few milliseconds and seconds. Other advantageous features of molecular systems over inorganic conductors and semiconductors are their flexibility, transparency, low-density etc. The ultimate objectives of molecular spintronics are the construction of cheaper spintronic devices by using molecular materials and reduction of the sizes of device in the contest towards miniaturization.[88] In 2002, organic spintronics was born with the pioneer work by Dediu et al. on sexithienyl molecule (a prototypical organic semiconductor).[84b] Organic molecules have weak spin–orbit coupling as well as hyperfine interactions which leads to the enviable properties such as ultra-miniaturization and very low power consumption. Moreover, organic molecules have the spin polarization which persists over greater time and distance than in conventional semiconductors or metals. Therefore, the capacity to manipulate electron

spin in organic materials offers a new way towards spin electronics from fundamental and technological viewpoints.

Normally molecular spintronic device is constructed either by placing a magnetic molecule sandwiched between two non-magnetic electrodes or by placing a nonmagnetic molecule to two ferromagnetic electrodes (Figure 1.5).[89] However, the first one is considered as true molecular spintronic device where spin-polarized transport properties are controlled by magnetic molecule mainly, rather than the electrodes. The surfaces of the electrode used in a molecular junction are generally metallic such as Al, Ni, Au etc. On the other hand graphene nanoribbons (GNRs) especially zigzag graphene nanoribbons (ZGNRs) are selected as prospective electrodes in covalent−organic molecular devices due to the high carrier mobility as well as long spin relaxation length.[90] There are many theoretical and experimental results that focus on the spin dependent transport of various molecular systems.[91] A review of literature about the transport property of spin polarized molecular systems such as metal complexes, SMMs and organic radical is discussed below.

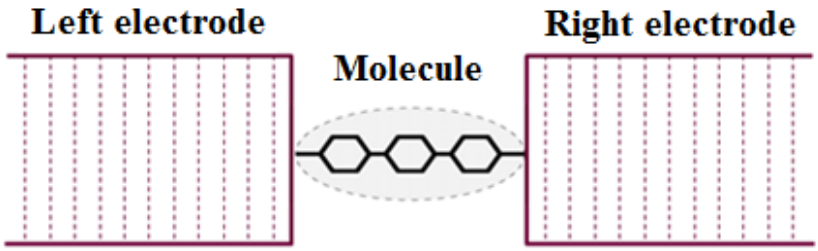

Figure 1.5 The Electrode–Molecule–Electrode transport structure.

In molecular spintronics, sizeable giant magnetoresistance (GMR) and perfect spin filtering are two significant issues. A perfect spin filter is a system which transport all spin-up (or spin-down) carriers through a channel and blocks all the spin-down (or spin-up) carriers. Spin filtering with high-efficiency was found in four-coordinate planar Fe complexes with armchair single-walled carbon nanotube (ASWCNT) electrodes[92] and in iron phthalocyanine (FePc) molecules with gold (Au) electrodes.[93] Shen et al. have investigated the spin transport of transition metal (M) phthalocyanines (where M is Mn, Fe, Co, Ni, Cu, Zn) and showed that a perfect spin filter is obtained with Mn and Fe metal center with high spin-polarization up to 100%.[94] Zhao et al. have studied the spin polarized as well as thermospin polarized transport properties of transition metal (Mn, Fe, Co, Ni) phthalocyanine dimer based molecular junction and it is found that Mn based system is a potential candidate for the development of multifunctional spintronic as well as spin caloritronic devices.[95] They have also investigated that sizeable GMR/thermal-GMR effects and perfect spin/thermal-spin filtering can be obtained in the Mn- phthalocyanine dimer.[95] Among the transition metal derivatives, dithiolene complexes have attracted interest due to their unique optical, conductive, superconductive and magnetic properties.[96] In 1994,

a field effect transistor based on nickel dithiolene complex was first synthesized and showed somewhat high mobility.[97] Huong et al. have studied theoretically the charge transport characteristics of transition metal (M) dithiolene complexes (where M = Ni, Fe and Mn) and observed that Ni complexes are non-polarized, but Fe and Mn complexes show high degree of spin polarization, and therefore used as excellent spin filtering materials.[98] The spin transport phenomenon was also reported in the transition metal salophenes[99] and dibenzotetraaza [4]annulene complexes.[100] The transport properties of dibenzotetraazaannulene-based systems shows the multi-functional properties such as switching, GMR, rectifying, dual spin filtering effects.[101] In past few years much attention was taken to determine the electronic transport through a SMM and it is a promising field full of interesting challenges for both the theoreticians and experimentalists.[102] A fundamental link between spintronics and molecular electronics can be made by using molecular magnetic materials and particularly using single-molecule magnets. SMMs are consisted of inner magnetic core which is surrounded by organic ligands that can fit them or connect them into junctions or on surfaces.[103] The advantages of SMMs over magnetic nanoparticles are that SMMs are completely monodispersed. The electronic transport through a SMM coupled to nonmagnetic electrodes was mostly studied by the experimentalists, however it is suggested that when the leads are ferromagnetic, the spin-polarized current can manipulate the magnetic state of a SMM.[104] The spin polarized current can even reverse the magnetization of SMM.[105] Barnaś and coworkers have shown that the spin polarized current can reverse the spin of a SMM and the reversal process may be observed in current when the voltage is increased in time.[105a] Magnetic materials of coordination compounds are a source of inspiration in the field of molecular spintronics. The double-decker type SMM phthalocyaninato-Tb(III) ($TbPc_2$) molecule is exploited in spintronics devices, such as spin valves,[106] spin transistors,[107] and spin quantum bits.[108] Many interesting effects such as tunnel magnetoresistance (TMR)[109] and spin-diode behavior[110] results from the exchange coupling between the core spin and lowest unoccupied molecular orbital (LUMO).

From last decades, the area of quantum spin transport properties of organic molecular junctions and molecular spintronic devices has achieved an ample enthusiasm.[111] The engineering of spin transport in graphene,[112] small conjugated organic molecules,[113] magnetic molecules[114] and stable organic radicals[115] has gained a remarkable attention for their huge applications in molecular spintronic devices. On the other hand, linear chains of carbon atoms is predicted to have excellent properties for various transport related applications.[116] Cumulene wires are well known for the application in nanoelectronics.[117] In organic molecular devices, different novel quantum effects, such as giant magnetoresistance (GMR),[118] rectifying,[119] spin filtering[120] and Kondo effect,[121] have been reported. Organic radicals can be used as building blocks for functional molecular materials, half-metals, organic light-emitting diodes, spin filters, batteries etc.[122] In stable organic radicals, the degeneracy of α and β spin-orbitals break and one particular spin can remain close to the Fermi energy level (E_F) of the electrodes. As a result the transmission of one particular spin is

manifested over the other which is the essential criterion for a spin filter.[115c] Sen and Chakrabarti have studied a very small sized ferromagnetically coupled cobalt-benzene-cobalt (CBC) molecular spin filter with extraordinary spin injection coefficient.[123] Chen et al. have designed 1, 4-dinitrobenzene with boron doping sandwiched between two zigzag-edge graphene nanoribbon (ZGNR) electrodes which shows rectifying effects, large spin-filtering, and negative differential resistance.[124] Herrmann and coworkers have reported the molecular spintronic materials based on the organic radical systems.[115c] They have found that the conduction properties of radical systems may vary depending on the molecular conformation as well as the way by which the molecules is absorbed on the electrodes.[115c] They have also shown that the transport property does not directly depend on the MO occupations. However, the number of α and β electrons has an effect on the central subsystem MO shapes and energies that control the transmission. HOMO and LUMO play fundamental roles in the transport properties[125] and the Fermi levels exist somewhere in between the HOMO and the LUMO. Deng et al. have studied theoretically the spin transport of acene molecules containing four aromatic rings in the GNRs based molecular junctions with Nitrogen dopant and investigated the spin dependent electronic transport properties.[126] It is found that the designed system displays a diode behavior with large rectification ratio with high-efficiency spin-filtering, and such molecular system has important theoretical significance as well as practical value in molecular circuits in future.[126] Tagami et al. have used the poly-(4-phenoxyl-1,2-phenylenevinylene) radical molecule that bridges between the two gold electrodes.[127] Zhang et al.'s investigations demonstrate the spin-polarized transport properties of pyridinium-based radicals sandwiched between two Al electrodes and the molecular device have promising potential future applications.[128] Recently molecular devices are experimentally designed where a single organic molecule is fixed between GNR electrodes at room temperature.[129] Caliskan et al. have investigated that the conductance depends on the length and strength of the acenes rings attached to Ni electrodes and these systems have potential applications in molecular spin valves.[130] They have also investigated the spin resolved transport through $N@C_{20}$ endohedral fullerene molecule placed between Au electrodes and it is found that $N@C_{20}$ can be used as a potential molecule for spintronic applications.[131] Sevov et al. investigated that pyridinium-based radicals may be used as low potential electrolytes for flow batteries.[132]

1.6 Objectives of the thesis

The objective of the thesis is to study the magnetic features and applicability of different spin polarized molecular systems and the transport property of molecules with varying conformation. The defined objectives of the thesis are as follows:

(1) To investigate the transport and magnetic properties of diradical substituted molecular wires of different length and to understand the effect of length on such properties (**Chapter 3: Effect of length on the transport and magnetic properties of diradical substituted molecular wires**).

(2) Designing chiral organic magnetic molecules based on allene and chiral cumulene couplers and investigate the variation of magnetic property with the increase in chiral centers within the coupler (**Chapter 4: A perspective on designing chiral organic magnetic molecules with unusual behavior in magnetic exchange coupling**).

(3) Designing diradicals based on conjugated and cumulated couplers and investigate the different factors that affect the magnetic and transport properties of such systems (**Chapter 5: Magnetic and transport properties of conjugated and cumulated molecules: the π-System enlightens part of the story**).

(4) To study the magnetic tone in heteroallene and heterocumulene based diradicals and to investigate the role of conformation and spin density on magnetic exchange coupling of such systems (**Chapter 6: Magnetic modulation in heteroallene and heterocumulene based *tert*-butyl nitroxide diradicals: spin delocalization and conformation play crucial roles**).

1.7 References

(1) Du Trémolet de Lacheisserie, É.; Gignoux, D.; Schlenker, M. (**2005**). *Magnetism: Fundamentals*. Springer.pp. 3–6. ISBN 0-387-22967-1.
(2) (a) Tamaki, H.; Zhong, Z. J.; Matsumoto, N.; Kida, S.; Koikawa, M.; Achiwa, N.; Hashimoto, Y.; Okawa, H. *J. Am. Chem. Soc.* **1992**, *114*, 18, 6974–6979. (b) Miyasaka, H.; Saitoh, A.; Abe, S. *Coord. Chem. Rev.* **2007**, *251*, 2622–2664. (c) Okawa, H.; Mitsumi, M.; Ohba, M.; Kodera, M.; Matsumoto, N. *Bull. Chem. Soc. Jpn.* **1994**, *67*, 2139–2144. (d) Tanase, S.; Reedijk, J. *Coord. Chem. Rev.* **2006**, *250*, 2501–2510. (e) Ohba, M.; Okawa, H. *Coord. Chem. Rev.* **2000**, *198*, 313-328. (f) Saalfrank, R.W.; Bernt, I. *Curr. Opin. Solid State Mater. Sci.* **1998**, *3*, 407-413.(g) Matthews, C. J.; Avery, K.; Xu, Z.; Thompson, L. K.; Zhao, L.; Miller, D. O.; Biradha, K.; Poirier, K.; Zaworotko, M. J.; Wilson, C.; Goeta, A. E.; Howard, J. A. K. *Inorg. Chem.* **1999**, *38*, 5266-5276.
(3) (a) Ratera, I.; Jaume Veciana, J. *Chem. Soc. Rev.* **2012**, *41*, 303–349. (b) Iwamura, H. *Adv. Phys. Org. Chem.* **1991**, *26*, 179-253. (c) Dougherty, D. A. *Acc. Chem. Res.*

1991, *24*, 88-94. (d) Iwamura, H.; Koga, N. *Acc. Chem. Res.* **1993**, *26*, 346-351. (e) Matsuda, K.; Iwamura, H. *Curr. Opin. Solid State Mater. Sci.* **1997**, *2*, 446-450.
(4) (a) Crayston, J. A.; Devine, J. N.; Walton, J. C. *Tetrahedron*, **2000**, *56*, 7829-7857. (b) Miller, J. S.; Epstein, A. J. *MRS Bull.* **2000**, *25*, 21-30.
(5) (a) Itoh K.; Kinoshita, M. *Molecular Magnetism*, Gordon and Breach, Amsterdam (Kodansha asco publisher, Tokyo), (**2000**). (b) Lahti, P. M. *Magnetic Properties of Organic Materials*, Marcel Dekker, New York (**1999**).
(6) Verdaguer, M. *Polyhedron* **2001**, *20*, 1115-1128.
(7) Miller, J.S. *Mater. Today* **2014**, *17*, 224–235.
(8) Kahn, O. (**1993**). *Molecular Magnetism*. John Wiley & Sons, Singapore.
(9) Bleaney, B.; Bowers, K.D. *Proc. R. Soc. A* **1952**, *214*, 451-465.
(10) Wickman, H. H.; Trozzolo, A. M.; Williams, H. J.; Hull, G. W.; Merritt, F. R. *Phys. Rev.* **1967**, *155*, 563-566.
(11) (a) Tamura, M.; Nakazawa, Y.; Shiomi, D.; Nozawa, K.; Hosokoshi, Y.; Ishikawa, M.; Takahashi, M.; Kinoshita, M. *Chem. Phys. Lett.* **1991**, *186*, 401–404. (b) Nakazawa, Y.; Tamura, M.; Shirakawa, N.; Shiomi, D.; Takahashi, M.; Kinoshita, M.; Ishikawa, M. *Phys. Rev. B* **1992**, *46*, 8906–8914.
(12) (a) Sessoli, R.; Tsai, H.-L; Schake, A.R.; Wang, S.; Vincent, J.B.; Folting, K.; Gatteschi, D.; Christou, G.; Hendrickson, D.N. *J. Am. Chem. Soc.* **1993**, *115*, 1804-1816. (b) Packwood, D. M., Reaves, K. T., Federici, F. L., Katzgraber, H. G., & Teizer, W. *Proc. R. Soc. A* **2013**, *469*, 20130373.
(13) Green, J. E., Wook Choi, J., Boukai, A., Bunimovich, Y., Johnston-Halperin, E., DeIonno, E.; Luo, Y.; Sheriff, B. A.; Xu, K.; Shin, Y. S.; Tseng, H. –R.; Stoddart, J. F.; Heath, J. R. *Nature* **2007**, *445*, 414–418.
(14) (a) Gatteschi, D.; Sessoli, R.; Villain, J. Molecular Nanomagnets; Oxford University Press: Oxford, U.K., **2006**. (b) Gatteschi, D. *Adv. Mater.***1994**, *6*, 635−645.
(15) (a) Coronado, E.; Epsetin, A. J. *J. Mater.Chem.* **2009**, *19*, 1670−1671. (b) Bogani, L.; Wernsdorfer, W. *Nat. Mater.* **2008**, *7*, 179−186.
(16) Leuenberger, M. N.; Loss, D. *Nature* **2001**, *410*, 789−793.
(17) Rumberger, E. M.; Zakharov, L. N.; Rheingold, A. L.; Hendrickson, D. N. *Inorg. Chem.* **2004,** *43*, 6531-6533.
(18) (a) Barra, A. L.; Gatteschi D.; Sessoli, R. *Chem. Eur. J.*, **2000**, *6*, 1608-1614. (b) Wieghardt, K.; Pohl, K.; Jibril I.; Huttner, G. *Angew. Chem., Int. Ed. Engl.*, **1984**, *23*, 77-78.
(19) Castro, S. L.; Sun, Z. M.; Grant, C. M.; Bollinger, J. C.; Hendrickson, D. N.; Christou, G. *J. Am. Chem. Soc.* **1998**, *120*, 2365.
(20) (a) Sessoli, R.; Powell, A. K. *Coord. Chem. Rev.* **2009**, *253*, 2328–2341. (b) Feltham, H. L. C.; Brooker, S. *Coord. Chem. Rev.* **2014**, *276*, 1–33. (c) Zhang, P.; Guo, Y. –N.; Tang, J. *Coord. Chem. Rev.* **2013**, *257*, 1728–1763. (d) Layfield, R. *Organometallics*, **2014**, *33*, 1084–1099. (e) Pointillart, F.; Cador, O.; Guennic, B. L.; Ouahab, L. *Coord. Chem. Rev.* **2017**, *346*, 150–175. (f) Liu, K.; Zhang, X.; Meng, X.; Shi, W.; Cheng, P.; Powell, A. K. *Chem. Soc. Rev.* **2016**, *45*, 2423–2439. (g) McAdams, S. G.; Ariciu, A. -M.; Kostopoulos, A. K.; Walsh, J. P. S.; Tuna, F. *Coord. Chem. Rev.* **2017**, *346*, 216–239.

(21) (a) Wang, Y.-L.; Gu, B.; Ma, Y.; Xing, C.; Wang, Q.-L.; Li, L.-C.; Cheng, P.; Liao, D.-Z. *CrystEngComm.* **2014**, *16*, 2283-2289. (b) Silva, M.R.; Martín-Ramos, P.; Coutinho, J.T.; Pereira, L.C.J.; Martín-Gil, J. *Dalton Trans.* **2014**, *43*, 6752-6761. (c) Li, Q.-W.; Liu, J.-L.; Jia, J.-H.; Leng, J.-D.; Lin, W.-Q.; Chen, Y.-C.; Tong, M.-L. *Dalton Trans.* **2013**, *42*, 11262-11270. (d) Jiménez, J.-R.; Díaz-Ortega, I. F.; Ruiz, E.; Aravena, D.; Pope, S. J. A.; Colacio, E.; Herrera, J.M. *Chem. Eur. J.* **2016**, *22*, 14548–14559. (e) Costes, J.P.; Titos-Padilla, S.; Oyarzabal, I.; Gupta, T.; Duhayon, C.; Rajaraman, G.; Colacio, E. *Chem. Eur. J.* **2015**, *21*, 15785 – 15796. (f) Ren, M.; Xu, Z.-L.; Bao, S.-S.; Wang, T.-T.; Zheng, Z.-H.; Ferreira, R.A.S.; Zheng, L.-M.; Carlos, L.D. *Dalton Trans.* **2016**, *45*, 2974-2982.

(22) Zhang, K.; Montigaud, V.; Cador, O.; Li, G. –P.; Guennic, B. L.; Tang, J. -K.; Wang, Y. –Y. *Inorg. Chem.* **2018**, *57*, 8550-8557.

(23) (a) Meihaus, K. R.; Long, J. R. *Dalton Trans.* **2015**, *44*, 2517−2528. (b) Cooper, O. J.; Mills, D. P.; McMaster, J.; Moro, F.; Davies, E. S.; Lewis, W.; Blake, A. J.; Liddle, S. T. *Angew. Chem.* **2011**, *123*, 2431−2434. (c) Mills, D. P.; Moro, F.; McMaster, J.; van Slageren, J.; Lewis, W.; Blake, A. J.; Liddle, S. T. *Nat. Chem.* **2011**, *3*, 454−460. (d) Antunes, M. A.; Pereira, L. C.; Santos, I. C.; Mazzanti, M.; Marcalo, J.; Almeida, M. *Inorg. Chem.* **2011**, *50*, 9915−9917. (e) King, D. M.; Tuna, F.; McMaster, J.; Lewis, W.; Blake, A. J.; McInnes, E. J.; Liddle, S. T. *Angew. Chem., Int. Ed.* **2013**, *52*, 4921−4924. (f) Rinehart, J. D.; Long, J. R. *J. Am. Chem. Soc.* **2009**, *131*, 12558−12559. (g) Mougel, V.; Chatelain, L.; Pécaut, J.; Caciuffo, R.; Colineau, E.; Griveau, J. C.; Mazzanti, M. *Nat. Chem.* **2012**, *4*, 1011−1017. (h) Pereira, L. C.; Camp, C.; Coutinho, J. T.; Chatelain, L.; Maldivi, P.; Almeida, M.; Mazzanti, M. *Inorg. Chem.* **2014**, *53*, 11809−11811.

(24) Gaggioli, C. A.; Gagliardi, L. *Inorg. Chem.* **2018**, *57*, 8098-8105.

(25) (a) Gomberg, M. *J. Am. Chem. Soc*. **1900**, *22*, 757-771. (b) Gomberg, M. *J. Am. Chem. Soc*., **1901**, *23*, 496-502. (c) Gomberg, M. *Chem. Rev*. **1924**, *1*, 91-141.

(26) (a) Leonid Sheps, L.; Andrew C. Crowther, A. C.; Christopher G. Elles, C. G.; F. Fleming Crim, F. F. *J. Phys. Chem. A* **2005**, *109*, 4296-4302. (B) Gibian, M. J.; Corley, R. C. *Chemical Reviews*. **1973**, *73*, 441-464. (C) Rozantsev, E. G.; Loshadkin, D. V. *Designed Monomers and Polymers.* **2001**, *4*, 281–300.

(27)(a) Kahn, O. Magnetism: A Supramolecular Function, Kluwer, Dordrecht, **1996**. (b) Itoh, K.; Kinoshita, M. *Molecular Magnetism*, Kodansha (Gordon and Breach), Tokyo, **2000**. (c) Power, P. P. *Chem. Rev*. **2003**, *103*, 789-810.(d)Tang, B.; Zhao, J.; Xu, J. –F.; Zhang, X. *Chem. Sci.* **2020**, *11*, 1192-1204.(e) Ventosa, N.; Ruiz, D.; Rovira, C.; Veciana, J. *Mol. Cryst. Liq. Cryst*. **1993**, *232*, 333-342. (f) Ballester, M. *Adv. Phys. Org. Chem*. **1989**, *25*, 267-445. (g) Armet, O.; Veciana, J.; Rovira, C.; Riera, J.; Castaner, J.; Molins, E.; Rius, J.; Miravitlles, C.; Olivella, S.; Brichfeus, J. *J. Phys. Chem*. **1987**, *91*, 5608-5616. (h) Ballester, M.; Pascual, I.; Riera, J.; Castaner, J. *J. Org. Chem*. **1991**, *56*, 217-225. (i) Domingo, V. M.; Castaner, J. *J. Chem. Soc.,Chem. Commun*. **1995**, 895-896.

(28) Li, Z.; Moalin, M.; Zhang, M.; Vervoort, L.; Mommers, A.; Haenen G. R. M. M. *Int. J. Mol. Sci.* **2020**, *21*, 2033.

(29) (a) Shiomi, D.; Ito, K.; Nishizawa, M.; Sato, K.; Takui, T.; Itoh, K. *Syn. Metals* **1999**, *103*, 2271-2272.(b) Romero, F. M.; Ziessel, R.; Bonnet, M.; Pontillon, Y.; Ressouche, E.; Schweizer, J.; Delley, B.; Grand, A.; Paulsen, C. *J. Am. Chem. Soc*. **2000**, *122*, 1298-1309. (c) Nagashima, H.; Irisawa, M.; Yoshioka, N.; Inoue, H. *Mol. Cryst. Liq. Cryst. Sci.Technol. Sect. A* **2002**, *376*, 371-376.(d) Rajadurai, C.; Ivanova, A.; Enkelmann, V.; Baumgarten, M. *J. Org. Chem*. **2003**, *68*, 9907-9915.(f) Deumal, M.; Robb, M. A.; Novoa, J. J. *Polyhedron* **2003**, *22*, 1935-1944. (g) Ishida, T.; Iwamura, H. *J. Am. Chem. Soc*. **1991**, *113*, 4238-4241. (h) Kanno, F.; Inoue, K.; Koga, N.; Iwamura, H. *J. Phys. Chem.* **1993**, *97*, 13267-13272. (i) Inoue, K.; Iwamura, H. *J. Am. Chem. Soc*. **1994**, *116*, 3173-3174. (j) Iwamura, H.; Inoue, K. *Adv. Mater*. **1996**, *8*, 73-76. (k) Inoue, K. *π- Electron Magnetism.* **2001**, *100*, 61-91.

(30) (a) Ali, M. E.; Roy, A. S.; Datta, S. N. *J. Phys. Chem. A* **2007**, *111*, 5523–5527. (b) Wautelet, P.; Le Moigne, J.; Videva, V.; Turek, P. *J. Org. Chem.* **2003**, *68*, 8025–8036.(c) Ali, M. E.; Datta, S. N. *J. Phys. Chem. A* **2006**, *110*, 2776–2784. (d) Latif, I. A.; Singh, V. P.; Bhattacharjee, U.; Panda, A.; Datta, S. N. *J. Phys. Chem. A* **2010**, *114*, 6648–6656. (e) Ali, M. E.; Datta, S. N. *J. Phys. Chem. A* **2006**, *110*, 10525–10527.

(31) Nogami, T.; Ishida, T.; Yasui, M.; Iwasaki, F.; Takeda, N.; Ishikawa, M.; Kawakami, T.; Yamaguchi, K. *Bull. Chem. Soc. Japan* **1996,** *69***,** 1841-1848.

(32) Kuhn, R.; Trischmann, H. *Angew. Chem., Int. Ed. Engl.* **1963**, *2*, 155.

(33) (a) Hicks, R. G. *Can. J. Chem*. **2004**, *82*, 1119-1127. (b) Hicks, R. G.; Lemaire, M. T.; Öhrström, L.; Richardson, J. F.; Thompson, L. K.; Xu, Z. *J. Am. Chem. Soc*. **2001**, *123*, 7154-7159.

(34) Hicks, R. G.; Hooper, R. *Inorg. Chem.* **1999**, *38*, 284-286.

(35) (a) Hicks, R. G.; Ohrstrom, L.; Patenaude, G. W. *Inorg. Chem.* **2001**, *40*, 1865-1870. (b) Koivisto, B. D.; Ichimura, A. S.; McDonald, R.; Lemaire, M. T.; Thompson, L. K.; Hicks, R. G. *J. Am. Chem. Soc.* **2006**, *128*, 690-691.(c) Koivisto, B. D.; Hicks, R. G. *Coord. Chem. Rev.* **2005**, *249*, 2612-2630.

(36) (a) Mukai, K.; Konishi, K.; Nedachi, K.; Takeda, K. *J. Magn. Magn.Mater*. **1995**, *140*, 1449-1450. (b) Neugebauer, F. A.; Fisher, H.; Siegel, R. *Chem. Ber.***1988**, *121*, 815-822.

(37) (a) Mukai, K.; Nedachi, K.; Takiguchi, M.; Kobayashi, T.; Amaya, K. *Chem. Phys. Lett*. **1995,** *238*, 61-64. (b) Kremer, R. K.; Kanellakopulos, B.; Bele, P.; Brunner, H.; Neugebauer, F. A. *Chem. Phys. Lett*. **1994**, *230*, 255-259. (c) Mito, M.; Nakano, H.; Kawae, T.; Hitaka, M.; Takagi, S.; Deguchi, H.; Suzuki, K.; Mukai, K.; Takeda, K. *J. Phys. Soc. Jpn*. **1997**, *66*, 2147-2156. (d) Mukai, K.; Nuwa, M.; Morishita, T.; Muramatsu, T.; Kobayashi, T. C.; Amaya, K. *Chem. Phys. Lett*. **1997**, *272*, 501-505. (e) Mukai, K.; Wada, N.; Jamali, J. B.; Achiwa, N.; Narumi, Y.; Kindo, K.; Kobayashi, T.; Amaya, K. *Chem. Phys. Lett*. **1996**, *257*, 538-544.

(38) Ballester, M. *Acc. Chem. Res*. **1985**, *18*, 380-387.

(39) (a) Haddon, R. C. *Nature* **1975**, *256*, 394–396. (b) Cordes, A. W.; Haddon, R. C.; Oakley, R. T. *Phosphorus. Sulfur. Silicon Relat. Elem.* **2004**, *179*, 673–684.

(40) Rawson, J. M.; Alberola, A.; Whalley, A. *J. Mater. Chem.* **2006**, *16*, 2560-2575.

(41) (a) Vegas, A.; Perez-Salazar, A.; Banister, A. J.; Hey, R. G. *J. Chem. Soc., Dalt. Trans.* **1980**, 1812–1815. (b) Haynes, D. A. *CrystEngComm* **2011**, *13*, 4793-4805.
(42) (a) Stubbe, J.; Van der Donk, W.A. *Chem. Rev.***1998**, *98*,705–762. (b) Amorati, R.; Lucarini, M.; Mugnaini, V.; Pedulli, G. F.; Minisci, F.; Recupero, F.; Fontana, F.; Astolfi, P.; Greci, L. *J. Org. Chem.* **2003**, *68*, 1747-1754.
(43) (a) Hubbel, W. L.; Gross, A.; Langen, R.; Lietzow, M.A. *Curr. Opin.Struct. Biol.* **1998**, *8*, 649-656. (b) Fanucci G.E.; Cafiso, D.S. *Curr.Opin.Struct. Biol.* **2006**, *16*, 644-653. (c) Roques, N.; Mugnaini, V.; Veciana, J. *Top. Curr. Chem.* **2010**, *293*, 207-258.
(44) (a) Gatteschi, D. *Adv. Mater.* **1994**, *6*, 635-645. (b) Train, C.; Noreland, L.; Baumgarten, M. *Coord. Chem. Rev.* **2009**, *253*, 2342-2351.
(45) (a) Hamachi, K.; Matsuda, K.; Itoh, T.; Iwamura,H. *Bull. Chem. Soc. Jpn.* **1998**, *71*, 2937-2943. (b) Matsuda, K.; Irie, M. *J. Am. Chem. Soc.* **2000**, *122*, 7195-7201. (c) Matsuda, K.; Irie, M. *J. Am. Chem. Soc.* **2000**, *122*, 8309-8310.(d) Matsuda, K.; Irie, M. *Mol. Cryst. Liq. Cryst.* **2000**, *345*, 155-160.
(46) (a) Vyas, S.; Ali, M. E.; Hossain, E.; Patwardhan, S.; Datta, S. N. *J. Phys. Chem. A* **2005**, *109*, 4213–4215. (b) Barone, V.; Bencini, A.; Matteo, A. di. *J. Am. Chem. Soc.* **1997**, *7863*, 10831–10837. (c) Latif, I. a; Panda, A.; Datta, S. N. *J. Phys. Chem. A* **2009**, *113*, 1595–1600. (d) Bhattacharya, D.; Shil, S.; Misra, A.; Klein, D. J. *Theor. Chem. Acc.* **2009**, *127*, 57–67.
(47) Ziessel, R.; Stroh, C.; Heise, H.; Khler, F. H.; Turek, P.; Claiser, N.; Souhassou, M.; Lecomte, C. *J. Am. Chem. Soc*. **2004**, *126*, 12604-12613.
(48) Catala, L.; Le Moigne, J.; Gruber, N.; Novoa, J. J.;Rabu, P.; Belorizky, E.; Turek, P. *Chem. Eur. J* **2005**, *11*, 2440-2454.
(49) Trindle, C.; Datta, S. N.; Mallik, B. *J. Am. Chem. Soc.* **1997**, *119*, 12947-12951.
(50) (a) Bhattacharya, D.; Misra, A. *J. Phys. Chem. A*, **2009**, *113*, 5470–5475. (b) Paul, S.; Misra, A. *J. Phys. Chem. A.* **2010**, *114*, 6641-. 6647. (c) S. Paul, A. Misra, *J. Chem. Theory Comput.* 2**012**, *8*, 843-853.
(51) Coey, J. M. D. *Magnetism and Magnetic Materials*, Cambridge University Press, Cambridge, U.K., **2010**, ISBN 13: 9780521816144.
(52) Bhattacharya, D.; Shil, S.; Misra, A.; Klein, D. J. *Theor. Chem. Acc.* **2010**, *127*, 57-67.
(53) (a) Shil, S.; Misra, A. *J. Phys. Chem. A* **2010**, *114*, 2022-2027. (b) Saha, A.; Latif, I. A.; Datta, S.N. *J. Phys. Chem. A* **2011**, *115*, 1371-1379. (c) Ali, Md. E.; Staemmler, V.; Illas, F.; Oppeneer, P.M.; *J. Comput. Theory Chem.* **2013**, *9*, 5216-5220.
(54) (a) Rancurel, C.; Heise, H.; Köhler, F. H.; Schatzschneider, U.; Rentschler, E.; Vidal-Gancedo, J.; Veciana, J.; Sutter, J. –P. *J. Phys. Chem. A* **2004**, *108*, 5903-5914. (b) Polo, V.; Alberola, A.; Andres, J.; Anthony, J.; Pilkington, M. *Phys. Chem. Chem. Phys.* **2008**, *10*, 857–864. (c) Bhattacharya, D.; Shil, S.; Panda, A.; Misra, A. *J. Phys. Chem. A* **2010**, *114*, 11833–11841. (d) Barclay, T. M.; Hicks, R. G.; Ichimura, A. S.; Patenaude, G. W. *Can. J. Chem.* **2002**, *80*, 1501–1506.
(55) Ali, M. E.; Datta, S. N. *J. Phys. Chem. A* **2006**, *110*, 13232–13237.
(56) (a) Ghosh, R.; Seal, P.; Chakrabarti, S. *J. Phys. Chem. A* **2010**, *114*, 93-96. (b) Seal, P.; Chakrabarti, S. *J. Phys. Chem. A* **2008**, *112*, 3409-3413.

(57) (a) Miller, J. S.; Drillon, M. D. *Magnetism: Molecules to Materials II*; Wiley-VCH: Weinheim, Germany, **2001**. (b) Rajca, A. *Chem. Eur. J.* **2002**, *8*, 4834-4841.
(58) (a) Pappas, C. Physics **2012**, *5*, 28. (b) Togawa, Y.; Koyama, T.; Takayanagi, K.; Mori, S.; Kousaka, Y.; Akimitsu, J.; Nishihara, S.; Inoue, K.; Ovchinnikov, A. S.; Kishine, *J. Phys. Rev. Lett.* **2012**, *108*, 107202.
(59) (a) Crivillers, N.; Mas-Torrent, M.; Vidal-Gancedo, J.; Veciana, J.; Rovira, C. *J. Am. Chem. Soc.* **2008**, *130*, 5499–5506. (b) Yulikov, M.; Lueders, P.; Warsi, M.F.; Chechik, V.; Jeschke, G. *Phys. Chem. Chem. Phys.* **2012**, *14*, 10732–10746. (c) Miller, J. S.; Gatteschi, D. *Chem. Soc. Rev.* **2011**, *40*, 3065–3066.
(60) (a) Boehme, C.; Lupton, J. M. *Nat. Nanotechnol.* **2013**, *8*, 612−615. (b) Sun, D.; Ehrenfreund, E.; Vardeny, Z. V. *Chem.Commun. (Cambridge)* **2014**, *50*, 1781−1793.
(61) (a) Oyaizu, K.; Nishide, H. *Adv. Mater.* **2009**, *21*, 2339–2344.(b) Tomlinson, E. P.; Hay, M. E.; Boudouris, B. W. *Macromolecules* **2014**, *47*, 6145 –6158.(c) Lloveras, V.; Vidal-Gancedo, J.; Figueira-Duarte, T. M.; Nierengarten, J. -F.; Novoa, J. J.; Mota, F.; Ventosa, N.; Rovira, C.; Veciana, J. *J. Am. Chem. Soc.* **2011**, *133*, 5818–5833.
(62) (a) Matsumoto, K.; Hyodo, F.; Matsumoto, A.; Koretsky, A. P.; Sowers, A. L.; Mitchell, J. B.; Krishna, M. C. *Clin. Cancer Res.* **2006**, *12*, 2455–2462. (b) Metz, J. M.; Smith, D.; Mick, R.; Lustig, R.; Mitchell, J.; Cherakuri, M.; Glatstein, E.; Hahn, S. M. *Clin. Cancer Res.* **2004**, *10*, 6411–6417. (c) Huang, Z.; Jiang, J.; Belikova, N. A.; Stoyanovsky, D. A.; Kagan, V. E.; Mintz, A. H. *J. Neuro-Oncol.* **2010**, *100*, 1–8. (d) Francese, G.; Dunand, F. A.; Loosli, C.; Merbach, A. E.; Decurtins, S. *Magn. Reson. Chem.* **2003**, *41*, 81–83.
(63) (a) Bosman, A. W.; Janssen, R. A. J.; Meijer, E. W. *Macromolecules* **1997**, *30*, 3606–3611. (b) Han, H. J.; Sebby, K. B.; Singel, D. J.; Cloninger, M. J. *Macromolecules* **2007**, *40*, 3030–3033. (c) Lei, X. G.; Jockusch, S.; Turro, N. J.; Tomalia, D. A.; Ottaviani, M. F. *J. Colloid Interface Sci.* **2008**, *322*, 457–464.(d) Fukuzaki, E.; Takahashi, N.; Imai, S.; Nishide, H.; Rajca, A. *Polym. J.* **2005**, *37*, 284–293. (e) Badetti, E.; Lloveras, V.; Wurst, K.; Sebastián, R. M.; Caminade, A. -M.; Majoral, J. -P.; Veciana, J.; Vidal-Gancedo, J. *Org. Lett.* **2013**, *15*, 3490–3493.(f) Badetti, E.; Lloveras, V.; Muñoz-Gómez, J. L.; Sebastián, R. M.; Caminade, A. -M.; Majoral, J. P.; Veciana, J.; Vidal-Gancedo, J. *Macromolecules* **2014**, *47*, 7717–7724.
(64) Hansda, S.; Pal, A. K.; Datta, S. N. *J. Phys. Chem. C* **2015**, *119*, 3754-3761.
(65) Mañeru, D. R.; Moreira, I. P. R.; Illas, F. *J. Am. Chem. Soc.* **2016**, *138*, 5271-5275.
(66) Michinobu, T.; Inui, J.; Nishide, H. *Org. Lett.* **2003**, *5*, 2165-2168.
(67) Kaneko, T.; Abe, H.; Teraguchi, M.; Aoki, T. *Macromolecules* **2013**, *46*, 2583−2589.
(68) Lao, K. -U.; Tsou, P. -K.; Lankau, T.; Yu, C. -H.; *Phys. Chem. Chem. Phys.* **2012**, *14*, 138–147.
(69) (a) Allemand, P. -M.; Khemani, K. C.; Koch, A.; Wudl, F.; Holczer, K.; Donavan, S.; Gruner, G.; Thompson, J. D. *Science* **1991**, *253*, 301-302.(b) Mihailovic, D.; Arcon, D.; Venturini, P.; Blinc, R.; Omerzu, A.; Cevc, P. *Science* **1995**, *268*, 400-402.(c) Narymbetov, B.; Omerzu, A.; Kabanov, V. V.; Tokumoto, M.; Kobayashi, H.;

Mihailovic, D. *Nature* **2000**, *407*, 883-885. (d) Mrzel, A.; Cevc, P.; Omerzu, A.; Mihailovic, D. *Phys. Rev. B* **1996**, *53*, R2922-R2925. (e) Omerzu, A.; Mihailovic, D.; Tokumoto. M. *Phys. Rev. B* **2000**, *61*, R11883-R11885. (f) Tanaka, K.; Asai, Y.; Sato, T.; Kuga, T.; Yamabe, T.; Tokumoto, M. *Chem. Phys. Lett.* **1996**, *259*, 574-578.
(70) Rajca, A.; Utamapanya, S.; Thayumanavam, S. *J. Am. Chem. Soc.* **1992**, *144*, 1884-1885.
(71)(a) Rajca, A.; Wongsriratanakul, J.; Rajca, S. *Science* **2001**, *294*, 1503-1505. (b) Rajca, A.; Wongsriratanakul, J.; Rajca, S. *J. Am. Chem. Soc.* **2004**, *126*, 6608-6626; (c) Rajca, A.; Lu, K.; Rajca, S. *J. Am. Chem. Soc.***1997**, *119*, 10335-10345;(d) Rajca, A. *Adv. Phys. Org. Chem.* **2005**, *40*, 153-199; (e) Rajca, A. *Chem. Rev.* **1994**, *94*, 871-893.
(72) (a) Fang, S.; Lee, M.-S.; Hrovat, D. A.; Borden, W. T. *J. Am. Chem. Soc.* **1995**, *117*, 6727−6731. (b) Wenthold, P. G.; Kim, J. B.; Lineberger, W. C. *J. Am. Chem. Soc.* **1997**, *119*, 1354−1359. (c) Zhang, G.; Li, S.; Jiang, Y. *Tetrahedron* **2003**, *59*, 3499−3504. (d) Mañeru, D. R.; Pal, A. K.; Moreira, I.; de, P. R.; Datta, S. N.; Illas, F. *J. Chem. Theory Comput.* **2014**, *10*, 335−345. (e) Pal, A. K.; Mañeru, D. R.; Latif, I. A.; Moreira, I.; de, P. R.; Illas, F.; Datta, S. N. *Theor. Chem. Acc.* **2014**, *133*, 1472.
(73) Song, M.; Song, X.; Bu, Y. *Organometallics* **2017**, *36*, 1505-1514.
(74) Yang, Y.; Liu, C.; Xu, X.; Meng, Z.; Tong, W.; Ma, Z.; Zhou, C.; Sun, Y.; Sheng, Z. *Polym. Chem.* **2018**, *9*, 5499-5503.
(75) Wernsdorfer, W. *Int. J. Nanotechnology* **2010**, *7*, 497-522.
(76) (a) Moore, G. E. *Electronics* **1965**, *38*, 114–117. (b) Moore, G. E. *IEDM Tech. Digest* **1975**, 11–13.
(77) Waldrop, M. M. *Nature* **2016**, *530*, 144-147.
(78) Baibich, M. N.; Broto, J. M.; Fert, A.; Dau, F. N. V.; Petroff, F.; Etienne, P.; Creuzet, G.; Friederich, A.; Chazelas, J. *Phys. Rev. Lett.***1988**, *61*, 2472–2475.
(79) (a) Mosca, D.H.; Petroff, F.; Fert, A.; Schroeder, P. A.; Pratt, W.P.; Laloee, R. *J. Mag. Mag. Mat.* **1991**, *94*, L1-L5. (b) Schad, R.; Potter, C.D.; Belien, P.; Verbanck, G.; Moshchalkov, V.V.; Bruynseraede, Y. *Appl. Phys. Lett.* **1994**, *64*, 3500.
(80) (a) Žutic, I.; Das Sarma, S. *Rev. Mod. Phys.* **2004**, *76*, 323–410. (b) Wolf, S. A.; Awschalom, D. D.; Buhrman, R. A.; Daughton, J. M.; von Molnár, S.; Roukes, M. L.; Chtchelkanova, A. Y.; Treger, D. M.; *Science* **2001**, *294*, 1488–1495.
(81) Miyzaki, T.; Tezuka, N. *J. Mag. Mag. Mat.* **1995**, *139*, L231.
(82) Moodera, J.S.; Kinder, L.R.; Wong. M.; Meservey, R. *Phys. Rev. Lett.* **1995**, *74*, 3273.
(83) (a) Zhu, H. J.; Ramsteiner, M.; Kostial, H.; Wassermeier, M.; Schönherr, H.-P.; Ploog, K. H. *Phys. Rev. Lett.* **2001**, *87*, 016601. (b) Malajovich, I.; Kikkawa, J. M.; Awschalom, D. D.; Berry, J. J.; Samarth, N. *Phys. Rev. Lett.* **2000**, *84*, 1015. (c) Labella, V. P.; Bullock, D. W.; Z. Ding, Z.; Emery, C.; Venkatesan, A.; Oliver, W. F.; Salamo, G. J.; Thibado, P. M.; M. Mortazavi, M. *Science*, **2001**, *292*, 1518-1521.
(84) (a) Schmidt, G. *J. Phys. D. Appl. Phys.* **2005**, *38*, R107-R122. (b) Dediu, V.; Murgia, M.; Matacotta, F. C.; Taliani, C.; Barbanera, S. *Solid State Commun.* **2002**, *122*, 181-184. (c) Xiong, Z.H.; Wu, D.; Vardeny, Z.V.; Shi, J. *Nature* **2004**, *427*, 821-

824. (d) Lou, X.; Adelmann, C.; Crooker, S. A.; Garlid, E. S.; Zhang, J.; Reddy, K.S.M.; Flexner, S. D.; Palmstrom, C. J.; Crowell, P. A. Nat. Phys. **2007,** *3*, 197-202.
(85) (a) Datta, S.; Das. B. *Appl. Phys. Lett.* **1990**, *56*, 665-667. (b) Ohno, Y.; Young, D. K.; Beschoten, B.; Matsukura, F.; Ohno, H.; Awschalom, D.D. *Nature*. **1999**, *402*, 790-792. (c) Appelbaum, I.; Huang, B.; Monsma, D. J. *Nature* **2007**, *447*, 295-298.
(86) (a) Chappert, C.; Fert, A.; Nguyen Van Dau, F. *Nat. Mater.* **2007**, *6*, 813–823. (b) Parkin, S. S. P., Hayashi, M., Thomas, L. *Science* **2008**, *320*, 190–194.
(87) Tsukagoshi, K.; Alphenaar, B.; Ago, H. *Nature* **1999**, *401*, 572-574.
(88) Camarero, J.; Coronado, E. *J. Mater. Chem.,* **2009**, *19*, 1678.
(89) (a) Bogani, L.; Wernsdorfer, W. *Nat. Mater.* **2008,** *7*, 179-186. (b) Atodiresei, N.; Brede, J.; Lazic, P.; Caciuc, V.; Hoffmann, G.; Wiesendanger, R.; Blugel, S. *Phys. Rev. Lett.* **2010**, *105*, 066601. (c) Wan, H.; Zhou, B.; Chen, X.; Sun, C. Q.; Zhou, G. *J. Phys. Chem. C* **2012**, *116*, 2570-2574. (d) Thomas, L.; Lionti, F.; Ballou, R.; Gatteschi, D.; Sessoli, R.; Barbara, B. *Nature* **1996**, *383*, 145-147. (e) Cremades, E.; Pemmaraju, C. D.; Sanvito, S.; Ruiz, E. *Nanoscale* **2013**, *5*, 4751-4757.
(90) (a) Wu, Q. H.; Zhao, P.; Chen, G. *Org. Electron.* **2015**, *25*, 308-316. (b) Li, X.B.; Gao, H.; Wan, H.Q.; Li, H.L.; Zhou, G.H. *Chem. Phys. Lett.* **2014**, *610*, 298-302.
(91) (a) Chen, W.; Xu, N.; Wang, B. L.; Bian, B. A. *Phys. Lett. A.* **2014**, *378*, 2020-2023. (b) Zu, F.X.; Gao, G.Y.; Fu, H.H.; Xiong, L.; Zhu, S.C.; Li, P.; Yao, K.L. *Appl. Phys. Lett.* **2015**, *107*, 252403. (c) Zhu, L.; Yao, K. L.; Liu, Z. L. *Appl. Phys. Lett.***2010**, *96*, 082115. (d) Li, E. Y.; Marzari, N. *ACS Nano.* **2011**, *5*, 9726-9736. (e) Maslyuk, V. V.; Bagrets, A.; Meded, V.; Arnold, A.; Evers, F.; Brandbyge, M.; Bredow, T.; Mertig, I. *Phys. Rev. Lett.* **2006**, *97*, 097201. (f) Mannini, M.; Pineider, F.; Sainctavit, P.; Danieli, C.; Otero, E.; Sciancalepore, C.; Talarico, A. M.; Arrio, M.; Cornia, A.; Gatteschi, D.; Sessoli, R. *Nature Mater.* **2009**, *8*, 194-197. (g) Xiang, H.;Yang, J.; Hou, J. G.; Zhu, Q. *J. Am. Chem. Soc.* **2006**, *128*, 2310-2314. (h) Shen, X.; Yi, Z.; Shen, Z.; Zhao, X.; Wu, J.; Hou, S.; Sanvito, S. *Nanotechnology.* **2009**, *20*, 385401. (i) Zhou, L.; Yang, S.W.; Ng, M. F.; Sullivan, M. B.; Tan, V. B. C.; Shen, L. *J. Am. Chem.Soc.* **2008**, *130*, 4023-4027. (j) Pemmaraju, C. D.; Rungger, I.; Sanvito, S. *Phys. Rev. B.* **2009**, *80*, 104422. (k) Shukla, S. K.; Sanvito, S. *Phys. Rev. B.* **2009**, *80*, 184429.
(92) Huang, J.; Wang, W. Y.; Yang, S. F.; Su, H. B.; Li, Q. X.; Yang, J. L. *Chem. Phys. Lett.* **2012**, *539-540*, 102-106.
(93) Deng, X. Q.; Zhang, Z. H.; Tang, G. P.; Fan, Z. Q.; Sun, L.; Li, C. X. *Org. Electron.* **2016**, *35*, 1-5.
(94) Shen, X.; Sun, L. L.; Yi, Z. L.; Benassi, E.; Zhang, R. X.; Shen, Z. Y.; Sanvito, S.; Hou, S. M.*Phys. Chem. Chem. Phys*., **2010**, *12*, 10805-10811.
(95) Zhao, P.; Chen, G. *J.Chem. Phys.* **2018**, *149*, 134305.
(96) (a) Shojaei, F.; Hahn, J. R. *Chem. Mater.* **2014**, *26*, 2967-2974. (b) Huang, X.; Sheng, P.; Tu, Z.; Zhang, F.; Wang, J.; Geng, H.; Zou, Y.; Di, C.; Yi, Y.; Sun, Y.; Xu, W.; Zhu, D. *Nature. Commun.* **2015**, *6*, 7408. (c) Sarkar, S.; Pramanik, A.; Sarkar, P. *Chem. Phys.* **2016**, *478*, 173-177. (d) Chakravarty, C.; Mandal, B.; Sarka, P. *J. Phys. Chem. C* **2016**, *120*, 28307-28319. (e) Clough, C. A. J.; Skelton, J. M.; Dowbes, C. A.;

Rosa, A. A.; Yoo, J. W.; Walsh, A.; Melot, B. C.;Marinescu, S. C. *J. Am. Chem. Soc.* **2017**, *139*, 10863-10867.
(97) Pearson, C.; Moore, A. J.; Gibson, J. E.; Bryce, M. R.; Petty, M. C. *Thin Solid Films*. **1994**, *244*, 932-935.
(98) Huong, V. T. T.; Tai, T. B.; Jiang, J. –C.; Nguyen,M. T.; *Phys. Chem. Chem. Phys.* **2017**, *19*, 32536-32543.
(99) Peng, J.; Zhou, W. -X.; Chen, K. -Q. *Phys. Lett*. A. **2014**, *378*, 3126-3130.
(100) Wu, Q. H.; Zhao, P.; Su, Y.; Li S. J.; Gou, J. H. *RSC Adv*. **2015**, *5*, 52938-52944.
(101) Wu, Q. H.; Zhao, P.; Chen, G. *Org. Electron.* **2015**, *25*, 308-316.
(102) (a) Heersche, H. B.; Groot, Z. D.; Folk, J. A.; van der Zant, H. S. J.; Romeike, C.; Wegewijs, M. R.; Zobbi, L.; Barreca, D.; Tondello, E.; Cornia, A. *Phys. Rev. Lett.***2006**, *96*, 206801. (b) Voss, S.; Zander, O.; Fonin, M.; Rüdiger, U.; Burgert, M.; Groth, U. *Phys. Rev. B* **2008**, *78*, 155403. (c) Ni, C.; Shah, S.; Hendrickson, D.; Bandaru, P. R. *Appl. Phys. Lett.* **2006**, *89*, 212104. (d) Jo, M.-H.; Grose, J. E.; Baheti, K.; Deshmukh, M. M.; Sokol, J. J.; Rumberger, E. M.; Hendrickson, D. N.; Long, J. R.; Park, H.; Ralph, D. C. *Nano Lett*. **2006**, *6*, 2014-2020. (e) Kim, G.-H.; Kim, T.-S. *Phys. Rev. Lett*. **2004**, *92*, 137203. (f) Henderson, J. J.; Ramsey, C. M.; del Barco, E.; Mishra, A.; Christou, G. *J. Appl. Phys*. **2007**, *101*, 09E102. (g) Romeike, C.; Wegewijs, M. R.; Hofstetter, W.; Schoeller, H. *Phys. Rev. Lett*. **2006**, 96, 196601. (h) Romeike, C.; Wegewijs, M. R.; Schoeller, H. *Phys. Rev. Lett*. **2006**, *96*, 196805. (i) Misiorny, M.; Barnaś, J. *Europhys.Lett*. **2007**, *78*, 27003.
(103) (a) Christou, G.; Gatteschi, D.; Hendrickson, D. N.; Sessoli, R. *Mater. Res. Soc. Bull.* **2000**, *25*, 66–71. (b) Gatteschi, D.; Sessoli, R.; Villain, J. *Molecular Nanomagnets* (Oxford Univ. Press, New York, **2007**). (c) Naitabdi, A.; Bucher, J.-P.; Gerbier, P.; Rabu, P.; Drillon, M. *Adv. Mater*.**2005**, *17*,1612–1616. (d) Fleury, B.; Catala,L.; Huc,V.; David,C.; Zhong,W.Z.; Jegou,P.;Baraton,L.; Palacin,S.; Albouy, P. –A.; Mallah, T. *Chem. Comm.* **2005**, 2020–2022. (e) Coronado, E.; Forment-Aliaga, A.; Gaita-Ariño, A.; Giménez-Saiz, C.; Romero, F. M.; Wernsdorfer ,W. *Angew. Chem. Int. Ed.* **2004**, *43***,** 6152–6156.
(104) (a) Misiorny, M.; Barnaś, J. *Phys. Rev. B* **2007**, *75*, 134425. (b) Misiorny, M.; Barnaś, J. *Phys. Status Solidi B* **2009**, *246*, 695.
(105) (a) Timm, C.; Elste, F. *Phys. Rev. B* **2006**, *73*, 235304. (b) Misiorny, M.; Barnaś, J. *Phys. Rev. B* **2008**, *77*, 172414.
(106) (a) Urdampilleta, M.; Klyatskaya, S.; Cleuziou, J.P.; Ruben, M.; Wernsdorfer, W. *Nat. Mater.* **2011**, *10*, 502–506. (b) Urdampilleta, M.; Nguyen, N.V.; Cleuziou, J.P.; Klyatskaya, S.; Ruben, M.; Wernsdorfer, W. *Int. J. Mol. Sci.* **2011**, *12*, 6656–6667.
(107) Vincent, R.; Klyatskaya, S.; Ruben, M.; Wernsdorfer, W.; Balestro, F. *Nature* **2012**, *488*, 357–360.
(108) Thiele, S.; Balestro, F.; Ballou, R.; Klyatskaya, S.; Ruben, M.; Wernsdorfer, W. *Science* **2014**, *344*, 1135–1138.
(109) (a) Misiorny, M.; Barnaś, J. *Phys. Rev. B* **2007**, *76*, 054448. (b) Misiorny, M.; Weymann, I.; Barnaś, J. *Phys. Rev. B* **2011**, *84*, 035445. (c) Misiorny, M.; Barnaś, J.

Phys. Rev. B **2009**, *79*, 224420. (d) Misiorny, M.; Weymann, I.; Barnaś, J. *Phys. Rev. Lett.* **2011**, *106*, 126602.
(110) Misiorny, M.; Barnaś, J. *Europhys. Lett.* **2010**, *89*, 18003.
(111) (a) Larade, B.; Taylor, J.; Mehrez, H.; Guo, H. *Phys. Rev. B* **2001**, *64*, 075420. (b) Sotthewes, K.; Geskin, V.; Heimbuch, R.; Kumar, A.; Zandvliet, H. J. W. *APL. Mat.* **2014**, *2*, 010701. (c) Tsukagoshi, K.; Alphenaar, B. W.; Ago, H. *Nature* **1999**, *401*, 572-574. (d) Ouyang, M.; Awschalom, D. D. *Science* **2003**, *301*, 1074-1078. (e) Pati, R.; Senapati, L.; Ajayan, P. M.; Nayak, S. K. *Phys. Rev. B* **2003**, *68*,100407.
(112) (a) Datta, S. Electronic Transport in Mesoscopic Systems, (Cambridge University Press, New York, 1997). (b) Chun, D.; Cheng, Y.; Wudl, F. *Angew. Chem. Int. Ed.* **2008**, *47*, 8380 –8385. (c) Mondal, R.; Shah, B. K.; Neckers, D. C. *J. Am. Chem. Soc.* **2006**, *128*, 9612-9613. (d) Tonshoff, C.; Bettinger, H. F. *Angew. Chem. Int. Ed.* **2010**, *49*, 4125-4128. (e) Anthony, J. *Angew. Chem. Int. Ed.* **2008**, *47*, 452 – 483.
(113) (a) Meng, H.; Bendikov, M.; Mitchell, G.; Helgeson,R.; Wuld, F.; Bao, Z.; Siegrist, T.; Kloc, C.; Chen, C. –H. *Adv. Mater.* **2003**, *15*, 1090-1093. (b) Katz, H. E. *Chem. Mat.* **2004**, *16*, 4748-4756.
(114) (a) Bendikov, M.; Duong, H. M.; Starkey, K.; Houk, K. N.; Carter, E. A. Wudl , F. *J. Am. Chem. Soc.* **2004**, *126*, 7416-7417. (b) Hachmann, J.; Dorando, J. J.; Aviles, M.; Chan, G. K. *J. Chem. Phys.* **2007**, *127*, 134309. (c) Hajgato, B.; Szieberth, D.; Geerlings, P.; Proft, F. D.; Deleuze, M.S. *J. Chem. Phys.* **2009**, *131*, 224321. (d) Qu, Z.; Zhang, D.; Liu, C.; Jiang, Y. *J. Phys. Chem. A* **2009**, *113*, 7909-7914. (e) Szulczewski, G.; Sanvito, S.; Coey, J. M. D. *Nat. Mater* **2009**, *8*, 693-695.
(115) (a) Sanvito, S. *Chem. Soc. Rev.* **2011**, *40*, 3336-3355. (b) Mas-Torrent, M.; Crivillers, N.; Mugnaini, V.; Ratera, I.; Rovira, C.; Veciana, J. *J. Mater.Chem.* **2009**, *19*, 1691-1695. (c) Herrmann, C.; Solomon, G. C.; Ratner, M. A. *J. Am. Chem. Soc.* **2010**, *132*, 3682-3684. (d) Lee, J.; Lee, E.; Kim, S.; Bang, G. S.; Shultz, D. A.; Schmidt, R. D.; Forbes, M. D. E.; Lee, H. *Angew. Chem., Int. Ed.* **2011**, *50*, 4414-4418. (e) Yonekuta, Y.; Susuki, K.; Oyaizu, K.; Honda, K. *J. Am. Chem. Soc.* **2007**, *129*, 14128-14129. (f) McGuire, J.; Miras, Haralampos N.; Richards, E.; Sproules, S. *Chem. Sci.* **2019**, *10*, 1483-1491.
(116) (a) Zhao, X. L.; Ando, Y.; Liu, Y.; Jinno, M.; Suzuki, T. *Phys. Rev. Lett.*, **2003**, *90*, 187401. (b) Muramatsu, H.; Hayashi, T.; Kim, Y. A.; Shimamoto, D.; Endo, M.; Terrones, M.; Dresselhaus, M. S. *Nano Lett.*, **2008**, *8*, 237. (c) Kitaura, R.; Nakanishi, R.; Saito, T.; Yoshikawa, H.; Awaga, K.; Shinohara, H. *Angew. Chem., Int. Ed.*, **2009**, *48*, 8298.
(117) Prasongkit, J.; Grigoriev, A.; Wendin, G.; Ahuja, R. *Phys. Rev. B*: *Condens. Matter Mater. Phys.*, **2010**, *81*, 115404.
(118) Kim, W.Y.; Kim, K.S. *Nature Nanotech.* **2008**, *3*, 408-412.
(119) (a) Zhang, D.; Long, M.Q.; Zhang, X.J.; Xu, H. *RSC Adv.* **2015**, *5*, 96455-96463. (b) Deng, X.Q.; Zhang, Z.H.; Fang, Z.Q.; Tang, G.P. ; Sun, L.; Li, C.X. *Org. Electron.* **2016**, *32*, 41-46.(c) Zhao, P.; Wu, Q.H.; Liu, H.Y.; Liu, D.S.; Chen, G. *J. Mater. Chem. C.* **2014**, *2*, 6648-6654.

(120) (a) Zeng, M.G.; Shen, L.; Zhang, C.; Feng, Y.P. *Appl. Phys. Lett.* **2011**, *98*, 053101. (b) Deng, X.Q.; Zhang, Z.H.; Tang, G.P.; Fang, Z.Q.; Yang, C.H. *Carbon.* **2014**, *66*, 646-653.
(121) Lee, M.; Williams, J. R.; Zhang, S.; Frisbie, D.; Goldhaber-Gordon, D. *Phys. Rev. Lett.* **2011**, *107*, 256601.
(122) (a) Ratera, I.; Veciana, J. *Chem. Soc. Rev.***2012**, *41*, 303-349. (b) Lee, E.C.; Choi, Y.C.; Kim, W.Y.; Singh, N.J.; Lee, S.; Shim, J.H.; Kim, K.S. *Chem. Eur. J.* **2010**, *16*, 12141-12146. (c) Peng, Q.; Obolda, A.; Zhang, M.; Li, F. *Angew. Chem. Int. Ed.***2015**, *54*, 7091-7095. (d) Sugawara, T.; Komatsu, H.; Suzuki, K. *Chem. Soc. Rev.* **2011**, *40*, 3105-3118. (e) Nakahara, K.; Iwasa, S.; Satoh, M.; Morioka, Y.; Iriyama, J.; Suguro, M.; Hasegawa, E. *Chem. Phys. Lett.***2002**, *359*, 351-354. (f) Xu, L.; Yang, F.; Su, C.; Ji, L.; Zhang, C. *Electrochim. Acta* **2014**, *130*, 148-155. (g) Dardenne, N.; Blase, X.; Hautier, G.; Charlier, J. –C.; Rignanese, G. M. *J. Phys. Chem. C* **2015**, *119*, 23373-23378.
(123) Sen, S.; Chakrabarti, S. *J. Am. Chem. Soc.* **2010**, *132*, 15334–15339.
(124) Chen, W.; Mao, W.; Bian, B.; Xu, N.; Chen, R.; Li, X-a.; Wang, L. *Comput. Theor. Chem.* **2016**, *1091*, 85-91.
(125) (a) Tour, J. M.; Kozaki, M.; Seminario, J. M. *J. Am. Chem. Soc.*, **1998**, *120*, 8486. (b) Modelli, A.; Venuti, M.; Scagnolari, F.; Contento, M.; Jones, D. *J. Phys. Chem. A*, **2001**, *105*, 219. (c) Distefano, G.; Jones, D.; Guerra, M.; Favaretto, L.; Modelli, L.; Mengoli, G. *J. Phys. Chem*., **1991**, *95*, 9746. (d) Colle, M. D.; Cova, C.; Distefano, G.; Jones, D.; Modelli, A.; Comisso, N. *J. Phys. Chem. A* **1999**, *103*, 2828. (e) Bredas, J. L.; The´mans, B.; Fripiat, J. G.; Andre´, J. M.; Chance, R. R. *Phys. Rev. B: Condens. Matter Mater. Phys.* **1984**, *29*, 6761.
(126) Deng, Y.-X.; Chen, S.-Z.; Zeng, Y.; Zhou, W.-X.; Chen, K.-Q.*Org. Electron.* **2017**, *50*, 184-190.
(127) Tagami, K.; Tsukada, M. *J. Phys. Chem. B* **2004**, *108*, 6441–6444.
(128) Zhang, J.; Xu, B.; Qin. Z. *Phys. Lett. A* **2018**, *382*, 1226-1230.
(129) Prins, F.; Barreiro, A.; Ruitenberg, J. W.; Seldenthuis, J. S.; Aliaga-Alcalde, N.; Vandersypen, L.M.K.; van der Zant, H. S. J. *Nano Lett.* **2011**, *11*, 4607–4611.
(130) Caliskan, S.; Laref, A. *Sci. Rep.* **2015**, *4*, 7363.
(131) Caliskan, S.*Physica E: Low-dimensional Systems and Nanostructures.***2018**, *99*, 43–50.
(132) Sevov, C.S.; Hickey, D.P.; Cook, M.E.; Robinson, S.G.; Barnett, S.; Minteer, S.D.; Sigman, M.S.; Sanford, M.S. *J. Am. Chem. Soc.* **2017**, *139*, 2924-2927.

CHAPTER 2

Theoretical background

The theoretical background for the estimation of the magnetic exchange coupling constant (*J*) is described in this chapter. The theoretical background for the determination of the transport property of molecules is also discussed here.

2.1 Introduction

The quantification of magnetic nature of molecular systems renders a wide area for theoretical exertion. The magnetic property of a molecule or radical can be estimated by the magnetic exchange coupling constant (*J*). In diradical species *J* is quantified by the difference in energy between triplet and the singlet states.

For many electron systems, the Hartree-Fock (HF) method provides a solution of Schrödinger equation based on variational principle. The main limitation of HF method is that the electrons are moving independently, and they have no correlation. After that different post-HF methods such as coupled cluster methods or configuration interaction methods are introduced. Though, an adequate computation of *J* can be achieved through Post-HF methods, they are not so popular as they are immensely resource intensive.[1] In recent years density functional theory-based approach is extensively used to compute the magnetic exchange coupling constant.

2.2 Density Functional Theory

DFT is the powerful methodology that overcomes the inadequacy of HF and computational cost of post-HF methods by using the electronic density as the basic variable instead of the multi-electronic wave function. In DFT formalism the electronic energy *E* of the systems can be expressed as the functional of electron density $E(\rho)$. Density functional theory-based methodology is easy to use compared to the *ab initio* methodology due to the low time consumption and flexibility. Besides, for a large system the complexity in the wave function is increased, however the electron density sustains the same number of variables which is independent on the size of the system. In late 1920s,[2] the concept of density functional was emerged for the first time from the work of Fermi and Thomas.

The energy functional have three terms i.e., the kinetic energy (KE), potential energy from the external field and the electron-electron interaction energy and can be written as;

$$E[\rho] = T[\rho] + V_{ext}[\rho] + V_{ee}[\rho]. \tag{2.1}$$

The external potential energy is expressed as

$$V_{ext}[\rho] = \int \hat{V}_{ext}\, \rho(r) dr. \tag{2.2}$$

Though KE has a common form for every system, the major problem in earlier DFT formalism is the difficulties in representing the KE of a system. In Kohn-Sham approach, the KE functional have split into two different parts to overcome this problem. The first part represents the kinetic energy of non-interacting particles and

this part can be calculated exactly and another part that comes from the introduction of a small correction term due to the electron-electron interactions.

Here we introduce the quantity $E_{xc}[\rho]$ which is called the exchange-correlation energy and represented as

$$E_{xc}[\rho] = (T[\rho] - T_s[\rho]) + (V_{ee}[\rho] - V_H[\rho]). \quad (2.3)$$

i.e., E_{xc} is the sum of the error made by using a non-interacting kinetic energy and by treating the electron-electron interaction classically.

Therefore, the energy functional can be written as

$$E[\rho] = T_s[\rho] + V_{ext}[\rho] + V_H[\rho] + E_{xc}[\rho]. \quad (2.4)$$

The exchange correlation energy (E_{xc}) is often decomposed as

$$E_{xc}[\rho] = E_x[\rho] + E_c[\rho]. \quad (2.5)$$

Where E_x is the exchange energy due to the interactions between the electrons with same spin and E_c is the correlation energy due to the interactions between the electrons having opposite spins. The respective functional are the exchange functional and the correlation functional.

In Kohn-Sham approach the system is composed of *n* non-interacting electrons described by a single determinantal wavefunction in *n* "orbitals"Ψ_i. The kinetic energy is represented as,

$$T_s[\rho] = -\frac{1}{2}\sum_i^n \langle \Psi_i | \nabla^2 | \Psi_i \rangle. \quad (2.6)$$

The suffix represents that this is the kinetic energy of a system with non-interacting electrons and not the true kinetic energy.

The ground state electron density $\rho(r)$ can be written as

$$\rho(r) = \sum_i^n |\Psi_i|^2. \quad (2.7)$$

The electron–electron Coulomb interaction which is known as the Hartree energy can be represented in terms of density as

$$V_H[\rho] = \frac{1}{2}\int \frac{\rho(r_1)\rho(r_2)}{|r_1 - r_2|} dr_1 dr_2 \,. \tag{2.8}$$

The Kohn-Sham equation needs to solve in order to obtain the Kohn-Sham orbital. For which application of variational principle to the electronic energy $E(\rho)$ is needed.

$$\hat{h}_i \Psi_i(r_i) = \varepsilon_i \Psi_i(r_i) \tag{2.9}$$

Here $\hat{h}_i$ and ε_i signify the Kohn-Sham Hamiltonian and the respective orbital energy. The Kohn-Sham Hamiltonian has the form

$$\hat{h}_i = \left[-\frac{1}{2}\nabla^2 + v_{ext}(r) + \int \frac{\rho(r')}{|r - r'|} dr' + v_{xc}(r)\right] \tag{2.10}$$

Where V_{xc} is a local potential which is the functional derivative of exchange correlation energy with respect to the density and is given by

$$v_{xc}(r) = \frac{\delta E_{xc}[\rho]}{\delta \rho} \,. \tag{2.11}$$

After obtaining the initial set of Kohn-Sham orbitals, they are used to get the electron density from eq. (2.7). The process is repeated again and again until the E_{xc} and the density meet the certain convergence criteria.

2.3 Spin Hamiltonian and magnetic exchange coupling constant (*J*)

The magnetic exchange interaction between two magnetic centers 1and 2 is generally expressed by the phenomenological Heisenberg spin Hamiltonian

$$\hat{H} = -2J\, \hat{S}_1 . \hat{S}_2 \tag{2.12}$$

Where $\hat{S}_1$and $\hat{S}_2$ are the respective spin angular momentum operators and J is the effective exchange coupling constant between two magnetic sites. For a diradical system, a negative J value indicates the antiferromagnetic interaction with anti-parallel orientation of the spins (S = 0) in the ground state and the positive J value indicates the ferromagnetic interaction with parallel spins (S = 1) in the ground state.

The magnetic exchange coupling constant for a diradical with one unpaired electron on each site can be represented as

$$E_{HS} - E_{LS} = -2J. \tag{2.13}$$

Though the single determinantal wave function properly represent the high spin state of a molecule, it cannot adequately signify the singlet state of a molecule in unrestricted formalism which causes spin contamination in such calculations. Multiconfigurational approach can describe the pure spin states in proper way. Many research groups have done the theoretical study using multiconfigurational techniques. However, these methods are computationally very expensive and are difficult to apply in large systems. The broken symmetry method is the way out of this difficulty.

2.4 Broken symmetry approach

Till now broken symmetry (BS) approach is the best technique proposed by Noodleman and coworkers to calculate the *S*-*T* energy gap as well as the magnetic exchange coupling constant (*J*).[3] Though the arguments are given in terms of wavefunction theory, the formalism is mostly applied in DFT framework. To determine the magnetic exchange coupling constant, the triplet state ($<S^2> = 2$, in case of diradical) from unrestricted formalism and a broken-symmetry (BS) solution is required. According to Noodleman, a state of lowered space symmetry and mixed spin symmetry is obtained when two singly occupied orbital of spin bearing monomers interact by overlapping in self-consistent field procedure. This state is known as the broken symmetry state.

Following are the three spin-projected equations that differ in their applicability depending on the extent of overlap between the magnetic orbitals. When the interaction between magnetic orbitals are sufficiently small, the expression for evaluating magnetic exchange coupling constant is given by Giensberg, Noodleman and Davidson.[3,4]

$$J = -\frac{E_{HS} - E_{BS}}{S^2_{max}} \tag{2.14}$$

where E_{HS} and E_{BS} represents the energies of the high-spin (HS) and BS states respectively.

On the other hand, Bencini et al.[5] and Ruitz et al.[6] have proposed an expression given in eq. 2.15 to estimate *J* which is applicable for large interaction with large overlap integral that usually occurs for binuclear transition metal complexes.

$$J = -\frac{E_{HS} - E_{BS}}{S_{max}(S_{max}+1)} \tag{2.15}$$

However, the spin projected method given by Yamaguchi[7] to evaluate the magnetic exchange coupling constant is given in eq. 2.16 that are applicable for whole range of coupling strengths.

$$J = -\frac{E_{HS} - E_{BS}}{\langle S^2\rangle_{HS} - \langle S^2\rangle_{BS}} \tag{2.16}$$

In my thesis work, I have used the eq. 2.16 given by Yamaguchi to determine the magnetic exchange coupling constant (*J*) values.

2.5 Electron transport (Density functional method)

A general approach to determine whether a molecule can transport electrical current or not, is to look at their current vs. voltage (*I-V*) profile. As an unbalanced situation arises under an applied bias voltage, the transport phenomena of a system deviate from equilibrium proviso. Therefore, nonequilibrium green's function method (NEGF)[8] is used to address the inadequacy of nonequilibrium behavior of the transport property. In addition to the *I-V* plot, the transmission probabilities also give an insight about the transport property of molecular systems.

The standard Kohn-Sham one-electron Hamiltonian (within the nonlocal-pseudopotential approximation) is written as[9]

$$\hat{H} = \hat{T} + \sum_I V_I^{local}(r) + \sum_I \hat{V}_I^{KB} + V^H(r) + V^{xc}(r). \tag{2.17}$$

Where *I* is an atom index, the kinetic energy operator $\hat{T} = -\frac{1}{2}\nabla^2$, the total Hartree and XC potentials are represented by $V^H(r)$and$V^{xc}(r)$, the local and nonlocal Kleiman and Bylander (KB) parts of pseudopotential of the atom *I* are $V_I^{local}(r)$and $\hat{V}_I^{KB}$.

In Landauer approach,[10] a single molecule (or in general a nanoscopic structure) is sandwiched between to two macroscopic electrodes. The zero-temperature conductance (G) is determined by

$$G(V) = \frac{dI(V)}{dV} \tag{2.18}$$

where I is the current and V is the bias voltage. The zero-bias conductance (for low voltages) is given by

$$G = G_0 T(E_F) \tag{2.19}$$

Where G_0 is the conductance quantum, $G_0 = 2e^2/h$. T is the transmission function and often calculated for zero bias. The electronic structure and thus T may change considerably under a large applied bias. Transmission measures the tendency for an electron to tunnel over the junction. E_F is the Fermi energy of the electrodes.

Molecular transport properties through electrode-molecule-electrode junction uses the Landauer–Imry–Büttiker approximation,[10] with nonequilibrium Green's functions (NEGF)[8] and spin-unrestricted Kohn-Sham density functional theory (UKSDFT).[11]

In the coherent tunnelling regime (i.e., for short molecular bridges with large gap between the one-particle energy levels and Fermi energies of the electrodes and for low temperature) the current ($I_s(V)$) for electron spins s ∈ {α, β } relates to the transmission function $Ts(E, V)$ by the following equation[12]

$$I_s(V) = \frac{e}{h}\int_{E_F-\frac{eV}{2}}^{E_F+\frac{eV}{2}} dE T_S(E,V) \tag{2.20}$$

Here h Planck's constant, e is the unit charge, V is the symmetrically applied finite bias voltage, E is the energyand $T_S(E,V)$ is the transmission function. The number of electrons on the molecule is supposed to be constant in time. In the Landauer–Imry–Büttiker approximation,[10] zero voltage conductance ($(dI/dV)_{V=0}$) is proportional to $T(E_F)$. Therefore, it is reasonable to take integration over $E_F - \frac{eV}{2}$ to $E_F + \frac{eV}{2}$.

In the NEGF approach, T_S can be calculated from a trace over matrices ($\Gamma_{L/R,s}$) that describes the coupling of central region to the left and right electrodes, and the retarded and advanced Green's functions ($G_{C,s}^{r/a}$) of the electrode-molecule-electrode system[13] as

$$T_S(E,V) = tr\left(\Gamma_{R,s} G_{C,s}^{r} \Gamma_{L,s} G_{C,s}^{a}\right) \tag{2.21}$$

The advanced Green's function is the complex conjugate of the retarded Green's function.

For a finite cluster electrode-molecule-electrode System, $\Gamma_{X,s}$ and $G^r_{C,s}$ are calculated from the Fock and overlap matrices.[12]

$$\Gamma_{X,s} = 2\,Im\left[\left(ES_{XC} - H_{XC,s}\right)^{\dagger} g_{X,s}\left(ES_{XC} - H_{XC,s}\right)\right] \tag{2.22}$$

$$G^r_{C,s} = \left(ES_C - H_{C,s} + i\,\frac{1}{2}\Gamma_{R,s} + i\,\frac{1}{2}\Gamma_{L,s}\right)^{-1} \tag{2.23}$$

The overlap and Fock matrices are divided into central, right-electrode and left-electrode regions. $H_{XC,s}$ and S_{XC} represent the coupling block of molecule and electrode X in the Fock and overlap matrix, respectively. Whereas the molecule (i.e., "central region") subblocks of these matrices are designated by the subscript C. $g_{X,s}$ is the Green's function matrices of the isolated and infinite electrodes.

In my thesis work, I have calculated the transmission property using the ARTAIOS code developed by Herrmann et al.[12,14,15]

2.6 References

(1) Orio, M.; Pantazis, D. A.; Neese, F. *Photosynth. Res*. **2009**, *102*, 443-453.
(2) Fermi, E. *Rend. Accad. Naz. Lincei.* **1927**, *6*, 602-607. (b) Thomas, L. H. *Proc. Cambridge Philos. Soc.* **1927**, *23*, 542-548.
(3) (a) Noodleman, L. *J. Chem. Phys.* **1981**, *74*, 5737-5743. (b) Noodleman, L.; Baerends, E. J. *J. Am. Chem.* Soc. **1984**, *106*, 2316-2327. (c) Noodleman, L.; Davidson, E. R. *Chem. Phys.* **1986**, *109*, 131-143. (d) Noodleman, L.; Peng, C. Y.; Case, D. A.; Mouesca, J.-M. *Coord. Chem. Rev.* **1995**, *144*, 199-244.
(4) Ginsberg, A. P. *J. Am. Chem. Soc.* **1980**, *102*, 111-117.
(5) (a) Bencini, A.; Totti, F.; Daul, C. A.; Doclo, K.; Fantucci, P.; Barone, V. *Inorg. Chem.* **1997**, *36*, 5022-5030. (b) Bencini, A.; Gatteschi, D.; Totti, F.; Sanz, D. N.; McClevrty, J. A.;Ward, M. D. *J. Phys. Chem. A* **1998**, *102*, 10545.
(6) Ruiz, E.; Cano. J.; Alvarez, S.; Alemany, P. *J. Comput. Chem.* **1999**, *20*, 1391-1400.
(7) (a) Yamaguchi, K.; Takahara, Y.; Fueno, T.; Nasu, K. *Jpn. J. Appl. Phys.* **1987**, *26*, L1362. (b) Yamaguchi, K.; Jensen, F.; Dorigo, A.; Houk, K. N. *Chem. Phys. Lett.* **1988**, *149*, 537-542. (c) Yamaguchi, K.; Takahara, Y.; Fueno, T.; Houk, K. N. *Theo. Chim. Acta* **1988**, *73*, 337.
(8) Mahan, G. D. *Many-particle Physics*; Plenum Press: New York, **1990**.

(9) Soler, J. M.; Artacho, E.; Gale, J. D.; García, A.; Junquera, J.; Ordejón, P.; Sánchez-Portal, D. *J. Phys.: Condens. Matter*.**2002**, *14*, 2745-2779.
(10) (a) Landauer, R. *IBM J. Res. De*V.**1957**, *1*, 223–231. (b) M. Buttiker, Y. Imry, R. Landauer and S. Pinhas, *Phys. Rev. B.***1985**, *31*, 6207-6215.
(11) (a) Kohn, W.; Sham, L. J. *Phys. Re*v. **1965**, *140*, 1133–1138. (b) Hohenberg, P.; Kohn, W. *Phys. Re*v. **1964**, *136*, 864–871.
(12) Herrmann, C.; Solomon, G. C.; Ratner,M. A. *J. Am. Chem. Soc.* **2010**, *132*, 3682-3684.
(13) (a) Caroli, C.; Combescot, R.; Nozieres, P.; Saint-James, D. *J. Phys. C: Solid State Phys.* **1971**, *4*, 916–929. (b) Meir, Y.; Wingreen, N. S. *Phys. Re*v. *Lett.* **1992**, *68*, 2512–2516.
(14) Herrmann, C.; Solomon, G. C.; Subotnik, J. E.; Mujica, V.; Ratner, M. A. *J. Chem. Phys.* **2010**, *132*, 024103(1–17).
(15) Herrmann, C.; Groß, L.; Steenbock, T.; Solomon. G. C. Artaios — a transport code for postprocessing quantum chemical electronic structure calculations, **2008-2014.**

CHAPTER 3

Effect of length on the transport and magnetic properties of diradical substituted molecular wires

Abstract

In the third chapter we investigate the effect of the length of unsaturated organic molecular wires and radical substituted wires on the conduction properties of hybrid devices. At the same time, we also study the effect of length of unsaturated radical substituted organic molecular wire on the magnetic properties. It was found that the value of magnetic exchange coupling constant (*J*) depends on the distance between spin centers. In order to measure the transmission characteristics of these conjugated molecular wires, we have designed a molecular bridge structure where the phenyl based molecular system containing conjugated multiple bonds of varying length is used as a bridging fragment between two semi-infinitely widened Au_9 fcc clusters along Au(111) direction. A state of the art non-equilibrium Green's function (NEGF) method coupled with the density functional theory (DFT) based approach has been applied on this two-probe molecular bridge system to understand its electrical transport characteristics. It was observed that the molecular wires with smaller length show higher transmission. The transmission spectra of the ferromagnetically coupled diradical based molecular wires show similar behavior to those of the wires without any substitution. Hence, there is no effect of radical substitution on transport properties for ferromagnetically coupled diradical based molecular wires, whereas for antiferromagnetically coupled systems, the scenario is different.

3.1 Introduction

The term molecular wire is usually employed in molecular electronics to signify molecular scale objects which conduct electrical current with a highly preferential axis for conduction. Electrical conduction properties of molecular wires have been the focus of many studies in recent years.[1-4] Individual molecular wires are divided into two categories.[1] The first category is based on n-alkane chains [CH_3-$(CH_2)_{n-1}$] which have large (~6 eV or greater) band gap separating their highest occupied molecular orbital (HOMO) and their lowest unoccupied molecular orbital (LUMO) and are relatively insulating.[5,6] The second category is based on conjugated molecules that have a small (2-4 eV) HOMO-LUMO gap and behaves like ordinary semiconductor.[7-9] This second category of molecules are rigid and possess delocalized π-electrons. Jalili et al. investigated the effect of the length of the molecular wire on the conduction spectra of organic nanowires,[3] where the *I-V* curve for thiophenthiol based systems is non-ohmic in nature. Recently, a hybrid device is designed where gold nano particles are connected by saturated organic molecules of different lengths (alkanedithiol chains)[2] and it is observed that the conductivity increases with the length of the molecule. Electron tunneling through molecular wire has also been studied as a function of the length and chemical structure of the molecule by Magoga et al.[4] They have found that the tunneling phenomenon through a molecular wire relies on the damping factor and the contact conductance. The effect of bond length alternation on transport behavior has also been experimentally and theoretically demonstrated.[10] A study of charge and spin transport through *para*-phenylene oligomers reveals that the oligomeric *para*-phenylene bridge can act as a molecular wire for the charge recombination reaction. The rate of charge transport through such molecules decreases exponentially when the super-exchange mechanism dominates.[11] The decay constants (β) of diradical substituted conjugated molecular wires have been studied by Nishizawa et al. and they found that β is well correlated with the electronic transmission.[12]

In this work we investigate the transport property of two molecular wires of different lengths (Figure 3.1) to show the effect of the length of the wire on the electrical transport property. In this context we have designed six diradicals (Figure 3.2) by substituting methylene radical at different positions in molecular wire 1 to generate series 1 and similarly ten diradicals based on molecular wire 2 to generate the systems of series 2 (Figure 3.3) to study the effect of spin polarization on the transport property and the dependence of magnetic coupling on the distance between the radical centers. The wires we have studied here are addition polymers, and such polymers are important for application in the electronic industry.[13] The effects of entropy, the amount of molecules and their root-mean-square end-to-end distance on the physical properties of polymers are very important issues and these points were properly discussed by Lu et al.[14,15]

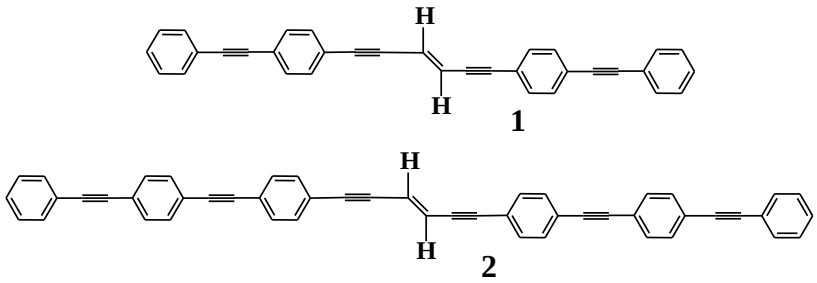

Figure 3.1 Two molecular wires (1 and 2) on which transport calculations have been carried out.

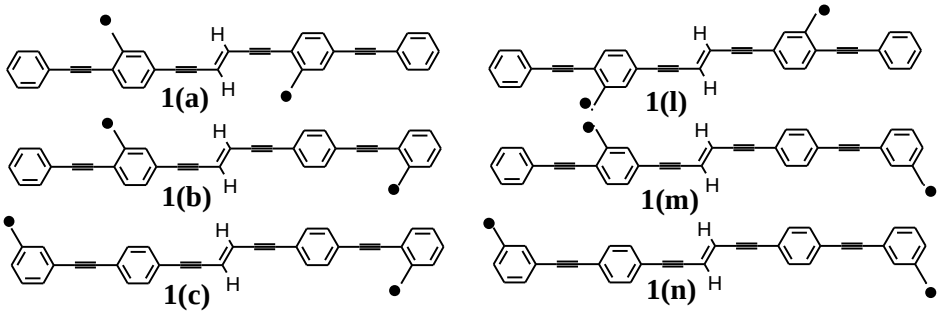

Figure 3.2 Designed diradical based molecular wire 1.

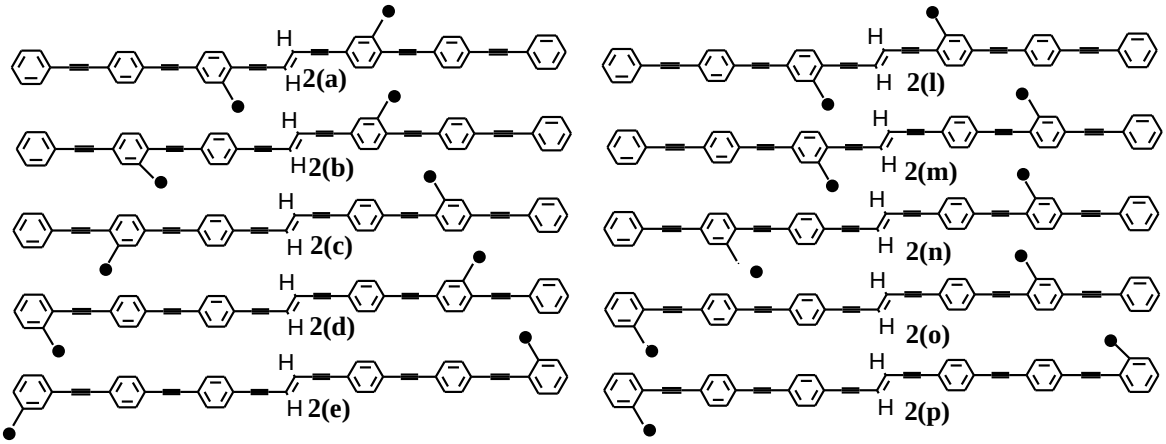

Figure 3.3 Designed diradical based molecular wire 2.

3.2 Theoretical and computational methodology

In order to determine the transport properties of the system, we need to describe the finite left electrode-molecular region-right electrode part of the infinite system. For this purpose, the gold-cluster-dithiolate-gold-cluster system has been divided into three sub systems: left gold cluster, central dithiolate, right gold cluster as

illustrated in Figure 3.4. Wires with radical substitutions are also treated in similar manner. The magnetic properties of the diradicals are calculated on the structures without –SH and gold cluster.

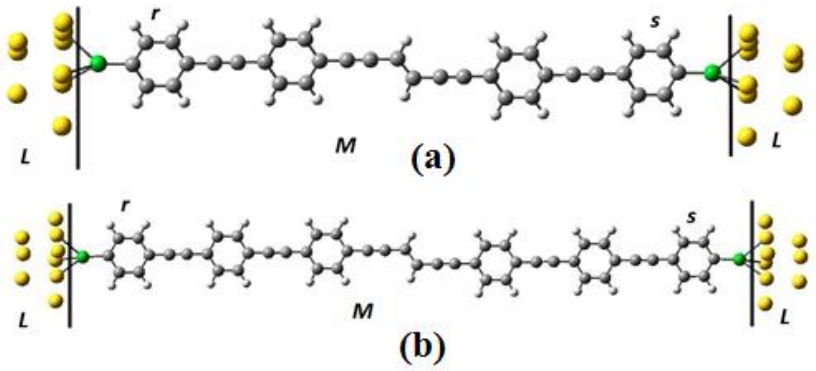

Figure 3.4 (a) and (b) are the Au-molecule-Au two probe structures designed primarily for the transport calculation. The gray, white, yellow and green colors represent carbon, hydrogen, gold and sulfur atoms respectively. *r* and *s* are two different sites of the molecular wire.

We calculated the transmission property using ARTAIOS code developed by Herrmann et al.[16,17] In this approach the dithiol molecule has been optimized in the unrestricted DFT framework with B3LYP functional and 6-31G(d,p) basis set using Gaussian09 quantum chemical package[18] and then the hydrogen atoms are stripped off and the resulting neutral dithiolate is placed between two Au_9 fcc clusters. The bond length between sulfur and Au (111) surface has been chosen to be 2.48 Å with Au-Au distances of 2.88 Å as in extended gold crystals. Fock and overlap matrices required for the transport calculation is obtained by single point calculation in Gaussian09W program package. For the transport calculation we employ B3LYP functional and the LANL2DZ basis set to avoid ghost transmission.[17] Transmission function is calculated within the Landaur approximation based on a Green's function approach using the post processing tool ARTAIOS.

Yoshizawa and coworkers have developed an orbital rule to predict the right connections between the molecule and the electrodes.[19,20] The rule is, (1) the sign of the product of the orbital coefficients at sites *r* and *s* in the HOMO should be different from the sign of the product of the orbital coefficients at sites *r* and *s* in the LUMO, (2) sites *r* and *s* should have the large amplitude of HOMO and LUMO. We computed the coefficients of HOMO and LUMO of both the wires (in Figure 3.5) that are given in Table 3.1 and a right connection has been made between the molecule and the electrodes following the Yoshizawa's rule.[19,20]

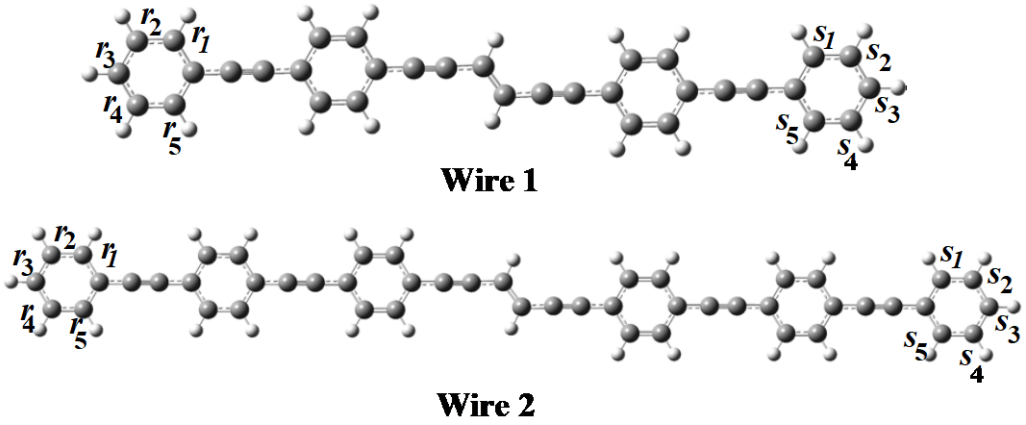

Figure 3.5 Molecular wire1 and molecular wire 2.

Table 3.1 Orbital coefficients for molecular wire 1 and wire 2 (B3LYP/6-31G(d,p)).

Site	Orbital	Molecular wire 1		Molecular wire 2	
		HOMO	LUMO	HOMO	LUMO
r_1	$2p_Z$	0.0725	0.0708	-0.0477	-0.0408
r_2	$2p_Z$	-0.0205	0.0142	0.0129	-0.0071
r_3	$2p_Z$	-0.0863	-0.0823	0.0560	0.0464
r_4	$2p_Z$	-0.0205	0.0142	0.0130	-0.0071
r_5	$2p_Z$	0.0721	0.0705	-0.0477	-0.0408
s_1	$2p_Z$	0.0721	-0.0705	-0.0485	0.0402
s_2	$2p_Z$	-0.0205	-0.0142	0.0143	0.0082
s_3	$2p_Z$	-0.0863	0.0823	0.0572	-0.0465
s_4	$2p_Z$	-0.0205	-0.0142	0.0130	0.0059
s_5	$2p_Z$	0.0725	-0.0708	-0.0502	0.0424

The interaction between two magnetic sites 1 and 2, is generally expressed by Heisenberg spin Hamiltonian

$$\hat{H} = -2J\hat{S}_1 \bullet \hat{S}_2 \qquad (1)$$

Where $\hat{S}_1$ and $\hat{S}_2$ are the respective spin angular momentum operators and J is the exchange coupling constant. The positive value of J indicates the ferromagnetic interaction while the negative value indicates the antiferromagnetic interaction between two magnetic sites. For a diradical containing one unpaired electron on each site, J can be represented as:

$$E_{(S=1)} - E_{(S=0)} = -2J. \qquad (2)$$

Many researchers[21-28] have developed different formalisms to evaluate *J* using unrestricted spin polarized broken symmetry (BS) solution, depending on the extent of magnetic interaction between two magnetic sites. The equation for evaluating *J* proposed by Ginsberg[23] Noodleman[24] and Davidson[25] is applicable when interaction between two magnetic orbitals is small. On the other hand the expression proposed by Bencini[26,27] and co workers and Ruitz et al.[28] is applicable for large interaction. Nevertheless, the well known expression given by Yamaguchi[29] is applicable for both strong and weak overlap limits. Following the well established[30,31] and widely applied method,[30-35] we use the Yamaguchi [29] formula for evaluation of *J* in this work, which is given by:

$$J = \frac{(E_{BS} - E_{HS})}{\langle S^2 \rangle_{HS} - \langle S^2 \rangle_{BS}} \tag{3}$$

Where E_{BS}, E_{HS} and $\langle S^2 \rangle_{BS}$, $\langle S^2 \rangle_{HS}$ are the energy and average spin square values for corresponding BS and high spin states.

3.3 Results and discussion

3.3.1 Transport properties of the molecular wires 1 and 2

Zero bias transmission spectra of the molecular wires are given in Figure 3.6. The horizontal axis corresponds to the electron energy *E* incident from the electrode. The Fermi energy of bulk gold is −5.53 eV.[36] but a Fermi energy of −5.0 eV is used from DFT calculations.[37] For our calculation the Fermi energy is taken to be −5.0 eV.

We can see from Figure 3.6 that the molecular wire 1 has higher transmission near the Fermi level compared to the molecular wire 2, which implies that the smaller wire is more efficient for electrical transport.[2]

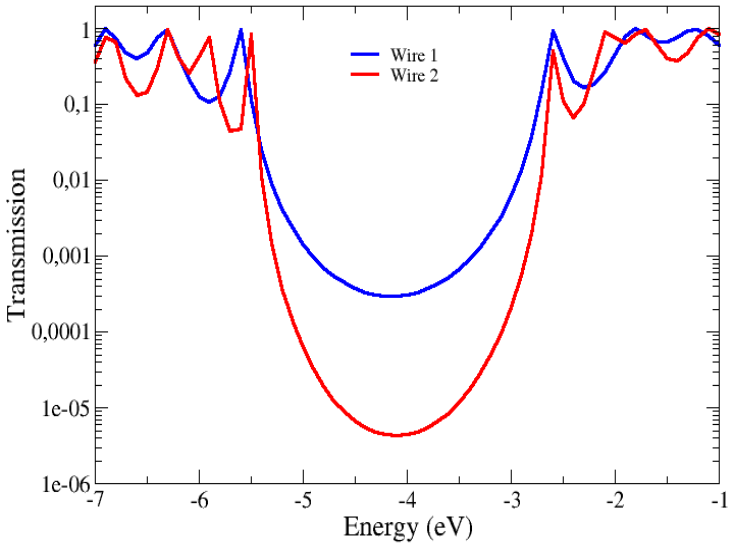

Figure 3.6 Transmission spectra of the molecular wire 1 and molecular wire 2 at zero bias.

Now from the structures of the two molecular wires one may expect that the conductivity of a system increases with increasing the number of π electrons. But organic molecules are not usually very rigid. The flexing and bending of bonds change the overlap between different orbitals. If all the benzene rings in the molecule are in the same plane, the *p* orbitals have maximum overlap that leads to lowest resistance. On the other hand the complete misalignment between the rings leads to highest resistance. The decrease in transmission with the increase in the length of the wire can also be explained by Pauling's bond order[38] which is proportional to the transmission. According to this concept with increasing phenyl ring in a molecular wire Pauling's bond order decreases exponentially and hence the transmission is also decreased.

3.3.2 Molecular orbitals of wire 1 and 2

Molecular orbitals contain all the quantum mechanical information about electronic structures of a molecule. To understand the transport property through a molecule it is necessary to study the molecular orbitals because they offer spatial conduction channels for electron transport.[39] Localization of orbitals can significantly change the transport properties. External electric field is an appropriate stimulus to tune the MOs of a molecule. It has been shown that the MOs of a molecule with and without electrode atoms at their end have similar characteristics under external electric field.[40] Following this analogy and following one of our recent works[41] we apply electric field (parallel to the molecule**)** taking the optimized geometry (without thiol groups and lead atoms at their ends) to study the change of molecular orbital under external electric field.

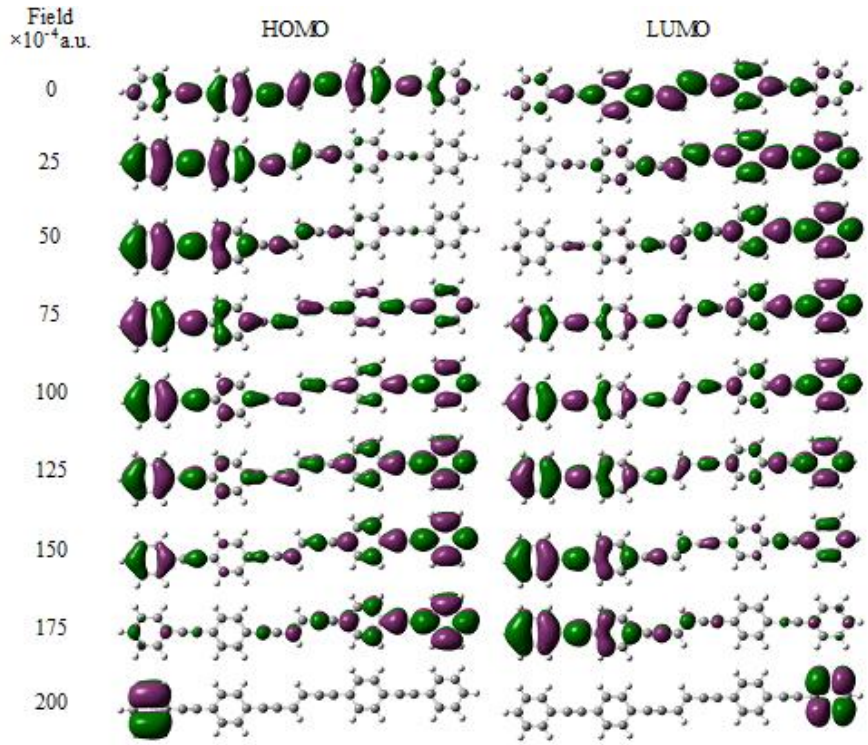

Figure 3.7 Molecular orbitals of the wire 1 under different electric fields.

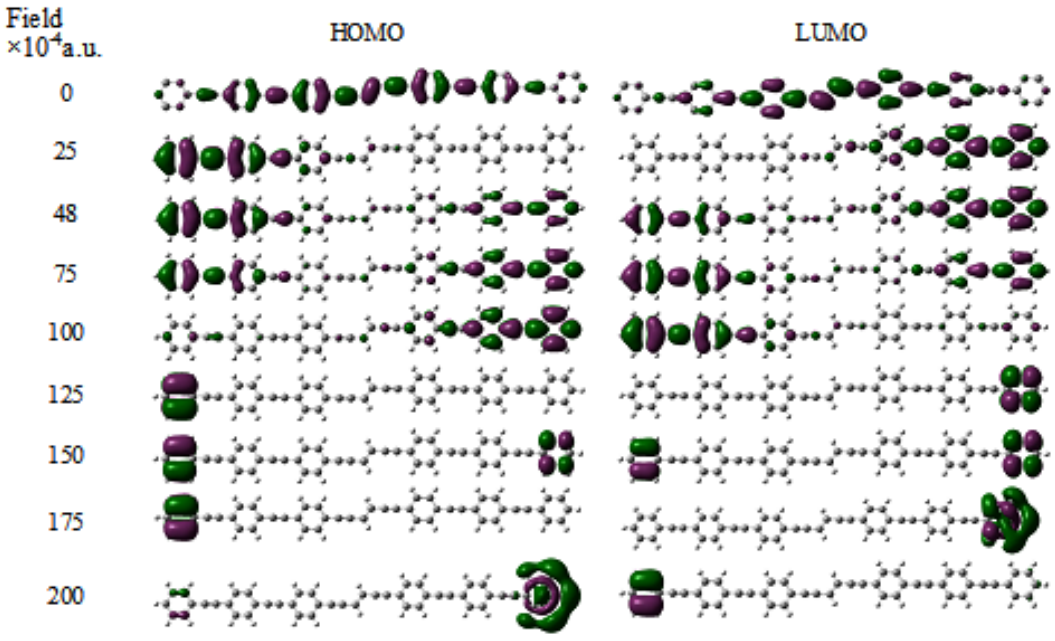

Figure 3.8 Molecular orbitals of the wire 2 under different electric fields.

We can see from Figure 3.7 and Figure 3.8 that at zero external electric field the HOMO and LUMO spreads over the entire molecule. After the application of external electric field MOs are squeezed to few atoms for both the wires. If we closely look at the MOs of wire 1 we can see that the HOMO and the LUMO always collectively spread over all the molecules (except field 0.02 a.u.). However, for wire 2, HOMO and LUMO cannot cover the whole molecule even jointly. Thus with the application of external electric field there is a large separation in the spatial distribution of HOMO-LUMO for molecular wire 2 as compared to wire 1.

3.3.3 Magnetic exchange coupling constant of the diradical substituted molecular wires

We have substituted the molecular wires with two methylene radicals such that the diradical show ferromagnetic and antiferromagnetic interaction according to the spin alternation rule[42] and we change the position of the radicals to vary the distance between the radical centers. The calculated magnetic exchange coupling constant of the diradical are presented in Table 3.2 and Table 3.3. We have also plotted the magnetic exchange coupling constant as a function of the distance between radical centers (Figure 3.9). We can see that with increasing the distance between radical centers magnetic exchange coupling constant value decreases. The distance dependent exchange coupling constant of π–conjugated molecular wires have been studied by Nishizawa et al. and found the similar results.[12]

Table 3.2 The energy (a.u.),$\langle S^2 \rangle$ and magnetic exchange coupling constant (J in cm^{-1}) values of the diradical based molecular wire 1 (B3LYP/6-31G(d,p)).

Diradicals		**Triplet**	**BS**	***J* (cm^{-1})**
1(a)	**Energy (a.u.)**	-1384.81939	-1384.81859	168.83
	$\langle S^2 \rangle$	2.12	1.08	
1(b)	**Energy (a.u.)**	-1384.81940	-1384.81926	30.42
	$\langle S^2 \rangle$	2.08	1.08	
1(c)	**Energy (a.u.)**	-1384.81786	-1384.81784	4.39
	$\langle S^2 \rangle$	2.08	1.08	
1(l)	**Energy (a.u)**	-1384.81813	-1384.81843	-67.38
	$\langle S^2 \rangle$	2.084	1.108	
1(m)	**Energy (a.u.)**	-1384.81680	-1384.81685	-10.21
	$\langle S^2 \rangle$	2.084	1.089	
1(n)	**Energy (a.u.)**	-1384.815334	-1384.81534	-1.58
	$\langle S^2 \rangle$	2.076	1.077	

Table 3.3 The energy (a.u.),$\langle S^2 \rangle$ and magnetic exchange coupling constant (J in cm^{-1}) values of the diradical based molecular wire 2 (B3LYP/6-31G(d,p)).

Diradicals		Triplet	BS	$J(cm^{-1})$
2(a)	Energy (a.u.)	-1999.26030	-1999.25949	169.36
	$\langle S^2 \rangle$	2.123	1.082	
2(b)	Energy (a.u.)	-1999.25952	-1999.25938	30.42
	$\langle S^2 \rangle$	2.10	1.09	
2(c)	Energy (a.u.)	-1999.25940	-1999.25938	4.39
	$\langle S^2 \rangle$	2.09	1.09	
2(d)	Energy (a.u.)	-1999.26018	-1999.26017	2.19
	$\langle S^2 \rangle$	2.08	1.08	
2(e)	Energy (a.u.)	-1999.25866	-1999.25866	0.15
	$\langle S^2 \rangle$	2.078	1.078	
2(l)	Energy (a.u.)	-1999.25951	-1999.26173	-500.10
	$\langle S^2 \rangle$	2.076	1.100	
2(m)	Energy (a.u.)	-1999.25984	-1999.26023	-85.55
	$\langle S^2 \rangle$	2.092	1.107	
2(n)	Energy (a.u.)	-1999.25953	-1999.25959	-14.81
	$\langle S^2 \rangle$	2.089	1.093	
2(o)	Energy (a.u.)	-1999.26034	-1999.26035	-2.57
	$\langle S^2 \rangle$	2.085	1.086	
2(p)	Energy (a.u.)	-1999.26113	-1999.26113	-0.44
	$\langle S^2 \rangle$	2.079	1.079	

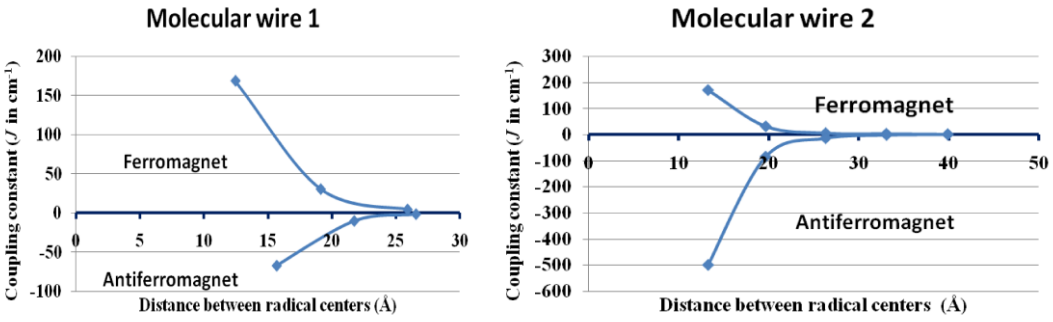

Figure 3.9 Plot of magnetic exchange coupling constants as a function of distance between the radical centers.

3.3.4 Spin density distribution between diradical centers

The spin density of DFT based approach can give us an insight about the spin polarization mechanism in the molecule for magnetic exchange. The spin density of high-spin states of the diradical are represented in Figure 3.10 and Figure 3.11. It is clear that with increasing distance between the radical centers spin polarization decreases; hence the coupling constant also decreases. Therefore, it is obvious that after certain distances between two spin centers spin polarization is no longer effective although the molecule has strong π network. Another important thing is that the magnetic exchange between two spin centers depends only on the environment in between them, not on the outsider substitution.

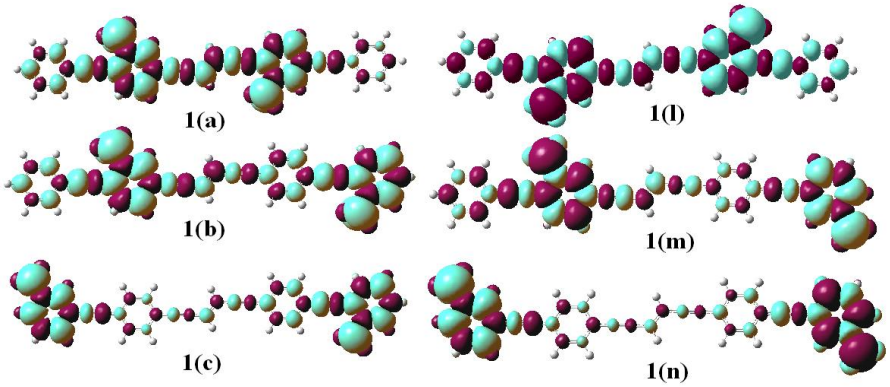

Figure 3.10 Spin density distributions of the ferromagnetically coupled diradicals (high spin state) and antiferromagnetically coupled diradicals (BS state) based on molecular wire 1.

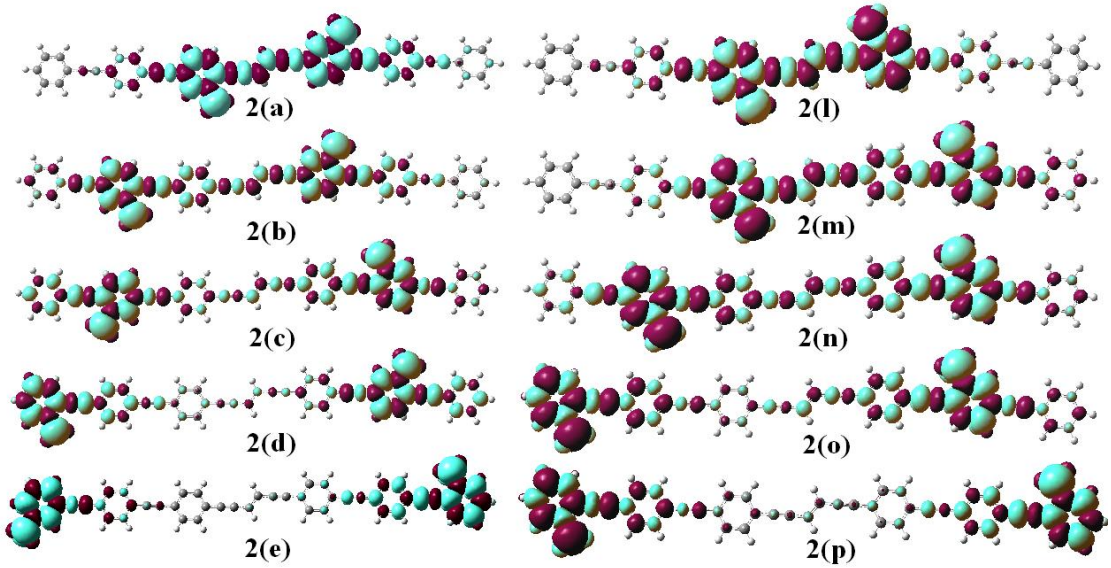

Figure 3.11 Spin density distributions of the ferromagnetically coupled diradicals (high spin state) and antiferromagnetically coupled diradicals (BS state) based on molecular wire 2.

3.3.5 Transport property of the diradical substituted molecular wires

We have studied the transport property of the diradical substituted molecular wires to see the effect of radical substitution on the transport behavior of the molecular wires. The transmission spectra of the diradical substituted wires with varying lengths are presented in Figure 3.12 and Figure 3.13, where we can see that the molecular wires belonging to the same series show almost similar transmission (for ferromagnetically coupled diradicals) however series 1 exhibits higher transmission than series 2. Again comparing the transmission for molecular wire without radical substitution (Figure 3.6), we observe the same result with radical substitution. Hence it can be concluded that the transport property of the molecular wire is independent of radical substitution, whereas, the magnetic exchange coupling constant of the diradical decreases with increasing distance between the radical centers. Stasiw et al. have studied that for donor−bridge−acceptor systems, there is a large variation in magnetic exchange coupling and electronic coupling as a function of bridge conformation.[43] For our designed molecular wires (consist of several aromatic phenyl rings along with radical substitution on the rings), when transmission occurs through the wire, possibly only local transmission of the aromatic rings appear on the Fermi level of the electrode and the radicals are not participated to the transmission of that region, which may be the reason for the same transmission after radical substitution in the ferromagnetic diradicals, but for antiferromagnetic diradicals, there is a small variation in transmission characteristics between radical substituted molecular wires.

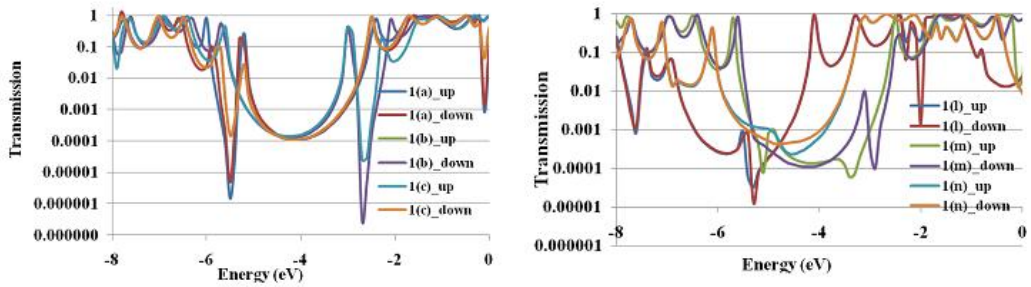

Figure 3.12 The transmission spectra of the diradical substituted molecular wire 1 [1(a)-1(c) high spin state; 1(l)-1(n) BS state].

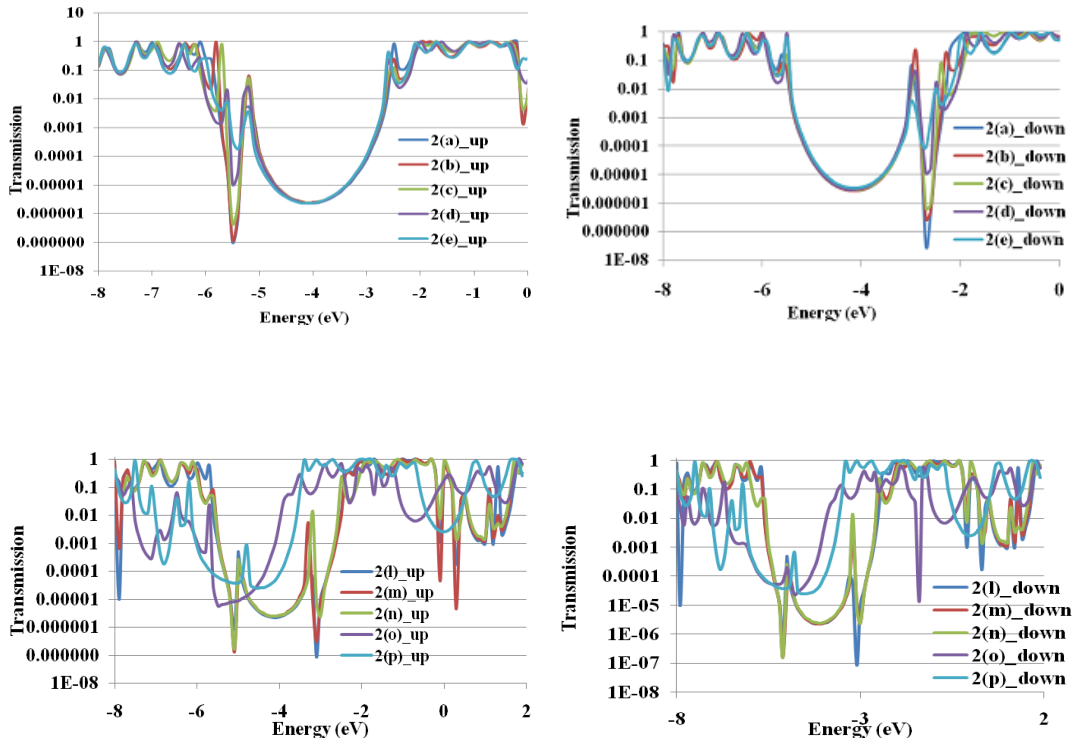

Figure 3.13 The transmission spectra of the diradical substituted molecular wire 2 [2(a)-2(e) high spin state; 2(l)-2(p) BS state].

3.4 Conclusion

To summarize, we studied the effect of the length of molecular wires on the electrical transport properties. We found that the molecular wires (addition polymer) with smaller length show higher transmission, i.e., higher conduction. Another important point is that the magnetic exchange coupling constant of the radical substituted molecular wire depends only on the distance between the spin centers, not on the outsider substitution. The transmission of the molecular wire without radical substitution shows similar observations as that of the wire with radical substitution for ferromagnetically coupled diradicals; however, the transmission characteristics are slightly affected by the antiferromagnetic diradicals.

3.5 References

(1) Tian, W.; Datta, S.; Hong, S.; Reifenberger, R.; Henderson, J. I.; Kubiak, C. P. *J. Chem. Phys.* **1998**, *109*, 2874-2882.
(2) Kober, S.; Gotesman, G.; Naaman, R. *J. Phys. Chem. Lett*. **2013**, *4*, 2041-2045.
(3) Jalili, S.; Rafi-Tabar, H. *Phys. Rev. B* **2005**, *71*, 165410(1-9).
(4) Magoga, M.; Joachim, C. *Phys. Rev. B* **1997**, *56*, 4722-4729.
(5) Durig, U.; Zuger, O.; Michel, B.; Haussling, L.; Ringsdorf, H. *Phys.Rev. B* **1993**, *48*, 1711-1717.
(6) Boulas, C.; Davidovits, J. V.; Rondelez, F.; Vuillaume, D. *Phys. Rev. Lett*. **1996**, *76*, 4797-4800.
(7) Bumm, L. A.; Arnold, J. J.; Cygan, M. T.; Dunbar, T. D.; Burgin, T. P.; Jones, L.; II, Allara, D. L.; Tour, J. M.; Weiss, P. S. *Science* **1996**, *271*, 1705-1707.
(8) Andres, R.P.; Bein, T.; Dorogi, M.; Feng, S.; Henderson, J. I.; Kubiak, C. P.; Mahoney, W.; Osifchin, R.G.; Reifenberger, R.G. *Science* **1996**, *272*, 1323-1325.
(9) Reed, M. A.; Zhou, C.; Muller, C. J.; Burgin, T. P.; Tour, J. M. *Science* **1997**, *278*, 252-254.
(10) Kushmerick, J. G.; Holt, D. B.; Pollack, S. K.; Ratner, M. A.; Yang, J. C.; Schull, T. L.; Naciri, J.; Moore, M. H.; Shashidhar, R. *J. Am. Chem. Soc*. **2002**, *124*, 10654-10655.
(11) Weiss, E. A.; Ahrens, M. J.; Sinks, L. E.; Gusev, A. V.; Ratner, M. A.; Wasielewski, M. R. *J. Am. Chem. Soc.* **2004**, *126*, 5577-5584.
(12) Nishizawa, S.; Hasegawa, J.-Y.; Matsuda, K. *J. Phys. Chem. C* **2013**, *117*, 26280-26286.
(13) Samuel, I. D. W. *Philos. Trans. R. Soc., A,* **2000**, *358*, 193–210.
(14) Lu, H.; Leng, J.; Du, S. *Soft Matter,* **2013**, *9*, 3851–3858.
(15) Lu, H.; Du, S. *Polym. Chem.,* **2014**, *5*, 1155–1162.
(16) Herrmann, C.; Solomon, G. C.; Ratner, M. A. *J. Am. Chem. Soc.* **2010**, *132*, 3682-3684.
(17) Herrmann, C.; Solomon, G. C.; Subotnik, J. E.; Mujica, V.; Ratner, M. A. *J. Chem. Phys.* **2010**, *132*, 024103 (1-17).
(18) Frisch, M. J.; Trucks, G. W.; Schlegel, H. B.; Scuseria, G. E.; Robb, M. A.; Cheeseman, J. R.; Scalmani, G.; Barone, V.; Mennucci, B.; Petersson, G. A.; et.al. Gaussian09; Gaussian, Inc.: Wallingford, CT, **2009**.
(19) Yoshizawa, K. *Acc. Chem. Res.* **2012**, *45*, 1612-1621;
(20) Yoshizawa, K.; Tada, T.; Staykov, A. *J. Am. Chem. Soc*. **2008**, *130*, 9406-9413.
(21) Noodleman, L. *J. Chem. Phys*. **1981**, *74*, 5737.
(22) Noodleman, L.; Baerends, E. J. *J. Am. Chem. Soc*. **1984**, *106*, 2316-2327.
(23) Ginsberg, A. P. *J. Am. Chem. Soc*. **1980**, *102*, 111-117.
(24) Noodleman, L.; Peng, C. Y.; Case, D. A.; Mouesca, J. M. *Coord. Chem. Rev*. **1995**, *144*, 199-244.
(25) Noodleman, L.; Davidson, E. R. *Chem. Phys*. **1986**, *109*, 131-143.

(26) Bencini, A.; Totti, F.; Daul, C. A.; Doclo, K.; Fantucci, P.; Barone, V. *Inorg. Chem*. **1997**, *36*, 5022-5030.
(27) Bencini, A.; Gatteschi, D.; Totti, F.; Sanz, D. N.; McClevrty, J. A.; Ward, M. D. *J. Phys. Chem. A* **1998**, *102*, 10545.
(28) Ruiz, E.; Cano, J.; Alvarez, S.; Alemany, P. *J. Comput. Chem*. **1999**, *20*, 1391-1400.
(29) Yamaguchi, K.; Takahara, Y.; Fueno, T.; Nasu, K. *Jpn. J. Appl. Phys*. **1987**, *26*, L1362.
(30) Ali, Md. E.; Datta, S. N. *J. Phys. Chem. A* **2006**, *110*, 2776-2784.
(31) Ali, Md. E.; Datta, S. N. *J. Phys. Chem. A* **2006,** *110***,** 13232-13237**.**
(*32)* Polo, V.; Alberola, A.; Andres, J.; Anthony, J.; Pilkington, M. Phys. *Chem. Chem. Phys.* **2008**, *10*, 857-864.
(33) Bhattacharya, D.; Misra, A. *J. Phys. Chem. A* **2009,** *113*, 5470-5475**.**
(34) Paul, S.; Misra, A. *THEOCHEM* **2009**, *907*, 35-40.
(35) Paul, S.; Misra, A. *THEOCHEM* **2009**, *895*, 156-160,
(36) Ashcroft, N.W.; Mermin, N.D, Solid *State Physics*, Holt, Rinehart and Winston, New York, **1976**.
(37) F. Pauly, J. K. Viljas, J. C. Cuevas, G. Schön, *Phys. Rev. B,* **2008**, *77*, 155312.
(38) Stuyver, T.; Fias, S.; Proft, De F.; Geerlings, P, *Chem. Phys. Lett.* **2015**, *630*, 51-56.
(39) Kim, W. Y.; Kim, K. S. *Acc. Chem. Res*. **2010**, *43*, 111-120.
(40) Choi, Y. C.; Kim, W. Y.; Park, K. –S.; Tarakeshwar, P.; Kim, K. S.; Kim, T. –S.; Lee, J. Y. *J. Chem. Phys*. **2005**, *122*, 094706 (1-6).
(41) Shil, S.; Misra, A. *RSC Adv.* **2013**, *3*, 14352-14362.
(42) Trindle, C.; Datta, S. N. *Int. J. Quantum Chem.* **1996**, *57*, 781-799.
(43) Stasiw, D. E.; Zhang, J.; Wang, G.; Dangi, R.; Stein, B. W.; Shultz, D.A.; Kirk, M.L.; Wojtas, L.; Sommer, R. D. *J. Am. Chem.Soc*. **2015**, *137*, 9222-9225.

CHAPTER 4

A perspective on designing chiral organic magnetic molecules with unusual behavior in magnetic exchange coupling

Abstract

In the fourth chapter we have designed a total of nine diradical based organic chiral magnetic molecules with allene and cumulene couplers and subsequently the magnetic property has been studied by DFT. It is found that with an increase in length of the coupler, a remarkable increase in spin density within the coupler takes place. An increase in the length of the coupler reduces the energy of LUMO, and a smaller HOMO-LUMO gap facilitates stronger magnetic coupling and thereby a higher magnetic exchange coupling constant (*J*). This observation is supported by the occupation number of natural orbitals.

4.1 Introduction

Chirality is of utmost importance as it plays a key role not only in the life forms but also in pharmaceutical, agricultural and other chemical industries.[1] At present, chiral organic molecules are of extensive interest to organic chemists as well as pharmaceutical chemists.[2] Galán-Mascarós et al. have synthesized molecular materials with ferromagnetism, metal-like conductivity and chirality.[3] When chirality appears in the structure of atoms in a solid having unpaired electrons, the chiral lattice favor a screw like arrangement of the magnetic moments of unpaired electrons, but they must compete with ferromagnetic exchange, that attempts to align all the magnetic moments in the same direction. These chiral lattice are known as chiral magnets.[4] On the other hand, chiral magnetic molecules with ferromagnetic interaction can also be regarded as chiral magnet.[5] Stable chiral magnets are important ingredients for future data storage, spintronic device[6] and other applications for their fascinating properties.[4] The most important phenomena shown by chiral magnets are the magneto-chiral effect which occurs in chiral media in presence of a magnetic field.[7] The synthesized chiral magnets are mainly inorganic or metallo-organic in nature.[8,9] It is observed that chiral magnets, particularly manganese silicide (MnSi), a cubic intermetallic compound that has no inversion symmetry i.e, with a noncentrosymmetric crystal structure,[10] have attracted interest over the last few years and they may one day reach a degree of functionality similar to that of chiral liquid crystals.[4] But in last few decades, the search for new ferromagnetic materials based on organic diradicals has generated tremendous interest.[11-13] Organic radicals[11] have been widely studied for their versatile applicability in the field of magnetism,[14] and for their superconductivity,[15] spintronic properties,[16] photomagnetic behaviour[17] and so on. In case of organic diradicals, the magnetic interaction between two radical centers normally depends on the couplers which connect the radical centers.[18] A series of nitronylnitroxide (NN) diradicals with linear conjugated couplers have been studied by Ali and Datta, and they reported that the magnetic exchange coupling constant value decreases gradually with increasing conjugation length of the coupler.[19] It has been found that chains containing sp-hybridized carbon atoms are fascinating due to their unique linear structure and interesting physical properties.[20] Allenes (1, 2-propadiene derivatives) are an important class of compounds and have gained increasing attraction as interesting building blocks in synthetic organic chemistry.[21] Cumulenes with odd number of carbon atoms have π-systems that are spatially orthogonal with each other and therefore these systems contain a chiral axis and their two pairs of substituent are in two perpendicular planes, giving rise to enantiomers.[22] Skibar et al. have synthesized cumulenes containing 7 carbon atoms.[23] Januszewski et al. also have synthesized and predicted the properties of long cumulenes containing up to 10 carbon atoms.[24] Cumulenes find major application in molecular machines (nano-mechanics), molecular wires (nano-electronics), nonlinear optics, and molecular sensors due to their unique electronic structures.[25] It is found that among all conjugated oligomers, cumulene wires with odd number of carbon atoms show the highest conductance with metallic-like ballistic transport behavior.[26]

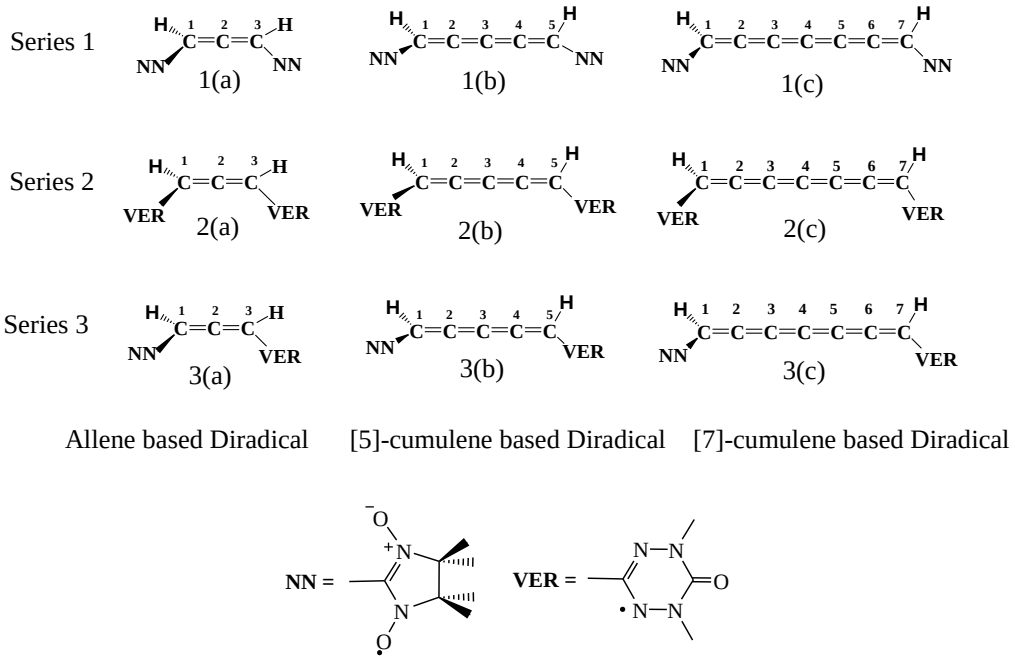

Figure 4.1 Allene- and cumulene-based diradicals. [5] and [7] indicates the number of carbon atoms in a coupler.

We have designed allene and cumulene (containing odd number of carbon atoms) based diradical systems that are shown in Figure 4.1 and have studied the magnetic property of these diradicals in detailed as an estimation of the intramolecular exchange coupling constant is necessary before synthesizing a successful magnetic material based on organic diradicals or transition metal complexes. These designed molecules may be used as molecular building block for organic chiral magnetic solids.

4.2 Theoretical Background

The magnetic exchange interaction between two magnetic sites 1 and 2 is generally express by the Heisenberg spin Hamiltonian $\hat{H} = -2J\hat{S}_1 \bullet \hat{S}_2$, where $\hat{S}_1$ and $\hat{S}_2$ are the respective spin angular momentum operators and J is the exchange coupling constant between two magnetic centers. When J is positive, the high-spin state is lower in energy, and the coupling is said to be ferromagnetic. A negative value of J is representative of antiferromagnetic interaction in the diradical and a low-spin state is the ground state. For a diradical containing a single unpaired electron on each site, J can be represented as $E_{(S=1)} - E_{(S=0)} = -2J$.

Multiconfiguration approaches are suitable to describe pure spin states in an appropriate manner; but these methods are resource intensive and not used in this work. To circumvent this issue, broken symmetry (BS) approach by Noodleman et

al.[27-30] in DFT framework is a more useful alternative to evaluate *J* that can eventually lead to an estimate of the energy of diradical singlet. The ideal BS state is a weighted average of the singlet and the triplet, and has an M_S equal to zero. The ideal triplet (T) state has an $\langle S^2 \rangle$ = 2, whereas $\langle S^2 \rangle$ = 1 in the ideal BS state and that results E(BS) $-E$(T) =J. However in actual calculation approximate $\langle S^2 \rangle$ values are obtained, and hence BS solution is often found to be spin contaminated. Therefore, a correction is needed to calculate the coupling constant.

The spin projected formula given by Yamaguchi[31-34] for the evaluation of magnetic exchange coupling constant (*J*) is free from such spin contamination and applicable for both low and high overlap between magnetic orbitals, which can be written as $J = (E_{BS} - E_{HS}) \Big/ \left(\left\langle S^2 \right\rangle_{HS} - \left\langle S^2 \right\rangle_{BS} \right)$ where E_{BS}, E_{HS}, $\langle S^2 \rangle_{BS}$, and $\langle S^2 \rangle_{HS}$ are the energies and average spin square values for the BS and high-spin states, respectively.

4.3 Computational Strategy

The molecular structure of all the diradicals have been fully optimized in each spin state by hybrid exchange-correlation functionals B3LYP and M06 in combination with 6-311++G(d,p) basis set within the unrestricted formalism using Gaussian09 quantum chemical package.[35] A broken symmetry (BS) singlet solution has been performed for mixing of the HOMO and the LUMO. To obtain open shell BS singlet solution "guess=mix" keyword is used. The magnetic exchange coupling constant (*J*) value for each molecule has been estimated from the energies of triplet and BS states at the same level of theory using the spin projected formula given by Yamaguchi.[31-34] To confirm the enantiomeric nature of our designed systems, we analyze the vibrational circular dichroism (VCD) spectra using freq= vcd keyword. Detailed analyses of geometrical parameters, the spin density distribution, molecular orbital as well as natural orbital occupancies have been calculated with the optimized geometry.

4.4 Results and Discussion

It is well-known that the two enantiomers of a chiral compound show optical rotation value of same angle but in opposite direction in presence of plane-polarized light. The absolute configuration of a chiral molecule can be determined from its vibrational circular dichroism (VCD) spectrum as the VCD spectra of the two enantiomers of a chiral molecule are equal in magnitude and opposite in sign.[2] Here we have tried to verify the enantiomeric relationship between our designed chiral molecules. For series 2 diradicals (in Figure 4.2), calculated VCD spectra (in Figure 4.3) confirm the stereochemistry as well as the enantiomeric relationship between them.

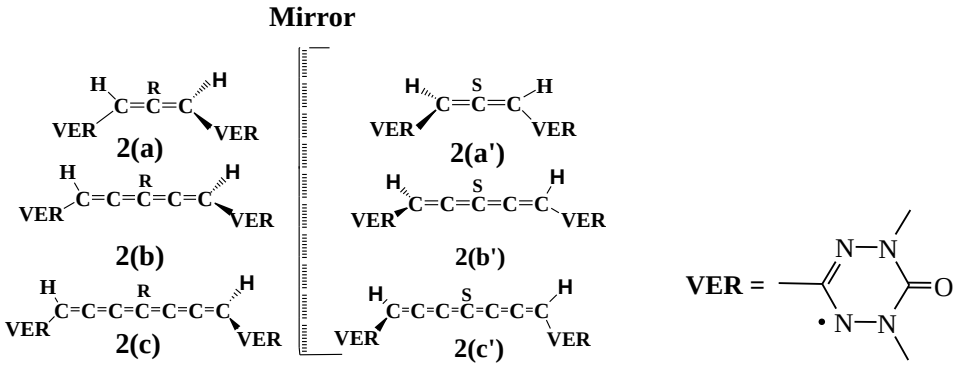

Figure 4.2 *R* and *S* configuration of the designed diradicals of series 2.

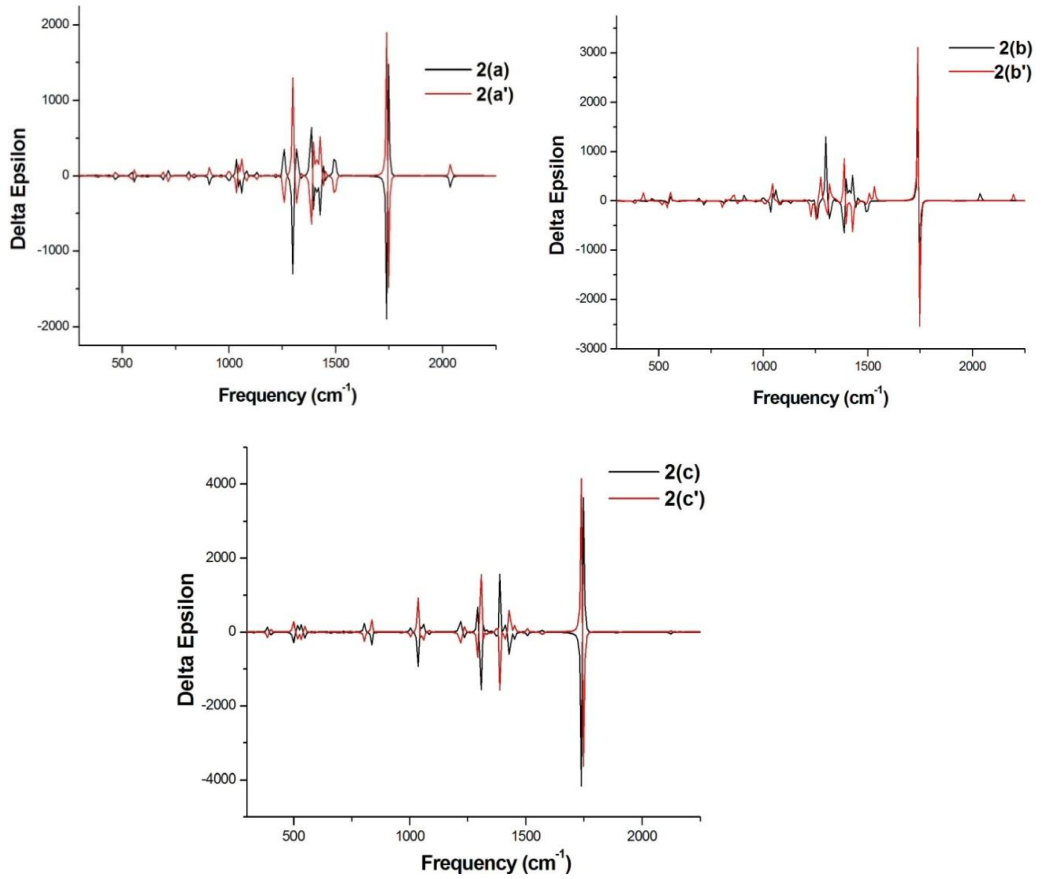

Figure 4.3 VCD spectra of two enantiomers of series 2 (We have calculated the VCD spectra of the diradicals using B3LYP functional and 6-311++G(d,p) basis set on the top of optimized geometry of M06 functional with 6-311++G(d,p) basis set).

The other diradicals (series 1 and series 3) have similar couplers; therefore it is obvious that they will follow the same trend as series 2. The point here is that the form of the Hamiltonian guarantees the magnetic exchange coupling constant of the diradical based chiral enantiomers to be equal in magnitude.

4.4.1 Magnetic exchange coupling constant

The calculated magnetic exchange coupling constants of all the diradicals are listed in Table 4.1. The consistency of magnetic exchange coupling constant values have been confirmed using two different exchange-correlation functionals (B3LYP and M06). It is observed that although the values of coupling constants are different for different methods, they follow the similar trend. From Table 4.1 it is observed that with the increase in chain length of the coupler from the allene based diradical to the [5]-cumulene based diradical, the magnetic exchange coupling constant increases almost 2-fold, and again upon the transition from the [5]-cumulene based diradical to the [7]-cumulene based diradical, the coupling constant further increases approximately by 2-fold, which contradicts the fact that the level of magnetic exchange decreases with an increase in the length of conjugated systems.[19] Therefore, it can be argued that there must be a major contribution of the coupler in magnetic exchange pathway and this observation demands a detailed investigation of electronic structure of these couplers. If we compare the coupling constant of same coupler with different radicals, we can see that the NN based diradicals have highest coupling constant and VER based diradicals have lowest one, combination of two radicals NN and VER gives the coupling constant in between. Thus, we can conclude that the nitronyl nitroxide radical is more suitable for obtaining a coupling constant higher than that of verdazyl radical with allene and cumulene couplers.

Table 4.1 The energy (a.u.),$\langle S^2 \rangle$ and magnetic exchange coupling constant (J in cm^{-1}) of designed diradicals (from series 1 to series 3).

		B3LYP/6-311++G(d,p)			M06/6-311++G(d,p)			
Systems		**Triplet**	**BS**	***J***		**Triplet**	**BS**	***J***
1(a)	E	-1183.41922	-1183.41900	47.66	E	-1182.62355	-1182.62326	63.17
	$\langle S^2 \rangle$	2.136	1.123		$\langle S^2 \rangle$	2.134	1.116	
1(b)	E	-1259.59164	-1259.59117	99.09	E	-1258.73505	-1258.73440	146.28
	$\langle S^2 \rangle$	2.207	1.166		$\langle S^2 \rangle$	2.134	1.158	
1(c)	E	-1335.76802	-1335.76716	171.28	E	-1334.85150	-1334.85020	244.31
	$\langle S^2 \rangle$	2.319	1.217		$\langle S^2 \rangle$	2.384	1.215	
2(a)	E	-1016.17752	-1016.17745	15.30	E	-1015.50571	-1015.50560	22.96
	$\langle S^2 \rangle$	2.050	1.046		$\langle S^2 \rangle$	2.050	1.044	
2(b)	E	-1092.34903	-1092.34889	30.36	E	-1091.61679	-1091.61658	45.00
	$\langle S^2 \rangle$	2.068	1.056		$\langle S^2 \rangle$	2.073	1.054	
2(c)	E	-1168.52398	-1168.52373	53.17	E	-1167.73165	-1167.73123	86.95
	$\langle S^2 \rangle$	2.100	1.068		$\langle S^2 \rangle$	2.132	1.068	
3(a)	E	-1099.79801	-1099.79788	28.33	E	-1099.06411	-1099.06393	39.14
	$\langle S^2 \rangle$	2.092	1.085		$\langle S^2 \rangle$	2.090	1.080	
3(b)	E	-1175.97033	-1175.97007	55.84	E	-1175.17589	-1175.17552	78.62
	$\langle S^2 \rangle$	2.136	1.114		$\langle S^2 \rangle$	2.143	1.109	
3(c)	E	-1252.14603	-1252.14557	95.42	E	-1251.29167	-1251.29093	147.65
	$\langle S^2 \rangle$	2.209	1.151		$\langle S^2 \rangle$	2.258	1.156	

We have calculated the absolute energy values of the diradicals as $\frac{1}{2}[E_{NN}^{T} + E_{VER}^{T}]$ and for mixed radical systems given in Table 4.2 and found that for allene based diradicals the energy difference is as small as 0.00036 a.u. and for longer cumulene there is no energy difference at all, which suggests that the interaction between radicals at the two ends of the molecules is not radical specific and decreases with an increase in the length of the carbon chain.

Table 4.2 Absolute energies of the diradicals as $\frac{1}{2}[E_{NN}^{T} + E_{VER}^{T}]$ and for mixed radical systems in their triplet state (E_{NN}^{T} represents the energy of series 1 diradicals, E_{VER}^{T} represents the energy of series 2 diradicals, and E_{Mixed} represents the energy of series 3 diradicals).

Systems	E_{NN}^{T} **(a.u.)**	E_{VER}^{T}**(a.u.)**	$\overline{E}_{\text{pure}} = \frac{1}{2}[E_{NN}^{T} + E_{VER}^{T}]$**(a.u.)**	E_{Mixed} **(a.u.)**	$\Delta E = (\overline{E}_{\text{Pure}} - E_{\text{Mixed}})$ **(a.u.)**
Allene based Diradical	-1183.41922	-1016.17752	-1099.79837	-1099.79801	-0.00036
[5]-cumulene based Diradical	-1259.59164	-1092.34903	-1175.97034	-1175.97033	0.00001
[7]-cumulene based Diradical	-1335.76802	-1168.52398	-1252.14600	-1252.14603	0.00003

4.4.2 Spin density distribution

The spin density of DFT based approach can give us an insight about the spin polarization mechanism for magnetic exchange coupling within the molecule. Exchange coupling constant between two magnetic sites largely depends on the delocalization of π-electron densities between them. Hence, to understand the anomalous increase in magnitude of *J*, we have done the spin density distribution analysis. Hund's rule based spin density alternation rule[36,37] helps to predict the nature of magnetic interaction for diradicals with different couplers. Ferromagnetic exchange coupling takes place between two spin centers when they are connected by even number of conjugated bonds and antiferromagnetism occurs for odd number of bonds.[36,37] Spin density distribution of the diradicals in their high-spin states (Figure 4.4) confirm that all these diradicals have intramolecular ferromagnetic coupling.

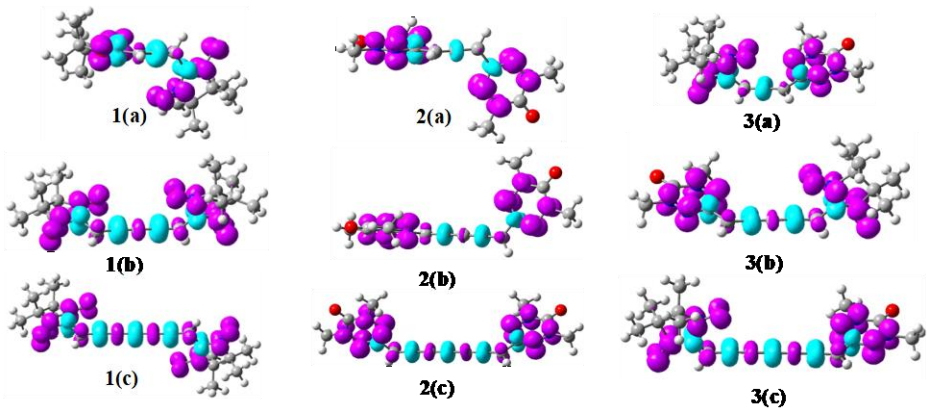

Figure 4.4 Spin density plot of all the designed diradicals in their triplet states (B3LYP/6-311++G(d,p)), (iso value 0.004), magenta and sky colors represent the α and β spins respectively.

The spin density on different atoms of coupler and also the total spin density of coupler in designed diradicals are reported in Table 4.3. Hermann et al. have proposed that cumulene based systems with even number of carbon centers, the spin delocalization onto the chain increases as the length of the chain gets longer.[38] For our designed systems it is also found that with increase in chain length of the coupler, spin density on different atoms of coupler as well as the total spin density on coupler increases, which is quite contradictory from the concept that with increase in chain length of conjugated systems the spin density on the coupler reduces.[19] Hence as argued in the previous subsection, there must be some special reason which facilitates the spin polarization in such systems.

Table 4.3 Spin density distribution on each atom of coupler and total spin density of coupler in designed diradicals in their triplet state (B3LYP/6-311++G(d,p)).

Systems	**Spin density on different atoms of coupler**							**Total spin density**
	C_1	C_2	C_3	C_4	C_5	C_6	C_7	
1(a)	0.0768	-0.2655	0.0768	--------	--------	--------	--------	-0.1120
1(b)	0.1072	-0.2664	0.1572	-0.2665	0.1071	--------	--------	-0.1614
1(c)	0.1501	-0.3004	0.2041	-0.3196	0.2041	-0.3004	0.1501	-0.2120
2(a)	0.0616	-0.141	0.0616	-------	--------	--------	--------	-0.0177
2(b)	0.0831	-0.1341	0.0652	-0.1341	0.0831	--------	--------	-0.0366
2(c)	0.1223	-0.1659	0.0899	-0.1396	0.0899	-0.1659	0.1223	-0.0470
3(a)	0.0638	-0.1862	0.0683	---------	--------	--------	--------	-0.0541
3(b)	0.1025	-0.2095	0.114	-0.1969	0.0953	--------	-------	-0.0946
3(c)	0.1437	-0.2437	0.1711	-0.2488	0.1469	-0.2316	0.1362	-0.1262

4.4.3 Spin polarization

Chiral allene and cumulene couplers contain even number of π-bonds in perpendicular planes; therefore the two end π-bonds are perpendicular to each other. A close inspection of the spin density plot in Figure 4.5 for series 1 diradicals point to the fact that the spin density distribution of π-electrons of two end carbon atoms of the coupler are individually directed along two Cartesian axes (y and z direction). But for rest of the carbon atoms within the coupler, spin polarization of π-electrons is along both the y and z directions collectively, causing a large accumulation of spin density for the middle carbons of the coupler chain. Plausible mechanistic pathway of spin polarization within the coupler is shown in Figure 4.6.

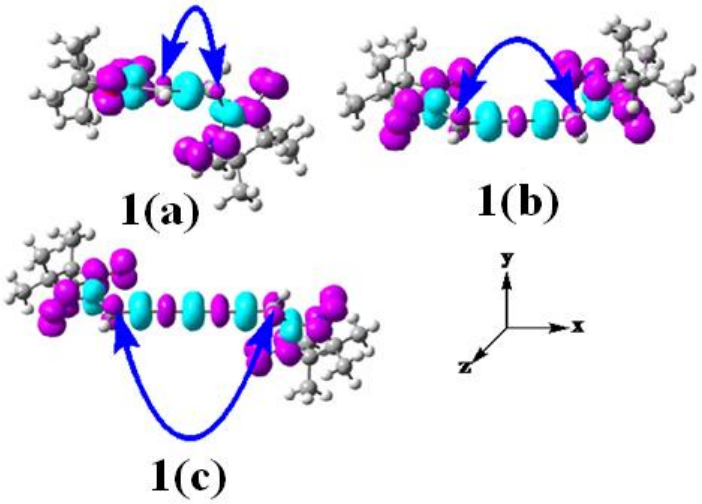

Figure 4.5 Spin density plot for the diradicals of series 1 in their triplet states (B3LYP/6-311++G(d,p)) (iso value 0.004), magenta and sky colors represent the α and β spins respectively. Blue arrow represents two end carbons of coupler.

To explain the increase in spin density upon addition of carbon center within the coupler, and simultaneously to explain the contradictory behavior of spin polarization in cumulenes with that of conjugated systems (*i.e.*, alternating σ and π bonds), detailed investigation of mechanistic pathway of spin polarization was conducted. Figure 4.6 shows that the two end carbons in allene based diradical contain one π-bonding electron on each of them, but the central carbon contains two π-bonding electrons in two different *p* orbitals at a time. Therefore, for allene based diradicals, spin polarization is greater in middle carbon compared to the end carbons. Now while comparing the allene based diradical with [5]-cumulene based diradical, one finds that former contains only one carbon with two π-electrons at central region of the coupler but later contains three carbons with two π-electrons on each. As a result [5]-cumulene based diradical has higher accumulation of spin density on each carbon of coupler compared to allene based diradical. A similar trend in [7]-cumulene based diradical is also observed. Thus, one can surmise that spin polarization

increases considerably with increase in the number of carbon centers of coupler in cumulene systems.

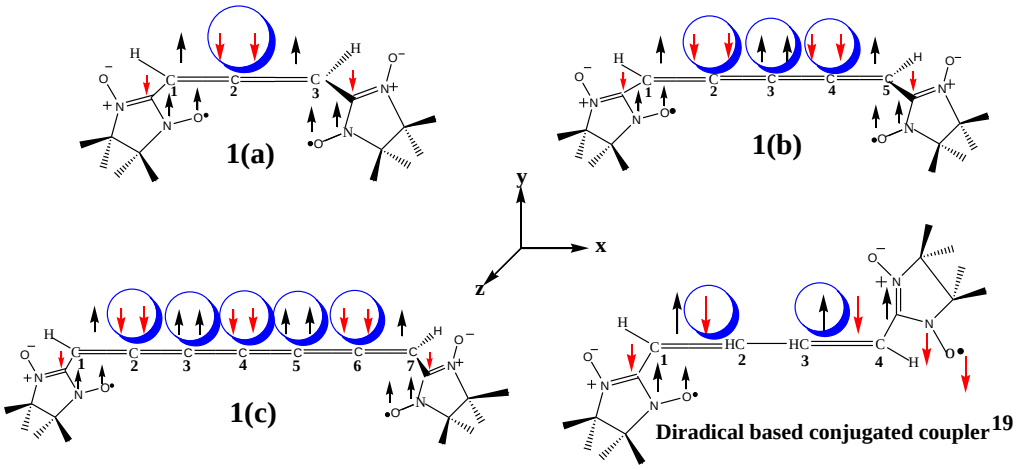

Figure 4.6 Spin polarization of π electron within the coupler (for series 1).

Upon comparison of the spin density of cumulene with that of the conjugated coupler, it is found that for conjugated coupler based diradicals, each carbon atom of the coupler contains one π-electron on each and no such enhancement of spin polarization occurs; moreover, a decrease in spin density with an increase in the chain length of the coupler is observed as the distance between the radical centers increases. Figure 4.7 is a plot of the coupling constant versus the distance between the radical centers that clearly shows the variation of the coupling constant with distance.

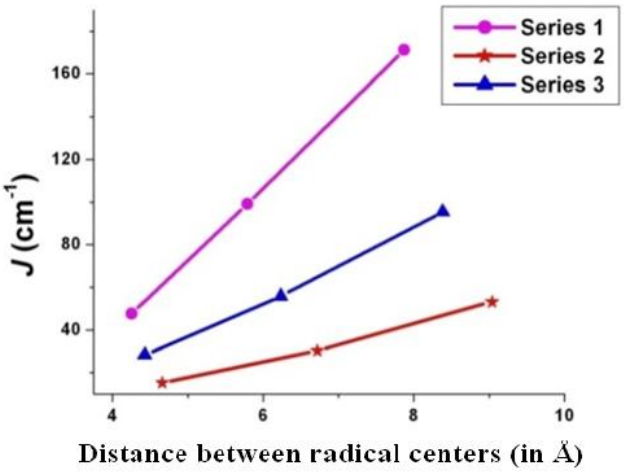

Figure 4.7 Plot of magnetic exchange coupling constant vs. distance (in Å) between radical centers (B3LYP/6-311++G(d,p)).

Therefore a high level of accumulation of spin density within the coupler overcomes the distance factor between the radical centers in case of cumulene based diradicals and higher magnetic exchange coupling results with the increase in the length of the coupler.

4.4.4 Molecular structures

A small change in molecular structure can lead to a drastic change in the magnetic coupling constant.[39] Therefore, it is important to study the molecular structure of the allene and cumulene based diradicals in order to understand their magnetic behavior. The optimized geometrical parameters of our designed diradicals are reported in Table 4.4 and Table 4.5.

Table 4.4 Bond distance between two atoms and the average bond distance of the couplers for the designed diradicals in their triplet state (B3LYP/6-311++G(d,p)). All bonds are in pm unit. (L is the connecting atom of left radical center and R is the connecting atom of right radical center respectively).

System	Bond distance						Average bond distance	Distance between C_1-L	Distance between C_3-R	Distance Between C_5-R	Distance between C_7-R
	C_1=C_2	C_2=C_3	C_3=C_4	C4=C_5	C_5=C_6	C_6=C_7					
1(a)	131.1	131.1	-------	-------	-------	-------	131.1	143.8	143.8	--------	--------
1(b)	132.6	127.0	127.0	132.6	-------	-------	129.8	142.8	--------	142.8	--------
1(c)	133.3	126.4	128.1	128.1	126.4	133.3	129.3	142.3	--------	--------	142.3
2(a)	130.7	130.7	-------	-------	-------	-------	130.7	147.3	147.3	--------	--------
2(b)	131.9	127.2	127.2	131.9	-------	-------	129.5	146.6	--------	146.6	--------
2(c)	132.3	126.7	128.0	128.0	126.7	132.3	129.0	146.2	--------	--------	146.2
3(a)	131.3	130.5	-------	-------	-------	-------	130.1	144.0	147.2	--------	--------
3(b)	132.6	126.9	127.3	131.8	-------	-------	129.7	142.9	--------	146.5	--------
3(c)	133.3	126.3	128.3	127.9	126.8	132.4	129.2	142.3	--------	--------	146.2

The most important structural aspect is the bond distance alteration of the cumulene moiety. Our calculations predict a distinct alternation of adjacent C=C bonds, the first and last bond lengths for all the diradicals are approximately close to the double bond length in ethylene (132pm). The central double bond distance in [5]-cumulene based diradicals are approximately 127pm and their values are in between the double bond length in ethylene (132pm) and the C≡C triple bond length in acetylene (121.2 pm).The central bond distance for [7]-cumulene are also approximately 128 pm and double bond lengths elsewhere in the bridge chain equal 126 pm and their values are in between the double bond length in ethylene (132pm) and the C≡C triple bond length in acetylene (121.2 pm). When two different groups are included, all the

double bond lengths become unequal (see series3). These different bond lengths are indicative of electronically different bonding situations.

Another important point is that the average C-C bond length tends to decrease with increase in cumulene chain length in a particular series, as for series 1 the values are 131.1pm, 129.8pm, and 129.3 pm for 1 (a), 1(b) and 1(c) respectively and this is closer to a C=C double bond distance, as expected. It is observed that with decrease in the average bond length in each series, there is a possibility of increase in s-character of the coupler. The higher the s-character the greater is the electronegativity of that atom, and higher is the possibility to localize the spin density on that atom, which facilitates the higher spin densities on the coupler with increase in length. From Table 4.4 it is also clear that with increase in length of the coupler the distance between carbon atoms of the coupler and the radical centers decreases in each series, therefore the conjugation between the coupler and the radical center increases. Thus, ultimately a better π-interaction results with the increase in the chain length of the coupler.

The computed bond angle between the carbon atoms in the coupler are described in Table 4.5. It is confirmed that the bond angle of the coupler deviates from the exact angle of allene (180º), hence they are the systems with a nonlinear C=C=C framework, and are characterized by slightly deviated orthogonal π-bonds. This bending is higher in case of allene based diradicals compared to cumulene based diradicals. For this the allene π-system is significantly disturbed, and the central carbon atom is no longer sp-hybridized as in typical all-carbon allenes. Now, comparing diradical substituted allene with their higher homologue it is found that with increase in the chain length the middle allene counterpart goes nearly 180º (e.g, for 1(a) $\angle c_1\text{-}c_2\text{-}c_3$=173.87º, for 1(b) $\angle c_2\text{-}c_3\text{-}c_4$=177.97º, and for 1(c) $\angle c_3\text{-}c_4\text{-}c_5$=179.8º). Hence, there is relatively strong π-interaction with increasing chain length in each series and the coupling constant increases accordingly.

Table 4.5 Bond angle for the couplers in the diradicals in series 1-3 in their triplet state (B3LYP/6-311++G(d,p)).

Systems	**Bond angle/ º**				
	$\angle c_1\text{-}c_2\text{-}c_3$	$\angle c_2\text{-}c_3\text{-}c_4$	$\angle c_3\text{-}c_4\text{-}c_5$	$\angle c_4\text{-}c_5\text{-}c_6$	$\angle c_5\text{-}c_6\text{-}c_7$
1(a)	173.87	---------	---------	----------	---------
1(b)	174.35	177.97	174.35	--------	---------
1(c)	174.33	178.42	179.8	178.41	174.33
2(a)	177.92	----------	----------	---------	----------
2(b)	178.12	179.76	178.11	---------	----------
2(c)	178.13	179.88	179.95	179.87	178.14
3(a)	175.75	---------	----------	----------	----------
3(b)	174.54	178.49	178.23	---------	----------
3(c)	174.44	178.59	179.76	179.83	178.11

4.4.5 Molecular orbital analysis

The shape of molecular orbitals play a major role in determining the magnetic properties of the diradicals, electronic transport etc.[40] Frontier molecular orbitals (FMOs) of all the axially chiral allene and cumulene based diradical are presented in Figure 4.8. According to Borden and co-workers when the nonbonding molecular orbitals of a diradical have no atoms in common i.e., disjoint in nature, the diradicals favor antiferromagnetic state as ground state. The non-disjoint SOMOs favor ferromagnetic ground state. From Figure 4.8 one can see that α-SOMOs of diradicals in series 1 and 2 are non-disjoint and α-SOMOs of diradicals in series 3 are disjoint although all the diradicals are ferromagnetic in nature.

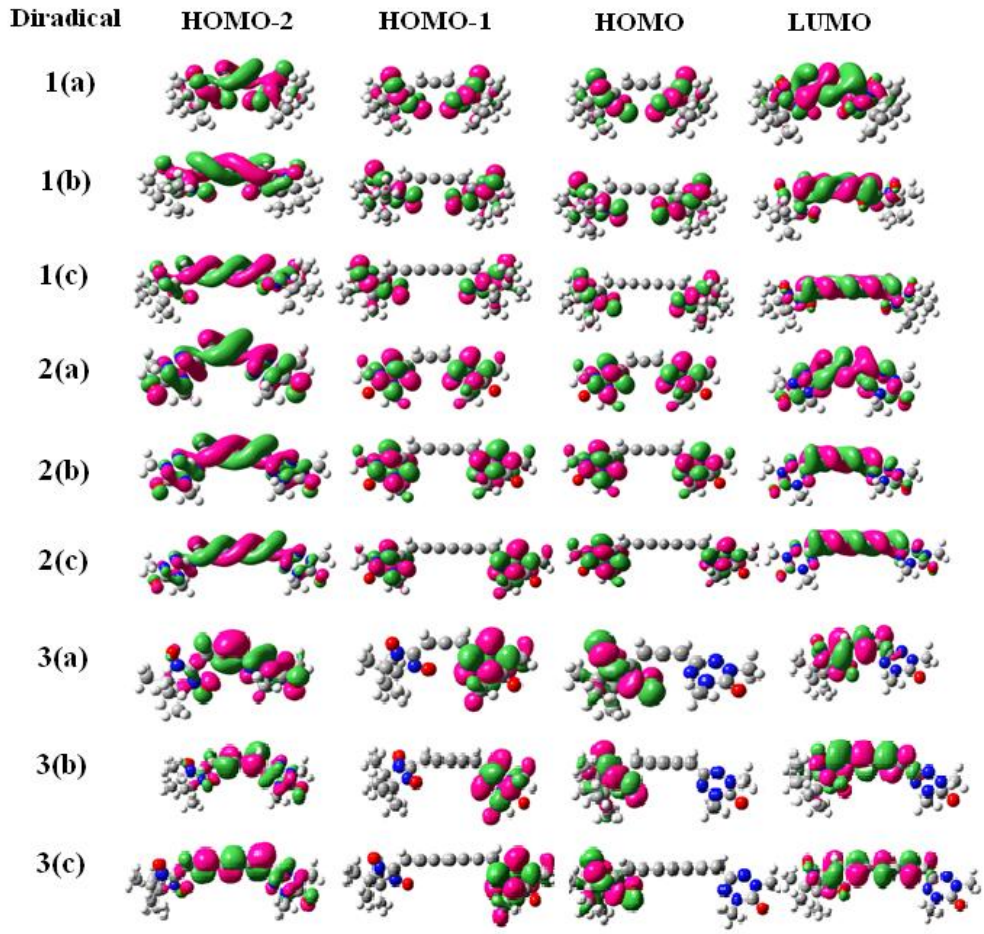

Figure 4.8 Spatial distribution of molecular orbitals of all the diradicals in their triplet states (B3LYP/6-311++G(d,p)) (iso value 0.02), green and pink colors represent the different phase of the orbital coefficients.

We have carried out molecular orbital analysis of diradical 1 and 2 with varying geometry given in Figure 4.9, to check the stability of non-disjoint nature of the SOMOs and found that the SOMOs are unaltered upon structural changes. Thus Borden's analogy [41,42] which is derived for alternant hydrocarbons does not fit for the disjoint diradicals in series 3. Thus, it may be surmised that Borden's analogy which is derived for alternant hydrocarbons does not fit for these diradicals and such systems follow a different mechanism for magnetic interaction.

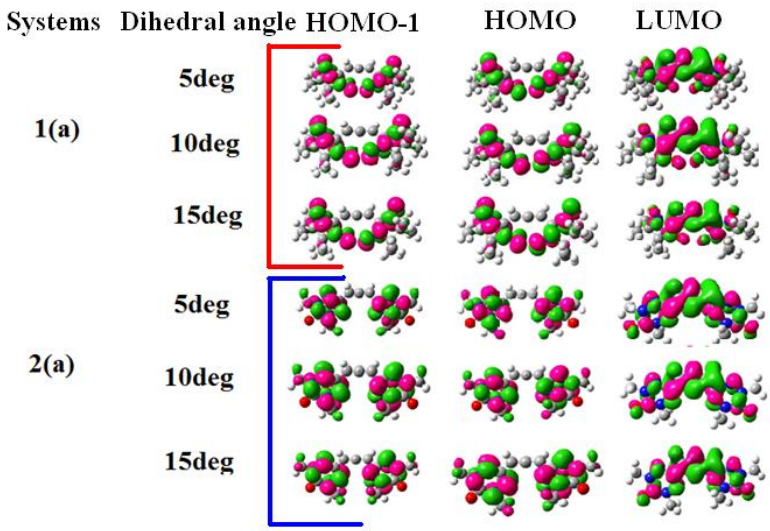

Figure 4.9 Spatial distribution of molecular orbitals of the diradicals with varying geometry in their triplet states (B3LYP/6-311++G(d,p)) (iso value 0.02), green and pink colors represent the different phase of the orbital coefficients.

The molecular orbital analysis of the BS determinant of diradical based allene in Figure 4.10 shows that for 1(a) and 2(a) diradicals, the α-HOMO and β-HOMO are on the two individual radical centers. However α-SOMOs of the triplet state for those diradicals are distributed collectively on two radical centers. But for series 3 diradicals (3(a)) the shape of α-HOMO and β-HOMO of BS determinant and α-SOMOs of triplet state are same. Therefore, the SOMOs of BS determinant and triplet state are not exactly same for all the diradicals but are distributed only over radical centers.

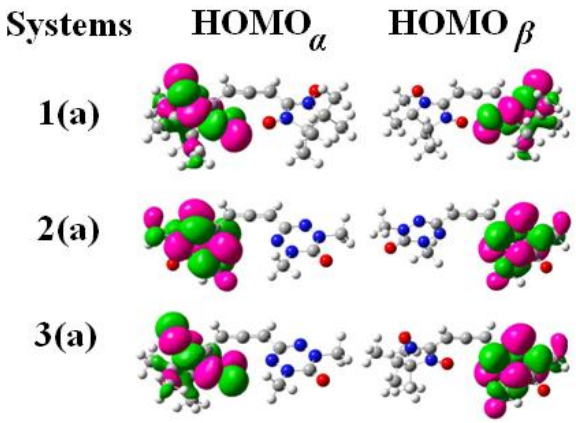

Figure 4.10 The molecular orbital of the diradicals (HOMO$_\alpha$ and HOMO$_\beta$) in their Broken symmetry state (B3LYP/6-311++G(d,p)) (iso value 0.02), green and pink colors represent the different phase of the orbital coefficients.

4.4.6 Mechanism of magnetic interaction

Molecular orbital takes an important role to understand the magnetic coupling between two radical centers. It is known that the SOMOs are mainly responsible for magnetic interaction in diradicals through itinerant exchange[41-44] and the low SOMO–SOMO gap or degenerate SOMOs produces strong magnetic exchange coupling constant. The SOMO–SOMO energy gap, HOMO–LUMO energy gap for the designed diradicals are listed in Table 4.6. We observe from the Table 4.6 that for series 1 and 2, the two SOMOs are almost degenerate although they have different values of *J* in each series. Another interesting point is that for diradicals 3(a) and 3(b) SOMO–SOMO gap is highest and equal in magnitude but shows the different *J* values. So, the SOMO–SOMO gap is not the only guiding factor to determine the extent of magnetic interaction, there must be some other factor which guides magnetic exchange. In couple of our recent works, we have studied that the SOMO–SOMO gap is not responsible for the strength of magnetic coupling, rather HOMO–LUMO gap plays a more important role.[39,45,46] If we focus on the energy difference between HOMO and LUMO in this study, it has been found that on going from diradical based allene to its higher homologue ([5]- and [7]-cumulene) in each series, there is a smooth decrease in HOMO–LUMO energy gap. Hermann et al. also have showed that the α-HOMO–α-LUMO gaps decreases with increasing carbon chain lengths of cumulene based systems containing even number of carbon centers.[38] Therefore, it can be concluded that diradicals with low HOMO–LUMO gap facilitates the strong magnetic coupling constant and the diradicals based on allene and cumulene couplers with low HOMO–LUMO gap will be the promising candidate to design chiral organic magnetic molecules.

Table 4.6 Energy (in eV) of HOMO–2, HOMO–1, HOMO and LUMO for all the diradicals and the energy difference (in eV) between SOMO1 $(HOMO)_{\alpha}$–SOMO2 $(HOMO–1)_{\alpha}$ (ΔE_{SS}) and $HOMO_{\alpha}$–$LUMO_{\alpha}$ (ΔE_{HL}) and magnetic exchange coupling constant (J in cm^{-1}) in their triplet state (B3LYP/6-311++G(d,p)).

System	E_{HOMO-2}	E_{HOMO-1}	E_{HOMO}	E_{LUMO}	ΔE_{SS}	ΔE_{HL}	J
1(a)	-6.89275	-5.29989	-5.29309	-1.58143	0.01	3.71	47.66
1(b)	-6.54971	-5.39002	-5.38653	-2.36083	0.00	3.03	99.09
1(c)	-6.29637	-5.47614	-5.47329	-2.83002	0.00	2.64	171.28
2(a)	-7.06015	-5.59234	-5.57656	-1.44088	0.02	4.14	15.30
2(b)	-6.65889	-5.63969	-5.63901	-2.28864	0.00	3.35	30.36
2(c)	-6.39022	-5.68584	-5.68584	-2.83331	0.00	2.85	53.17
3(a)	-6.89035	-5.49982	-5.36784	-1.64687	0.13	3.72	28.33
3(b)	-6.53529	-5.57941	-5.44784	-2.44366	0.13	3.00	55.84
3(c)	-6.29033	-5.61574	-5.52594	-2.73263	0.09	2.79	95.42

Our designed diradicals based on allene, [5]- and [7]-cumulene coupler (containing odd number of carbon atoms) has two π-conjugations that are mutually perpendicular to each other. Imamura and Aoki have proposed that polyyne has two π-conjugated systems mutually perpendicular to each other and both the π-conjugations have a tendency to follow a bond alternation that originates a competition in between them.[47-49] With increase in the length of the polyyne chain, a remarkable transition in the molecular structure takes place from almost equidistant bond structure to an intensely alternating bond structure, that causes a lifting of the HOMO level and a lowering of LUMO level. As a result there is a sudden decrease in HOMO–LUMO gap with increase in the length of the polyyne chains. The orbital phases of two mutually perpendicular π-conjugations for our designed diradicals are shown in Figure 4.11.

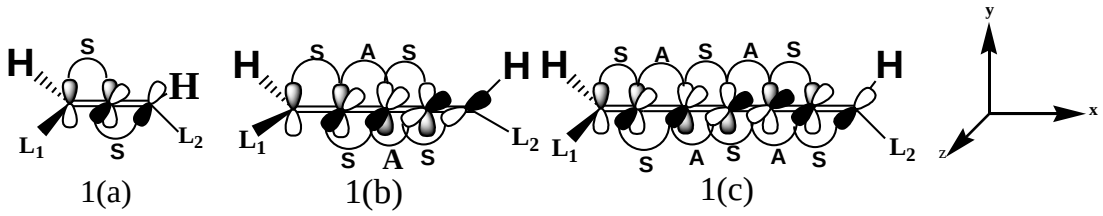

Figure 4.11 Structure of allene based diradical and cumulenes based diradical with phases of HOMO–2. S indicates symmetric and A indicates antisymmetric in the phase of MO. L_1 and L_2 are the left and right radical centers respectively.

For our designed diradicals $HOMO_\alpha$ and $(HOMO–1)_\alpha$ are the nonbonding molecular orbitals, therefore the energy of LUMO decreases and HOMO–2 energy increases remarkably (shown in Figure 4.12) that satisfy the proposal of Imamura et al.[47-49] As a result there is a decrease in the $HOMO_\alpha$–$LUMO_\alpha$ and $(HOMO–2)_\alpha$–$(HOMO–1)_\alpha$ energy gaps.

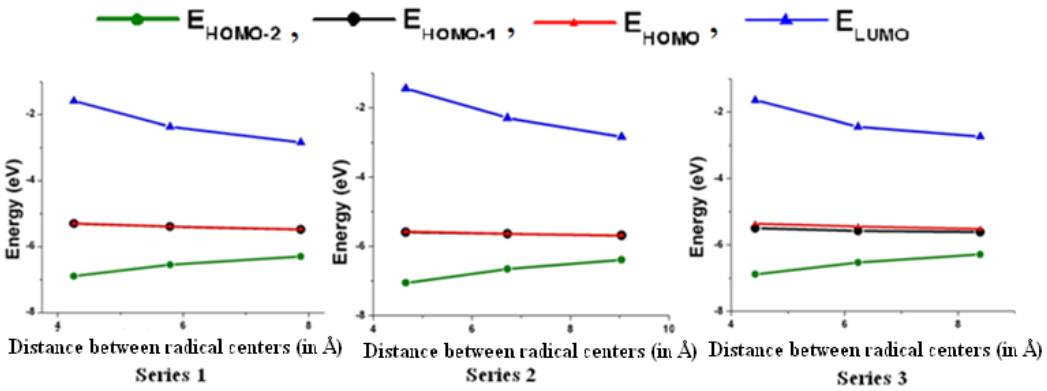

Figure 4.12 Plot of energy vs. distance between radical centers (in Å) for the series 1-3 in their triplet state (B3LYP/6-311++g(d,p)).

To determine the role of LUMO in the magnetic exchange coupling constant, we have computed the electron occupation in LUMO and HOMO–2 and SOMOs (Table 4.7).

Table 4.7 Natural orbital occupation of the diradicals in the triplet state (B3LYP/6-311++G(d,p)).

Systems	HOMO–2	HOMO–1	HOMO	LUMO
1(a)	1.968	1.0	1.0	0.032
1(b)	1.952	1.0	1.0	0.048
1(c)	1.924	1.0	1.0	0.073
2(a)	1.990	1.0	1.0	0.009
2(b)	1.986	1.0	1.0	0.014
2(c)	1.980	1.0	1.0	0.020
3(a)	1.969	1.0	1.0	0.031
3(b)	1.954	1.0	1.0	0.046
3(c)	1.931	1.0	1.0	0.069

From Table 4.7 we can see that LUMOs have considerable amount of occupation. Therefore, it can be assumed that the LUMO takes part in the exchange mechanism. Here, we can see that in case of diradicals (c) in all the series 1-3, the LUMO has the

highest occupation in their respective series. The higher occupation in the LUMO favors strong intramolecular magnetic exchange coupling between the radical centers. Therefore, there is a correlation between the LUMO occupation and magnetic exchange coupling constant.

4.5 Conclusion

All the designed diradicals have ferromagnetic interaction that increases on addition of chiral centers within the coupler. Spin density distribution analysis shows that with the increase in the length of the coupler, enhancement of spin polarization along the coupler takes place and the probability to localize the spin density on each chiral center increases. Addition of chiral centers within the coupler lowers the energy of LUMO and a lower HOMO-LUMO gap facilitates a stronger magnetic coupling and a higher magnetic exchange coupling constant (*J*) results. From natural orbital occupancies it is found that with increasing chain length of chiral coupler the occupancy of LUMO increases. Furthermore, non-applicability of Borden's rule indicates that a good way of predicting the ground state of the diradical systems having allene and [n]-cumulene coupler should be by Hund's rule based spin density alternation. A close inspection of *J* values shows that NN stands for a better choice of radical center over VER and mixed radicals. Thereby, it is expected that this trend might inspire synthetic chemists to synthesis NN- based chiral magnetic molecule with high ferromagnetic interaction. The diradicals with an [n]-cumulene coupler with n being an even number will show antiferromagnetic behavior according to the spin alternation rule. These antiferromagnetic diradicals will be discussed elsewhere.

4.6 References

(1) Nguyen, L. A.; He, H.; Pham-Huy, C. *Int. J. Biomed. Sci*. **2006**, ***2***, 85–100.
(2) Stephens, P. J.; Devlin, F. J.; Pan, J.-J. *Chirality.* **2008**, *20*, 643–663.
(3) Galán-Mascarós, J. R.; Coronado, E.; Goddard, P. A.; Singleton, J.; Coldea, A. I.; Wallis, J. D.; Coles, S. J.; Alberola, A. *J. Am. Chem. Soc*. **2010**, *132*, 9271.
(4) Pappas, C. *Physics* **2012**, *5*, 28.
(5) Train, C.; Gheorghe, R.; Krstic, V.; Chamoreau, L.-M.; Ovanesyan, N.S.; Rikken, G.L.J.A.; Gruselle, M.; Verdaguer, M. *nat. mater.* **2008**, *7*, 729-734.
(6) Togawa, Y.; Koyama, T.; Takayanagi, K.; Mori, S.; Kousaka, Y.; Akimitsu, J.; Nishihara, S.; Inoue, K.; Ovchinnikov, A. S.; Kishine, J. *Phys. Rev. Lett*. **2012**, *108*, 107202.
(7) Wagnière, G. H. *Chem Phys.***1999**, *245*,165–173.

(8) Bordács, S.; Kézsmárki, I.; Szaller, D.; Demko, L.; Kida, N.; Murakawa, H.; Onose, Y.; Shimano, R.; Rõõm, T.; Nagel, U.; Miyahara, S.; Furukawa, N.; Tokura, Y. *Nat. Phys*. **2012**, *8*, 734.
(9) Minguet, M.; Luneau, D.; Paulsen, C.; Lhotel, E.; Gorski, A.; Waluk, J.; Amabilino, D.B.; Veciana, J.; *Polyhedron* **2003**, *22*, 2349-2354.
(10) (a) Ishikawa, I.; Tajima, K. *Solid State Commun.* **1976**, *19*, 525-528.
(b) Yu, X. Z.; Onose, Y.; Kanazawa, N.; Park, J.H.; Han, J.H.; Matsui, Y.; Nagaosa, N.; Tokura, Y. *Nature* **2010,** *465*, 901-904.
(11) Kahn, O. Molecular Magnetism, VCH, New York, 1993.
(12) Coronado E, Delhae` P, Gatteschi D, Molecular magnetism: from molecular assemblies to devices; Miller J. S. (Eds); NATO ASI Series E321, vol 321, Kluwer, Dordrecht, 1996.
(13) Benelli, C.;Gatteschi, D. *Chem.Rev.* **2002**, *102*, 2369-2387.
(14) Lahti, P. M. Magnetic Properties of Organic Materials, Marcel Dekker, New York, 1999.
(15) (a) Kobayashi , H.; Kobayashi , A.; Cassoux, P.; *Chem. Soc. Rev*.**2000**, *29*, 325–333. (b) Uji, S.; Shinagawa, H.; Terashima, T.; Yakabe, T.; Terai , Y.; Tokumoto, M.; Kobayashi, A.; Tanaka, H.; Kobayashi, H. *Nature*.**2001**, *410*, 908–910.
(16) (a) Prinz ,G. A. *Science*, **1998**, *282*, 1660–1663. (b) Emberly, E. G.; Kirczenow, G. *Chem. Phys*. **2002**, *281*, 311–324.
(17) (a) Matsuda, K.; Matsuo, M.; Irie, M. *J. Org. Chem*.**2001**, *66*, 8799–8803. (b) Tanifuji, N.; Irie, M.; Matsuda, K. *J. Am. Chem. Soc*.**2005**, *127*, 13344–13353.
(18) (a) Bhattacharya, D.; Misra, A. *J. Phys. Chem. A*, **2009**, *113*, 5470–5475. (b) Bhattacharya, D.**;** Shil, S.; Misra, A.; Klein, D. J. *Theor. Chem. Acc*., **2010**, *127*, 57–67. (c) Bhattacharya, D.; Shil, S.; Panda, A.; Misra, A. *J. Phys. Chem. A*, **2010**, *114*, 11833–11841.
(19) Ali, Md. E.; Dutta, S.N. *J. Phys. Chem. A* **2006**, *110*, 2776-2784.
(20) (a) Tobe, Y.; Wakabayashi, T.; in *Acetylene Chemistry: Chemistry, Biology, and Material Science* (Eds.: F. Diederich, P. J. Stang, R. R. Tykwinski), Wiley-VCH, Weinheim,**2005**, pp. 387 – 426. (b) Chalifoux, W. A.; Tykwinski, R. R. *Chem. Rec*.**2006**, *6*, 169 –182. c) Shi Shun, A. L. K.; Tykwinski, R. R. *Angew. Chem. Int. Ed*.**2006,** *45*, 1034 – 1057. (d) Raton, B. Polyynes: Synthesis, Properties, and Applications; Cataldo, F. (Eds); Taylor & Francis, **2005**.
(21) Taylor, D. R. *Chem. Rev*.**1967**, *67*, 317.
(22) Hendon, C.H.; Tiana, D.; Murray, A.T.; Carbery, D.R.; Walsh, A. *Chem. Sci*., **2013**, *4*, 4278–4284.
(23) Skibar, W.; Kopacka, H.; Wurst, K.; Salzmann, C.; Ongania, K.H.; Biani, F.F.D.; Zanello.P.; Bildstein, B. *Organometallics* **2004**,*23*,1024-1041.
(24) (a)Januszewski, J.A.; Tykwinski, R.R.; *Chem. Soc. Rev.* **2014**, *43*, 3184-3203.
(b) Januszewski, J.A.; Wendinger, D.; Methfessel, C.D.; Hampel, F.; Tykwinski, R.R.; *Angew. Chem. Int. Ed*.**2013**, *52*, 1817 –1821.
(25) Gu, X.; Kaiser, R.I.; Mebel, A.M. *Chem. Phys. Chem.* **2008**, *9*, 350–369.
(26) Prasongkit, J.; Grigoriev, A.; Wendin. G.; Ahuja, R. *Phys. Rev. B* **2010**, *81*, 115404.

(27) Noodleman, L. *J. Chem. Phys.***1981**, *74*, 5737−5743.
(28) Noodleman, L.; Baerends, E. J. *J. Am. Chem. Soc.***1984**, *106*, 2316−2327.
(29) Noodleman, L.; Davidson, E. R. *Chem. Phys.***1986**, *109*, 131−143.
(30) Noodleman, L.; Peng, C. Y.; Case, D. A.; Mouesca, J. -M. *Coord. Chem. Rev.***1995**, *144*, 199−244.
(31) Yamaguchi, K.; Fukui, H.; Fueno, T. *Chem.Lett.***1986**, *15*, 625−628.
(32) Yamaguchi, K.; Takahara, Y.; Fueno, T.; Nasu, K. *Jpn. J. Appl. Phys.***1987**, *26*, L1362−L1364.
(33) Yamaguchi, K.; Jensen, F.;Dorigo, A.; Houk, K. N. *Chem.Phys. Lett.* **1988**, *149*, 537−542.
(34) Yamaguchi, K.; Takahara, Y.; Fueno, T.; Houk, K. N. *Theor. Chim. Acta* **1988**, *73*, 337−364.
(35) Frisch, M. J.; Trucks, G. W.; Schlegel, H. B.; Scuseria, G. E.; Robb, M. A.; Cheeseman, J. R.; Scalmani, G.; Barone, V.; Mennucci, B.; Petersson, G. A.; Nakatsuji, H.; Caricato, M.; Li, X.; Hratchian, H. P.; Izmaylov, A. F.; Bloino, J.; Zheng, G.; Sonnenberg, J. L.; Hada, M.; Ehara, M.; Toyota, K.; Fukuda, R.; Hasegawa, J.; Ishida, M.; Nakajima, T.; Honda, Y.; Kitao, O.; Nakai, H.; Vreven, T.; Montgomery, J. A., Jr.; Peralta, J. E.; Ogliaro, F.; Bearpark, M.; Heyd, J. J.; Brothers, E.; Kudin, K. N.; Staroverov, V. N.; Kobayashi, R.; Normand, J.; Raghavachari, K.; Rendell, A.; Burant, J. C.; Iyengar, S. S.; Tomasi, J.; Cossi, M.; Rega, N.; Millam, M. J.; Klene, M.; Knox, J. E.; Cross, J. B.; Bakken, V.; Adamo, C.; Jaramillo, J.; Gomperts, R.; Stratmann, R. E.; Yazyev, O.; Austin, A. J.; Cammi, R.; Pomelli, C.; Ochterski, J. W.; Martin, R. L.; Morokuma, K.; Zakrzewski, V. G.; Voth, G. A.; Salvador, P.; Dannenberg, J. J.; Dapprich, S.; Daniels, A. D.; Farkas, Ö.; Foresman, J. B.; Ortiz, J. V.; Cioslowski, J.; Fox, D. J. Gaussian, Inc., Wallingford CT, **2009**.
(36) Trindle, C.; Datta, S. N. *Int. J. Quantum Chem.***1996**, *57*, 781-799.
(37) Trindle, C.; Datta, S. N.; Mallik, B. *J. Am. Chem. Soc.***1997**, *119*, 12947-12951.
(38) Hermann, C.; Neugebauer, J.; Gladysz, J. A.; Reiher, M. *Inorg. Chem.* **2005**, *44*, 6174-6182.
(39) Shil, S.; Herrmann, C. *Inorg. Chem.* 2015, *54*, 11733–11740.
(40) Browne, W. R.; Hage, R.; Vos, J. G. *Coord.Chem. Rev.***2006**, *250*, 1653–1668.
(41) Borden, W.T.; Davidson, E.R. *J. Am. Chem. Soc.* **1977**, *99*, 4587–4594.
(42) Borden, W.T.; Davidson, E.R. *Acc. Chem. Res.* **1981**, *14*, 69–76.
(43) Constantinides, C. P.;Koutentis, P. A.; Schatz, J. *J. Am.Chem. Soc.* **2004**, *126*, 16232–16241.
(44) Zhang,G.; Li,S.; Jiang,Y.*J. Phys. Chem. A.* **2003**, *107*, 5573–5582.
(45) Shil, S.; Roy, M.; Misra, A. *RSC Adv.***2015**, *5*, 105574–105582.
(46) Bhattacharya, D.; Shil, S.; Misra, A.; Bytautas, L.; Klein, D. J. *Phys. chem. Chem. Phys.* **2015**, ***17***, 14223-14237.
(47) Aoki, Y.; Imamura, A. *J. Chem. Phys.***1995**, *103*, 9726.
(48) Imamura, A.; Aoki, Y. *Int. J. of Quantum Chem.* **2006**, *106*, 1924 –1933.
(49) Imamura, A.; Aoki, Y. *Int. J. of Quantum Chem.* **2013**, *113*, 423 –427.

CHAPTER 5

Magnetic and transport properties of conjugated and cumulated molecules: the π-system enlightens part of the story

Abstract

In the fifth chapter we have investigated the intramolecular magnetic exchange coupling constants (J) for a series of nitronyl nitroxide diradicals connected by a range of linear conjugated and cumulene couplers focusing on the unusual π-interaction properties within the couplers. Distance between radical centers, spin density within the couplers, as well as the dihedral angles between the radical centers and the plane of the coupler influence the strength of magnetic coupling. We also establish that with the increase in length of the coupler, the strength of magnetic interaction in conjugated and cumulated systems varies in a different way. Transport calculations show that with the increase in chain length, diradicals based on cumulene containing even number of carbon atoms act as better conductors than cumulenes with odd number of carbon atoms. It is also observed that with the increase in the length of the conjugated coupler based diradicals, transmission does not vary in a sequential way.

5.1 Introduction

The magnetic interactions of organic radicals[1] and methods of controlling their magnetic properties have been widely investigated for their potential applications in the field of magnetism,[2] superconductivity,[3,4] photomagnetism,[5,6] spintronics[7,8] including their use in spin field effect transistors, magnetic semiconductors, spin-polarized light-emitting diodes, spin valves, and so on.[9-12] On the other hand, tunable molecular wires that reconcile electronic communication,[13] energy transfer,[14] electron transfer,[15] charge transport [16] etc. have been sparkles in the eye of theoreticians and experimentalists.[17]

Spintronic elements whose transport properties are governed by antiferromagnetic interactions are also known.[18] Much efforts have been given over the past decades to the design and synthesis of π-conjugated molecular wires[19] (containing delocalized electrons) and it is a persistent challenge in molecular electronics to control the conductance and current flow through such systems. Getting high conductance is also of interest in the distance-dependent attenuation of electron transfer and transport.[20-22]

Among all carbon nanostructures, linear chains of carbon atoms have been predicted to have excellent properties for various transport related applications.[23-25] It is found that chains containing sp-hybridized carbon atoms are fascinating due to their unique linear structure and interesting physical properties.[26-29] Recently allenes have acquired major attraction as their reactivity and selectivity can be simply tuned by varying their electronic and steric effects with appropriate substituents.[30,31] Zhang et al. have shown that cumulenes act as semiconductors and polyynes as metallic monatomic chains by their rigidity, these properties make them promising for applications in nanotechnology.[32] Cumulenes and their substituted counterparts have also been used as elements for nonlinear optics, molecular sensors,[33] molecular machines (nanomechanics),[34] molecular wires (nano-electronics, which is an emerging field in structural chemistry). Skibar et al.[35] and Januszewski et al.[36,37] have synthesized and predicted the properties of long cumulene systems.

The magnetic interaction between two radical centers generally depends on the distance and the nature of the couplers.[38-42] The π-interaction as well as the spin-polarization through the coupler play a major role in controlling the magnitude and sign of the coupling constant.[43]An estimation of the exchange coupling constant is necessary before synthesizing a successful organic magnetic material based on organic diradicals. There are many systematic studies on the intramolecular magnetic coupling constants for organic diradicals linking with various couplers.[44-54] Recently we have studied the anomalous magnetic property of diradicals based on chiral allene and cumulene coupler (containing odd number of carbon atoms) where the π-orbitals at both end of the coupler are perpendicular to each other and may be used as building blocks for chiral magnets.[55] For cumulenes containing even number of carbon atoms,

the π-orbitals at both end of the cumulene chain are parallel to each other and hence have different electronic structure compared to that of odd cumulenes. On the other hand, conjugated systems have alternating double bonds. Therefore, as a continuation of our previous work,[55] we are motivated to investigate the effect of unusual π-interaction of cumulene based diradicals containing even number of carbon atoms as well as diradicals based on conjugated systems (shown in Figure 5.1) on the magnetic properties, as this will provide a completeness to this study. We use nitronyl nitroxide radicals as radical sources where the unpaired spin comes from the -NO group of the nitronyl nitroxide moiety.[56] In addition to that; we also study the coherent electronic transport characteristics of cumulene based diradicals (with both the odd and even number of carbon atoms) and the conjugated couplers.

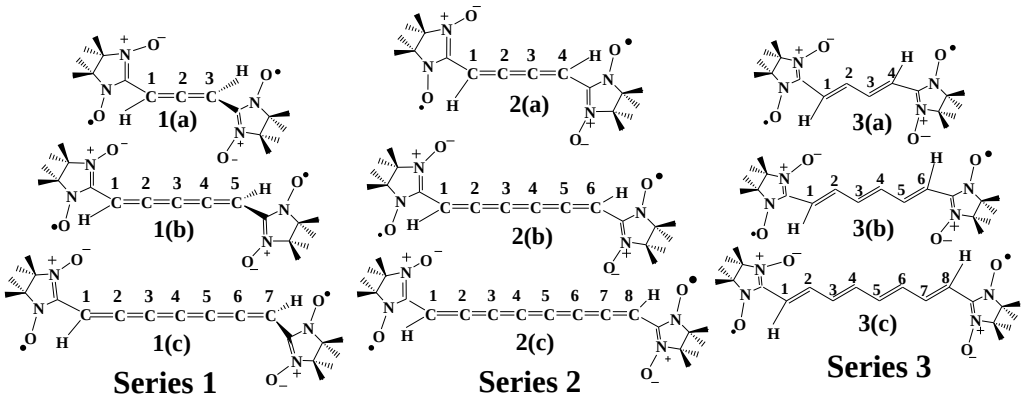

Figure 5.1 Designed diradicals based on allene, cumulene and the conjugated couplers. Series 1 represents the allene and cumulene based diradicals containing odd number of carbon atoms, Series 2 represents cumulene based diradicals containing even number of carbon atoms and Series 3 represents the diradical based on conjugated systems.

5.2 Theoretical background and computational strategy

The magnetic exchange interaction between two magnetic sites 1 and 2 is normally expressed by the Heisenberg spin Hamiltonian $\hat{H} = -2J\hat{S}_1 \bullet \hat{S}_2$, where $\hat{S}_1$ and $\hat{S}_2$ are the respective spin angular momentum operators and *J* is the effective exchange coupling constant between two magnetic sites. Positive sign of *J* means the coupling is ferromagnetic and the high-spin state is the lower energy state. A negative value of *J* is representative of antiferromagnetic interaction in the diradical and a low-spin state is the ground state. For a diradical having a single unpaired electron on each site, *J* can be represented as $E_{(S=1)} - E_{(S=0)} = -2J$.

Multi-configuration approaches are appropriate to describe pure spin states in a proper manner; but these methods are resource intensive and not used in this work. To circumvent this issue, broken symmetry (BS) approach proposed by Noodleman et al.[57-60] in DFT framework is a more useful alternative to evaluate *J* that can ultimately lead to an estimation of the energy of diradical singlets. The limiting form of the BS state is a weighted average of the singlet and the triplet, and has M_S =0. The ideal triplet (*T*) state has an $\langle S^2 \rangle$ = 2, whereas $\langle S^2 \rangle$= 1 in the ideal BS state and that results *E*(BS) −*E*(T) =*J*. However in actual calculation approximate $\langle S^2 \rangle$ values are obtained, and hence BS solution is often found to be spin contaminated. Therefore, a correction is needed to calculate the coupling constant. The spin projected formula given by Yamaguchi[61-64] for the estimation of magnetic exchange coupling constant (*J*) is capable of taking such spin contamination into account and applicable for both low and high overlaps between magnetic orbitals, that can be written as $J = (E_{BS} - E_{HS}) \Big/ \left(\left\langle S^2 \right\rangle_{HS} - \left\langle S^2 \right\rangle_{BS} \right)$where E_{BS}, E_{HS} and $\langle S^2 \rangle_{BS}$, $\langle S^2 \rangle_{HS}$ are the energy and average spin square values for corresponding BS and high-spin states.

All calculations related to magnetic properties have been done by Gaussian09 package.[65] The popular B3LYP exchange–correlation potential was used in combination with the 6-311++G(d,p) basis set within the unrestricted formalism for all geometry optimizations. Frequency calculation gives positive values for all these systems which confirm that the geometries are in local minima. To obtain open shell broken symmetry (BS) singlet solution "guess=(read,mix)" keyword is used for mixing of the HOMO and the LUMO. The magnetic exchange coupling constant (*J*) value for each molecule has been estimated from the energies of triplet and BS states at the same level of theory using the spin projected formula given by Yamaguchi.

In the coherent tunnelling regime the finite bias current ($I_s(V)$) conduction of electron spins through a gold-molecule-gold junction can be calculated by the following equation:

$$I_s(V) = \frac{e}{h} \int_{E_F - \frac{eV}{2}}^{E_F + \frac{eV}{2}} dE T_S(E,V) \qquad (1)$$

where *V* is the finite bias voltage, E_F is the Fermi energy, *E* is the energy and $T_S(E,V)$ is the transmission function. In the Landauer–Imry–Büttiker approximation,[66] the zero voltage conductance i.e., $(dI/dV)_{V=0}$ is proportional to $T(E_F)$. Therefore, it is reasonable to take integration over $E_F - \frac{eV}{2}$ to $E_F + \frac{eV}{2}$. The T_s can be calculated from the retarded ($\Gamma_{L/R,s}$) and advanced ($G_{C,sr/a}$) Green's function of the electrode-molecule-electrode system as

$$T_S(E,V) = tr\left(\Gamma_{R,s} G^r_{L,s} \Gamma_{L,s} G^a_{C,s}\right) \qquad (2)$$

The detailed theoretical approach we use here can be found in reference 67 and 68.

In order to obtain the transport properties of all the designed systems, instead of simply considering the prototypical diradical based on cumulene and conjugated couplers, we add polyacetylene chain (spacer groups, containing 4 carbon atoms), ensuring that there is no considerable interaction between the electrodes and any atom of the radical sites. The dithiol (obtained by replacing two end hydrogen atoms of polyyne chain by –SH group) molecule has been optimized and then the hydrogen atoms are stripped off and the resulting neutral dithiolate is placed between two electrodes (shown in Figure 5.2). Each electrode consists of nine gold atoms that are organized as a six-atom triangular fcc-gold (111)-surface connected to the molecule, with a second layer having three gold atoms. The bond length between sulfur and Au (111) surface has been chosen to be 2.48 Å and Au-Au distances of 2.88 Å as in extended gold crystals. Fock and overlap matrices required for the transport calculations are achieved by single point calculation in Gaussian09 program package.[65] For the transport calculation we employ B3LYP functional and the LANL2DZ basis set to avoid ghost transmission.[67] Basis sets of triple-zeta quality or higher sometime gives an artificially high transmission and possibly may give wrong conclusions about chemical trends. In such cases, transport persists when molecular atoms are substituted by basis functions alone (called "ghost atoms"). It is tested that the basis set of double zeta quality without polarization functions (e.g. Lanl2dz) gives negligible ghost transmission. This observation has been systematically studied by Herrmann and co-workers given in reference 67.

In order to obtain the transport properties, the designed systems have been divided into three sub systems: gold-cluster–dithiolate–gold-cluster as illustrated in Figure 5.2. We have calculated the transmission property using ARTAIOS code developed by Herrmann et al.[67-68]

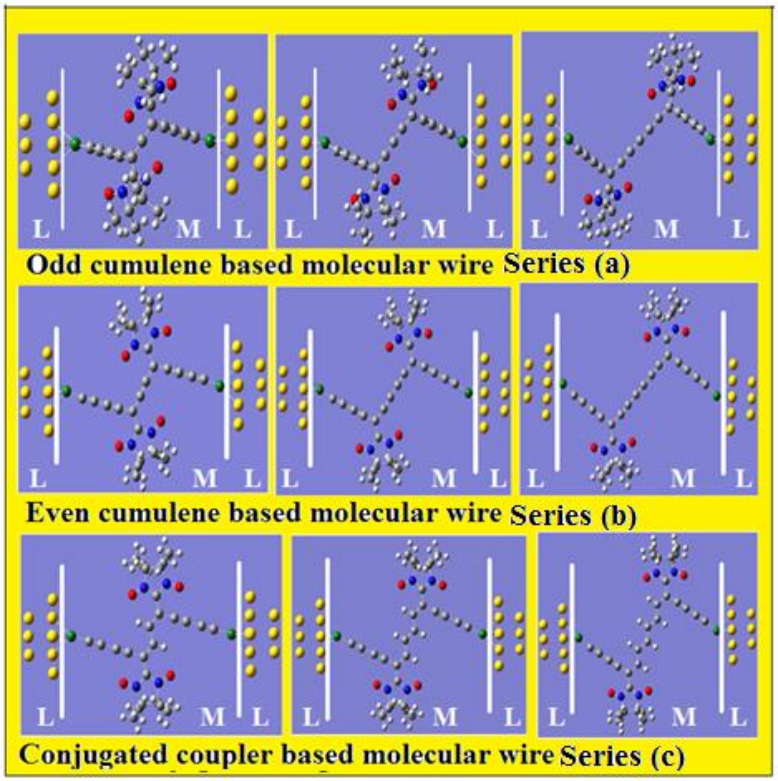

Figure 5.2 Designed diradical based systems on which transport calculations have been carried out (L stands for lead and M stands for molecule, the grey, white, red, blue, yellow and green colors represent carbon, hydrogen, oxygen, nitrogen, gold and sulfur atoms respectively). Series (a) represents odd cumulene based molecular wires, Series (b) represents even cumulene based molecular wires and Series (c) represents conjugated coupler based molecular wires.

5.3 Results and discussion

5.3.1 Magnetic exchange coupling constant

The calculation of *J* yields ferromagnetic interaction for linkers with an odd number of carbon atoms,[55] while antiferromagnetic coupling is predicted for diradicals connected by linkers with an even number of carbon atoms shown in Figure 5.3 (using B3LYP/6-311++G(d,p)). It is found that the increase in number of carbon atoms from odd cumulene connector to even cumulene connector causes a great contrast in magnitude as well as the change in sign of the magnetic exchange coupling constant values. It is also observed that with the increase in the number of carbon atoms of the coupler, the magnitude of *J* increases for both the series of odd and even cumulene based diradicals [the increase of *J* through the odd cumulene based diradical series is almost twice from 1(a) to 1(b) and from 1(b) to 1(c)],[55] while for conjugated couplers, the magnitude of *J* value decreases gradually. Therefore

cumulenes with even number of carbon atoms show an increase in coupling constant value with the increase in the distance between two radical centers; though opposite result is normally expected keeping parity with the conjugated systems. Thus together with the previous work[55] it provides completeness to this particular study. Therefore, it can be argued that there must be a major contribution of the π-interaction of the couplers in magnetic exchange pathways and this observation demands a detailed investigation of electronic structure of these couplers.

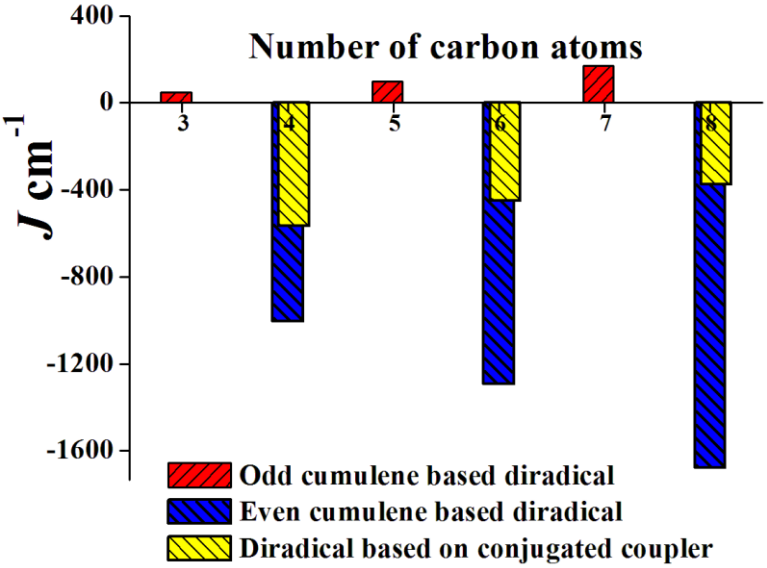

Figure 5.3 Plot of magnetic exchange coupling constant J (in cm^{-1}) vs. number of carbon atoms within the coupler (using B3LYP/6-311++G(d,p)). Red color represents the coupling constant for odd cumulene based diradical (series 1), blue color represents even cumulene based diradical (series 2), and yellow color represents diradical based on conjugated coupler (series 3).

B3LYP is a well-tested and widely used functional but it lacks dispersion correction and long range correction. Therefore, in addition to B3LYP, we compute the magnetic exchange coupling constant of our designed systems with dispersion corrected B3LYP (B3LYP-D) and to include long range correction we use CAM-B3LYP and the results are given in Table 5.1, Table 5.2 and Table 5.3. We found that there is no qualitative change of the magnetic exchange coupling constant due to dispersion correction and long range correction in the functional. All the functionals give qualitatively consistent results except CAM-B3LYP functional gives average spin square value far from 1 to the BS solution. Considering all these facts, we stick to the B3LYP functional for rest of the calculations.

Table 5.1 The energy (a.u.),$\langle S^2 \rangle$ and magnetic exchange coupling constant (J in cm^{-1}) of the odd cumulene based diradicals (taken from reference 55).

Diradicals			Triplet	BS	*J*
B3LYP/ 6-311++G(d,p)	1(a)	E(a.u.)	-1183.41922	-1183.41900	47.66
		$\langle S^2 \rangle$	2.136	1.123	
	1(b)	E	-1259.59164	-1259.59117	99.09
		$\langle S^2 \rangle$	2.207	1.166	
	1(c)	E(a.u.)	-1335.76802	-1335.76716	171.28
		$\langle S^2 \rangle$	2.319	1.217	
B3LYP-D/ 6-311++G(d,p)	1(a)	E(a.u.)	-1183.48377	-1183.48355	48.05
		$\langle S^2 \rangle$	2.136	1.124	
	1(b)	E	-1259.65614	-1259.65566	101.73
		$\langle S^2 \rangle$	2.208	1.169	
	1(c)	E(a.u.)	-1335.83327	-1335.83239	176.10
		$\langle S^2 \rangle$	2.320	1.223	
CAM-B3LYP/ 6-311++G(d,p)	1(a)	E(a.u.)	-1182.84108	-1182.84058	106.44
		$\langle S^2 \rangle$	2.261	1.235	
	1(b)	E	-1258.96336	-1258.96194	279.92
		$\langle S^2 \rangle$	2.453	1.340	
	1(c)	E(a.u.)	-1335.09014	-1335.08668	587.94
		$\langle S^2 \rangle$	2.824	1.529	

Table 5.2 The energy (a.u.),$\langle S^2 \rangle$ and magnetic exchange coupling constant (J in cm^{-1}) of the even cumulene based diradicals.

Diradicals			Triplet	BS	*J*
B3LYP/ 6-311++G(d,p)	2(a)	E(a.u.)	-1221.50674	-1221.51048	-1003.86
		$\langle S^2 \rangle$	2.119	1.302	
	2(b)	E	-1297.67951	-1297.68382	-1291.24
		$\langle S^2 \rangle$	2.137	1.404	
	2(c)	E(a.u.)	-1373.85534	-1373.86026	-1679.34
		$\langle S^2 \rangle$	2.156	1.513	
B3LYP-D/ 6-311++G(d,p)	2(a)	E(a.u.)	-1221.56528	-1221.56946	-1172.14
		$\langle S^2 \rangle$	2.118	1.335	
	2(b)	E(a.u.)	-1297.74438	-1297.74873	-1302.45
		$\langle S^2 \rangle$	2.137	1.406	
	2(c)	E(a.u.)	-1373.92099	-1373.92594	-1695.14
		$\langle S^2 \rangle$	2.156	1.515	
CAM-B3LYP/ 6-311++G(d,p)	2(a)	E(a.u.)	-1220.89356	-1220.90261	-3256.97
		$\langle S^2 \rangle$	2.226	1.616	
	2(b)	E(a.u.)	-1297.02294	-1297.03155	-3429.87
		$\langle S^2 \rangle$	2.253	1.703	
	2(c)	E(a.u.)	-1373.14718	-1373.15792	-6158.36
		$\langle S^2 \rangle$	2.296	1.913	

Table 5.3 The energy (a.u.),$\langle S^2 \rangle$ and magnetic exchange coupling constant (J in cm^{-1}) of the diradical based on conjugated systems.

Diradicals			Triplet	BS	*J*
B3LYP/ 6-311++G(d,p)	3(a)	E(a.u.)	-1222.77595	-1222.77989	-565.03
		$\langle S^2 \rangle$	2.117	1.225	
	3(b)	E	-1300.20673	-1300.20855	-450.12
		$\langle S^2 \rangle$	2.133	1.245	
	3(c)	E(a.u.)	-1377.63530	-1377.63681	-373.53
		$\langle S^2 \rangle$	2.147	1.264	
B3LYP-D/ 6-311++G(d,p)	3(a)	E(a.u.)	-1222.84466	-1222.84684	-536.49
		$\langle S^2 \rangle$	2.117	1.227	
	3(b)	E(a.u.)	-1300.27678	-1300.27863	-456.71
		$\langle S^2 \rangle$	2.133	1.247	
	3(c)	E(a.u.)	-1377.70835	-1377.70988	-379.74
		$\langle S^2 \rangle$	2.148	1.266	
CAM-B3LYP/ 6-311++G(d,p)	3(a)	E(a.u.)	-1222.17266	-1222.17652	-1029.03
		$\langle S^2 \rangle$	2.217	1.393	
	3(b)	E(a.u.)	-1299.55258	-1299.55564	-828.31
		$\langle S^2 \rangle$	2.249	1.439	
	3(c)	E(a.u.)	-1376.93172	-1376.93426	-699.12
		$\langle S^2 \rangle$	2.280	1.483	

Singlet and Triplet weightings[69] Considering a general BS state which is a nearly equal superposition of singlet (S) and triplet (T) states. We can write

$$\psi_{BS} = m\,\psi_S^{BS} + n\,\psi_T^{BS}$$

Where $m^2 \approx n^2 \approx 1/2$, $m^2 + n^2 = 1$ and $n^2 = 0.5\,\langle S^2 \rangle_{BS}$

Therefore $m^2 = 1 - 0.5\langle S^2 \rangle_{BS.}$ The net weights of singlet and triplet components in the BS solution are given in Table 5.4, Table 5.5, and Table 5.6.

Table 5.4 Percent Net Weight of Triplet and Singlet Components in the Computed BS Solution (B3LYP/6-311++G(d,p)). $\langle S^2 \rangle_{BS}$ values of series 1 diradicals are taken from ref 55.

System	singlet % weight ($100m^2$)	triplet % weight ($100n^2$)
1(a)	43.85	56.15
1(b)	41.70	58.30
1(c)	39.15	60.85
2(a)	34.90	65.10
2(b)	29.80	70.20
2(c)	24.35	75.65
3(a)	38.75	61.25
3(b)	37.75	62.25
3(c)	36.80	63.20

Table 5.5 Percent Net Weight of Triplet and Singlet Components in the Computed BS Solution (B3LYP-D/6-311++G(d,p)).

System	singlet % weight ($100m^2$)	triplet % weight ($100n^2$)
1(a)	43.80	56.20
1(b)	41.55	58.45
1(c)	38.85	61.15
2(a)	33.25	66.75
2(b)	29.70	70.30
2(c)	24.25	75.75
3(a)	38.65	61.35
3(b)	37.65	62.35
3(c)	36.70	63.30

Table 5.6 Percent Net Weight of Triplet and Singlet Components in the Computed BS Solution (CAM-B3LYP /6-311++G(d,p)).

System	singlet % weight ($100m^2$)	triplet % weight ($100n^2$)
1(a)	38.25	61.75
1(b)	33.00	67.00
1(c)	23.55	76.45
2(a)	19.20	80.80
2(b)	14.85	85.15
2(c)	4.35	95.65
3(a)	30.35	69.65
3(b)	28.05	71.95
3(c)	25.85	74.15

Factors affecting magnetic exchange coupling

The magnetic interaction depends on the distance *r* between the magnetic centers as *exp*(-*r*),[70] therefore for our designed systems one may expect a decrease in coupling constant value with the increase in the number of carbon atoms within the coupler (as the distance between radical centers also increases given in Table 5.7). But for odd-numbered cumulene series (1(a), 1(b), and 1(c)), the coupling constant is positive and increases in magnitude with the increase in number of carbon atoms in cumulene chain (shown in Figure 5.4). The relation is almost perfectly linear (R^2 =0.99, from regression analysis).

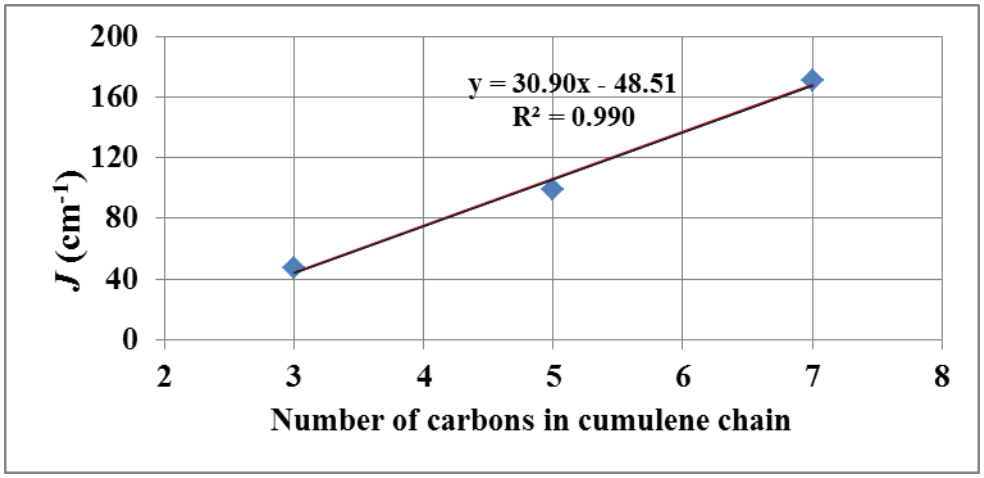

Figure 5.4 Plot of *J* (cm^{-1}) vs. number of carbon atoms in cumulene chain (regression analysis) for odd cumulene series (1(a), 1(b), and 1(c)) (using B3LYP/6-311++G(d,p)).

For even numbered cumulenes (2(a), (b), and (c)) the coupling constant also is linear with the increase in number of carbon atoms in cumulene chain (shown in Figure 5.5), but is negative, and larger in magnitude. The relation is almost perfectly linear (R^2 >0.99 from regression analysis).

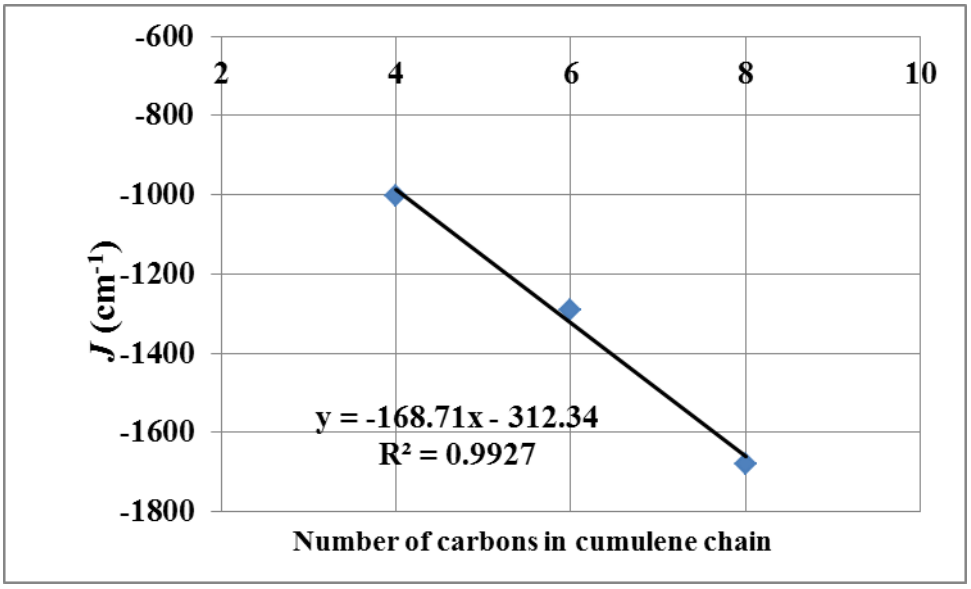

Figure 5.5 Plot of J (cm^{-1}) vs. number of carbon atoms in cumulene chain (regression analysis) for even cumulene series (2(a), (b), and (c)) (using B3LYP/6-311++G(d,p)).

Polo et al. have shown that the magnitude of J depends strongly on the planarity of the molecular structure of the diradical as more effective orbital overlap between the π-systems can thus be reached.[71] Shil et al. have also shown that when the coupler and the radical centers are in different planes, coupling between them decreases.[72] Therefore, there are certain factors (such as the distance between radical centers, spin polarization pathways, and the planarity of the molecular structure of the diradical), make it difficult to predict the values of J.

(i) Distance between radical centers *r* (in Å)

Table 5.7 Distance between radical centers r (in Å) (using B3LYP/6-311++G(d,p)).

System	*r* (in Å)	*J* (cm^{-1})	System	*r* (in Å)	*J* (cm^{-1})	System	*r* (in Å)	*J* (cm^{-1})
1(a)	4.256	47.66	2(a)	6.407	—1003.86	3(a)	6.989	—565.03
1(b)	5.790	99.09	2(b)	7.869	—1291.24	3(b)	9.263	—450.12
1(c)	7.873	171.28	2(c)	9.815	—1678.7	3(c)	11.391	—373.53

From the Table 5.7 it is clear that continuing from the smaller coupler to its higher homologues in each series, the distance between radical centers increases as expected. Therefore there should be a decrease in *J* values from smaller to the larger coupler as discussed earlier.[70] This trend is observed in the conjugated systems of series 3, but for cumulene couplers of series 1 and series 2, opposite result is found. This result clearly indicates that the magnitude of the coupling constant values not only depend on the distance between the radical centers but also on other factors which are discussed under subsequent points.

(ii) Spin density distribution on the coupler

The spin density of DFT based approach gives us an insight about the spin polarization mechanism for magnetic exchange coupling within the molecule. Hermann et al. have proposed that for cumulene systems (with even number of carbon centers), the spin delocalization onto the chain increases as the length of the chain gets longer.[73] From the spin density distribution plot of Figure 5.6 it is observed that for even cumulene based diradicals there is an accumulation of excess spin density on all the middle carbon atoms of the coupler i.e., along y and z direction collectively (represented by the red arrow). From Table 5.8 it is clear that the spin density on each carbon of the coupler and the average spin density increases with the increase in the length of the coupler. In our previous work we have shown that for odd cumulene based diradicals, a large accumulation of spin density within the coupler occurs due to the presence of two π-electrons at a time on each sp-carbon atom of the coupler,[55] and this also occurs for even cumulene based diradicals.

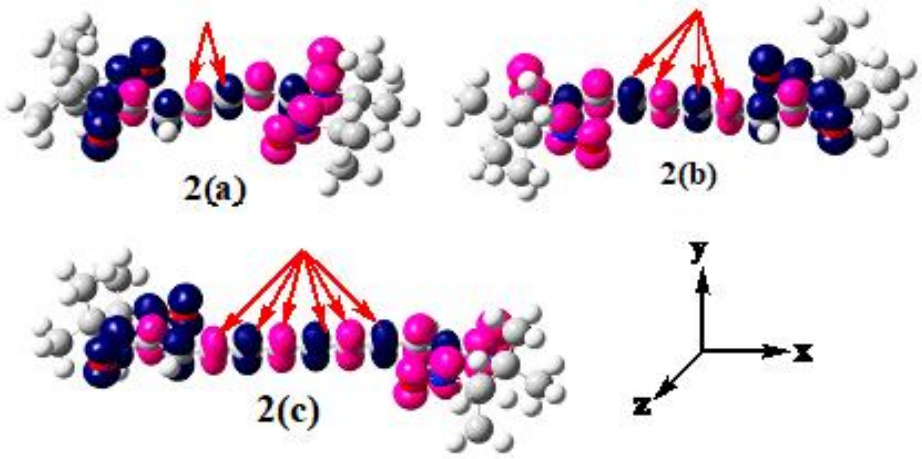

Figure 5.6 Spin density plot for the even cumulene based diradicals (series 2) in their BS states (B3LYP/6-311++G(d,p)) (iso value 0.004), magenta and blue colors represent the α and β spins respectively. Red arrow represents the carbons with excess spin density.

Table 5.8 Spin density distribution on each atom of the coupler of even cumulene-based diradicals in their BS state (B3LYP/6-311++G(d,p)).

System	Spin density on different atoms of coupler								Average spin density on each atom of the coupler
	C_1	C_2	C_3	C_4	C_5	C_6	C_7	C_8	
2(a)	0.2260	-0.2082	0.2082	-0.2260	-------	---------	--------	---------	0.2171
2(b)	0.2407	-0.2274	0.2484	-0.2484	0.2274	-0.2407	--------	---------	0.2388
2(c)	0.2630	-0.2510	0.2620	-0.2123	0.2123	-0.2619	0.2510	-0.2630	0.2471

But in case of conjugated systems spin density of the coupler is distributed in one direction only i.e., along y direction only (shown in Figure 5.7) and with the increase in length of the coupler, a decrease in average spin density is observed from Table 5.9. Therefore, spin density is one of the major factors that results the ultimate increases in *J* values for diradicals based on cumulene systems and decreases for diradicals based on conjugated couplers with the increase in number of carbon atoms of the coupler.

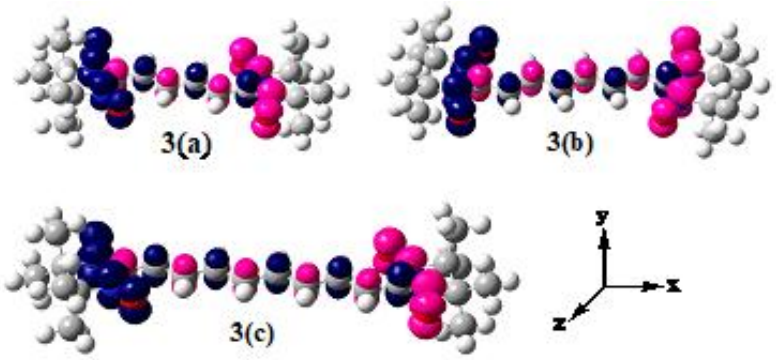

Figure 5.7 Spin density plot for the diradical based conjugated systems (series 3) in their BS states (B3LYP/6-311++G(d,p)) (iso value 0.004), magenta and blue colors represent the α and β spins respectively.

Table 5.9 Spin density distribution on each atom of the coupler of diradical based on conjugated systems in their BS state (B3LYP/6-311++G(d,p)).

System	Spin density on different atoms of coupler								Average spin density on each atom of the coupler
	C_1	C_2	C_3	C_4	C_5	C_6	C_7	C_8	
3(a)	0.1845	-0.1637	0.1637	-0.1845	--------	---------	--------	-------	0.1741
3(b)	0.1607	-0.1596	0.1342	-0.1342	0.1596	-0.1607	--------	-------	0.1515
3(c)	0.1704	-0.1639	0.1278	-0.1335	0.1335	-0.1278	0.1651	-0.1706	0.1491

(iii) Dihedral angle

The cumulenes – (C_n) – (where n either even or odd number of carbon atoms) have two orthogonal π-systems, while the conjugated systems – $(HC{=}CH)_k$ – have only one π-orbital (with k taking values 2, 3, and 4). For cumulene systems with nitronyl nitroxide end groups, the two types of perpendicular π-interactions are represented by red and blue arrows (in Figure 5.8(a) and (b)), whereas for conjugated systems only one π-interaction is shown by blue arrow (in Figure 5.8(c)). In odd cumulene based diradicals (Figure 5.8(a)), the extent of π-interaction between cumulene chain and the radical end groups are lower compared to the π-interaction in even cumulene based diradicals (Figure 5.8(b)). This is because for odd cumulenes, each type of π-interaction (represented by red/blue arrow in Figure 5.8(a)) can conjugate with one radical site at a time but not with the both radical end groups (as the two radical centers are not in same plane). But for even cumulene systems (Figure 5.8(b)), among the two π -interactions of the cumulene chain, one π -system (the π-interaction is represented by blue arrow) extends the length of the cumulene skeleton and can conjugate with both sides of end groups (Figure 5.8(b), where the two radical centers are in same plane).[36] Therefore for odd cumulene based diradicals, the perpendicular plane between two radical centers causes a small magnitude of coupling constant, but for even cumulene based diradicals, the planarity of two radical centers causes large magnitude of coupling constant values.

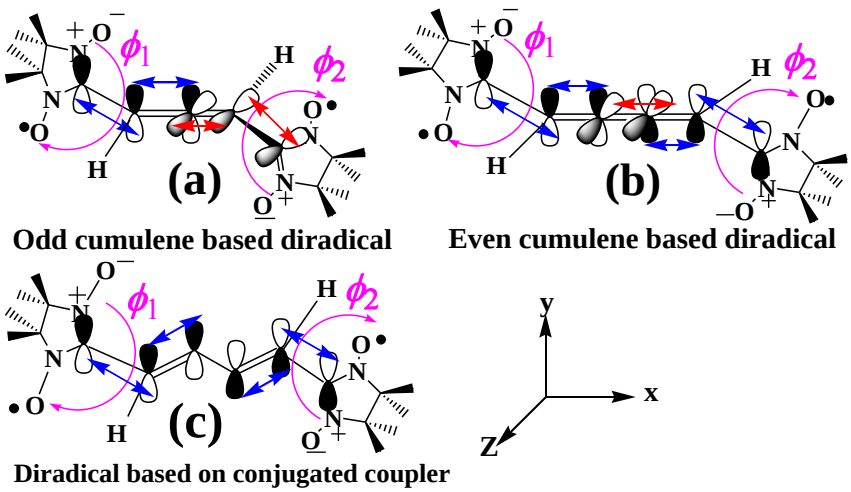

Figure 5.8 π-interaction of diradical based on cumulene and conjugated couplers. $\varphi_1$and φ_2 denote the dihedral angle between the plane of coupler and that of the nitronyl nitroxide radicals (blue arrow represents one π-interaction (i.e, overlap between p_y-p_y orbitals) and red arrow represents another π-interaction (i.e, p_z-p_z orbitals)). We have taken a representative figure from each series. (a) represents π-interaction of odd cumulene based diradicals, (b) represents π-interaction of even cumulene based diradicals, (c) represents π-interaction of diradical based on conjugated systems.

For even cumulene couplers, as the distance between radical sites increases the interaction may be expected to decline. However the increase in average spin density within the cumulene connector enhances the interaction. The net effect is small. For diradical based on conjugated couplers, there is only one π-interaction that can conjugate with both sets of end groups (shown in Figure 5.8(c)), but the increase in distance as well as the decrease in spin density within the coupler cause overall decrease in *J* value with increase in chain length of the coupler. Therefore, as a whole the π-interaction is the enlightening factor that controls the magnetic property of our designed systems.

5.3.2 Coherent electron transport through diradicals

Cumulene wires are known to be the potential candidates in nano-electronic applications.[74] Prasongkit et al. have theoretically studied the conductivity of cumulene based molecular wires and showed that all cumulenes yield higher conductance compared to other conjugated polymers, and for the odd-cumulene wires the conductance is still higher than that of even-cumulene wires as well as polyynes.[74] They also showed that the conductance of odd-cumulenes do not exhibit any marked dependence on the molecular length. However, Kondo et al. show an exponential decrease of transmission for oligo (p-phenylene) dithiolate wires with the increase in distance between two leads.[75] Apart from polyyne and cumulene systems, the polyene systems have a series of alternating single and double bonds through which transmission is possible.[76]

Magnetic molecules have wide applications in the field of spintronics.[77] In recent times organic radicals capable of constructing the spintronic devices like spin valves, spin filters, etc. are reported.[78] In order to design a diradical based electronic device it is important to understand the transport properties of the diradicals. Though much study has been made over the conductivity of cumulenes, in this section we try to understand the qualitative trend of transport property of the chiral cumulene based diradicals from our previous work[55] and the diradicals based on achiral cumulene and conjugated systems studied here. Schematic representations of the systems on which the transport property have been studied are given in Figure 5.9. Our comparison is based on the relative positions of transmission spectra with respect to each other, rather than on their absolute positions with respect to Fermi level of gold cluster. Therefore the addition of polyacetylene chain (spacer groups, containing 4 carbon atoms) at both ends of the cumulene and conjugated systems does not affect the transport property of the molecules under investigation because the acetylenic chains are conducting (also the relative positions of transmission spectra is not affected by the atom number of the electrode).

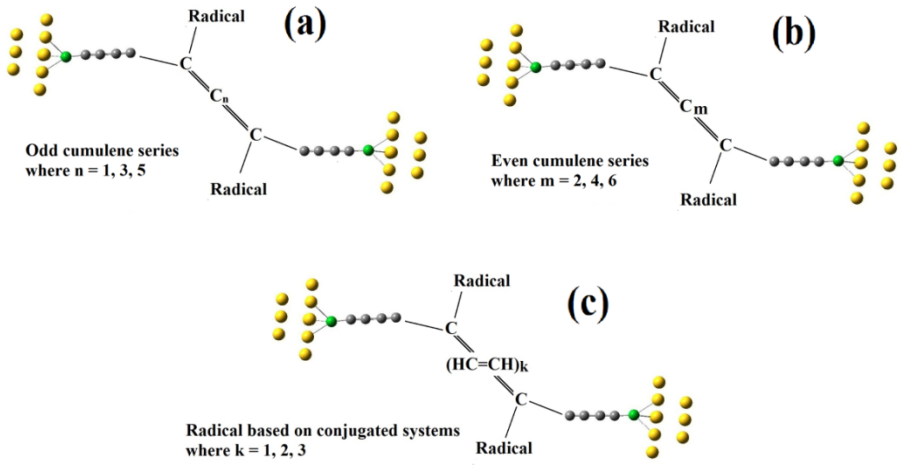

Figure 5.9 Schematic representation for the radical based systems on which the transport property have been studied.

For our designed systems (in Figure 5.9), the zero bias transmission spectra of the diradicals are given in Figure 5.10 (for α spin only). Usually the Fermi energy of bulk gold (−5.5 eV) is assumed,[79] but a Fermi energy of −5.0 eV is taken from DFT calculations.[80] For our calculation the Fermi energy is chosen to be −5.0 eV and marked with a dashed line in Figure 5.10 (therefore, when we compare the transmission spectra of our designed molecules, the shift in Fermi energy should be same for all the molecules with respect to Fermi level of gold cluster (-5 eV) and thus not affect qualitative comparisons based on the relative positions of transmission spectra of all the molecules with respect to each other). It is clear from Figure 5.10 that with the increase in length of the odd cumulene chains from [3]- to [5]-cumulene based diradicals and from [5]- to [7]- cumulene based diradicals (the number within the bracket represents the number of carbon atoms of the couplers within the two radical centers) the transmission decreases at the Fermi level (Figure 5.10(a)), but for even cumulene based diradicals from [4]- to [6]-cumulenes, transmission increases and after that (from [6]- to[8]-cumulene based diradicals) transmission value remains almost constant at the Fermi level (Figure 5.10(b)). Therefore, diradicals based on odd and even cumulene couplers show different characteristics of transmission. Moreover, Prasongkit et al. have shown that cumulene wire with odd number of carbon atoms gives higher transmission than that of the even one,[74] results from the high density of states of odd cumulene chains in lowest unoccupied molecular orbital levels that spans the Fermi level of the electrodes. But our calculation of cumulene based diradical shows the opposite trend (i. e., with the increase in length of the cumulene chain, even cumulene based diradicals have higher transmission compared to that of odd cumulene based diradicals). This is possibly due to the addition of radical within the cumulene systems. On the other hand transmission remains almost constant for diradical based on conjugated systems at the Fermi level marked with a dashed line at −5.0 eV (Figure 5.10(c)). For all of our designed systems, there is no difference

between α (in Figure 5.10) and β spin transmission (in Figure 5.11); therefore they have no spin filtering ability.

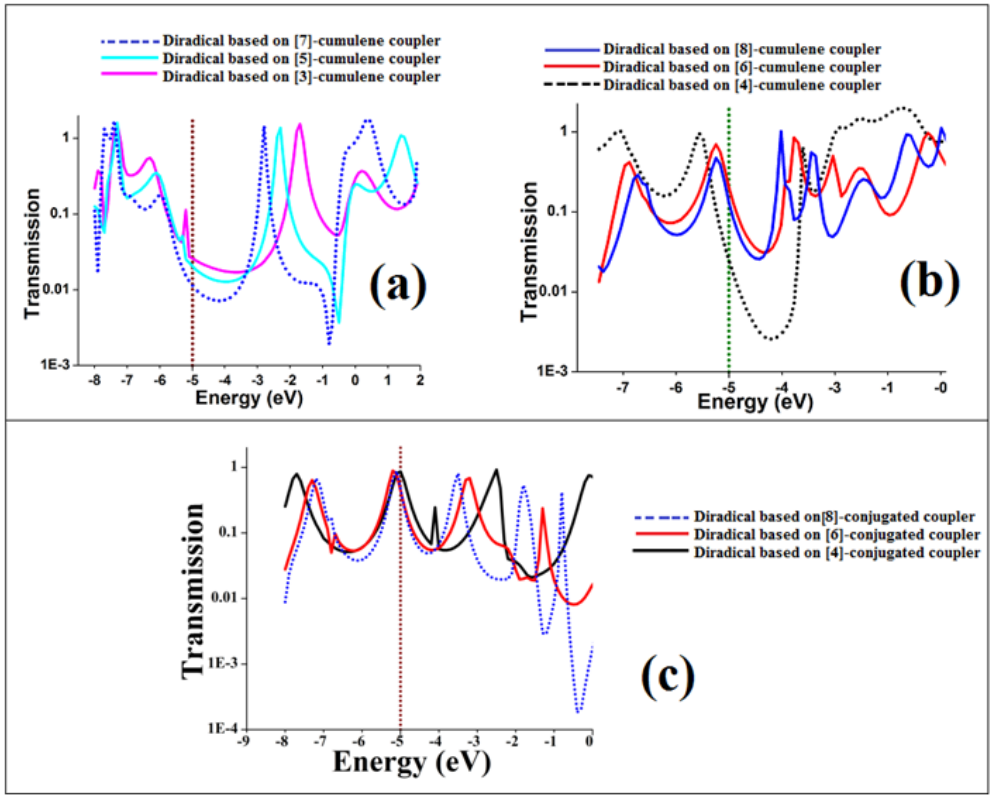

Figure 5.10 Transmission spectra of all the designed diradical based molecular wires (for α spin). (The transmission is expressed using a log scale). (a) represents the transmission spectra of odd cumulene based diradicals, (b) represents the transmission spectra of even cumulene based diradicals, (c) represents the transmission spectra of diradical based on conjugated systems.

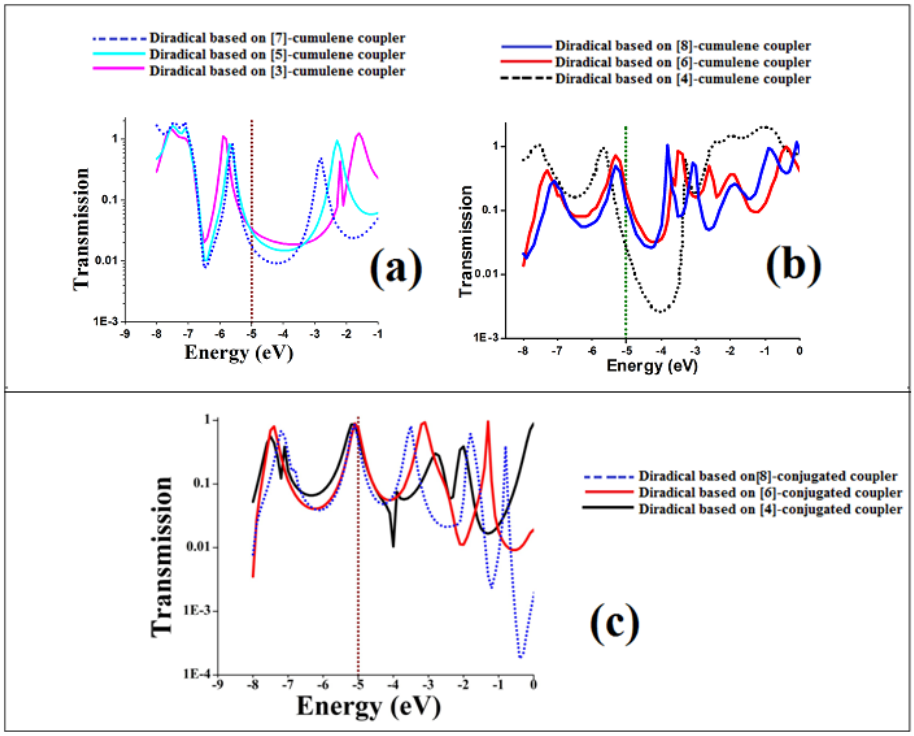

Figure 5.11 Transmission spectra of all the designed diradical based molecular wires (for β spin). (The transmission is expressed using a log scale). (a) represents the transmission spectra of odd cumulene based diradicals, (b) represents the transmission spectra of even cumulene based diradicals, (c) represents the transmission spectra of diradicals based on conjugated systems.

In order to understand the role of radical substitution on the transport property qualitatively, we have calculated the zero bias transmission spectra of cumulene and conjugated systems without radical centers shown in Figure 5.12.

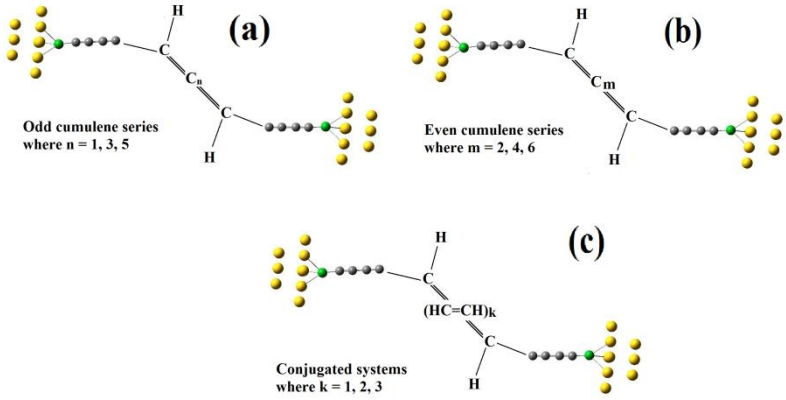

Figure 5.12 Schematic representations for the systems without radical centers on which the transport property have been studied.

For our designed systems without radical centers (in Figure 5.12), the zero bias transmission spectra are given in Figure 5.13.

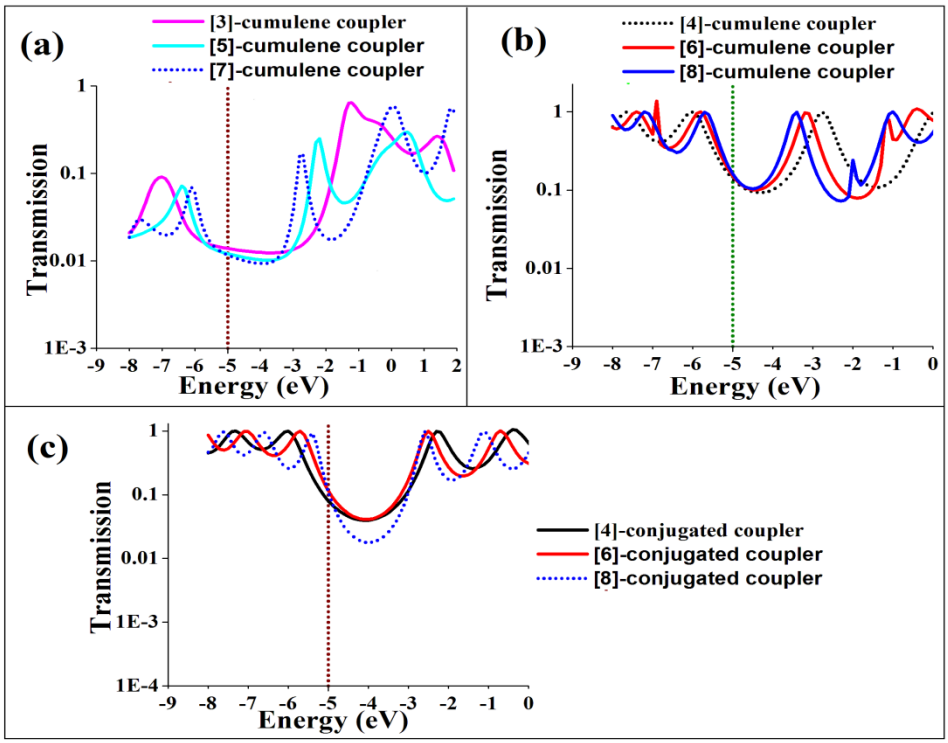

Figure 5.13 Transmission spectra of all the designed molecular wires without radical centers. (The transmission is expressed using a log scale). (a) represents transmission spectra of bare odd cumulene systems, (b) represents transmission spectra of bare even cumulene systems, and (c) represents transmission spectra of bare conjugated systems.

When we compare the results of diradical based systems (Figure 5.10(a) and Figure 5.10(b)) with that of bare systems (Figure 5.13(a) and Figure 5.13(b)); it is observed that, there is a variation in transmission with the increase in length of the odd and even cumulene based diradicals (in Figure 5.10(a) and Figure 5.10(b)), but for systems without radical centers (Figure 5.13(a), Figure 5.13(b)), the transmission remains constant at the Fermi level. Comparing the transmission value for diradicals based on conjugated systems with that of bare systems, it is found that for each set of molecules there is no variation of transmission values with the increase in chain length of the coupler. However, a higher transmission value is observed in case of radical based systems (Figure 5.10(c)) compared to bare systems (Figure 5.13(c)) at the Fermi level marked with a dashed line at −5.0 eV. Therefore, there is a contribution of radical substitution on the transport property.

Factors affecting transmission in radical substituted systems

(i) HOMO-LUMO energy gap

It is well known that the highest occupied molecular orbital (HOMO) and the lowest unoccupied molecular orbital (LUMO) play central roles for the transport properties[81-85] and the Fermi levels reside somewhere in between the HOMO and the LUMO. Schlicke et al. have proposed that if two radical centers are perpendicular to each other and also to the coupler, there is a loss of conjugation in between them, and that is reflected with an increase of the HOMO–LUMO gap, and further contributes to the low conductance.[86] Proppe et al. have suggested that in case of polyene systems the transmission increases at the Fermi level if there is a closer proximity of the HOMO energy and the Fermi energy.[87] Choi et al. showed that the molecular orbitals of a molecule with electrode atoms as well as without electrode atoms have similar orbital characteristics.[88] Therefore the transmission properties of a molecule between two electrodes can be manipulated by using our designed diradical systems (in Figure 5.1) without the gold electrodes. Hermann et al. also have shown that for cumulene based systems containing even number of carbon centers, the α-HOMO – α-LUMO gaps decreases with the increase in carbon chain length.[89] For our designed systems the frontier orbital energy are shown in Table 5.10 and Table 5.11. It is evident from these tables that, with the increase in the number of carbon atoms of the couplers in each series, frontier orbital energy splitting decreases gradually. Therefore an increase in transmission with the increase in number of carbon atoms in each series is expected. But from the transmission curve (Figure 5.10) it is clear that although the transmission characteristics show a predictable result to some extent for diradical based on even cumulene series, for diradical based on odd cumulenes and diradical based on conjugated systems the scenario is different. Hence, there must be some other factors guiding the situation.

Table 5.10 Energy (in eV) of $(HOMO-2)_\alpha$, $(HOMO-1)_\alpha$, $(HOMO)_\alpha$ and $(LUMO)_\alpha$ and Energy difference between $HOMO_\alpha$–$LUMO_\alpha$ (ΔE_{HL} in eV) for diradical based on odd cumulenes (B3LYP/6-311++G(d,p)) (taken from reference 55).

Systems	$(E_{HOMO-2})_\alpha$	$(E_{HOMO-1})_\alpha$	$(E_{HOMO})_\alpha$	$(E_{LUMO})_\alpha$	ΔE_{HL}
1(a)	-6.89275	-5.29989	-5.29309	-1.58143	3.71
1(b)	-6.54971	-5.39002	-5.38653	-2.36083	3.03
1(c)	-6.29637	-5.47614	-5.47329	-2.83002	2.64

Table 5.11 Energy (in eV) of $(HOMO-1)_{\alpha}$, $(HOMO)_{\beta}$, $(HOMO)_{\alpha}$ and $(LUMO)_{\alpha}$ and Energy difference between $HOMO_{\alpha}$–$LUMO_{\alpha}$ (ΔE_{HL} in eV) for diradical based on even cumulene and conjugated couplers (B3LYP/6-311++G(d,p)).

Systems	$(E_{HOMO-1})_{\alpha}$	$(E_{HOMO})_{\alpha}$	$(E_{HOMO})_{\beta}$	$(E_{LUMO})_{\alpha}$	ΔE_{HL}
2(a)	-5.98562	-5.43414	-5.43414	-2.71938	2.71
2(b)	-5.90437	-5.51172	-5.51172	-3.06425	2.45
2(c)	-5.85536	-5.57901	-5.57901	-3.29603	2.28
3(a)	-5.92453	-5.39471	-5.39471	-2.40915	2.99
3(b)	-5.71577	-5.38513	-5.38511	-2.56017	2.82
3(c)	-5.54832	-5.36897	-5.37308	-2.66809	2.70

(ii) Distance between leads (considering the distance between sulfur atoms)

In order to study the transmission characteristics, the sulfur atoms may be provided to connect the diradical based molecular wires into the close proximity of the gold electrode, so that the molecular wire can electronically couple to the electrode providing an electrode-sulfur—molecular wire-sulfur-electrode tunneling pathway. Therefore if the distance between two electrodes is small, a better transmission should be expected. For our designed systems the distances between two leads (i.e. between the sulfur atoms) are given in Table 5.12. It is found that, for both odd and even cumulene based diradicals as well as for diradical based on conjugated coupler, with the increase in number of carbon atoms, the distance between two sulfur atoms increases gradually. As a result, there should be a decrease in transmission value with the increase in distance between two electrodes for each series. But the transmission value shows different characteristics for each series. Therefore the two different factors (distance between two leads and the HOMO-LUMO energy gap) affect the transmission. For radical based on conjugated systems two factors counterbalance each other and ultimately a constant transmission value results (in Figure 5.10 (c)).

Table 5.12 Distance between two leads (in Å) (considering the distance between two sulfur atoms).

Systems	Distance between two leads (in Å)	Systems	Distance between two leads(in Å)	Systems	Distance between two leads(in Å)
1(a)	11.33	2(a)	15.53	3(a)	14.82
1(b)	13.32	2(b)	16.97	3(b)	15.72
1(c)	14.52	2(c)	18.56	3(c)	16.59

If the conjugation between the lead and the molecular region is better, higher transmission should be expected. At the same time, greater the distance between S and the rest of the molecular region, lower should be the transmission due to the lower possibility of tunneling of electrons from gold lead to molecular region and *vice versa*. For that reason the distance between S and nearest C has been considered. Though the S-C bond distance for even cumulene based diradicals and diradical based on conjugated systems are equal i.e., 1.68 Å (Figure 5.14 and Figure 5.15), from Figure 5.16 shows that for [3]-cumulene based diradicals as well as for [5]-cumulene based diradicals, the distance between S and C is 1.69Å i.e., remain unaltered, but for [7]-cumulene based diradicals the distance between S and C is 1.74 Å, hence there should be a decrease in transmission, that satisfies the transmission characteristics i.e., a decrease in transmission in [7]- cumulene based diradical systems (in Figure 5.10(a)).

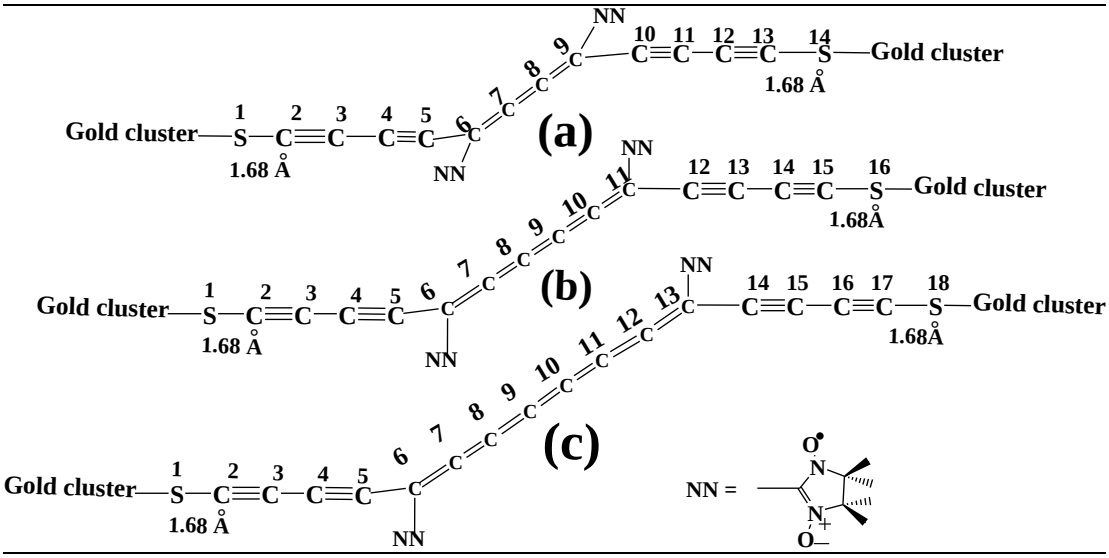

Figure 5.14 Designed even cumulene based molecular wires for the transport calculation.

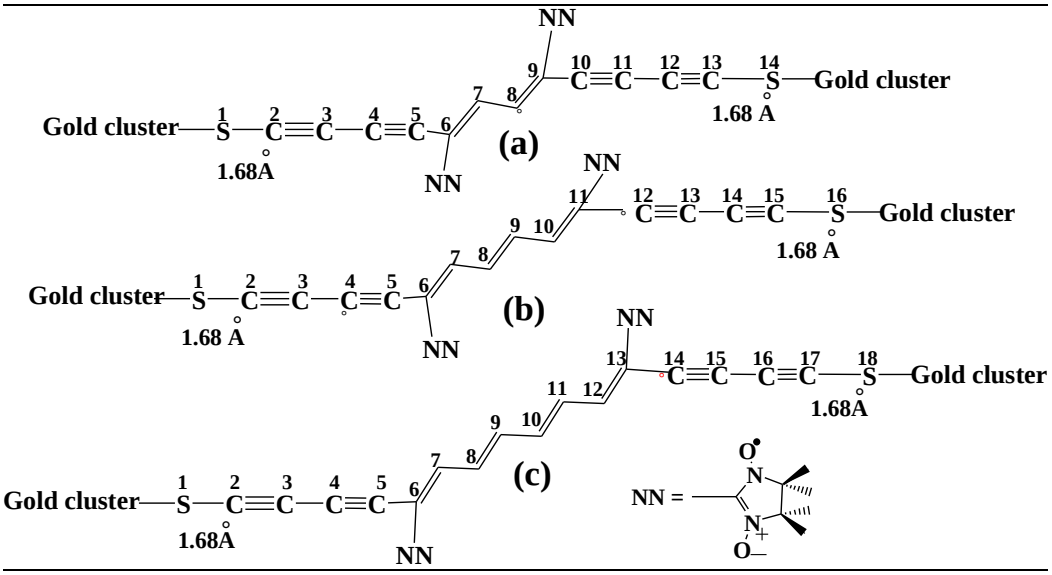

Figure 5.15 Designed conjugated system based molecular wires for the transport calculation.

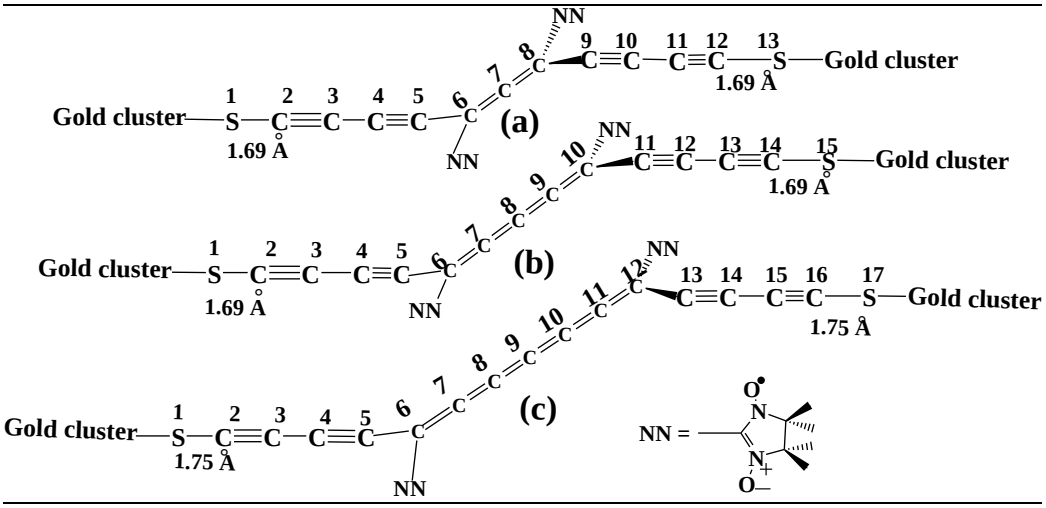

Figure 5.16 Designed odd cumulene based molecular wires for the transport calculation.

(iii) Spin density distribution within the coupler and radical centers

The spin density distributions of the molecular wires attached to the leads are given in Figure 5.17, Figure 5.18, and Figure 5.19.

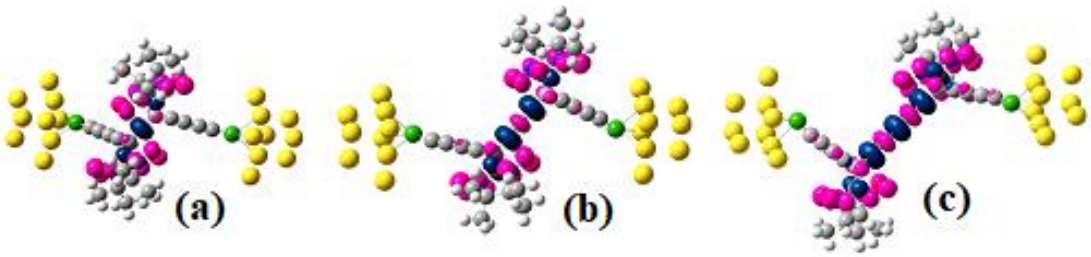

Figure 5.17 Spin polarization pathways within the odd cumulene based molecular wires (iso value 0.004). (a) represents the spin density distribution within allene based molecular wire, (b) represents the spin density distribution within cumulene (containing 5 carbon atoms) based molecular wire, (c) represents the spin density distribution within cumulene (containing 7 carbon atoms) based molecular wire.

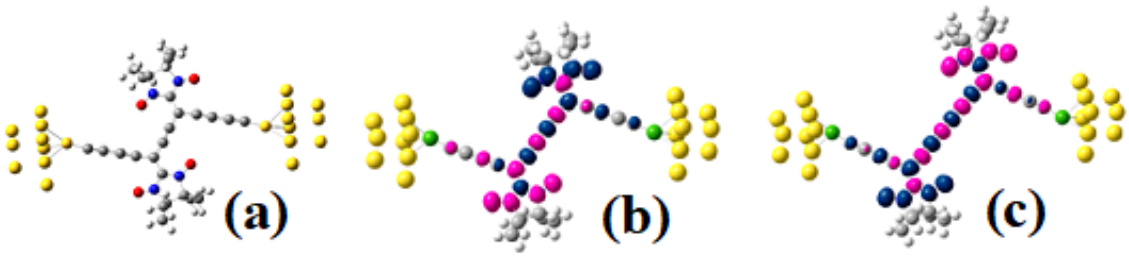

Figure 5.18 Spin polarization pathways within the even cumulene based molecular wires (iso value 0.004). (a) represents the spin density distribution within cumulene (containing 4 carbon atoms) based molecular wire, (b) represents the spin density distribution within cumulene (containing 6 carbon atoms) based molecular wire, (c) represents the spin density distribution within cumulene (containing 8 carbon atoms) based molecular wire.

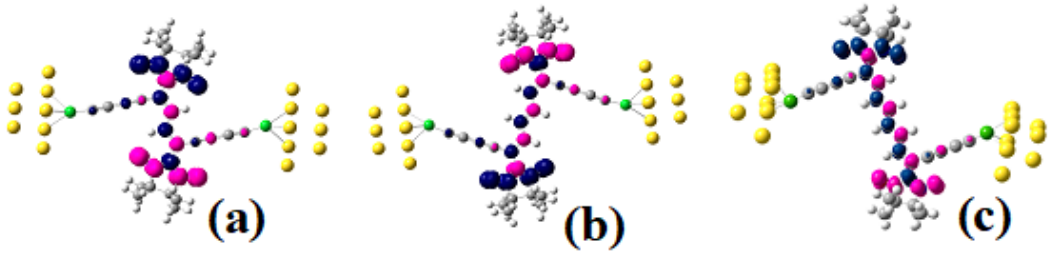

Figure 5.19 Spin polarization pathways within the molecular wires based on conjugated couplers (iso value 0.004). (a) represents the spin density distribution within conjugated systems (containing 4 carbon atoms) based molecular wire, (b) represents the spin density distribution within conjugated systems (containing 6 carbon atoms) based molecular wire, (c) represents the spin density distribution within conjugated systems (containing 8 carbon atoms) based molecular wire.

Figure 5.18 presents some interesting observation that needs further discussion. There seems to be no spin amplitude in the [4]-cumulene fragment in Figure 5.18 (a) but there is substantial amplitude along the chains of length [6]- and [8]-cumulene connector (Figure 5.18 (b) and Figure 5.18 (c)). The spin alternation rule predicts the alpha spin at a radical site will induce beta spin at a neighboring C, alpha at the next and so forth. If two alternating-spin patterns emanating from distinct sites interfere constructively then there will be strong amplitude along the connecting path, and if the interference is destructive there would be no amplitude. As a result of overall destructive interference in Figure 5.18 (a) a diamagnetic situation arises, whereas, in other cases constructive interference occur and high spin amplitude is observed in antiferromagnetic situation (in Figure 5.18(b), Figure 5.18(c)). Such systems can be exploited as logic gates in spintronic applications.[90] Therefore for the system represented in Figure 5.18(a) there occur a spin quenching when such systems are attached to the leads. Thus, an ultimate decrease in transmission in [4]-cumulene based diradicals is observed and a correlation of spin polarization and the transmission characteristics of our designed systems can be intuited.

So, it can be surmised that there are different guiding factors such as the HOMO-LUMO energy gap, distance between two leads as well as the spin polarization that causes the ultimate transmission characteristics in molecular junction transport. The preference of one factor over other causes an increase or decrease in transmission. Finally the origin of all the factors is the unusual π-interaction within the couplers that produce different transmission characteristics of our designed systems.

5.4 Conclusion

To sum up, there is a variation in *J* values for diradicals based on odd cumulene series, diradicals based on even cumulene series and diradicals based on conjugated couplers. It has been found that an existence of distinctive spin polarization pathway in cumulene systems (compared to conjugated systems), distance between two radical centers (that may possibly interrupt the spin polarization pathway) and a planar structure that allows better orbital overlap between π-systems compared to a non planar one, controls the magnetic exchange coupling constant values. Largely speaking, the unusual π-interaction within the coupler is the enlightening factor that controls the magnetic properties of our designed systems. It is also found that the frontier energy splitting, distance between two electrodes and the spin polarization pathways play a major role in determining transmission characteristics of our designed systems.

5.5 References

(1) Kahn, O. Molecular Magnetism. VCH, New York, **1993**.
(2) Lahti, P. M. Magnetic Properties of Organic Materials, Marcel Dekker, New York, **1999**.
(3) Kobayashi, H.; Kobayashi, A.; Cassoux, P. *Chem. Soc. Rev*. **2000**, *29*, 325.
(4) Uji, S.; Shinagawa, H.; Terashima, T.; Yakabe, T.; Terai, Y.; Tokumoto, M.; Kobayashi, A.; Tanaka, H.; Kobayashi, H. *Nature,* **2001**, *410*, 908.
(5) Matsuda, K.; Matsuo, M.; Irie. M. *J. Org. Chem.,* **2001**, *66*, 8799.
(6) Tanifuji, N.; Irie, M.; Matsuda. K. *J. Am. Chem. Soc*.**2005**, *127*, 13344.
(7) Prinz, G. A. *Science*, **1998**, ***282***, 1660.
(8) Emberly, E. G.; Kirczenow, G. *Chem. Phys*. **2002**, *281*, 311.
(9) Wang, F.; Vardeny. Z. V. *J. Mater. Chem.* **2009**, *19*, 1685.
(10) Michelfeit, M.; Schmidt, G.; Geurts, J.; Molenkamp, L. W. *Phys. Status Solidi*, **2008**, *205*, 656.
(11) Nguyen, T. D.; Ehrenfreund, E.; Vardeny, Z. V. *Science,* **2012**, *337*, 204.
(12) Yoo, J. W.; Chen, C. Y.; Jang, H. W.; Bark, C. W.; Prigodin, V. N.; Eom, C. B.; Epstein, A. J. *Nat. Mater.* **2010**, *9*, 638.
(13) Herrmann, C.; Elmisz, J. *Chem. Commun.* **2013**, *49*, 10456.
(14) Eng, M. P.; Albinsson, B. *Angew. Chem., Int. Ed.* **2006**, *45*, 5626.
(15) Wenger. O. S. *Acc. Chem. Res.,* **2011**, *44*, 25.
(16) Nitzan, A.; Ratner, M. A. *Science,* **2003**, *300*, 1384.
(17) Tao, N. J. *Nat. Nanotechnol.,* **2006**, *1*, 173.
(18) Park, B. G.; Wunderlich, J.; Martí, X.; Holý, V.; Kurosaki, Y.; Yamada, M.; Yamamoto, H.; Nishide, A.; Hayakawa, J.; Takahashi, H.; Shick, A. B.; Jungwirth, T. A. *Nat. Mater.,* **2011**, *10*, 347.

(19) Tour, J. M. *Acc. Chem. Res.*, **2000**, *33*, 791.
(20) Winkler, J. R.; Gray, H. B. *J. Am. Chem., Soc*. **2014**, *136*, 2930.
(21) Liu, H.; Wang, N.; Zhao, J.; Guo, Y.; Yin, X.; Boey, F. Y.C.; Zhang, H. *Chem. Phys. Chem*., **2008**, *9*, 1416.
(22) Khoo, K. H.; Chen, Y.; Li, S.; Quek, S. Y. *Phys. Chem. Chem. Phys.*, **2015**, *17*, 77.
(23) Zhao, X. L.; Ando, Y.; Liu, Y.; Jinno, M.; Suzuki, T. *Phys. Rev. Lett.* **2003,** *90*, 187401.
(24) Muramatsu, H.; Hayashi, T.; Kim, Y. A.; Shimamoto, D.; Endo, M.; Terrones, M.; Dresselhaus, M.S. *Nano. Lett*. **2008**, *8*, 237.
(25) Kitaura, R.; Nakanishi, R.; Saito, T.; Yoshikawa, H.; Awaga, K.; Shinohara, H. *Angew. Chem., Int. Ed.*, **2009**, *48*, 8298.
(26) Tobe, Y.; Wakabayashi, T. in *Acetylene Chemistry: Chemistry, Biology, and Material Science* (Eds.: F. Diederich, P. J. Stang, R. R. Tykwinski), Wiley-VCH, Weinheim, **2005**, pp. 387.
(27) Chalifoux, W. A.; Tykwinski, R. R. *Chem. Rec.*, **2006**, *6*, 169.
(28) Shi Shun, A. L. K.; Tykwinski, R. R. *Angew. Chem. Int,. Ed.* **2006**, *45*, 1034.
(29) Raton, B. Polyynes: Synthesis, Properties, and Applications; Cataldo, F. (Eds); Taylor & Francis, **2005.**
(30) Ma, S. *Acc. Chem. Res*. **2009**, *42*, 1679.
(31) Smadja. W. *Chem. Rev*. **1983**, *83*, 263.
(32) Zhang, Y.; Su, Y.; Wang, L.; Kong, E. S.-W.; Chen, X.; Zhang, Y. A. *Nanoscale Research Letters*, **2011**, *6*, 577.
(33) Gu, X.; Kaiser,R. I.; Mebel, A. M. *Chem. Phys. Chem.*, **2008**, *9*, 350.
(34) Weimer, M.; Hieringer, W.; Sala, F. D.; Gçrling, A. *Phys.*, **2005**, *309*, 77.
(35) Skibar, W.; Kopacka, H.; Wurst, K.; Salzmann, C.; Ongania, K. H.; Biani, F. F. D. ; Zanello, P. ; Bildstein, B. *Organometallics*, **2004**, *23*, 1024.
(36) Januszewski, J. A. ; Tykwinski, R.R. *Chem. Soc. Rev.*, **2014**, *43*, 3184.
(37) Januszewski, J. A. ; Wendinger, D.; Methfessel, C. D.; Hampel, F.; Tykwinski, R. R. *Angew. Chem. Int. Ed.*, **2013**, *52*, 1817.
(38) Bhattacharya, D.; Misra, A. *J. Phys. Chem. A*. **2009**, *113*, 5470.
(39) Bhattacharya, D.; Shil, S.; Misra, A.; Klein, D. J. *Theor. Chem. Acc*., **2010**, *127*, 57.
(40) Shil, S.; Sarbadhikary, P.; Misra, A. *RSC Adv*., **2016**, 6, 99467.
(41) Paul, S.; Misra, A. *J. Chem. Theory Comput.* **2012**, *8*, 843.
(42) Paul,S.; Misra, A. *J. Phys. Chem. A.***2010**, *114*, 6641.
(43) Ali, Md. E.; Datta, S. N. *J. Phys. Chem. A.* **2006**, *110*, 2776.
(44) Ko, K. C.; Cho, D.; Lee, J. Y. *J. Phys. Chem. A.* **2013**, *117*, 3561.
(45) Cho, D.; Ko, K.C.; Ikabata, Y.; Wakayama, K.; Yoshikawa, T.; Nakai, H.; Lee, J. Y. *J. Chem. Phys.* **2015**, *142*, 024318.
(46) Nam,Y.; Cho, D.; Lee, J. Y. *J. Phys. Chem. C* **2016**, *120*, 11237.
(47) Cho, D.; Ko, K. C.; Park, H.; Lee, J. Y. *J. Phys. Chem. C* **2015**, *119*, 10109.
(48) Cho, D.; Ko, K. C.; Lee,J. Y. *Int. J. Quant. Chem.* **2016**, *116*, 578.
(49) Ko, K. C.; Cho, D.; Lee, J. Y. *J. Phys. Chem. A* **2012**, *116*, 6837.

(50) Ko, K. C.; Son, S. U.; Lee, S. ; Lee, J. Y. *J. Phys. Chem. B* **2011**, *115*, 8401.
(51) Cho, D.; Ko, K. C.; Lee, J. Y. *J. Phys. Chem. A* **2014**, *118*, 5112.
(52) Ko, K. C.; Park, Y. G.; Cho, D.; Lee, J. Y. *J. Phys. Chem. A* **2014,** *118*, 9596.
(53) Song, M.; Song, X.; Bu, Y. *Chem. Phys. Chem.*, **2017**, *18*, 2487.
(54) Song, M.; Song, X.; Bu, Y. *J. Phys. Chem. C* **2017**, *121*, 21231.
(55) Sarbadhikary, P.; Shil, S.; Panda, A.; Misra, A. *J. Org. Chem,* **2016**, *81*, 5623.
(56) Tamura, M. ; Nakazawa, Y.; Shiomi, D.; Nozawa, K.; Hosokoshi, Y. ; Ishikawa, M.; Takahashi, M. ; Kinosita, M. *Chem. Phys. Lett.*, **1991**, *186***,** 401.
(57) Noodleman, L. *J. Chem. Phys.*, **1981**, *74*, 5737.
(58) Noodleman, L.; Baerends, E. *J. Am. Chem. Soc.*, **1984**, *106*, 2316.
(59) Noodleman, L.; Davidson, E. R. *Chem. Phys.***1986**, *109*, 131.
(60) Noodleman, L.; Peng, C. Y.; Case, D. A.; Mouesca, J. M. *Coord. Chem. Rev.*, **1995**, *144*, 199.
(61) Yamaguchi, K.; Fukui, H.; Fueno, T.*Chem. Lett.* **1986**, *15*, 625.
(62) Yamaguchi, K.; Takahara, Y.; Fueno, T.; Nasu, K. *Jpn. J. Appl. Phys.*, **1987**, *26*, L1362.
(63) Yamaguchi, K.; Jensen, F.; Dorigo, A.; Houk, K. N. *Chem. Phys. Lett.*, **1988**, *149*, 537.
(64) Yamaguchi, K.; Takahara, Y.; Fueno, T.; Houk, K. N. *Theor. Chim. Acta*, **1988**, *73*, 337.
(65) Frisch, M. J.; Trucks, G. W.; Schlegel, H. B.; Scuseria, G. E.; Robb, M. A.; Cheeseman, J. R.; Scalmani, G.; Barone, V.; Mennucci, B.; Petersson, G. A.; Nakatsuji, H.; Caricato, M.; Li, X.; Hratchian, H. P.; Izmaylov, A. F.; Bloino, J.; Zheng, G.; Sonnenberg, J. L.; Hada, M.; Ehara, M.; Toyota, K.; Fukuda, R.; Hasegawa, J.; Ishida, M.; Nakajima, T.; Honda, Y.; Kitao, O.; Nakai, H.; Vreven, T.; Montgomery, J. A., Jr.; Peralta, J. E.; Ogliaro, F.; Bearpark, M.; Heyd, J. J.; Brothers, E.; Kudin, K. N.; Staroverov, V. N.; Kobayashi, R.; Normand, J.; Raghavachari, K.; Rendell, A.; Burant, J. C.; Iyengar, S. S.; Tomasi, J.; Cossi, M.; Rega, N.; Millam, M. J.; Klene, M.; Knox, J. E.; Cross, J. B.; Bakken, V.; Adamo, C.; Jaramillo, J.; Gomperts, R.; Stratmann, R. E.; Yazyev, O.; Austin, A. J.; Cammi, R.; Pomelli, C.; Ochterski, J. W.; Martin, R. L.; Morokuma, K.; Zakrzewski, V. G.; Voth, G. A.; Salvador, P.; Dannenberg, J. J.; Dapprich, S.; Daniels, A. D.; Farkas, Ö.; Foresman, J. B.; Ortiz, J. V.; Cioslowski, J.; Fox, D. J. Gaussian, Inc., Wallingford CT, **2009**.
(66) Büttiker, M.; Imry, Y.; Landauer, R.; Pinhas, S. *Phys. Rev. B*, **1985**, *31*, 6207.
(67) Herrmann, C.; Solomon, G. C.; Subotnik, J. E.; Mujica, V.; Ratner, M. A. *J. Chem. Phys.***2010**, *132*, 024103 (1-17).
(68) Herrmann, C.; Solomon, G. C.; Ratner, M. A. *J. Am. Chem. Soc.*, **2010**, *132*, 3682.
(69) Latif, I. A.; Singh, V. P.; Bhattacharjee, U.; Panda, A.; Datta, S. N. *J. Phys. Chem. A*, **2010**, *114*, 6648–6656.
(70) Herring, C. Magnetism IIB, Direct exchange between well-separated atoms, 5, Eds. G.T. Rado and H. Suhl (**1966**) Academic Press, New York.
(71) Polo, V.; Alberola, A.; Andres, J.; Anthony, J.; Pilkington, M. *Phys. Chem. Chem. Phys*., **2008**, *10*, 857.

(72) Shil, S.; Roy, M.; Misra, A. *RSC Adv*., **2015**, *5*, 105574.
(73) Hermann, C.; Neugebauer, J.; Gladysz, J. A.; Reiher, M. *Inorg. Chem.* **2005**, *44*, 6174.
(74) Prasongkit, J. ; Grigoriev, A.; Wendin, G. ; Ahuja, R. *Phys. Rev. B,***2010**, *81*, 115404.
(75) Kondo, M.; Tada, T. ; Yoshizawa, K. *J. Phys. Chem. A* **2004**, *108*, 9143.
(76) Stuyver, T.; Fias, S. ; Proft, F. De. ; Geerlings, P. *J. Phys. Chem. C*, **2015**, *119*, 26390.
(77) Aravena, D.; Ruiz, E. *J. Am. Chem. Soc*. **2012**, *134*, 777.
(78) Herrmann, C.; Solomon, G. C.; Ratner, M. A. *J. Am. Chem. Soc.,* **2010**, *132*, 3682.
(79) Ashcroft, N. W.; Mermin, N. D. Solid *State Physics*, Holt, Rinehart and Winston, New York, **1976**.
(80) Pauly, F.; Viljas, J. K. ; Cuevas, J. C. ; Schön, G. *Phys. Rev. B,* **2008,** *77*, 155312.
(81) Tour, J. M.; Kozaki, M.; Seminario, J. M. *J. Am. Chem. Soc.,* **1998**,*120*, 8486.
(82) Modelli, A.; Venuti, M.; Scagnolari, F.; Contento, M.; Jones, D. *J. Phys. Chem. A,* **2001**,*105*, 219.
(83) Distefano, G.; Jones, D. ; Guerra, M. ; Favaretto, L. ; Modelli, A. ; Mengoli, G. *J. Phys. Chem.* **1991**, *95*, 9746.
(84) Colle, M. D.; Cova, C.; Distefano, G. ; Jones, D. ; Modelli, A. ; Comisso, N. *J. Phys. Chem. A.* **1999**,*103*, 2828.
(85) Brédas, J. L. ; Thémans, B.; Fripiat, J. G. ; André, J. M. ; Chance, R. R. *Phys. Rev. B,* **1984**,*29*, 6761.
(86) Schlicke, H.; Herrmann, C. *Chem. Phys. Chem.,* **2014**, *15*, 4011.
(87) Proppe, J.; Herrman, C. *J. Comput. Chem.* **2015**, *36*, 201.
(88) Choi, Y. C. ; Kim, W. Y. ; Park, K. S. ; Tarakeshwar, P.; Kim, K. S. ; Kim, T. S. ; Lee, J. Y. *Chem. Phys.*, **2005**, *122*, 094706.
(89) Hermann, C.; Neugebauer, J.; Gladysz, J. A.; Reiher. M. *Inorg. Chem.* **2005**, *44*, 6174.
(90) Chumak, A. V. ; Vasyuchka, V. I. ; Serga, A. A. ; Hillebrands, B. *Nat. Phys.* **2015**, *11*,453.

CHAPTER 6

Magnetic modulation in heteroallene and heterocumulene based *tert*-butyl nitroxide diradicals: spin delocalization and conformation play crucial roles

Abstract

We have theoretically investigated the magnetic property of heteroallene (>C=C=X−) and heterocumulene (>C=C=C=X−) based *tert*-butyl nitroxide diradicals (X is P/As). Calculation of magnetic exchange coupling constant (*J*) shows ferromagnetic interaction in heteroallene based diradicals. Whereas, in heterocumulene based diradicals, tuning of *J* value from antiferro- to ferro-magnetic state is observed from *Z*- to *E*- isomer. The essence of all findings is further explored by structural effects, spin density distribution and molecular orbital analysis. Delocalization of spin density from radical site to the coupler (in planar arrangement) is observed in spin distribution analysis. Moreover, the shapes of singly occupied molecular orbitals (SOMOs) advocate the delocalization of spin from radical center to the coupler. The typical feature of *tert*-butyl nitroxide radical creates spin delocalization along with spin polarization within the coupler. The *J* value of all diradicals strongly depends on the dihedral angle between radical center and coupler. The presence of heteroatom within the coupler produces major geometrical change that results magnetic crossover in heterocumulene based systems. Magneto-structural correlation shows that the change in dihedral angle tunes the magnetic property for both the *Z*- and *E*- isomers of heterocumulenes depending on the spin accumulation on two nearby magnetic centers. The energy gap between two consecutive SOMOs also supports this observation.

6.1 Introduction

Allene and cumulenes show interesting shapes and fascinating properties depending on the number of carbon atoms in the backbone chain[1,2] and have two types of π-bonds orthogonal to each other along their molecular axis. As allene and even cumulenes (containing even number of carbons) are structurally dissimilar, when the groups on end carbons are different, allene derivatives are chiral, whereas even cumulene derivatives show *Z*/*E* isomers.[3,4] Synthesis of long chain cumulenes and their characterization have been done by many researchers.[4-7]

There is a recent resurgence in studies relating to the switching of magnetic nature between ferromagnetic and antiferromagnetic states.[8-12] Normally the exchange interaction between two magnetic centers depends on the distance between radical centers as well as on the nature of the couplers.[13-15] However the interaction may follow different mechanisms[16] such as direct exchange, super exchange, ligand mediated exchange and so on. To search for excellent magnetic materials, the interaction between two magnetic centers connected through various couplers (such as conjugated chains and aromatic couplers) have been studied by different research groups.[13,17-22] In our previous works we have investigated the magnetic property of diradicals based on chiral allene as well as cumulene couplers and observed an anomalous magnetic behavior compared to the diradical based on conjugated systems.[23,24] Helical molecular orbitals of allene and cumulenes (with even number of double bonds) are investigated by notable researchers[25-27] and these systems can be tailored for use in enantioselective reactions.

Synthesis of heteroallenes,[28-31] in which one or more carbons are replaced by heavier elements of group 14 or 15, is a challenge in organometallic chemistry. Moreover heteroallene and heterocumulene (with 4 atoms in backbone chain) containing double bonded heavy elements, have attracted interest from a theoretical point of view because of their peculiar physicochemical properties.[29,32] Various types of phosphaallenes and phosphacumulenes −P=C=A (A=CR_2, PR, NR, C=PR, C=CR_2) have also been reported.[28,29] Märkl et al. in 1986 have synthesized phosphabutatriene −P=C=C=C< for the first time, a derivative with three cumulative double bonds.[33] On the other hand, though the stabilization of 1-arsabutatriene −As=C=C=C< is somewhat difficult due to the large size of arsenic, 1-Arsaallenes −As=C=C< have been first reported by Bouslikhane et al. which is stable towards air and moisture.[34] In the present study we have designed diradicals based on heteroallene (>C=C=X−) and heterocumulene (>C=C=C=X−) coupler where X is P/As.

The presence of heteroatom in the exchange pathway significantly influences magnetic exchange coupling.[35-37] Rancurel et al. have shown that the magnetic exchange between radical centers becomes more fragile when a heteroatom is introduced in the exchange pathway.[35] It is noted that when P atom bridges between

aminoxyl radical, exchange interaction depends on whether there is a participation of lone pair on P or not.[35] On the other hand, Polo et al. have opined that the introduction of heteroatom within the coupler may produce two or more inequivalent spin coupling pathways and the prediction of magnetic exchange interaction becomes more complicated.[36] Bhattacharya et al. investigated the spin leakage phenomenon of certain phosphoverdazyl systems and its effect on magnetic exchange coupling.[37] Herein, we are motivated to evaluate the potential effect of P/As atom substitution within the allene and cumulene couplers in mediating the exchange interaction between the two radical centers.

There are a number of stable organic radicals that are synthesized during last few decades.[38-43] Besides, lot of studies have been done predicting the magnetic property of molecules based on the *tert*-butyl nitroxide radical.[44-49] In the present investigation, we select the *tert*-butyl nitroxide as a spin source connected to heteroallene (>C=C=X−) and heterocumulene (>C=C=C=X−) coupler (X is P/As) and the systems studied are shown in Figure 6.1. The magnetic nature of these systems is quantified in DFT framework. The magnetic characteristics are rationalized through structural effects, spin density distributions, molecular orbital analysis and magneto-structural correlation.

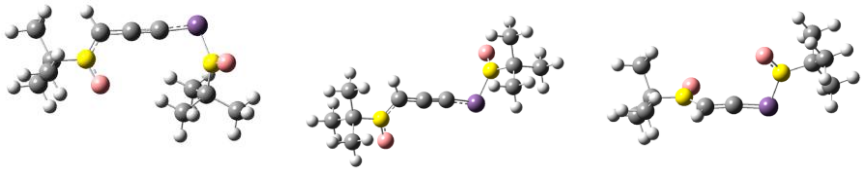

1(a) (Z-isomer) **1(b)** (E-isomer) **3**(Chiral)

P-substituted cumulene and allene based diradicals

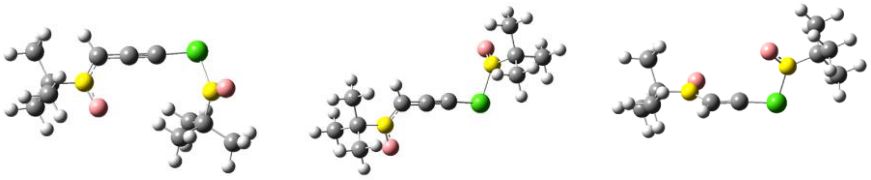

2(a) (Z-isomer) **2(b)** (E-isomer) **4**(Chiral)

As-substituted cumulene and allene based diradicals

Figure 6.1 Designed heteroallene and heterocumulene based diradicals where 1(a) and 1(b) represent *Z*- and *E*-isomer of P-substituted heterocumulene based diradicals, 2(a) and 2(b) represent *Z*- and *E*-isomer of As-substituted heterocumulene based diradicals, 3 and 4 represents the P- and As-substituted allene based diradicals. [Carbon, hydrogen, nitrogen, oxygen, phosphorus and arsenic atoms are depicted in grey, white, yellow, pink, purple, and green respectively].

6.2 Theoretical Background and Computational Strategy

For a system with two magnetic centers 1 and 2, the magnetic exchange interaction can be expressed by the phenomenological Heisenberg spin Hamiltonian $\hat{H} = -2J\hat{S}_1 \bullet \hat{S}_2$, where *J* is the effective exchange coupling constant between two magnetic centers of a diradical and $\hat{S}_1$ and $\hat{S}_2$ are the respective spin angular momentum operators. Positive sign of *J* indicates that the coupling is ferromagnetic and a negative value of *J* signifies the antiferromagnetic interaction in the diradical. For a diradical containing single unpaired electron on each magnetic site, *J* can be written as $E_{(S=1)} - E_{(S=0)} = -2J$.

Though the multiconfigurational approaches are suitable to describe pure spin states in an appropriate manner, these methods are not employed in this work as they are resource intensive. A more effective and useful alternative way with less computational effort is the Broken symmetry (BS) approach given by Noodleman et al.[50-53] in DFT framework. Many researchers have given different formulae for *J*.[54-56] However, the spin projected formula for the estimation of *J* has been given by Yamaguchi,[57-60] which is broadly applied and we also use this formula in this work $J = (E_{BS} - E_{HS}) \Big/ \left(\left\langle S^2 \right\rangle_{HS} - \left\langle S^2 \right\rangle_{BS} \right)$, where E_{HS}, E_{BS} and $\langle S^2 \rangle_{HS}$, $\langle S^2 \rangle_{BS}$, are the energy and average spin square values of corresponding high-spin and BS states.

Here, the molecular geometries of all the designed diradicals are fully optimized by hybrid exchange-correlation functional B3LYP, M06 and CAM-B3LYP (to include long range correction) using 6-311++G(d,p) basis set within unrestricted formalism. The open shell broken symmetry (BS) singlet solution has been obtained by using "guess=(read,mix)" keyword for mixing of HOMO and LUMO. Based on the energies of the triplet and the BS states at the same level of theory, *J* values of each molecule can be estimated using the spin projected formula given by Yamaguchi. Frequency calculation of all the diradicals gives positive values confirming that all the geometries are in local minima. Geometrical parameters of all the diradicals, the spin density distribution, and molecular orbital analysis are performed with the optimized geometry. All the calculations have been done by Gaussian 09 package.[61]

6.3 Result and Discussion

Magnetic exchange coupling constant

J values of all the designed diradicals are given in Table 6.1 Table 6.2 and Table 6.3 that are estimated using different exchange-correlation functionals (B3LYP, M06 and CAM-B3LYP) along with 6-311++G(d,p) basis set.

Table 6.1 The estimated energies (in a.u.) of triplet (T) state and broken symmetry (BS) state, corresponding $\langle S^2 \rangle$ values, and magnetic exchange coupling constant (*J*, in cm^{-1}) for all the diradicals (B3LYP/6-311++G(d,p)).

Diradicals	**$E_{(T)}$ ($\langle S^2 \rangle$)**	**$E_{(BS)}$ ($\langle S^2 \rangle$)**	***J* (cm^{-1})**
1(a) (*Z*–)	-1031.93594 (2.074)	-1031.93691 (1.011)	-200.27
2(a) (*Z*–)	-2926.44012 (2.065)	-2926.44051 (1.019)	-81.83
1(b) (*E*–)	-1031.93496 (2.074)	-1031.93427 (1.075)	151.59
2(b) (*E*–)	-2926.43915 (2.066)	-2926.43881 (1.059)	74.10
3	-993.83964 (2.054)	-993.83759(1.029)	440.0
4	-2888.33528 (2.067)	-2888.33305 (1.030)	471.97

Table 6.2 The estimated energies (in a.u.) of triplet (T) state and broken symmetry (BS) state, corresponding $\langle S^2 \rangle$ values, and magnetic exchange coupling constant (*J*, in cm^{-1}) for all the diradicals (M06 /6-311++G(d,p)).

Diradicals	**$E_{(T)}$ ($\langle S^2 \rangle$)**	**$E_{(BS)}$ ($\langle S^2 \rangle$)**	***J* (cm^{-1})**
1(a) (*Z*–)	-1031.41156 (2.068)	-1031.41288 (0.980)	-266.28
2(a) (*Z*–)	-2925.84247 (2.055)	-2925.84315(0.983)	-139.22
1(b) (*E*–)	-1031.40956 (2.071)	-1031.40907(1.054)	105.75
2(b) (*E*–)	-2925.83945(2.058)	-2925.83933(1.028)	24.54
3	-993.34352 (2.074)	-993.34048 (1.032)	640.65
4	-2887.76406(2.085)	-2887.76125(1.032)	585.68

Table 6.3 The estimated energies (in a.u.) of triplet (T) state and broken symmetry (BS) state, corresponding $\langle S^2 \rangle$ values, and magnetic exchange coupling constant (*J*, in cm^{-1}) for all the diradicals (CAM-B3LYP /6-311++G(d,p)).

Diradicals	**$E_{(T)}$ ($\langle S^2 \rangle$)**	**$E_{(BS)}$ ($\langle S^2 \rangle$)**	***J* (cm^{-1})**
1(a) (*Z*–)	-1031.56284 (2.156)	-1031.56360 (1.121)	-160.49
2(a) (*Z*–)	-2926.15818 (2.134)	-2926.15857 (1.107)	-83.34
1(b) (*E*–)	-1031.56149 (2.159)	-1031.56097 (1.156)	114.15
2(b) (*E*–)	-2926.15692 (2.139)	-2926.15654 (1.137)	83.23
3	-993.49053 (2.087)	-993.48833 (1.048)	464.72
4	-2888.07629 (2.115)	-2888.07376 (1.055)	523.84

There are certain issues associated with the calculated results that are discussed below.

(i) *J* values of heterocumulene based diradicals (isomers of 1 and 2) predict antiferromagnetic interaction in *Z*-isomers, while ferromagnetic interaction is observed in *E*-isomers. (ii) The magnitude of *J* value of heteroallene based diradicals (molecules 3 and 4) is higher than the heterocumulene based diradicals (isomers of 1 and 2 respectively), which is in contradiction to our previous study[24] where we have found that odd cumulene based diradicals have lesser magnitude of *J* value than that of the even cumulene based diradicals.

These observations demand a detailed investigation on the basis of the electronic structure analysis of the diradicals which are discussed in subsequent sections.

6.3.1 Structural characters and effects

Small changes in molecular structure can alter the *J* value significantly.[62] The strength of magnetic interaction depends on the distance between radical centers as well as the dihedral angle between radical center and coupler.[63-65] In this work, molecular structures of all the designed diradicals have been studied to understand their magnetic behavior.

6.3.1.1 Distance between radical centers

The extent of magnetic interaction is known to vary with the distance (*r)* between the magnetic centers as *exp*(-*r*).[66] For our designed systems (in Figure 6.1) the distance between radical centers are given in Table 6.4.

Table 6.4 Distance between radical centers *r* (in Å) for all the designed diradicals (using B3LYP/6-311++G(d,p)).

Systems	*r*	*J* (cm^{-1})	Systems	*r*	*J* (cm^{-1})
1(a) (*Z*-)	5.585	–200.27	2(a) (*Z*-)	5.622	-81.83
1(b) (*E*-)	6.858	151.59	2(b) (*E*-)	7.027	74.10
3	4.608	440.0	4	4.643	471.97

Table 6.4 shows that the distance between two radical centers increases from *Z*-isomer to *E*- isomer (in isomers of 1 and 2); consequently the magnitude of *J* value of *E*–isomers (1(b) and 2(b)) is lower than that of *Z*-isomers (1(a) and 2(a) respectively). The distance between radical centers of heteroallene based diradicals (3 and 4) are smaller compared to the respective heterocumulene based diradicals (isomers of 1 and 2 respectively) indicating the greater magnitude of *J* in heteroallene based diradical.

Photomagnetic crossover of several diradicals has already investigated where the trans-isomers are antiferromagnetic but cis-isomers are ferromagnetic (owing to the close proximity between radical centers that results direct exchange).[8] However for our designed *E*-isomer of heterocumulene based diradicals, the distance between two radical centers is sufficiently large (i.e., 6.858 Å for 1(b) and 7.027 Å for 2(b)), so a significant through-space direct exchange interaction between them is unlikely. Therefore the change in the sign of *J* value from *Z*- to *E*-isomer needs to be ascertained from some other criterion.

6.3.1.2 Dihedral angle

Several studies show that the magnitude of *J* strongly depends on the planarity of the molecular structure.[64,65] In one of our previous studies, we have shown that the coupling constant values of even cumulene based diradicals are higher than odd cumulene based diradicals; as for the later systems two radical centers are in perpendicular plane, while in former cases the radical centers are in the same plane.[24] In this work, the dihedral angle ϕ (q-r-r′-q′) between two radical centers R_1 and R_2 (considering only the connecting nitrogen atoms of two radical centers R_1 and R_2) shows that in heterocumulene based diradicals, the two N atoms of two radical centers are almost in same plane and in heteroallene based diradicals, the two N atoms of two radical centers are in perpendicular plane (given in Table 6.5). However the magnitude of *J* in heteroallene based diradicals is higher compared to heterocumulene based diradicals. To understand the fact we analyze the dihedral angle φ_1 (between R_1

and coupler) and φ_2 (between R_2 and coupler) in heterocumulene and heteroallene systems (in Figure 6.2) as given in Table 6.5.

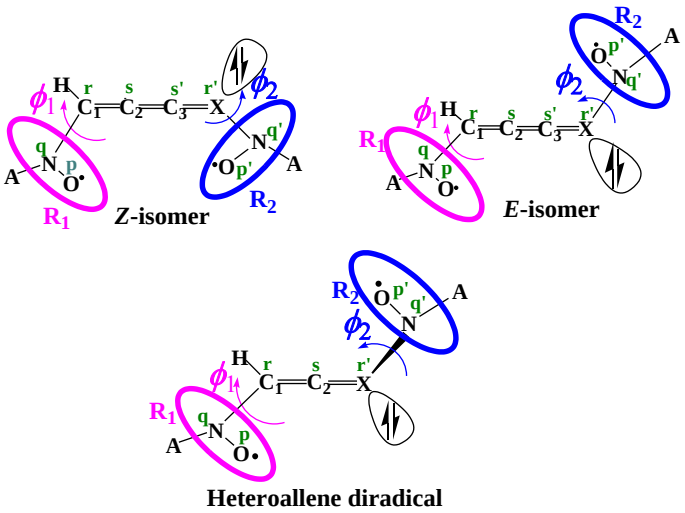

Figure 6.2 $\varphi_1$and φ_2 denote the dihedral angle between the plane of coupler and that of the nitroxide radicals (R_1 and R_2 respectively) and X denotes P/As, A stands for $-C(CH_3)_3$. R_1 and R_2 represents same radical center (–NO) but linked with different atoms (i.e., R_1 is connected to C_1 and R_2 is connected to X of the coupler).

Table 6.5 Dihedral angles from optimized geometry of heterocumulene and heteroallene based diradicals (using B3LYP/6-311++G(d,p)).

System	(Dihedral angle)°			J (cm^{-1})
	ϕ_1 (p-q-r-s)	ϕ_2 (p′-q′-r′-s′)	ϕ (q-r-r′-q′)	
1(a) (*Z*-)	–0.61	–104.11	–7.53	–200.27
1(b) (*E*-)	0.63	–93.97	176.43	151.59
2(a) (*Z*-)	–0.63	–101.93	–11.57	-81.83
2(b) (*E*-)	0.48	–98.41	174.96	74.10
System	ϕ_1 (p-q-r-s)	ϕ_2 (p′-q′-r′-s)	ϕ (q-r-r′-q′)	J (cm^{-1})
3	2.41	3.63	94.52	440.0
4	2.70	3.80	94.65	471.97

Table 6.5 shows that in heterocumulene based diradicals, R_1 and coupler are in same plane (dihedral angle $\phi_1 \approx 0^o$). However the dihedral angle ϕ_2 could not afford the planarity between R_2 and coupler due to the presence of lone pair of electrons on heteroatom (P/As). So a reduced delocalization of electrons occurs between the coupler and radical center (R_2). The extent of non planarity increases from *Z*- to *E*-isomer (ϕ_2), resulting smaller magnitude of *J* for *E*-isomers than the *Z*-isomer. On the other hand though heteroallene coupler has two types of perpendicular π-planes, dihedral angle φ_1 and φ_2 show that the radical centers are almost in same plane with the coupler (given in Table 6.5). Consequently a better interaction between radical

center and the coupler occurs that results higher magnitude of *J* value in heteroallene based diradicals (3 and 4) compared to heterocumulene based diradicals (1 and 2).

6.3.2 Spin density distribution

Spin density distribution is an important factor that tunes the interaction between different magnetic sites and has an effect on the sign of *J* values.[13,14] Distribution of spin density on each atom of the coupler and on the radical centers of all the diradicals (in their optimized structure) are given in Table 6.6 and Table 6.7. The concerns associated with these results are discussed in the following.

Table 6.6 Spin density distribution on each atom of the coupler of *Z*- and *E*-isomers of heterocumulene based diradicals in their BS state and triplet state respectively (B3LYP/6-311++G(d,p)).

Systems	R_1	C_1	C_2	C_3	X (P/As)	R_2
1(a) (*Z*-)	0.4761	–0.1943	0.2985	–0.2079	0.5798	–0.9619
2(a) (*Z*-)	–0.3950	0.1880	–0.2807	0.2477	–0.7333	0.9780
1(b) (*E*-)	0.4868	–0.1949	0.2892	–0.2386	0.6611	0.9544
2(b) (*E*-)	0.4109	–0.1874	0.2704	–0.2245	0.7224	0.9788

(i) Spin density distribution (given in Table 6.6) on *Z*-isomers (1(a) and 2(a)) follow the spin alternation rule.[67] However an unexpected outcome is obtained in the spin distribution i.e., although the spin density on R_2 (−NO) is almost unity, spin density on R_1 (−NO) is far less than unity and a large accumulation of spin density is observed on the heteroatom (P/As).

(ii) For *E*-isomers (1(b) and 2(b)), spin density (given in Table 6.6) on R_1 (−NO) is also far below from unity and heteroatom (X) have a large accumulation of spin density. Furthermore, a regular alternation of the spin density occurs within the R_1 and the coupler but the alternation breaks between X (P/As) and R_2 (−NO).

(iii) In heteroallene based diradicals (3 and 4), spin density distribution (given in Table 6.7) follow spin alternation between radical centers and the coupler. Unlike a large accumulation of spin density on heteroatom (P/As) as observed in heterocumulene based diradicals (isomers of 1 and 2), large amount of spin density is observed on C_2 of heteroallene coupler (in Table 6.7) and the spin density on R_1 (−NO) and R_2 (−NO) decreases to some extent from unity.

Table 6.7 Spin density distribution on each atom of the coupler of heteroallene based diradicals in their triplet state (B3LYP/6-311++G(d,p)).

Systems	R_1	C_1	C_2	X (P/As)	R_2
3	0.7886	–0.2205	0.6783	–0.1539	0.8889
4	0.7845	–0.2513	0.7367	–0.2285	0.9352

Such distribution of spin density on all the diradicals is quite astonishing. To understand the unusual type of spin density distribution on the magnetic center and coupler, we have studied a set of P-substituted allene and cumulene based diradicals by changing the radical center, i.e., instead of *tert*-butyl nitroxide radical, nitronyl nitroxide radical is considered as spin center and the designed systems are given in Figure 6.3. The magnetic exchange coupling constant values for those nitronyl nitroxide diradicals are given in Table 6.8. The spin density distribution (given in Table 6.9 and Table 6.10) for all the nitronyl nitroxide diradicals show that the spin density on the radical sites is almost unity and the coupler has very small spin density compared to the radical units. Thus, the spin density distribution on our designed *tert*-butyl nitroxide diradicals (Figure 6.1) reveals striking differences from that of the nitronyl nitroxide based diradicals. From this observation we can conclude that the radical unit (*tert*-butyl nitroxide radical) has a major role in such unusual type spin density distribution.

P substituted cumulene and allene based nitronyl nitroxide diradicals

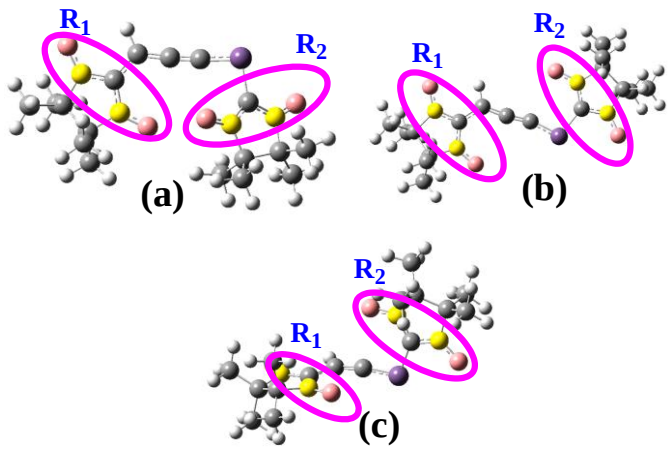

Figure 6.3 Designed nitronyl nitroxide diradicals based on heteroallene and heterocumulene couplers (with P-substitution). (a) and (b) represents *Z*- and *E*- isomer of heterocumulene based diradicals respectively, (c) represents the heteroallene based diradicals. [Carbon, hydrogen, nitrogen, oxygen, phosphorus atoms are depicted in grey, white, yellow, pink and purple respectively]. Here R_1 and R_2 (−NO−C−NO− group) are shown by magenta circle.

Table 6.8 The energy (a.u.),$\langle S^2 \rangle$ and magnetic exchange coupling constant (J in cm^{-1}) of all the nitronyl nitroxide diradicals (B3LYP/6-311++G(d,p)).

Diradicals	$E_{(T)}$ ($\langle S^2 \rangle$)	$E_{(BS)}$ ($\langle S^2 \rangle$)	J (cm^{-1})
S1(a) Z-	-1524.15524 (2.185)	-1524.15736 (1.309)	-529.76
S1(b) *E*-	-1524.15697 (2.144)	-1524.16057 (1.352)	-997.38
S1(c)	-1486.06429(2.149)	-1486.06405 (1.133)	52.62

From Table 6.8 it is observed that for heterocumulene based nitronyl nitroxide diradicals, both *Z*- and *E*- isomers show antiferromagnetic coupling and heteroallene based nitronyl nitroxide diradical shows ferromagnetic coupling as expected from spin density alternation rule.

Table 6.9 Spin density distribution on each atom of the coupler of *Z*- and *E*- isomers of P- substituted even cumulene based nitronyl nitroxide diradical in their BS state (B3LYP/6-311++G(d,p)).

Systems	**R_1 (−NO−C−NO−)**	**C_1**	**C_2**	**C_3**	**X**	**R_2 (−NO−C−NO−)**
S1(a) Z-	-1.1585	-0.2259	0.2055	-0.2234	0.3108	1.0489
S1(b) *E*-	-1.1820	-0.2486	0.1984	-0.2288	0.3030	1.1304

Table 6.10 Spin density distribution on each atom of the coupler of P- substituted allene based nitronyl nitroxide diradical in their high spin state (B3LYP/6-311++G(d,p)).

System	**R_1 (−NO−C−NO−)**	**C_1**	**C_2**	**X**	**R_2 (−NO−C−NO−)**
S1 (c)	1.0667	0.1173	-0.2831	0.0780	1.0548

Schatzschneider et al. have investigated that in *tert*-butyl phenyl nitroxides, a direct delocalization of unpaired electron occurs through the phenyl ring at the coplanar geometry and the delocalization decreases with increasing dihedral angle between radical group and phenyl ring.[68] The spin density distribution of *tert*-butyl nitroxide based diradicals (in Table 6.6 and Table 6.7) and of nitronyl nitroxide based diradicals (in Table 6.9 and Table 6.10) point out that in both the cases spin density spreads out onto the coupler. In nitronyl nitroxide diradicals, as the spin density on radical sites is almost unity (in Table 6.9 and Table 6.10), the delocalization of unpaired electrons of radical centers within the coupler is constrained. So, one can surmise that the spin density on the coupler arises from spin polarization within the coupler in nitronyl nitroxide diradicals.

For the heterocumulene based *tert*-butyl nitroxide diradicals (both *Z*- and *E*-isomers), dihedral angle (ϕ_1 in Table 6.5) suggest that R_1 (−NO) and the coupler are almost in same plane. Consequently along with the spin polarization, the additional contribution of spin density on the coupler and low contribution of spin density on R_1 is due to the spin delocalization (that occurs from the delocalization of unpaired electron between R_1 and the coupler as given in Table 6.6). However the dihedral angle (ϕ_2 in Table 6.5) between R_2 and coupler predict nonplanarity between them. The extent of delocalization of unpaired electron from R_2 to the coupler is negligible and the spin density on R_2 is almost one as seen in Table 6.6.

A plausible mechanistic pathway of the delocalization of unpaired electron from R_1 to the coupler is given in Figure 6.4. Here R_1 and the coupler together form one delocalized radical unit as shown by blue dotted line. The net magnetic coupling is due to the interaction between blue dotted radical unit and R_2. Similar delocalization of electron also observed in *E*-isomers. Table 6.6 shows that, at a certain dihedral angle (ϕ_2) in *E*-isomer, similar spin accumulates on two nearby magnetic centers that results ferromagnetic coupling. However in Z-isomer, antiferromagnetic coupling is observed owing to the opposite spin accumulation on two nearby magnetic centers (spin density plot is given in Figure 6.5 and Figure 6.6).

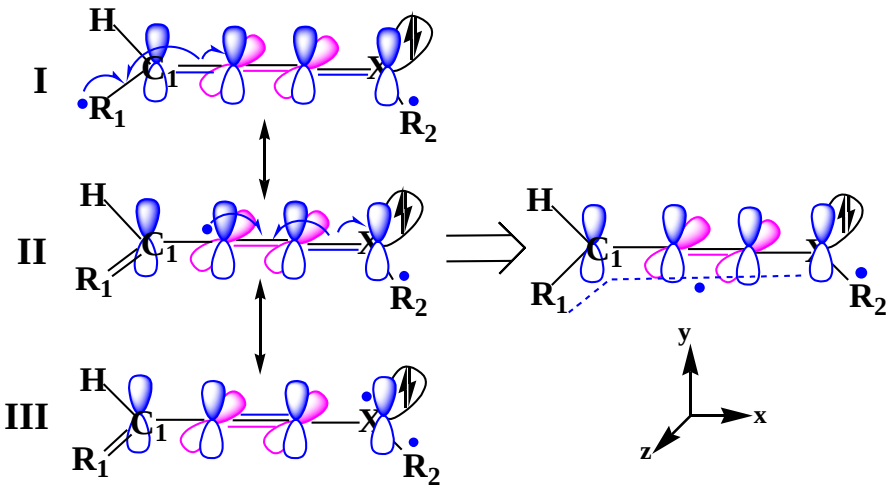

Figure 6.4 Delocalization of unpaired electron within the radical center (R_1) and the coupler in *Z*-isomer of heterocumulene based diradical. The magenta and blue lobes are two perpendicular *p* orbitals that form orthogonal π bonds in heteroatom substituted cumulene chain. Blue and magenta bonds are two perpendicular π bonds and blue arrows represents the electron delocalization pathways.

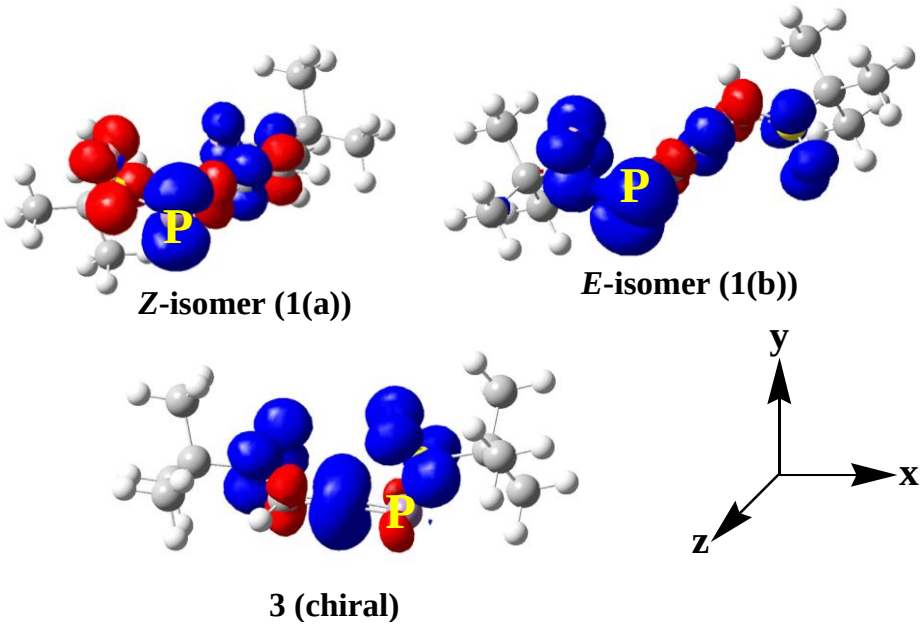

Z-isomer (1(a)) *E*-isomer (1(b))

3 (chiral)

Figure 6.5 Spin density plot for the *Z*–isomer of P-substituted cumulene based *tert*-butyl nitroxide diradicals (BS states) and *E*– isomer of P-substituted cumulene based *tert*-butyl nitroxide diradical (high spin states) and P-substituted allene based *tert*-butyl nitroxide diradical (high spin states) using (B3LYP/6-311++G(d,p)), (iso value 0.004), red and blue colors represent the α and β spins respectively.

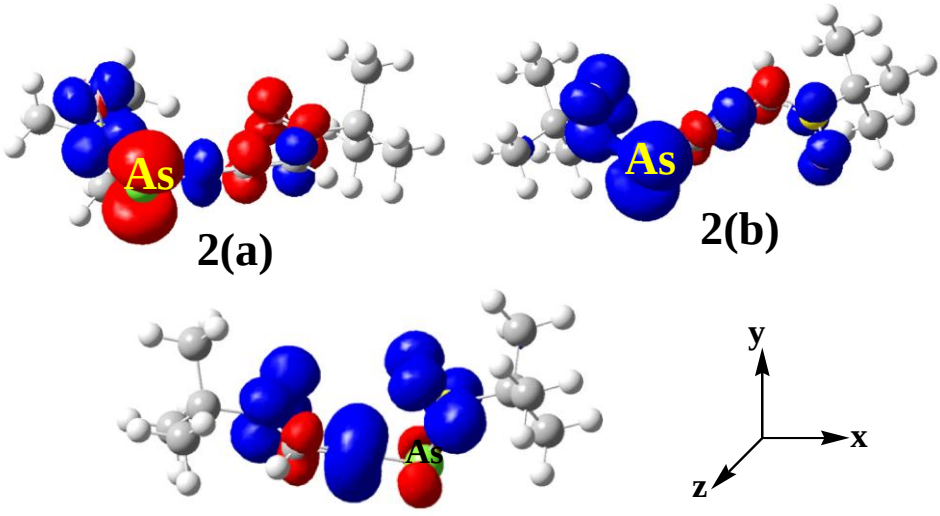

2(a) 2(b)

4

Figure 6.6 Spin density plot for the *Z*-isomer of As-substituted cumulene based *tert*-butyl nitroxide diradical (BS states) and *E*- isomer of As-substituted cumulene based *tert*-butyl nitroxide diradical (high spin states) and As-substituted allene based *tert*-butyl nitroxide diradical (high spin states) using (B3LYP/6-311++G(d,p)), (iso value 0.004), red and blue colors represent the α and β spins respectively.

For the heteroallene based diradicals, R_1 and the coupler are in same plane as observed from dihedral angle (ϕ_1 in Table 6.5). The delocalization of unpaired electron from R_1 to the coupler occurs smoothly which is shown in Scheme 1 of Figure 6.7. But the delocalization does not proceed beyond C_2, due to the presence of perpendicular π bonding orbital. Similarly, dihedral angle (ϕ_2 in Table 6.5) between coupler and radical center (R_2) shows that they are in almost same plane. The delocalization of unpaired electron occurs from R_2 to C_2 as shown in Scheme 2 of Figure 6.7. These two pathways collectively increase the spin density on C_2. Now the magnetic coupling is the result of the interaction between R_2 and blue dotted radical unit via the heteroatom.

The blue and magenta lobes are two orthogonal *p* orbitals in heteroallene chain and the blue and magenta dotted lines are two different electron delocalization pathways that are shown in Figure 6.7.

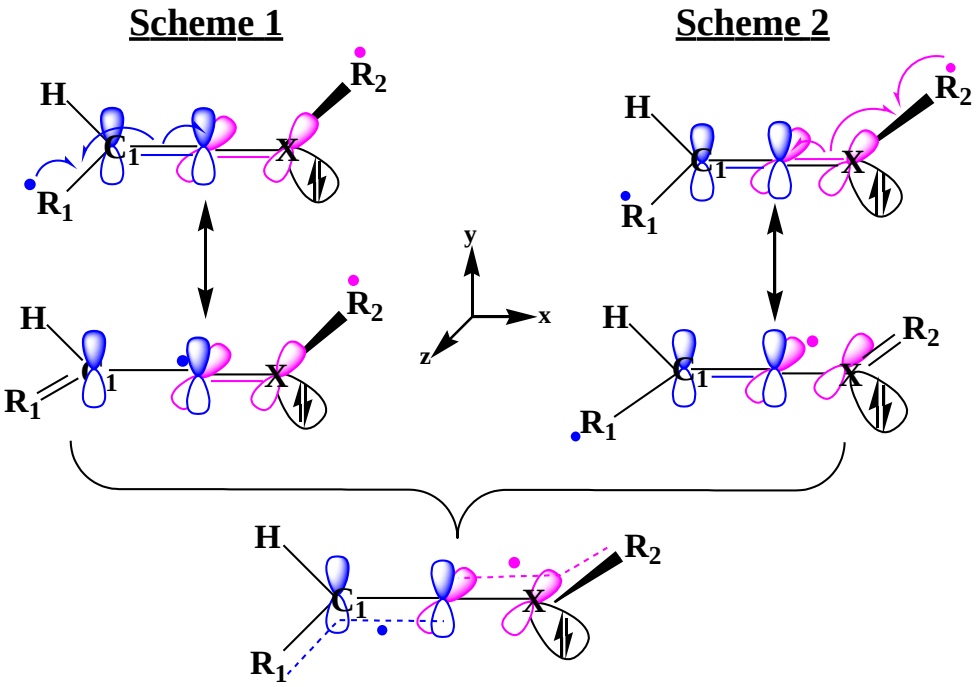

Figure 6.7 Delocalization of unpaired electron within the radical centers and coupler in heteroallene based diradicals.

6.3.3 Magneto-structural correlation

Though the *Z*- and *E*-forms are geometrical isomers that differ primarily by dihedral angle, the crossover of *J* values in heterocumulene based diradicals is quite interesting. Fang et al. have investigated that, if *tert*-butyl nitroxide radicals are twisted out of conjugation with the m-phenylene linker, the ability of ferromagnetic coupling reduces and antiferromagnetism arises depending on the dihedral angle between m-phenylene and the nitroxyl group.[46] Here we want to clarify how the dihedral angle ϕ_2 (Figure 6.2) affect the spin coupling between radical centers for both the P-substituted isomers of heterocumulene based diradicals. On the optimized geometry of 1(a) and 1(b) (using B3LYP/6-311++G(d,p)), single point calculation is done by changing the dihedral angle(ϕ_2) between –60º to –110º (at the same level of theory) with 10º interval. The change in magnetic exchange coupling constant value (*J*) with respect to the dihedral angle (φ_2) for both the isomers is given in Figure 6.8.

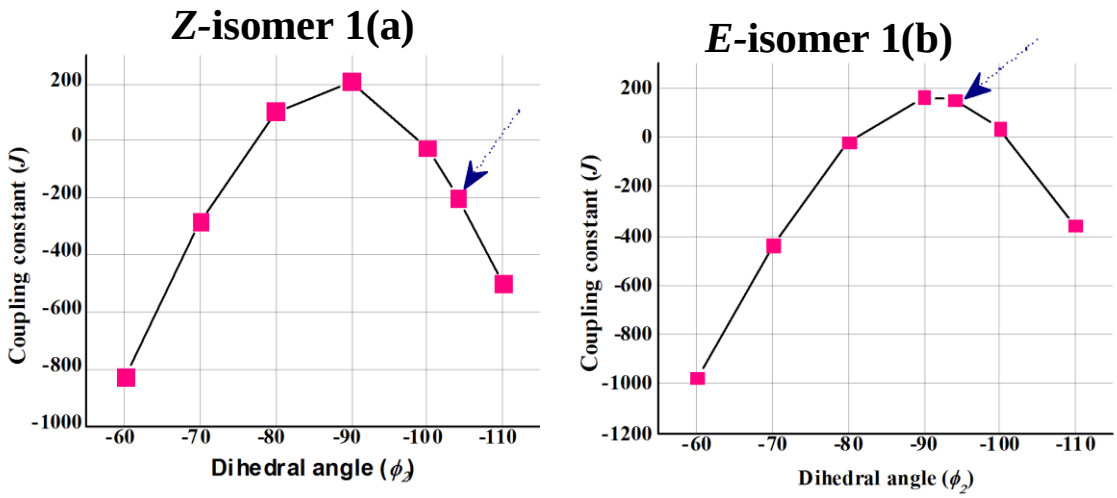

Figure 6.8 Coupling constant values (*J*, in cm^{-1}) of *Z*-isomer and *E*-isomer of P-substituted cumulene based diradicals by varying dihedral angle (φ_2, in degree) between the radical (R_2) and the coupler (B3LYP/6-311++G(d,p)).

Figure 6.8 clearly shows that for both the *E*- and *Z*-isomers (1(a) and 1(b)), a decreasing trend of antiferromagnetic *J* value is observed when twisting the dihedral angle φ_2 from –60º. A magnetic crossover between antiferro- and ferro-magnetic states occurs (for both the isomers) in the way of twisting the dihedral angle (ϕ_2) ≈ –80º and –100º. Hence we notice that ϕ_2 values are instrumental in tuning the *J* values. However the optimized geometry of *Z*-isomer has the ϕ_2 value –104.11º (in Table 6.5) which results antiferromagnetic coupling (shown in Figure 6.8 by a blue dotted arrow). Whereas, the optimized geometry of *E*-isomer shows that the ϕ_2 value is –93.97º (in Table 6.5) and a ferromagnetic coupling results (shown by a blue dotted

arrow in Figure 6.8). Thus from this section it is clear that a small change in dihedral angle in *Z*- and *E*-isomer is the major reason for the tuning of *J* values.

6.3.4 Molecular orbital analysis

In Section 6.3.2 we have interpreted that R_1 and coupler together form a delocalized radical unit which exhibits magnetic coupling with the other radical unit R_2 in heterocumulene based diradicals. To further justify this analysis, we scrutinize the molecular orbitals of all the P-substituted cumulene based diradicals (1(a) and 1(b)) that are sketched in Figure 6.9.

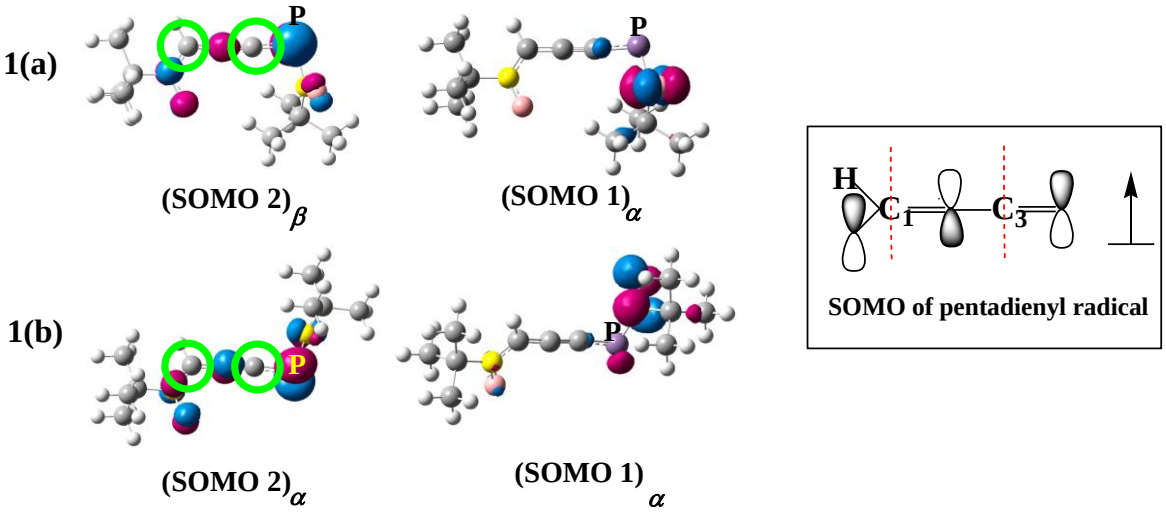

Figure 6.9 Spatial distribution of SOMOs of all the P-substituted cumulene based diradicals (1(a) and 1(b)) (B3LYP/6-311++G(d,p)) (iso value 0.06), blue and dark pink colors represent the different phase of the orbital coefficients. Within the inset, the SOMO of pentadienyl radical are shown. The red dotted lines represent nodal planes on C_1 and C_3.

It is clear from Figure 6.9 that, for both the *Z*- and *E*- isomers of P-substituted even cumulene based diradicals, SOMO1 is mostly located on the radical center R_2 and SOMO2 is mostly on the radical center R_1 as well as on the coupler. On the other hand, the molecular orbital analysis of nitronyl nitroxide based diradicals (specifically designed for comparison purpose as mentioned earlier and results are given in Figure 6.10) shows that the two SOMOs are centered exclusively on the radical centers. So the delocalization of unpaired electron is again confirmed from the MO analysis in *E*- and *Z*- isomers of P-substituted cumulene based *tert*-butyl nitroxide diradicals (1(a) and 1(b)).

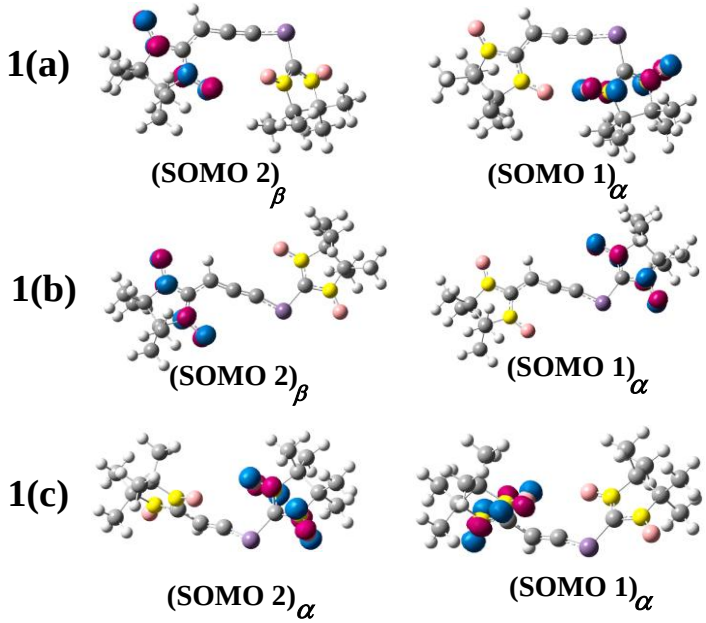

Figure 6.10 Spatial distribution of molecular orbitals of the P-substituted allene and cumulene based nitronyl nitroxide diradicals (B3LYP/6-311++G(d,p)) (iso value 0.06), blue and dark pink colors represent the different phase of the orbital coefficients.

Another notable point is that, SOMO2 of both 1(a) and 1(b) has two nodal points on C_1 and C_3 (green circle in Figure 6.9). If we consider the delocalization of unpaired electron from radical center R_1 to coupler (in Figure 6.4), it has the similar structure as that of SOMO of pentadienyl radical (inset in Figure 6.9). This observation confirms the mechanism of electron delocalization in our designed cumulene based systems. Similar analogy can also be put forward in case of As-substituted diradicals (2(a) and 2(b)) given in Figure 6.11.

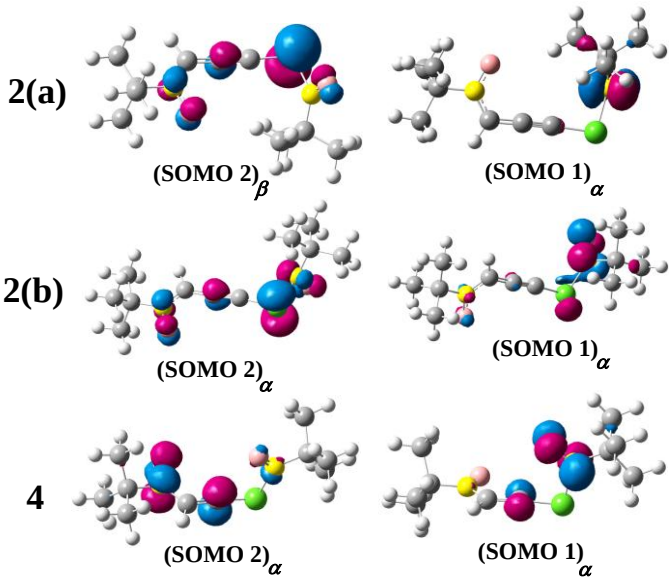

Figure 6.11 Spatial distribution of molecular orbitals of all the As-substituted cumulene and allene based *tert*-butyl nitroxide diradicals (B3LYP/6-311++G(d,p)) (iso value 0.06), blue and dark pink colors represent the different phase of the orbital coefficients.

For P-substituted allene based diradical (molecule 3 in Figure 6.1), SOMO2 has large coefficients on the radical center R_1 as well as on the coupler (on C_2) shown in Figure 6.12. Similarly SOMO1 has large coefficients on the R_2 as well as on the coupler (on C_2). The molecular orbital analysis again confirms the delocalization of radical unit as both the SOMOs spread over the radical center as well as the coupler. Moreover SOMO2 and SOMO1 have nodal points on C_1 and C_3 respectively (green circle in Figure 6.12). If we consider the SOMO of allyl radical, it has the well-known form shown in the inset of Figure 6.12 which has also one nodal point. This observation confirms the mechanism of electron delocalization between radical center and coupler (in two different planes) similar to that of the allyl radical. The molecular orbital of As-substituted allene based diradical is given in Figure 6.11.

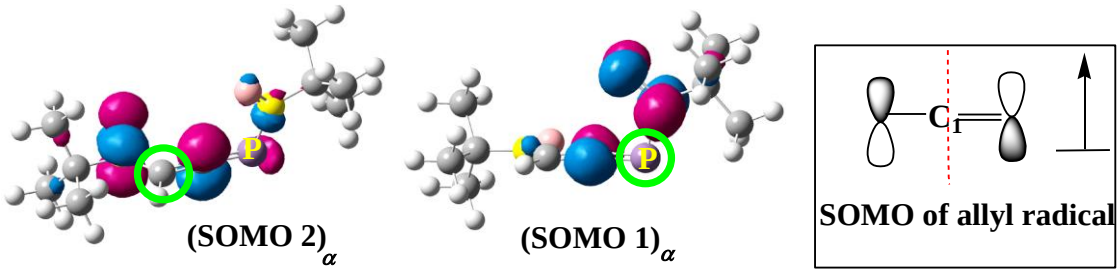

(SOMO 2)$_\alpha$ (SOMO 1)$_\alpha$

Molecule (3)

Figure 6.12 Spatial distribution of SOMOs of the allene based diradicals with P-substitution (B3LYP/6-311++G(d,p)) (iso value 0.05), blue and dark pink colors represent the different phase of the orbital coefficients. Within the inset, the SOMO of allyl radical are shown. The red dotted line represents nodal plane on C_1.

To understand the crossover of *J* value with change in dihedral angle (ϕ_2), we analyze the energy difference between two consecutive SOMOs of 1(a) and 1(b) at different dihedral angles given in Table 6.11. Frontier molecular orbital (FMO) energies of 1(a) and 1(b) are given in Table 6.12 and Table 6.13. According to Hoffmann[69] if the energy difference between two consecutive SOMOs is less than 1.5 eV, electrostatic repulsion between two degenerate orbitals increases and a spin-parallel orientation occurs with a triplet ground state. The critical value of ΔE_{SS} can be different for different systems.[70] From Table 6.11 it is clear that for both the 1(a) and 1(b), the ΔE_{SS} value decreases with change in φ_2 value from –60º to –90º and after that the ΔE_{SS} value increases with the change in φ_2 value. For *Z*-isomer, ΔE_{SS} value reaches to a minimum value at ϕ_2 value –80º and –90º, resulting a ferromagnetic coupling. But our optimized geometry have the φ_2 value –104.11º, so the antiferromagnetic coupling for *Z*-isomer results that are shown in Table 6.11. On the other hand, in *E*-isomer of even cumulene based diradical, ΔE_{SS} value reaches to a minimum value at ϕ_2 value –90º and –100º and our optimized geometry shows the φ_2 value is –93.97º. As a result ferromagnetic coupling is observed in *E*-isomer (shown in Table 6.11).

Table 6.11 Dihedral angle (φ_2, in degree), Energy difference (SOMO1 (HOMO)$_\alpha$)–(SOMO2 (HOMO-1)$_\alpha$)(ΔE_{SS}) and magnetic exchange coupling constant (J) in their triplet state (B3LYP/6-311++G(d,p)). The results for optimized geometries are given in bold face.

***Z*-isomer (1(a))**			***E*-isomer (1(b))**		
(φ_2)	**ΔE_{SS} (eV)**	**J(cm^{-1})**	**(φ_2)**	**ΔE_{SS} (eV)**	**J(cm^{-1})**
–60	0.718	–828.34	–60	0.790	–974.91
–70	0.470	–284.91	–70	0.555	–440.32
–80	0.209	102.60	–80	0.307	–21.57
–90	0.074	205.70	–90	0.072	164.19
–100	0.335	–26.44	**–93.97**	**0.0832**	**151.59**
–104.11	**0.442**	**–200.27**	–100	0.224	36.782
–110	0.594	–500.99	–110	0.474	–358.32

Table 6.12 Energy (in a.u.) of (SOMO 2)$_\alpha$, (SOMO 1)$_\alpha$ and (LUMO)$_\alpha$ for *Z*-isomer of P-substituted cumulene based *tert*-butyl nitroxide diradicals (B3LYP/6-311++G(d,p)).

Dihedral angle (*Z*-isomer)	**(SOMO 2)$_\alpha$ (a.u.)**	**(SOMO 1)$_\alpha$ (a.u.)**	**(LUMO)$_\alpha$ (a.u.)**
-60º	-0.21833	-0.19195	-0.06811
-70º	-0.21444	-0.19718	-0.06902
-80º	-0.21021	-0.20253	-0.06986
-90º	-0.2082	-0.20549	-0.07067
-100º	-0.21341	-0.20112	-0.07147
-104.11º	-0.21556	-0.1993	-0.0718
-110º	-0.21855	-0.19674	-0.07222

Table 6.13 Energy (in a.u.) of (SOMO 2)$_\alpha$, (SOMO 1)$_\alpha$ and (LUMO)$_\alpha$ for *E*-isomer of P-substituted cumulene based *tert*-butyl nitroxide diradicals (B3LYP/6-311++G(d,p)).

Dihedral angle (*E*-isomer)	**(SOMO 2)$_\alpha$ (a.u.)**	**(SOMO 1)$_\alpha$ (a.u.)**	**(LUMO)$_\alpha$ (a.u.)**
-60º	-0.22067	-0.19164	-0.06798
-70º	-0.21672	-0.19631	-0.06873
-80º	-0.2125	-0.2012	-0.06941
-90º	-0.2085	-0.20585	-0.07009
-93.97º	-0.20883	-0.20577	-0.07038
-100º	-0.21163	-0.20338	-0.07082
-110º	-0.21657	-0.19917	-0.07158

6.4 Conclusion

To sum up, we primarily discuss the magnetic property of heteroallene and heterocumulene based *tert*-butyl nitroxide diradicals, where the latter shows *E*- and *Z*-isomers. Heteroallene based diradicals manifest ferromagnetic coupling whereas heterocumulene based diradicals show tuning of *J* values from antiferromagnetic to ferromagnetic state on going from *Z*- to *E*-isomer. The heteroatom (P/As) substitution in allene and cumulene couplers causes some geometrical changes due to the presence of lone pair of electrons on the heteroatom. Along with spin polarization, a delocalized radical unit is formed from the radical center to the coupler in all the *tert*-butyl nitroxide diradicals. The shapes of the SOMOs also assure the delocalization of unpaired electron within the coupler. Magneto-structural correlation shows that for both the *E*- and *Z*-isomers, magnetic crossover occurs at a certain range of dihedral angles depending on the spin accumulation on two nearby magnetic centers. From all these observations we conclude that the typical characteristics of *tert*-butyl nitroxide as a radical center and the presence of heteroatom within the coupler produce significant effect on our designed systems which show magnetic crossover associated with geometrical isomers in heterocumulene based systems.

6.5 References

(1) Taylor, D. R. *Chem. Rev.* **1967**, *67*, 317-359.
(2) Hendon, C.H.; Tiana, D.; Murray, A.T.; Carbery, D.R.; Walsh, A. *Chem. Sci*. **2013**, *4*, 4278–4284.
(3) Eliel, L. E.; Wilen, S. H. Stereochemistry of organic compounds; John Wiley & Sons: New York, **1994**; Chapter 9, p 539.
(4) Skibar, W.; Kopacka, H.; Wurst, K.; Salzmann, C.; Ongania, K.H.; Biani, F.F.D.; Zanello. P.; Bildstein, B. *Organometallics* **2004**, *23*, 1024-1041.
(5) Januszewski, J.A.; Tykwinski, R.R. *Chem. Soc. Rev.* **2014**, *43*, 3184-3203.
(6) Januszewski, J.A.; Wendinger, D.; Methfessel, C.D.; Hampel, F.; Tykwinski, *Angew. Chem. Int. Ed.* **2013**, *52*, 1817 –1821.
(7) Wendinger, D.; Tykwinski, R.R. *Acc. Chem. Res.* **2017**, *50*, 1468−1479.
(8) Shil, S.; Misra, A. *J. Phys. Chem. A* **2010**, *114*, 2022-2027.
(9) Bhattacharya, D.; Shil, S.; Misra, A. *J. Photochem. Photobiol., A* **2011**, *217*, 402−410.
(10) Zhang, F.; Song, X.; Bu, Y. *J. Phys. Chem. C* **2015**, *119*, 27930-27937.
(11) Saha, A.; Latif, I. A.; Datta, S.N. *J. Phys. Chem. A* **2011**, *115*, 1371-1379.
(12) Ali, Md. E.; Staemmler, V.; Illas, F.; Oppeneer, P.M. *J. Comput. Theory Chem.* **2013**, *9*, 5216-5220.
(13) Bhattacharya, D.; Misra, A. *J. Phys. Chem. A*, **2009**, *113*, 5470–5475.
(14) Shil, S.; Sarbadhikary, P.; Misra, A. *RSC Adv*. **2016**, *6*, 99467.

(15) Paul, S.; Misra, A. *J. Phys. Chem. A.* **2010**, *114*, 6641.
(16) Coey, J. M. D. Magnetism and magnetic materials, Cambridge University Press, Cambridge, U.K., **2010**, ISBN 13: 9780521816144.
(17) Latif, I. A.; Singh, V. P.; Bhattacharjee, U.; Panda, A.; Datta, S. N. *J. Phys. Chem. A* **2010**, *114*, 6648–6656.
(18) Ali, Md. E.; Datta, S.N. *J. Phys. Chem. A* **2006**, *110*, 2776-2784.
(19) Cho, D.; Ko, K. C.; Ikabata, Y.; Wakayama, K.; Yoshikawa, T.; Nakai, H.; Lee, J.Y. *J. Chem. Phys.* **2015**, *142*, 024318.
(20) Kolanji, K.; Postulka, L.; Wolf, B.; Lang, M.; Schollmeyer, D.; Baumgarten. M. *J. Org. Chem.* **2019**, *84*, 140−149.
(21) Song, M.; Song, X.; Bu, Y. *Chem. Phys. Chem.* **2017**, *18*, 2487-2498.
(22) Chen, D.; Deng, T.; Yang, L.; Bu, Y. *J. Phys. Chem. C* **2019**, *123*, 14152−14163.
(23) Sarbadhikary, P.; Shil, S.; Panda, A.; Misra, A. *J. Org. Chem*, **2016**, *81*, 5623.
(24) Sarbadhikary, P.; Shil, S.; Misra, A. *Phys. Chem. Chem. Phys.* **2018**, *20*, 9364-9375.
(25) Garner, M. H.; Hoffmann, R.; Rettrup, S.; Solomon, G.C. *ACS Cent. Sci.***2018**, *4*, 688-700.
(26) Garner, M. H.; Jensen, A.; Hyllested, L.; Solomon, G. C. *Chem. Sci.* **2019**, ***10***, 4598-4608.
(27) Aoki, Y.; Orimoto, Y.; Imamura, A. *ACS Cent. Sci.* **2018**, 4, 664-665.
(28) Appel, R. Multiple Bonds and Low Coordination in Phosphorus Chemistry, Georg Thieme Verlag: Stuttgart, Germany, **1990**; p 157.
(29) Escudié, J.; Ranaivonjatovo, H.; Rigon, L. *Chem. Rev.* **2000**, *100*, 3639-3696.
(30) Eichler, B.; West, R. *Adv. Organomet. Chem.* **2000**, *46*, 1-46.
(31) Escudié, J.; Ranaivonjatovo, H.; Bouslikhane, M.; Harouch, Y. E; Baiget, L.; Nemes, G.C. *Russ. Chem. Bull., Int. Ed.* **2004**, *53*, 1020-1033.
(32) Escudié, J.; Ranaivonjatovo, H. *Organometallics* **2007,** *26*, 1542-1559.
(33) Märkl, G.; Sejpka, H.; Dietl, S.; Nuber, B.; Ziegler, M. L. *Angew. Chem., Int. Ed. Engl*. **1986**, *25*, 1003-1004.
(34) Bouslikhane, M.; Gornitzka, H.; Ranaivonjatovo, H.; Escudié, J. *Organometallics* **2002**, *21*, 1531-1533.
(35) Rancurel, C.; Heise, H.; Köhler, F. H.; Schatzschneider, U.; Rentschler, E.; Vidal-Gancedo, J.; Veciana, J.; Sutter, J. –P. *J. Phys. Chem. A* **2004**, *108*, 5903-5914.
(36) Polo, V.; Alberola, A.; Andres, J.; Anthony, J.; Pilkington, M. *Phys. Chem. Chem. Phys.* **2008**, *10*, 857–864.
(37) Bhattacharya, D.; Shil, S.; Panda, A.; Misra, A. *J. Phys. Chem. A* **2010**, *114*, 11833–11841.

(38) Tamura, M.; Nakazawa, Y.; Shiomi, D.; Nozawa, K.; Hosokoshi, Y.; Ishikawa, M.; Takahashi, M.; Kinoshita, M. *Chem. Phys. Lett.* **1991**, *186*, 401-404.
(39) Ziessel, R.; Stroh, C.; Heise, H.; Köhler, F. H.; Turek, P.; Claiser, N.; Souhassou, M.; Lecomte, C. *J. Am. Chem. Soc.* **2004**, *126*, 12604-12613.
(40) Hicks, R. G.; Lemaire, M. T.; Öhrström, L.; Richardson, J. F.; Thompson, L. K.; Xu, Z. *J. Am. Chem. Soc*. **2001**, *123*, 7154-7159.
(41) Wautelet, P.; Catala, L.; Bieber, A.; Turek, P.; André, J.-J. *Polyhedron* **2001**, *20*, 1571-1576.
(42) Gomberg, M. *J. Am. Chem. Soc*. **1900**, *22*, 757-771.
(43) Gomberg, M. *Chem. Rev*. **1924**, *1*, 91-141.
(44) Kanno, F.; Inoue, K.; Koga, N.; Iwamura, H. *J. Am. Chem. Soc.***1993**, *115,* 847-850.
(45) Calder, A,; Forester, A. R.; James, P. *G.;* Luckhurst, G. R. *J. Am. Chem. Soc.* **1969**, *91,* 3724-3727.
(46) Fang, S.; Lee, M. –S.; Hrovat, D.A.; Borden, W.T. *J. Am. Chem. Soc.* **1995,** *117***,** 6727-6731.
(47) Jung, M.; Sharma, A.; Hinderberger, D.; Braun, S.; Schatzschneider, U.; Rentschler, E. *Inorg. Chem.* **2009**, *48*, 7244–7250.
(48) Oniciu, D. C.; Matsuda, K.; Iwamura, H. *J. Chem. Soc., Perkin Trans.* **1996**, *2*, 907-913.
(49) Inoue, K.; Iwamura, H. *J. Am. Chem. Soc.***1994,** *116***,** 3173-3174.
(50) Noodleman, L. *J. Chem. Phys.***1981**, *74*, 5737−5743.
(51) Noodleman, L.; Baerends, E. J. *J. Am. Chem. Soc.* **1984**, *106*, 2316−2327.
(52) Noodleman, L.; Davidson, E. R. *Chem. Phys.***1986**, *109*, 131−143.
(53) Noodleman, L.; Peng, C. Y.; Case, D. A.; Mouesca, J. -M. *Coord. Chem. Rev.***1995**, *144*, 199−244.
(54) Martin, R. L.; Illas, F. *Phys. Rev. Lett.* **1997**, *79*, 1539-1542.
(55) Caballol, R.; O. Castell, O.; Illas, F.; Moreira, I. de P. R.; Malrieu, J. P. *J. Phys. Chem. A* **1997**, *101*, 7860-7866.
(56) Paul, S.; Misra, A. *J. Chem. Theory Comput.* **2012**, *8*, 843−853.
(57)Yamaguchi, K.; Fukui, H.; Fueno, T. *Chem. Lett.* **1986**, *15*, 625−628.
(58) Yamaguchi, K.; Takahara, Y.; Fueno, T.; Nasu, K. *Jpn. J. Appl. Phys.***1987**, *26*, L1362−L1364.
(59) Yamaguchi, K.; Jensen, F.;Dorigo, A.; Houk, K. N. *Chem. Phys. Lett.* **1988**, *149*, 537−542.
(60) Yamaguchi, K.; Takahara, Y.; Fueno, T.; Houk, K. N. *Theor. Chim. Acta.* **1988**, *73*, 337−364.
(61) Frisch, M. J.; Trucks, G. W.; Schlegel, H. B.; Scuseria, G. E.; Robb, M. A.; Cheeseman, J. R.; Scalmani, G.; Barone, V.; Mennucci, B.; Petersson, G. A.; Nakatsuji, H.; Caricato, M.; Li, X.; Hratchian, H. P.; Izmaylov, A. F.; Bloino, J.; Zheng, G.; Sonnenberg, J. L.; Hada, M.; Ehara, M.; Toyota, K.; Fukuda, R.; Hasegawa, J.; Ishida, M.; Nakajima, T.; Honda, Y.; Kitao, O.; Nakai, H.; Vreven, T.; Montgomery, J. A., Jr.; Peralta, J. E.; Ogliaro, F.; Bearpark, M.; Heyd, J. J.; Brothers, E.; Kudin, K. N.; Staroverov, V. N.; Kobayashi, R.; Normand, J.; Raghavachari, K.;

Rendell, A.; Burant, J. C.; Iyengar, S. S.; Tomasi, J.; Cossi, M.; Rega, N.; Millam, M. J.; Klene, M.; Knox, J. E.; Cross, J. B.; Bakken, V.; Adamo, C.; Jaramillo, J.; Gomperts, R.; Stratmann, R. E.; Yazyev, O.; Austin, A. J.; Cammi, R.; Pomelli, C.; Ochterski, J. W.; Martin, R. L.; Morokuma, K.; Zakrzewski, V. G.; Voth, G. A.; Salvador, P.; Dannenberg, J. J.; Dapprich, S.; Daniels, A. D.; Farkas, Ö.; Foresman, J. B.; Ortiz, J. V.; Cioslowski, J.; Fox, D. J. Gaussian, Inc., Wallingford CT, **2009**.

(62) Shil, S.; Herrmann, C. *Inorg. Chem.* **2015**, *54*, 11733–11740.

(63) Ali, M. E.; Roy, A. S.; Datta, S. N. *J. Phys. Chem. A* **2007**, *111*, 5523–5527.

(64) Polo, V.; Alberola, A.; Andres, J.; Anthony, J.; Pilkington, M. *Phys. Chem. Chem. Phys*. **2008**, *10*, 857-864.

(65) Shil, S.; Roy, M.; Misra, A. *RSC Adv*. **2015**, *5*, 105574-105582.

(66) Herring, C. in Magnetism IIB, Direct exchange between well-separated atoms, ed. G.T. Rado and H. Suhl, Academic Press, New York, **1966**, vol. 5.

(67) Trindle, C.; Datta, S. N. *Int. J. Quantum Chem.***1996**, *57*, 781-799.

(68) Schatzschneider, U.; Rentschler, E. *J. Mol. Struct. (Theochem)* **2003**, 638, 163–168.

(69) Hoffmann, R.; Zeiss, G. D.; Dine, G. W. V. *J. Am. Chem. Soc*. **1968**, *90*, 1485.

(70) Zhang, G.; Li, S.; Jiang, Y. *J. Phys. Chem. A* **2003**, *107*, 5573-5582.

CHAPTER 7

Conclusions

A comprehensive conclusion of all the chapters is given here.

This part of the thesis contains the summary of preceding chapters which has been ploughed through. In first chapter we have discussed the different types of magnetic materials with their major applications. The stability as well as magnetic nature of organic radicals has also been elaborated. In the second part of this chapter, the transport property of different metal complexes, SMMs and radicals is discussed with their possible applications.

The second Chapter portrays the theoretical background for the estimation of the magnetic exchange coupling constant (*J*) of molecules. Among different variety of methodologies, the broken symmetry (BS) formalism in density functional theory (DFT) framework is found to come up with the optimal solution for the estimation of *J*. Starting from the expression of the phenomenological Heisenberg spin Hamiltonian, Giensberg, Noodleman and Davidson (GND) was given a popular formula for the evaluation of *J* value. However, the GND equation is applicable when the interaction between magnetic orbitals is sufficiently small. On the other hand, Bencini and Ruiz have proposed an expression to estimate *J* which is applicable where the overlap between the orbitals is large enough. However, the spin projected formula given by Yamaguchi is used to estimate the *J* values throughout my entire thesis work which is applicable for whole range of coupling strengths. The theoretical background for the estimation of transport property of molecules through green function-based technique in DFT framework has also been discussed.

In chapter three we have studied the effect of the length of molecular wires on the electrical transport properties. Several extended π-conjugated molecules have interesting applications as conducting nanowires, memory devices, and so on. In this chapter, we investigate the transport property of two molecular wires of different length which shows that the molecular wires of smaller length have higher transmission, i.e., higher conduction. The wires we have studied here are addition polymers and they are important for application in electronic industry. The magnetic exchange coupling constant of the radical substituted molecular wires (substituting each molecular wire with two methylene radical centers at two different positions) depend only on the distance between the spin centers, not on the outsider substitution. It is also observed that beyond certain distance between two radical centers, the spin polarization is no longer effective although the molecule have strong π network. The transmission of the molecular wire without radical substitution shows similar observations as that of the wire with radical substitution for ferromagnetically coupled diradicals. Our designed molecular wires consist of several aromatic phenyl rings along with radical substitution on the rings. When transmission occurs through the wire, possibly only local transmission of the aromatic rings appear on the Fermi level of the electrode and the radicals are not participated to the transmission of that region, which may be the reason for the same transmission after radical substitution in the ferromagnetic diradicals. But for antiferromagnetically coupled diradicals, there is a small variation in transmission characteristics between the radical substituted molecular wires.

In the fourth chapter we have discussed the magnetic property of diradicals based on allene and chiral cumulene coupler with ferromagnetic interaction that increases on addition of chiral centers within the coupler (where nitronyl nitroxide (NN) and verdazyl (VER) are used as radical center). Spin density distribution analysis shows that with the increase in length of the coupler, enhancement of spin polarization along the coupler takes place and the probability to localize the spin density on each chiral center increases (as all the middle carbons contain 2 π electrons on each). Addition of chiral centers within the coupler lowers the energy of LUMO and a lower HOMO-LUMO gap facilitates a stronger magnetic coupling. From natural orbital occupancies it is found that with increasing chain length of chiral coupler the occupancy of LUMO increases. Therefore, a correlation between the LUMO occupation and magnetic exchange coupling constant is intuited. It is well known that stable chiral magnets are important ingradients for future data storage, spintronic devices and other applications. But the synthesized chiral magnets are mainly inorganic or metallo-organic in nature. In our work, we have designed chiral organic magnetic molecules with ferromagnetic interaction. Therefore, these designed molecules may be used as molecular building blocks for organic chiral magnetic solids. Moreover, a close inspection of *J* values shows that NN- stands for a better choice of radical center over VER- and mixed radicals. Thereby, it is expected that this trend might inspire synthetic chemists to synthesis NN- based chiral magnetic molecule with high ferromagnetic interaction.

The fifth chapter presents a characteristic of variation in magnetic and transport properties of diradicals based on odd cumulene couplers, even cumulene couplers and conjugated couplers having different π interaction properties. During past decades, much efforts is given to design and synthesis of π-conjugated molecular wires containing delocalized electrons as it is a persistent challenge in molecular electronics to control the conductance and current flow through such systems. In this study we established that an existence of typical spin polarization pathway in cumulene systems (compared to conjugated systems), distance between two radical centers (that may perhaps interrupt the spin polarization pathway) and a planar structure that allows better orbital overlap between π-systems compared to a non-planar one, controls the magnetic exchange coupling constant values. Largely speaking, the unusual π-interaction within the coupler is the lighting factor that controls the magnetic properties of our designed systems. Transport calculations show that with the increase in chain length, diradicals based on even cumulene act as better conductors than odd cumulenes. Moreover, for all the diradicals, it is found that the distance between two electrodes, frontier energy splitting and the spin polarization pathways play a major role in determining transmission characteristics. Finally, the basis of all the factors is the unusual π-interaction within the couplers that produce different transmission characteristics of our designed systems.

In the sixth chapter, we primarily discuss the magnetic property of heteroallene and heterocumulene based *tert*-butyl nitroxide diradicals, where the latter shows *E*- and *Z*-isomers. There is a recent resurgence in studies relating to the switching of magnetic nature between ferromagnetic and antiferromagnetic states. Several studies show that the presence of heteroatom in the exchange pathway significantly influences the magnetic exchange coupling. On the other hand, heteroallene and heterocumulene (with 4 atoms in backbone chain) containing double bonded heavy elements, have attracted interest from a theoretical point of view because of their peculiar physicochemical properties. Herein, we are motivated to evaluate the potential effect of P/As atom substitution within the allene and cumulene couplers in mediating the exchange interaction between the two radical centers. Heteroallene based diradicals manifest ferromagnetic coupling whereas heterocumulene based diradicals show tuning of *J* values from antiferromagnetic to ferromagnetic state on going from *Z*- to *E*-isomer. The heteroatom (P/As) substitution in allene and cumulene couplers causes some geometrical changes due to the presence of lone pair of electrons on the heteroatom. Along with spin polarization, a delocalized radical unit is formed from the radical center to the coupler in all the *tert*-butyl nitroxide diradicals. The shapes of the SOMOs also assure the delocalization of unpaired electron within the coupler. Magneto-structural correlation shows that for both the *E*- and *Z*-isomers, magnetic crossover occurs at a certain range of dihedral angles depending on the spin accumulation on two nearby magnetic centers. From all these observations we conclude that the typical characteristics of *tert*-butyl nitroxide as a radical center and the presence of heteroatom within the coupler produce significant effect on our designed systems which show magnetic crossover associated with geometrical isomers in heterocumulene based systems.

BIBLIOGRAPHY

CHAPTER 1

(1) Du Trémolet de Lacheisserie, É.; Gignoux, D.; Schlenker, M. (**2005**). *Magnetism: Fundamentals*. Springer.pp. 3–6. ISBN 0-387-22967-1.
(2) (a) Tamaki, H.; Zhong, Z. J.; Matsumoto, N.; Kida, S.; Koikawa, M.; Achiwa, N.; Hashimoto, Y.; Okawa, H. *J. Am. Chem. Soc.* **1992**, *114*, 18, 6974–6979. (b) Miyasaka, H.; Saitoh, A.; Abe, S. *Coord. Chem. Rev.* **2007**, *251*, 2622–2664. (c) Okawa, H.; Mitsumi, M.; Ohba, M.; Kodera, M.; Matsumoto, N. *Bull. Chem. Soc. Jpn.* **1994**, *67*, 2139–2144. (d) Tanase, S.; Reedijk, J. *Coord. Chem. Rev.* **2006**, *250*, 2501–2510. (e) Ohba, M.; Okawa, H. *Coord. Chem. Rev.* **2000**, *198*, 313-328. (f) Saalfrank, R.W.; Bernt, I. *Curr. Opin. Solid State Mater. Sci.* **1998**, *3*, 407-413.(g) Matthews, C. J.; Avery, K.; Xu, Z.; Thompson, L. K.; Zhao, L.; Miller, D. O.; Biradha, K.; Poirier, K.; Zaworotko, M. J.; Wilson, C.; Goeta, A. E.; Howard, J. A. K. *Inorg. Chem.* **1999**, *38*, 5266-5276.
(3) (a) Ratera, I.; Jaume Veciana, J. *Chem. Soc. Rev.* **2012**, *41*, 303–349. (b) Iwamura, H. *Adv. Phys. Org. Chem.* **1991**, *26*, 179-253. (c) Dougherty, D. A. *Acc. Chem. Res.* **1991,** *24*, 88-94. (d) Iwamura, H.; Koga, N. *Acc. Chem. Res.* **1993**, *26*, 346-351. (e) Matsuda, K.; Iwamura, H. *Curr. Opin. Solid State Mater. Sci.* **1997**, *2*, 446-450.
(4) (a) Crayston, J. A.; Devine, J. N.; Walton, J. C. *Tetrahedron*, **2000**, *56*, 7829-7857. (b) Miller, J. S.; Epstein, A. J. *MRS Bull.* **2000**, *25*, 21-30.
(5) (a) Itoh K.; Kinoshita, M. *Molecular Magnetism*, Gordon and Breach, Amsterdam (Kodansha asco publisher, Tokyo), (**2000**). (b) Lahti, P. M. *Magnetic Properties of Organic Materials*, Marcel Dekker, New York (**1999**).
(6) Verdaguer, M. *Polyhedron* **2001**, *20*, 1115-1128.
(7) Miller, J.S. *Mater. Today* **2014**, *17*, 224–235.
(8) Kahn, O. (**1993**). *Molecular Magnetism*. John Wiley & Sons, Singapore.
(9) Bleaney, B.; Bowers, K.D. *Proc. R. Soc. A* **1952**, *214*, 451-465.
(10) Wickman, H. H.; Trozzolo, A. M.; Williams, H. J.; Hull, G. W.; Merritt, F. R. *Phys. Rev.* **1967**, *155*, 563-566.
(11) (a) Tamura, M.; Nakazawa, Y.; Shiomi, D.; Nozawa, K.; Hosokoshi, Y.; Ishikawa, M.; Takahashi, M.; Kinoshita, M. *Chem. Phys. Lett.* **1991**, *186*, 401–404. (b) Nakazawa, Y.; Tamura, M.; Shirakawa, N.; Shiomi, D.; Takahashi, M.; Kinoshita, M.; Ishikawa, M. *Phys. Rev. B* **1992**, *46*, 8906–8914.
(12) (a) Sessoli, R.; Tsai, H.-L; Schake, A.R.; Wang, S.; Vincent, J.B.; Folting, K.; Gatteschi, D.; Christou, G.; Hendrickson, D.N. *J. Am. Chem. Soc.* **1993**, *115*, 1804-1816. (b) Packwood, D. M., Reaves, K. T., Federici, F. L., Katzgraber, H. G., & Teizer, W. *Proc. R. Soc. A* **2013**, *469*, 20130373.

(13) Green, J. E., Wook Choi, J., Boukai, A., Bunimovich, Y., Johnston-Halperin, E., DeIonno, E.; Luo, Y.; Sheriff, B. A.; Xu, K.; Shin, Y. S.; Tseng, H. –R.; Stoddart, J. F.; Heath, J. R. *Nature* **2007**, *445*, 414–418.
(14) (a) Gatteschi, D.; Sessoli, R.; Villain, J. Molecular Nanomagnets; Oxford University Press: Oxford, U.K., **2006**. (b) Gatteschi, D. *Adv. Mater.***1994**, *6*, 635−645.
(15) (a) Coronado, E.; Epsetin, A. J. *J. Mater.Chem.* **2009**, *19*, 1670−1671. (b) Bogani, L.; Wernsdorfer, W. *Nat. Mater.* **2008**, *7*, 179−186.
(16) Leuenberger, M. N.; Loss, D. *Nature* **2001**, *410*, 789−793.
(17) Rumberger, E. M.; Zakharov, L. N.; Rheingold, A. L.; Hendrickson, D. N. *Inorg. Chem.* **2004,** *43*, 6531-6533.
(18) (a) Barra, A. L.; Gatteschi D.; Sessoli, R. *Chem. Eur. J.*, **2000**, *6*, 1608-1614. (b) Wieghardt, K.; Pohl, K.; Jibril I.; Huttner, G. *Angew. Chem., Int. Ed. Engl.*, **1984**, *23*, 77-78.
(19) Castro, S. L.; Sun, Z. M.; Grant, C. M.; Bollinger, J. C.; Hendrickson, D. N.; Christou, G. *J. Am. Chem. Soc*. **1998**, *120*, 2365.
(20) (a) Sessoli, R.; Powell, A. K. *Coord. Chem. Rev.* **2009**, *253*, 2328–2341. (b) Feltham, H. L. C.; Brooker, S. *Coord. Chem. Rev.* **2014**, *276*, 1–33. (c) Zhang, P.; Guo, Y. –N.; Tang, J. *Coord. Chem. Rev.* **2013**, *257*, 1728–1763. (d) Layfield, R. *Organometallics*, **2014**, *33*, 1084–1099. (e) Pointillart, F.; Cador, O.; Guennic, B. L.; Ouahab, L. *Coord. Chem. Rev.* **2017**, *346*, 150–175. (f) Liu, K.; Zhang, X.; Meng, X.; Shi, W.; Cheng, P.; Powell, A. K. *Chem. Soc. Rev*. **2016**, *45*, 2423–2439. (g) McAdams, S. G.; Ariciu, A. -M.; Kostopoulos, A. K.; Walsh, J. P. S.; Tuna, F. *Coord. Chem. Rev.* **2017**, *346*, 216–239.
(21) (a) Wang, Y.-L.; Gu, B.; Ma, Y.; Xing, C.; Wang, Q.-L.; Li, L.-C.; Cheng, P.; Liao, D.-Z. *CrystEngComm.* **2014**, *16*, 2283-2289. (b) Silva, M.R.; Martín-Ramos, P.; Coutinho, J.T.; Pereira, L.C.J.; Martín-Gil, J. *Dalton Trans.* **2014**, *43*, 6752-6761. (c) Li, Q.-W.; Liu, J.-L.; Jia, J.-H.; Leng, J.-D.; Lin, W.-Q.; Chen, Y.-C.; Tong, M.-L. *Dalton Trans.* **2013**, *42*, 11262-11270. (d) Jiménez, J.-R.; Díaz-Ortega, I. F.; Ruiz, E.; Aravena, D.; Pope, S. J. A.; Colacio, E.; Herrera, J.M. *Chem. Eur. J.* **2016**, *22*, 14548–14559. (e) Costes, J.P.; Titos-Padilla, S.; Oyarzabal, I.; Gupta, T.; Duhayon, C.; Rajaraman, G.; Colacio, E. *Chem. Eur. J.* **2015**, *21*, 15785 – 15796. (f) Ren, M.; Xu, Z.-L.; Bao, S.-S.; Wang, T.-T.; Zheng, Z.-H.; Ferreira, R.A.S.; Zheng, L.-M.; Carlos, L.D. *Dalton Trans.* **2016**, *45*, 2974-2982.
(22) Zhang, K.; Montigaud, V.; Cador, O.; Li, G. –P.; Guennic, B. L.; Tang, J. -K.; Wang, Y. –Y. *Inorg. Chem.* **2018**, *57*, 8550-8557.
(23) (a) Meihaus, K. R.; Long, J. R. *Dalton Trans.* **2015**, *44*, 2517−2528. (b) Cooper, O. J.; Mills, D. P.; McMaster, J.; Moro, F.; Davies, E. S.; Lewis, W.; Blake, A. J.; Liddle, S. T. *Angew. Chem.* **2011**, *123*, 2431−2434. (c) Mills, D. P.; Moro, F.; McMaster, J.; van Slageren, J.; Lewis, W.; Blake, A. J.; Liddle, S. T. *Nat. Chem.* **2011**, *3*, 454−460. (d) Antunes, M. A.; Pereira, L. C.; Santos, I. C.; Mazzanti, M.; Marcalo, J.; Almeida, M. *Inorg. Chem.* **2011**, *50*, 9915−9917. (e) King, D. M.; Tuna, F.; McMaster, J.; Lewis, W.; Blake, A. J.; McInnes, E. J.; Liddle, S. T. *Angew. Chem., Int. Ed.* **2013**, *52*, 4921−4924. (f) Rinehart, J. D.; Long, J. R. *J. Am. Chem. Soc.* **2009**, *131*, 12558−12559. (g) Mougel, V.; Chatelain, L.; Pécaut, J.; Caciuffo, R.; Colineau, E.;

Griveau, J. C.; Mazzanti, M. *Nat. Chem.* **2012**, *4*, 1011−1017. (h) Pereira, L. C.; Camp, C.; Coutinho, J. T.; Chatelain, L.; Maldivi, P.; Almeida, M.; Mazzanti, M. *Inorg. Chem.* **2014**, *53*, 11809−11811.
(24) Gaggioli, C. A.; Gagliardi, L. *Inorg. Chem.* **2018**, *57*, 8098-8105.
(25) (a) Gomberg, M. *J. Am. Chem. Soc*. **1900**, *22*, 757-771. (b) Gomberg, M. *J. Am. Chem. Soc*., **1901**, *23*, 496-502. (c) Gomberg, M. *Chem. Rev*. **1924**, *1*, 91-141.
(26) (a) Leonid Sheps, L.; Andrew C. Crowther, A. C.; Christopher G. Elles, C. G.; F. Fleming Crim, F. F. *J. Phys. Chem. A* **2005**, *109*, 4296-4302. (B) Gibian, M. J.; Corley, R. C. *Chemical Reviews*. **1973**, *73*, 441-464. (C) Rozantsev, E. G.; Loshadkin, D. V. *Designed Monomers and Polymers.* **2001**, *4*, 281–300.
(27)(a) Kahn, O. Magnetism: A Supramolecular Function, Kluwer, Dordrecht, **1996**. (b) Itoh, K.; Kinoshita, M. *Molecular Magnetism*, Kodansha (Gordon and Breach), Tokyo, **2000**. (c) Power, P. P. *Chem. Rev*. **2003**, *103*, 789-810.(d)Tang, B.; Zhao, J.; Xu, J. –F.; Zhang, X. *Chem. Sci.* **2020**, *11*, 1192-1204.(e) Ventosa, N.; Ruiz, D.; Rovira, C.; Veciana, J. *Mol. Cryst. Liq. Cryst*. **1993**, *232*, 333-342. (f) Ballester, M. *Adv. Phys. Org. Chem*. **1989**, *25*, 267-445. (g) Armet, O.; Veciana, J.; Rovira, C.; Riera, J.; Castaner, J.; Molins, E.; Rius, J.; Miravitlles, C.; Olivella, S.; Brichfeus, J. *J. Phys. Chem*. **1987**, *91*, 5608-5616. (h) Ballester, M.; Pascual, I.; Riera, J.; Castaner, J. *J. Org. Chem*. **1991**, *56*, 217-225. (i) Domingo, V. M.; Castaner, J. *J. Chem. Soc.,Chem. Commun*. **1995**, 895-896.
(28) Li, Z.; Moalin, M.; Zhang, M.; Vervoort, L.; Mommers, A.; Haenen G. R. M. M. *Int. J. Mol. Sci.* **2020**, *21*, 2033.
(29) (a) Shiomi, D.; Ito, K.; Nishizawa, M.; Sato, K.; Takui, T.; Itoh, K. *Syn. Metals* **1999**, *103*, 2271-2272.(b) Romero, F. M.; Ziessel, R.; Bonnet, M.; Pontillon, Y.; Ressouche, E.; Schweizer, J.; Delley, B.; Grand, A.; Paulsen, C. *J. Am. Chem. Soc*. **2000**, *122*, 1298-1309. (c) Nagashima, H.; Irisawa, M.; Yoshioka, N.; Inoue, H. *Mol. Cryst. Liq. Cryst. Sci.Technol. Sect. A* **2002**, *376*, 371-376.(d) Rajadurai, C.; Ivanova, A.; Enkelmann, V.; Baumgarten, M. *J. Org. Chem*. **2003**, *68*, 9907-9915.(f) Deumal, M.; Robb, M. A.; Novoa, J. J. *Polyhedron* **2003**, *22*, 1935-1944. (g) Ishida, T.; Iwamura, H. *J. Am. Chem. Soc*. **1991**, *113*, 4238-4241. (h) Kanno, F.; Inoue, K.; Koga, N.; Iwamura, H. *J. Phys. Chem.* **1993**, *97*, 13267-13272. (i) Inoue, K.; Iwamura, H. *J. Am. Chem. Soc*. **1994**, *116*, 3173-3174. (j) Iwamura, H.; Inoue, K. *Adv. Mater*. **1996**, *8*, 73-76. (k) Inoue, K. *π- Electron Magnetism.* **2001**, *100*, 61-91.
(30) (a) Ali, M. E.; Roy, A. S.; Datta, S. N. *J. Phys. Chem. A* **2007**, *111*, 5523–5527. (b) Wautelet, P.; Le Moigne, J.; Videva, V.; Turek, P. *J. Org. Chem.* **2003**, *68*, 8025–8036.(c) Ali, M. E.; Datta, S. N. *J. Phys. Chem. A* **2006**, *110*, 2776–2784. (d) Latif, I. A.; Singh, V. P.; Bhattacharjee, U.; Panda, A.; Datta, S. N. *J. Phys. Chem. A* **2010**, *114*, 6648–6656. (e) Ali, M. E.; Datta, S. N. *J. Phys. Chem. A* **2006**, *110*, 10525–10527.
(31) Nogami, T.; Ishida, T.; Yasui, M.; Iwasaki, F.; Takeda, N.; Ishikawa, M.; Kawakami, T.; Yamaguchi, K. *Bull. Chem. Soc. Japan* **1996,** *69***,** 1841-1848.
(32) Kuhn, R.; Trischmann, H. *Angew. Chem., Int. Ed. Engl.* **1963**, *2*, 155.

(33) (a) Hicks, R. G. *Can. J. Chem*. **2004**, *82*, 1119-1127. (b) Hicks, R. G.; Lemaire, M. T.; Öhrström, L.; Richardson, J. F.; Thompson, L. K.; Xu, Z. *J. Am. Chem. Soc*. **2001**, *123*, 7154-7159.
(34) Hicks, R. G.; Hooper, R. *Inorg. Chem.* **1999**, *38*, 284-286.
(35) (a) Hicks, R. G.; Ohrstrom, L.; Patenaude, G. W. *Inorg. Chem.* **2001**, *40*, 1865-1870. (b) Koivisto, B. D.; Ichimura, A. S.; McDonald, R.; Lemaire, M. T.; Thompson, L. K.; Hicks, R. G. *J. Am. Chem. Soc.* **2006**, *128*, 690-691.(c) Koivisto, B. D.; Hicks, R. G. *Coord. Chem. Rev.* **2005**, *249*, 2612-2630.
(36) (a) Mukai, K.; Konishi, K.; Nedachi, K.; Takeda, K. *J. Magn. Magn.Mater*. **1995**, *140*, 1449-1450. (b) Neugebauer, F. A.; Fisher, H.; Siegel, R. *Chem. Ber*.**1988**, *121*, 815-822.
(37) (a) Mukai, K.; Nedachi, K.; Takiguchi, M.; Kobayashi, T.; Amaya, K. *Chem. Phys. Lett*. **1995,** *238*, 61-64. (b) Kremer, R. K.; Kanellakopulos, B.; Bele, P.; Brunner, H.; Neugebauer, F. A. *Chem. Phys. Lett*. **1994**, *230*, 255-259. (c) Mito, M.; Nakano, H.; Kawae, T.; Hitaka, M.; Takagi, S.; Deguchi, H.; Suzuki, K.; Mukai, K.; Takeda, K. *J. Phys. Soc. Jpn*. **1997**, *66*, 2147-2156. (d) Mukai, K.; Nuwa, M.; Morishita, T.; Muramatsu, T.; Kobayashi, T. C.; Amaya, K. *Chem. Phys. Lett*. **1997**, *272*, 501-505. (e) Mukai, K.; Wada, N.; Jamali, J. B.; Achiwa, N.; Narumi, Y.; Kindo, K.; Kobayashi, T.; Amaya, K. *Chem. Phys. Lett*. **1996**, *257*, 538-544.
(38) Ballester, M. *Acc. Chem. Res*. **1985**, *18*, 380-387.
(39) (a) Haddon, R. C. *Nature* **1975**, *256*, 394–396. (b) Cordes, A. W.; Haddon, R. C.; Oakley, R. T. *Phosphorus. Sulfur. Silicon Relat. Elem.* **2004**, *179*, 673–684.
(40) Rawson, J. M.; Alberola, A.; Whalley, A. *J. Mater. Chem.* **2006**, *16*, 2560-2575.
(41) (a) Vegas, A.; Perez-Salazar, A.; Banister, A. J.; Hey, R. G. *J. Chem. Soc., Dalt. Trans.* **1980**, 1812–1815. (b) Haynes, D. A. *CrystEngComm* **2011**, *13*, 4793-4805.
(42) (a) Stubbe, J.; Van der Donk, W.A. *Chem. Rev*.**1998**, *98*,705–762. (b) Amorati, R.; Lucarini, M.; Mugnaini, V.; Pedulli, G. F.; Minisci, F.; Recupero, F.; Fontana, F.; Astolfi, P.; Greci, L. *J. Org. Chem.* **2003**, *68*, 1747-1754.
(43) (a) Hubbel, W. L.; Gross, A.; Langen, R.; Lietzow, M.A. *Curr. Opin.Struct. Biol.* **1998**, *8*, 649-656. (b) Fanucci G.E.; Cafiso, D.S. *Curr.Opin.Struct. Biol.* **2006**, *16*, 644-653. (c) Roques, N.; Mugnaini, V.; Veciana, J. *Top. Curr. Chem.* **2010**, *293*, 207-258.
(44) (a) Gatteschi, D. *Adv. Mater.* **1994**, *6*, 635-645. (b) Train, C.; Noreland, L.; Baumgarten, M. *Coord. Chem. Rev.* **2009**, *253*, 2342-2351.
(45) (a) Hamachi, K.; Matsuda, K.; Itoh, T.; Iwamura,H. *Bull. Chem. Soc. Jpn.* **1998**, *71*, 2937-2943. (b) Matsuda, K.; Irie, M. *J. Am. Chem. Soc*. **2000**, *122*, 7195-7201. (c) Matsuda, K.; Irie, M. *J. Am. Chem. Soc.* **2000**, *122*, 8309-8310.(d) Matsuda, K.; Irie, M. *Mol. Cryst. Liq. Cryst.* **2000**, *345*, 155-160.
(46) (a) Vyas, S.; Ali, M. E.; Hossain, E.; Patwardhan, S.; Datta, S. N. *J. Phys. Chem. A* **2005**, *109*, 4213–4215. (b) Barone, V.; Bencini, A.; Matteo, A. di. *J. Am. Chem. Soc.* **1997**, *7863*, 10831–10837. (c) Latif, I. a; Panda, A.; Datta, S. N. *J. Phys. Chem. A* **2009**, *113*, 1595–1600. (d) Bhattacharya, D.; Shil, S.; Misra, A.; Klein, D. J. *Theor. Chem. Acc.* **2009**, *127*, 57–67.

(47) Ziessel, R.; Stroh, C.; Heise, H.; Khler, F. H.; Turek, P.; Claiser, N.; Souhassou, M.; Lecomte, C. *J. Am. Chem. Soc*. **2004**, *126*, 12604-12613.
(48) Catala, L.; Le Moigne, J.; Gruber, N.; Novoa, J. J.;Rabu, P.; Belorizky, E.; Turek, P. *Chem. Eur. J* **2005**, *11*, 2440-2454.
(49) Trindle, C.; Datta, S. N.; Mallik, B. *J. Am. Chem. Soc.* **1997**, *119*, 12947-12951.
(50) (a) Bhattacharya, D.; Misra, A. *J. Phys. Chem. A*, **2009**, *113*, 5470–5475. (b) Paul, S.; Misra, A. *J. Phys. Chem. A.* **2010**, *114*, 6641-. 6647. (c) S. Paul, A. Misra, *J. Chem. Theory Comput.* 2**012**, *8*, 843-853.
(51) Coey, J. M. D. *Magnetism and Magnetic Materials*, Cambridge University Press, Cambridge, U.K., **2010**, ISBN 13: 9780521816144.
(52) Bhattacharya, D.; Shil, S.; Misra, A.; Klein, D. J. *Theor. Chem. Acc.* **2010**, *127*, 57-67.
(53) (a) Shil, S.; Misra, A. *J. Phys. Chem. A* **2010**, *114*, 2022-2027. (b) Saha, A.; Latif, I. A.; Datta, S.N. *J. Phys. Chem. A* **2011**, *115*, 1371-1379. (c) Ali, Md. E.; Staemmler, V.; Illas, F.; Oppeneer, P.M.; *J. Comput. Theory Chem.* **2013**, *9*, 5216-5220.
(54) (a) Rancurel, C.; Heise, H.; Köhler, F. H.; Schatzschneider, U.; Rentschler, E.; Vidal-Gancedo, J.; Veciana, J.; Sutter, J. –P. *J. Phys. Chem. A* **2004**, *108*, 5903-5914. (b) Polo, V.; Alberola, A.; Andres, J.; Anthony, J.; Pilkington, M. *Phys. Chem. Chem. Phys.* **2008**, *10*, 857–864. (c) Bhattacharya, D.; Shil, S.; Panda, A.; Misra, A. *J. Phys. Chem. A* **2010**, *114*, 11833–11841. (d) Barclay, T. M.; Hicks, R. G.; Ichimura, A. S.; Patenaude, G. W. *Can. J. Chem.* **2002**, *80*, 1501–1506.
(55) Ali, M. E.; Datta, S. N. *J. Phys. Chem. A* **2006**, *110*, 13232–13237.
(56) (a) Ghosh, R.; Seal, P.; Chakrabarti, S. *J. Phys. Chem. A* **2010**, *114*, 93-96. (b) Seal, P.; Chakrabarti, S. *J. Phys. Chem. A* **2008**, *112*, 3409-3413.
(57) (a) Miller, J. S.; Drillon, M. D. *Magnetism: Molecules to Materials II*; Wiley-VCH: Weinheim, Germany, **2001**. (b) Rajca, A. *Chem. Eur. J.* **2002**, *8*, 4834-4841.
(58) (a) Pappas, C. Physics **2012**, *5*, 28. (b) Togawa, Y.; Koyama, T.; Takayanagi, K.; Mori, S.; Kousaka, Y.; Akimitsu, J.; Nishihara, S.; Inoue, K.; Ovchinnikov, A. S.; Kishine, *J. Phys. Rev. Lett.* **2012**, *108*, 107202.
(59) (a) Crivillers, N.; Mas-Torrent, M.; Vidal-Gancedo, J.; Veciana, J.; Rovira, C. *J. Am. Chem. Soc.* **2008**, *130*, 5499–5506. (b) Yulikov, M.; Lueders, P.; Warsi, M.F.; Chechik, V.; Jeschke, G. *Phys. Chem. Chem. Phys.* **2012**, *14*, 10732–10746. (c) Miller, J. S.; Gatteschi, D. *Chem. Soc. Rev.* **2011**, *40*, 3065–3066.
(60) (a) Boehme, C.; Lupton, J. M. *Nat. Nanotechnol.* **2013**, *8*, 612−615. (b) Sun, D.; Ehrenfreund, E.; Vardeny, Z. V. *Chem.Commun. (Cambridge)* **2014**, *50*, 1781−1793.
(61) (a) Oyaizu, K.; Nishide, H. *Adv. Mater.* **2009**, *21*, 2339–2344.(b) Tomlinson, E. P.; Hay, M. E.; Boudouris, B. W. *Macromolecules* **2014**, *47*, 6145 –6158.(c) Lloveras, V.; Vidal-Gancedo, J.; Figueira-Duarte, T. M.; Nierengarten, J. -F.; Novoa, J. J.; Mota, F.; Ventosa, N.; Rovira, C.; Veciana, J. *J. Am. Chem. Soc.* **2011**, *133*, 5818–5833.
(62) (a) Matsumoto, K.; Hyodo, F.; Matsumoto, A.; Koretsky, A. P.; Sowers, A. L.; Mitchell, J. B.; Krishna, M. C. *Clin. Cancer Res.* **2006**, *12*, 2455–2462. (b) Metz, J. M.; Smith, D.; Mick, R.; Lustig, R.; Mitchell, J.; Cherakuri, M.; Glatstein, E.; Hahn, S. M. *Clin. Cancer Res.* **2004**, *10*, 6411–6417. (c) Huang, Z.; Jiang, J.; Belikova, N.

A.; Stoyanovsky, D. A.; Kagan, V. E.; Mintz, A. H. *J. Neuro-Oncol.* **2010**, *100*, 1–8. (d) Francese, G.; Dunand, F. A.; Loosli, C.; Merbach, A. E.; Decurtins, S. *Magn. Reson. Chem.* **2003**, *41*, 81–83.

(63) (a) Bosman, A. W.; Janssen, R. A. J.; Meijer, E. W. *Macromolecules* **1997**, *30*, 3606–3611. (b) Han, H. J.; Sebby, K. B.; Singel, D. J.; Cloninger, M. J. *Macromolecules* **2007**, *40*, 3030–3033. (c) Lei, X. G.; Jockusch, S.; Turro, N. J.; Tomalia, D. A.; Ottaviani, M. F. *J. Colloid Interface Sci.* **2008**, *322*, 457–464.(d) Fukuzaki, E.; Takahashi, N.; Imai, S.; Nishide, H.; Rajca, A. *Polym. J.* **2005**, *37*, 284–293. (e) Badetti, E.; Lloveras, V.; Wurst, K.; Sebastián, R. M.; Caminade, A. -M.; Majoral, J. -P.; Veciana, J.; Vidal-Gancedo, J. *Org. Lett.* **2013**, *15*, 3490–3493.(f) Badetti, E.; Lloveras, V.; Muñoz-Gómez, J. L.; Sebastián, R. M.; Caminade, A. -M.; Majoral, J. P.; Veciana, J.; Vidal-Gancedo, J. *Macromolecules* **2014**, *47*, 7717–7724.

(64) Hansda, S.; Pal, A. K.; Datta, S. N. *J. Phys. Chem. C* **2015**, *119*, 3754-3761.

(65) Mañeru, D. R.; Moreira, I. P. R.; Illas, F. *J. Am. Chem. Soc.* **2016**, *138*, 5271-5275.

(66) Michinobu, T.; Inui, J.; Nishide, H. *Org. Lett*. **2003**, *5*, 2165-2168.

(67) Kaneko, T.; Abe, H.; Teraguchi, M.; Aoki, T. *Macromolecules* **2013**, *46*, 2583−2589.

(68) Lao, K. -U.; Tsou, P. -K.; Lankau, T.; Yu, C. -H.; *Phys. Chem. Chem. Phys.* **2012**, *14*, 138–147.

(69) (a) Allemand, P. -M.; Khemani, K. C.; Koch, A.; Wudl, F.; Holczer, K.; Donavan, S.; Gruner, G.; Thompson, J. D. *Science* **1991**, *253*, 301-302.(b) Mihailovic, D.; Arcon, D.; Venturini, P.; Blinc, R.; Omerzu, A.; Cevc, P. *Science* **1995**, *268*, 400-402.(c) Narymbetov, B.; Omerzu, A.; Kabanov, V. V.; Tokumoto, M.; Kobayashi, H.; Mihailovic, D. *Nature* **2000**, *407*, 883-885. (d) Mrzel, A.; Cevc, P.; Omerzu, A.; Mihailovic, D. *Phys. Rev. B* **1996**, *53*, R2922-R2925. (e) Omerzu, A.; Mihailovic, D.; Tokumoto. M. *Phys. Rev. B* **2000**, *61*, R11883-R11885. (f) Tanaka, K.; Asai, Y.; Sato, T.; Kuga, T.; Yamabe, T.; Tokumoto, M. *Chem. Phys. Lett.* **1996**, *259*, 574-578.

(70) Rajca, A.; Utamapanya, S.; Thayumanavam, S. *J. Am. Chem. Soc.* **1992**, *144*, 1884-1885.

(71)(a) Rajca, A.; Wongsriratanakul, J.; Rajca, S. *Science* **2001**, *294*, 1503-1505. (b) Rajca, A.; Wongsriratanakul, J.; Rajca, S. *J. Am. Chem. Soc.* **2004**, *126*, 6608-6626; (c) Rajca, A.; Lu, K.; Rajca, S. *J. Am. Chem. Soc.***1997**, *119*, 10335-10345;(d) Rajca, A. *Adv. Phys. Org. Chem.* **2005**, *40*, 153-199; (e) Rajca, A. *Chem. Rev.* **1994**, *94*, 871-893.

(72) (a) Fang, S.; Lee, M.-S.; Hrovat, D. A.; Borden, W. T. *J. Am. Chem. Soc.* **1995**, *117*, 6727−6731. (b) Wenthold, P. G.; Kim, J. B.; Lineberger, W. C. *J. Am. Chem. Soc.* **1997**, *119*, 1354−1359. (c) Zhang, G.; Li, S.; Jiang, Y. *Tetrahedron* **2003**, *59*, 3499−3504. (d) Mañeru, D. R.; Pal, A. K.; Moreira, I.; de, P. R.; Datta, S. N.; Illas, F. *J. Chem. Theory Comput.* **2014**, *10*, 335−345. (e) Pal, A. K.; Mañeru, D. R.; Latif, I. A.; Moreira, I.; de, P. R.; Illas, F.; Datta, S. N. *Theor. Chem. Acc.* **2014**, *133*, 1472.

(73) Song, M.; Song, X.; Bu, Y. *Organometallics* **2017**, *36*, 1505-1514.

(74) Yang, Y.; Liu, C.; Xu, X.; Meng, Z.; Tong, W.; Ma, Z.; Zhou, C.; Sun, Y.; Sheng, Z. *Polym. Chem.* **2018**, *9*, 5499-5503.

(75) Wernsdorfer, W. *Int. J. Nanotechnology* **2010**, *7*, 497-522.
(76) (a) Moore, G. E. *Electronics* **1965**, *38*, 114–117. (b) Moore, G. E. *IEDM Tech. Digest* **1975**, 11–13.
(77) Waldrop, M. M. *Nature* **2016**, *530*, 144-147.
(78) Baibich, M. N.; Broto, J. M.; Fert, A.; Dau, F. N. V.; Petroff, F.; Etienne, P.; Creuzet, G.; Friederich, A.; Chazelas, J. *Phys. Rev. Lett.***1988**, *61*, 2472–2475.
(79) (a) Mosca, D.H.; Petroff, F.; Fert, A.; Schroeder, P. A.; Pratt, W.P.; Laloee, R. *J. Mag. Mag. Mat.* **1991**, *94*, L1-L5. (b) Schad, R.; Potter, C.D.; Belien, P.; Verbanck, G.; Moshchalkov, V.V.; Bruynseraede, Y. *Appl. Phys. Lett.* **1994**, *64*, 3500.
(80) (a) Žutic, I.; Das Sarma, S. *Rev. Mod. Phys.* **2004**, *76*, 323–410. (b) Wolf, S. A.; Awschalom, D. D.; Buhrman, R. A.; Daughton, J. M.; von Molnár, S.; Roukes, M. L.; Chtchelkanova, A. Y.; Treger, D. M.; *Science* **2001**, *294*, 1488–1495.
(81) Miyzaki, T.; Tezuka, N. *J. Mag. Mag. Mat.* **1995**, *139*, L231.
(82) Moodera, J.S.; Kinder, L.R.; Wong. M.; Meservey, R. *Phys. Rev. Lett.* **1995**, *74*, 3273.
(83) (a) Zhu, H. J.; Ramsteiner, M.; Kostial, H.; Wassermeier, M.; Schönherr, H.-P.; Ploog, K. H. *Phys. Rev. Lett.* **2001**, *87*, 016601. (b) Malajovich, I.; Kikkawa, J. M.; Awschalom, D. D.; Berry, J. J.; Samarth, N. *Phys. Rev. Lett.* **2000**, *84*, 1015. (c) Labella, V. P.; Bullock, D. W.; Z. Ding, Z.; Emery, C.; Venkatesan, A.; Oliver, W. F.; Salamo, G. J.; Thibado, P. M.; M. Mortazavi, M. *Science*, **2001**, *292*, 1518-1521.
(84) (a) Schmidt, G. *J. Phys. D. Appl. Phys.* **2005**, *38*, R107-R122. (b) Dediu, V.; Murgia, M.; Matacotta, F. C.; Taliani, C.; Barbanera, S. *Solid State Commun.* **2002**, *122*, 181-184. (c) Xiong, Z.H.; Wu, D.; Vardeny, Z.V.; Shi, J. *Nature* **2004**, *427*, 821-824. (d) Lou, X.; Adelmann, C.; Crooker, S. A.; Garlid, E. S.; Zhang, J.; Reddy, K.S.M.; Flexner, S. D.; Palmstrom, C. J.; Crowell, P. A. Nat. Phys. **2007,** *3*, 197-202.
(85) (a) Datta, S.; Das. B. *Appl. Phys. Lett.* **1990**, *56*, 665-667. (b) Ohno, Y.; Young, D. K.; Beschoten, B.; Matsukura, F.; Ohno, H.; Awschalom, D.D. *Nature*. **1999**, *402*, 790-792. (c) Appelbaum, I.; Huang, B.; Monsma, D. J. *Nature* **2007**, *447*, 295-298.
(86) (a) Chappert, C.; Fert, A.; Nguyen Van Dau, F. *Nat. Mater.* **2007**, *6*, 813–823. (b) Parkin, S. S. P., Hayashi, M., Thomas, L. *Science* **2008**, *320*, 190–194.
(87) Tsukagoshi, K.; Alphenaar, B.; Ago, H. *Nature* **1999**, *401*, 572-574.
(88) Camarero, J.; Coronado, E. *J. Mater. Chem.*, **2009**, *19*, 1678.
(89) (a) Bogani, L.; Wernsdorfer, W. *Nat. Mater.* **2008,** *7*, 179-186. (b) Atodiresei, N.; Brede, J.; Lazic, P.; Caciuc, V.; Hoffmann, G.; Wiesendanger, R.; Blugel, S. *Phys. Rev. Lett.* **2010**, *105*, 066601. (c) Wan, H.; Zhou, B.; Chen, X.; Sun, C. Q.; Zhou, G. *J. Phys. Chem. C* **2012**, *116*, 2570-2574. (d) Thomas, L.; Lionti, F.; Ballou, R.; Gatteschi, D.; Sessoli, R.; Barbara, B. *Nature* **1996**, *383*, 145-147. (e) Cremades, E.; Pemmaraju, C. D.; Sanvito, S.; Ruiz, E. *Nanoscale* **2013**, *5*, 4751-4757.
(90) (a) Wu, Q. H.; Zhao, P.; Chen, G. *Org. Electron.* **2015**, *25*, 308-316. (b) Li, X.B.; Gao, H.; Wan, H.Q.; Li, H.L.; Zhou, G.H. *Chem. Phys. Lett.* **2014**, *610*, 298-302.
(91) (a) Chen, W.; Xu, N.; Wang, B. L.; Bian, B. A. *Phys. Lett. A.* **2014**, *378*, 2020-2023. (b) Zu, F.X.; Gao, G.Y.; Fu, H.H.; Xiong, L.; Zhu, S.C.; Li, P.; Yao, K.L. *Appl. Phys. Lett.* **2015**, *107*, 252403. (c) Zhu, L.; Yao, K. L.; Liu, Z. L. *Appl. Phys.*

*Lett.***2010**, *96*, 082115. (d) Li, E. Y.; Marzari, N. *ACS Nano.* **2011**, *5*, 9726-9736. (e) Maslyuk, V. V.; Bagrets, A.; Meded, V.; Arnold, A.; Evers, F.; Brandbyge, M.; Bredow, T.; Mertig, I. *Phys. Rev. Lett.* **2006**, *97*, 097201. (f) Mannini, M.; Pineider, F.; Sainctavit, P.; Danieli, C.; Otero, E.; Sciancalepore, C.; Talarico, A. M.; Arrio, M.; Cornia, A.; Gatteschi, D.; Sessoli, R. *Nature Mater.* **2009**, *8*, 194-197. (g) Xiang, H.;Yang, J.; Hou, J. G.; Zhu, Q. *J. Am. Chem. Soc.* **2006**, *128*, 2310-2314. (h) Shen, X.; Yi, Z.; Shen, Z.; Zhao, X.; Wu, J.; Hou, S.; Sanvito, S. *Nanotechnology.* **2009**, *20*, 385401. (i) Zhou, L.; Yang, S.W.; Ng, M. F.; Sullivan, M. B.; Tan, V. B. C.; Shen, L. *J. Am. Chem.Soc.* **2008**, *130*, 4023-4027. (j) Pemmaraju, C. D.; Rungger, I.; Sanvito, S. *Phys. Rev. B.* **2009**, *80*, 104422. (k) Shukla, S. K.; Sanvito, S. *Phys. Rev. B.* **2009**, *80*, 184429.

(92) Huang, J.; Wang, W. Y.; Yang, S. F.; Su, H. B.; Li, Q. X.; Yang, J. L. *Chem. Phys. Lett.* **2012**, *539-540*, 102-106.

(93) Deng, X. Q.; Zhang, Z. H.; Tang, G. P.; Fan, Z. Q.; Sun, L.; Li, C. X. *Org. Electron.* **2016**, *35*, 1-5.

(94) Shen, X.; Sun, L. L.; Yi, Z. L.; Benassi, E.; Zhang, R. X.; Shen, Z. Y.; Sanvito, S.; Hou, S. M.*Phys. Chem. Chem. Phys*., **2010**, *12*, 10805-10811.

(95) Zhao, P.; Chen, G. *J.Chem. Phys.* **2018**, *149*, 134305.

(96) (a) Shojaei, F.; Hahn, J. R. *Chem. Mater.* **2014**, *26*, 2967-2974. (b) Huang, X.; Sheng, P.; Tu, Z.; Zhang, F.; Wang, J.; Geng, H.; Zou, Y.; Di, C.; Yi, Y.; Sun, Y.; Xu, W.; Zhu, D. *Nature. Commun.* **2015**, *6*, 7408. (c) Sarkar, S.; Pramanik, A.; Sarkar, P. *Chem. Phys.* **2016**, *478*, 173-177. (d) Chakravarty, C.; Mandal, B.; Sarka, P. *J. Phys. Chem. C* **2016**, *120*, 28307-28319. (e) Clough, C. A. J.; Skelton, J. M.; Dowbes, C. A.; Rosa, A. A.; Yoo, J. W.; Walsh, A.; Melot, B. C.;Marinescu, S. C. *J. Am. Chem. Soc.* **2017**, *139*, 10863-10867.

(97) Pearson, C.; Moore, A. J.; Gibson, J. E.; Bryce, M. R.; Petty, M. C. *Thin Solid Films*. **1994**, *244*, 932-935.

(98) Huong, V. T. T.; Tai, T. B.; Jiang, J. –C.; Nguyen,M. T.; *Phys. Chem. Chem. Phys.* **2017**, *19*, 32536-32543.

(99) Peng, J.; Zhou, W. -X.; Chen, K. -Q. *Phys. Lett.* A. **2014**, *378*, 3126-3130.

(100) Wu, Q. H.; Zhao, P.; Su, Y.; Li S. J.; Gou, J. H. *RSC Adv.* **2015**, *5*, 52938-52944.

(101) Wu, Q. H.; Zhao, P.; Chen, G. *Org. Electron.* **2015**, *25*, 308-316.

(102) (a) Heersche, H. B.; Groot, Z. D.; Folk, J. A.; van der Zant, H. S. J.; Romeike, C.; Wegewijs, M. R.; Zobbi, L.; Barreca, D.; Tondello, E.; Cornia, A. *Phys. Rev. Lett.***2006**, *96*, 206801. (b) Voss, S.; Zander, O.; Fonin, M.; Rüdiger, U.; Burgert, M.; Groth, U. *Phys. Rev. B* **2008**, *78*, 155403. (c) Ni, C.; Shah, S.; Hendrickson, D.; Bandaru, P. R. *Appl. Phys. Lett.* **2006**, *89*, 212104. (d) Jo, M.-H.; Grose, J. E.; Baheti, K.; Deshmukh, M. M.; Sokol, J. J.; Rumberger, E. M.; Hendrickson, D. N.; Long, J. R.; Park, H.; Ralph, D. C. *Nano Lett*. **2006**, *6*, 2014-2020. (e) Kim, G.-H.; Kim, T.-S. *Phys. Rev. Lett*. **2004**, *92*, 137203. (f) Henderson, J. J.; Ramsey, C. M.; del Barco, E.; Mishra, A.; Christou, G. *J. Appl. Phys.* **2007**, *101*, 09E102. (g) Romeike, C.; Wegewijs, M. R.; Hofstetter, W.; Schoeller, H. *Phys. Rev. Lett*. **2006**, 96, 196601. (h) Romeike, C.; Wegewijs, M. R.; Schoeller, H. *Phys. Rev. Lett*. **2006**, *96*, 196805. (i) Misiorny, M.; Barnaś, J. *Europhys.Lett*. **2007**, *78*, 27003.

(103) (a) Christou, G.; Gatteschi, D.; Hendrickson, D. N.; Sessoli, R. *Mater. Res. Soc. Bull.* **2000**, *25*, 66–71. (b) Gatteschi, D.; Sessoli, R.; Villain, J. *Molecular Nanomagnets* (Oxford Univ. Press, New York, **2007**). (c) Naitabdi, A.; Bucher, J.-P.; Gerbier, P.; Rabu, P.; Drillon, M. *Adv. Mater.***2005**, *17*,1612–1616. (d) Fleury, B.; Catala,L.; Huc,V.; David,C.; Zhong,W.Z.; Jegou,P.;Baraton,L.; Palacin,S.; Albouy, P. –A.; Mallah, T. *Chem. Comm.* **2005**, 2020–2022. (e) Coronado, E.; Forment-Aliaga, A.; Gaita-Ariño, A.; Giménez-Saiz, C.; Romero, F. M.; Wernsdorfer ,W. *Angew. Chem. Int. Ed.* **2004**, *43***,** 6152–6156.

(104) (a) Misiorny, M.; Barnaś, J. *Phys. Rev. B* **2007**, *75*, 134425. (b) Misiorny, M.; Barnaś, J. *Phys. Status Solidi B* **2009**, *246*, 695.

(105) (a) Timm, C.; Elste, F. *Phys. Rev. B* **2006**, *73*, 235304. (b) Misiorny, M.; Barnaś, J. *Phys. Rev. B* **2008**, *77*, 172414.

(106) (a) Urdampilleta, M.; Klyatskaya, S.; Cleuziou, J.P.; Ruben, M.; Wernsdorfer, W. *Nat. Mater.* **2011**, *10*, 502–506. (b) Urdampilleta, M.; Nguyen, N.V.; Cleuziou, J.P.; Klyatskaya, S.; Ruben, M.; Wernsdorfer, W. *Int. J. Mol. Sci.* **2011**, *12*, 6656–6667.

(107) Vincent, R.; Klyatskaya, S.; Ruben, M.; Wernsdorfer, W.; Balestro, F. *Nature* **2012**, *488*, 357–360.

(108) Thiele, S.; Balestro, F.; Ballou, R.; Klyatskaya, S.; Ruben, M.; Wernsdorfer, W. *Science* **2014**, *344*, 1135–1138.

(109) (a) Misiorny, M.; Barnaś, J. *Phys. Rev. B* **2007**, *76*, 054448. (b) Misiorny, M.; Weymann, I.; Barnaś, J. *Phys. Rev. B* **2011**, *84*, 035445. (c) Misiorny, M.; Barnaś, J. *Phys. Rev. B* **2009**, *79*, 224420. (d) Misiorny, M.; Weymann, I.; Barnaś, J. *Phys. Rev. Lett.* **2011**, *106*, 126602.

(110) Misiorny, M.; Barnaś, J. *Europhys. Lett.* **2010**, *89*, 18003.

(111) (a) Larade, B.; Taylor, J.; Mehrez, H.; Guo, H. *Phys. Rev. B* **2001**, *64*, 075420. (b) Sotthewes, K.; Geskin, V.; Heimbuch, R.; Kumar, A.; Zandvliet, H. J. W. *APL. Mat.* **2014**, *2*, 010701. (c) Tsukagoshi, K.; Alphenaar, B. W.; Ago, H. *Nature* **1999**, *401*, 572-574. (d) Ouyang, M.; Awschalom, D. D. *Science* **2003**, *301*, 1074-1078. (e) Pati, R.; Senapati, L.; Ajayan, P. M.; Nayak, S. K. *Phys. Rev. B* **2003**, *68*,100407.

(112) (a) Datta, S. Electronic Transport in Mesoscopic Systems, (Cambridge University Press, New York, 1997). (b) Chun, D.; Cheng, Y.; Wudl, F. *Angew. Chem. Int. Ed.* **2008**, *47*, 8380 –8385. (c) Mondal, R.; Shah, B. K.; Neckers, D. C. *J. Am. Chem. Soc.* **2006**, *128*, 9612-9613. (d) Tonshoff, C.; Bettinger, H. F. *Angew. Chem. Int. Ed.* **2010**, *49*, 4125-4128. (e) Anthony, J. *Angew. Chem. Int. Ed.* **2008**, *47*, 452 – 483.

(113) (a) Meng, H.; Bendikov, M.; Mitchell, G.; Helgeson,R.; Wuld, F.; Bao, Z.; Siegrist, T.; Kloc, C.; Chen, C. –H. *Adv. Mater.* **2003**, *15*, 1090-1093. (b) Katz, H. E. *Chem. Mat.* **2004**, *16*, 4748-4756.

(114) (a) Bendikov, M.; Duong, H. M.; Starkey, K.; Houk, K. N.; Carter, E. A. Wudl , F. *J. Am. Chem. Soc.* **2004**, *126*, 7416-7417. (b) Hachmann, J.; Dorando, J. J.; Aviles, M.; Chan, G. K. *J. Chem. Phys.* **2007**, *127*, 134309. (c) Hajgato, B.; Szieberth, D.; Geerlings, P.; Proft, F. D.; Deleuze, M.S. *J. Chem. Phys.* **2009**, *131*, 224321. (d) Qu,

Z.; Zhang, D.; Liu, C.; Jiang, Y. *J. Phys. Chem. A* **2009**, *113*, 7909-7914. (e) Szulczewski, G.; Sanvito, S.; Coey, J. M. D. *Nat. Mater* **2009**, *8*, 693-695.

(115) (a) Sanvito, S. *Chem. Soc. Rev.* **2011**, *40*, 3336-3355. (b) Mas-Torrent, M.; Crivillers, N.; Mugnaini, V.; Ratera, I.; Rovira, C.; Veciana, J. *J. Mater.Chem.* **2009**, *19*, 1691-1695. (c) Herrmann, C.; Solomon, G. C.; Ratner, M. A. *J. Am. Chem. Soc.* **2010**, *132*, 3682-3684. (d) Lee, J.; Lee, E.; Kim, S.; Bang, G. S.; Shultz, D. A.; Schmidt, R. D.; Forbes, M. D. E.; Lee, H. *Angew. Chem., Int. Ed.* **2011**, *50*, 4414-4418. (e) Yonekuta, Y.; Susuki, K.; Oyaizu, K.; Honda, K. *J. Am. Chem. Soc.* **2007**, *129*, 14128-14129. (f) McGuire, J.; Miras, Haralampos N.; Richards, E.; Sproules, S. *Chem. Sci.* **2019**, *10*, 1483-1491.

(116) (a) Zhao, X. L.; Ando, Y.; Liu, Y.; Jinno, M.; Suzuki, T. *Phys. Rev. Lett.*, **2003**, *90*, 187401. (b) Muramatsu, H.; Hayashi, T.; Kim, Y. A.; Shimamoto, D.; Endo, M.; Terrones, M.; Dresselhaus, M. S. *Nano Lett.*, **2008**, *8*, 237. (c) Kitaura, R.; Nakanishi, R.; Saito, T.; Yoshikawa, H.; Awaga, K.; Shinohara, H. *Angew. Chem., Int. Ed.*, **2009**, *48*, 8298.

(117) Prasongkit, J.; Grigoriev, A.; Wendin, G.; Ahuja, R. *Phys. Rev. B*: *Condens. Matter Mater. Phys.*, **2010**, *81*, 115404.

(118) Kim, W.Y.; Kim, K.S. *Nature Nanotech.* **2008**, *3*, 408-412.

(119) (a) Zhang, D.; Long, M.Q.; Zhang, X.J.; Xu, H. *RSC Adv.* **2015**, *5*, 96455-96463. (b) Deng, X.Q.; Zhang, Z.H.; Fang, Z.Q.; Tang, G.P. ; Sun, L.; Li, C.X. *Org. Electron.* **2016**, *32*, 41-46.(c) Zhao, P.; Wu, Q.H.; Liu, H.Y.; Liu, D.S.; Chen, G. *J. Mater. Chem. C.* **2014**, *2*, 6648-6654.

(120) (a) Zeng, M.G.; Shen, L.; Zhang, C.; Feng, Y.P. *Appl. Phys. Lett.* **2011**, *98*, 053101. (b) Deng, X.Q.; Zhang, Z.H.; Tang, G.P.; Fang, Z.Q.; Yang, C.H. *Carbon.* **2014**, *66*, 646-653.

(121) Lee, M.; Williams, J. R.; Zhang, S.; Frisbie, D.; Goldhaber-Gordon, D. *Phys. Rev. Lett.* **2011**, *107*, 256601.

(122) (a) Ratera, I.; Veciana, J. *Chem. Soc. Rev.***2012**, *41*, 303-349. (b) Lee, E.C.; Choi, Y.C.; Kim, W.Y.; Singh, N.J.; Lee, S.; Shim, J.H.; Kim, K.S. *Chem. Eur. J.* **2010**, *16*, 12141-12146. (c) Peng, Q.; Obolda, A.; Zhang, M.; Li, F. *Angew. Chem. Int. Ed.***2015**, *54*, 7091-7095. (d) Sugawara, T.; Komatsu, H.; Suzuki, K. *Chem. Soc. Rev.* **2011**, *40*, 3105-3118. (e) Nakahara, K.; Iwasa, S.; Satoh, M.; Morioka, Y.; Iriyama, J.; Suguro, M.; Hasegawa, E. *Chem. Phys. Lett.***2002**, *359*, 351-354. (f) Xu, L.; Yang, F.; Su, C.; Ji, L.; Zhang, C. *Electrochim. Acta* **2014**, *130*, 148-155. (g) Dardenne, N.; Blase, X.; Hautier, G.; Charlier, J. –C.; Rignanese, G. M. *J. Phys. Chem. C* **2015**, *119*, 23373-23378.

(123) Sen, S.; Chakrabarti, S. *J. Am. Chem. Soc.* **2010**, *132*, 15334–15339.

(124) Chen, W.; Mao, W.; Bian, B.; Xu, N.; Chen, R.; Li, X-a.; Wang, L. *Comput. Theor. Chem.* **2016**, *1091*, 85-91.

(125) (a) Tour, J. M.; Kozaki, M.; Seminario, J. M. *J. Am. Chem. Soc.*, **1998**, *120*, 8486. (b) Modelli, A.; Venuti, M.; Scagnolari, F.; Contento, M.; Jones, D. *J. Phys. Chem. A*, **2001**, *105*, 219. (c) Distefano, G.; Jones, D.; Guerra, M.; Favaretto, L.; Modelli, L.; Mengoli, G. *J. Phys. Chem.*, **1991**, *95*, 9746. (d) Colle, M. D.; Cova, C.; Distefano, G.; Jones, D.; Modelli, A.; Comisso, N. *J. Phys. Chem. A* **1999**, *103*, 2828.

(e) Bredas, J. L.; The´mans, B.; Fripiat, J. G.; Andre´, J. M.; Chance, R. R. *Phys. Rev. B: Condens. Matter Mater. Phys.* **1984**, *29*, 6761.
(126) Deng, Y.-X.; Chen, S.-Z.; Zeng, Y.; Zhou, W.-X.; Chen, K.-Q.*Org. Electron.* **2017**, *50*, 184-190.
(127) Tagami, K.; Tsukada, M. *J. Phys. Chem. B* **2004**, *108*, 6441–6444.
(128) Zhang, J.; Xu, B.; Qin. Z. *Phys. Lett. A* **2018**, *382*, 1226-1230.
(129) Prins, F.; Barreiro, A.; Ruitenberg, J. W.; Seldenthuis, J. S.; Aliaga-Alcalde, N.; Vandersypen, L.M.K.; van der Zant, H. S. J. *Nano Lett.* **2011**, *11*, 4607–4611.
(130) Caliskan, S.; Laref, A. *Sci. Rep.* **2015**, *4*, 7363.
(131) Caliskan, S.*Physica E: Low-dimensional Systems and Nanostructures.***2018**, *99*, 43–50.
(132) Sevov, C.S.; Hickey, D.P.; Cook, M.E.; Robinson, S.G.; Barnett, S.; Minteer, S.D.; Sigman, M.S.; Sanford, M.S. *J. Am. Chem. Soc.* **2017**, *139*, 2924-2927.

CHAPTER 2

(1) Orio, M.; Pantazis, D. A.; Neese, F. *Photosynth. Res*. **2009**, *102*, 443-453.
(2) Fermi, E. *Rend. Accad. Naz. Lincei*. **1927**, *6*, 602-607. (b) Thomas, L. H. *Proc. Cambridge Philos. Soc*. **1927**, *23*, 542-548.
(3) (a) Noodleman, L. *J. Chem. Phys.* **1981**, *74*, 5737-5743. (b) Noodleman, L.; Baerends, E. J. *J. Am. Chem.* Soc. **1984**, *106*, 2316-2327. (c) Noodleman, L.; Davidson, E. R. *Chem. Phys.* **1986**, *109*, 131-143. (d) Noodleman, L.; Peng, C. Y.; Case, D. A.; Mouesca, J.-M. *Coord. Chem. Rev.* **1995**, *144*, 199-244.
(4) Ginsberg, A. P. *J. Am. Chem. Soc.* **1980**, *102*, 111-117.
(5) (a) Bencini, A.; Totti, F.; Daul, C. A.; Doclo, K.; Fantucci, P.; Barone, V. *Inorg. Chem.* **1997**, *36*, 5022-5030. (b) Bencini, A.; Gatteschi, D.; Totti, F.; Sanz, D. N.; McClevrty, J. A.;Ward, M. D. *J. Phys. Chem. A* **1998**, *102*, 10545.
(6) Ruiz, E.; Cano. J.; Alvarez, S.; Alemany, P. *J. Comput. Chem.* **1999**, *20*, 1391-1400.
(7) (a) Yamaguchi, K.; Takahara, Y.; Fueno, T.; Nasu, K. *Jpn. J. Appl. Phys.* **1987**, *26*, L1362. (b) Yamaguchi, K.; Jensen, F.; Dorigo, A.; Houk, K. N. *Chem. Phys. Lett.* **1988**, *149*, 537-542. (c) Yamaguchi, K.; Takahara, Y.; Fueno, T.; Houk, K. N. *Theo. Chim. Acta***1988**, *73*, 337.
(8) Mahan, G. D. *Many-particle Physics*; Plenum Press: New York, 1990.
(9) Soler, J. M.; Artacho, E.; Gale, J. D.; García, A.; Junquera, J.; Ordejón, P.; Sánchez-Portal, D. *J. Phys.: Condens. Matter*.**2002**, *14*, 2745-2779.
(10) (a) Landauer, R. *IBM J. Res. De*V.**1957**, *1*, 223–231. (b) M. Buttiker, Y. Imry, R. Landauer and S. Pinhas, *Phys. Rev. B.***1985**, *31*, 6207-6215.
(11) (a) Kohn, W.; Sham, L. J. *Phys. Re*v. **1965**, *140*, 1133–1138. (b) Hohenberg, P.; Kohn, W. *Phys. Re*v. **1964**, *136*, 864–871.
(12) Herrmann, C.; Solomon, G. C.; Ratner,M. A. *J. Am. Chem. Soc.***2010**, *132*, 3682-3684.

(13) (a) Caroli, C.; Combescot, R.; Nozieres, P.; Saint-James, D. *J. Phys. C: Solid State Phys.* **1971**, *4*, 916–929. (b) Meir, Y.; Wingreen, N. S. *Phys. Re*v. *Lett.* **1992**, *68*, 2512–2516.
(14) Herrmann, C.; Solomon, G. C.; Subotnik, J. E.; Mujica, V.; Ratner, M. A. *J. Chem. Phys.* **2010**, *132*, 024103(1–17).
(15) Herrmann, C.; Groß, L.; Steenbock, T.; Solomon. G. C. Artaios — a transport code for postprocessing quantum chemical electronic structure calculations, **2008-2014.**

CHAPTER 3

(1) Tian, W.; Datta, S.; Hong, S.; Reifenberger, R.; Henderson, J. I.; Kubiak, C. P. *J. Chem. Phys.* **1998**, *109*, 2874-2882.
(2) Kober, S.; Gotesman, G.; Naaman, R. *J. Phys. Chem. Lett*. **2013**, *4*, 2041-2045.
(3) Jalili, S.; Rafi-Tabar, H. *Phys. Rev. B* **2005**, *71*, 165410(1-9).
(4) Magoga, M.; Joachim, C. *Phys. Rev. B* **1997**, *56*, 4722-4729.
(5) Durig, U.; Zuger, O.; Michel, B.; Haussling, L.; Ringsdorf, H. *Phys.Rev. B* **1993**, *48*, 1711-1717.
(6) Boulas, C.; Davidovits, J. V.; Rondelez, F.; Vuillaume, D. *Phys. Rev. Lett*. **1996**, *76*, 4797-4800.
(7) Bumm, L. A.; Arnold, J. J.; Cygan, M. T.; Dunbar, T. D.; Burgin, T. P.; Jones, L.; II, Allara, D. L.; Tour, J. M.; Weiss, P. S. *Science* **1996**, *271*, 1705-1707.
(8) Andres, R.P.; Bein, T.; Dorogi, M.; Feng, S.; Henderson, J. I.; Kubiak, C. P.; Mahoney, W.; Osifchin, R.G.; Reifenberger, R.G. *Science* **1996**, *272*, 1323-1325.
(9) Reed, M. A.; Zhou, C.; Muller, C. J.; Burgin, T. P.; Tour, J. M. *Science* **1997**, *278*, 252-254.
(10) Kushmerick, J. G.; Holt, D. B.; Pollack, S. K.; Ratner, M. A.; Yang, J. C.; Schull, T. L.; Naciri, J.; Moore, M. H.; Shashidhar, R. *J. Am. Chem. Soc*. **2002**, *124*, 10654-10655.
(11) Weiss, E. A.; Ahrens, M. J.; Sinks, L. E.; Gusev, A. V.; Ratner, M. A.; Wasielewski, M. R.
J. Am. Chem. Soc. **2004**, *126*, 5577-5584.
(12) Nishizawa, S.; Hasegawa, J.-y.; Matsuda, K. *J. Phys. Chem. C* **2013**, *117*, 26280-26286.
(13) I. D. W. Samuel, *Philos. Trans. R. Soc., A,* **2000**, 358, 193–210.
(14) H. Lu, J. Leng and S. Du, *Soft Matter,* **2013**, 9, 3851–3858.
(15) H. Lu and S. Du, *Polym. Chem.*, **2014**, 5, 1155–1162.
(16) Herrmann, C.; Solomon, G. C.; Ratner, M. A. *J. Am. Chem. Soc.* 2010***, 132,*** 3682-3684.
(17) Herrmann, C.; Solomon, G. C.; Subotnik, J. E.; Mujica, V.; Ratner, M. A. *J. Chem. Phys.* **2010**, *132*, 024103 (1-17).

(18) Frisch, M. J.; Trucks, G. W.; Schlegel, H. B.; Scuseria, G. E.; Robb, M. A.; Cheeseman, J. R.; Scalmani, G.; Barone, V.; Mennucci, B.; Petersson, G. A.; et.al. Gaussian09; Gaussian, Inc.: Wallingford, CT, 2009.
(19) Yoshizawa, K. *Acc. Chem. Res.* **2012**, *45*, 1612-1621;
(20) Yoshizawa, K.; Tada, T.; Staykov, A. *J. Am. Chem. Soc*. **2008**, *130*, 9406-9413.
(21) Noodleman, L. *J. Chem. Phys*. **1981**,*74*, 5737.
(22) Noodleman, L.; Baerends, E. J. *J. Am. Chem. Soc*. **1984**, *106*, 2316-2327.
(23) Ginsberg, A. P. *J. Am. Chem. Soc*. **1980**, *102*, 111-117.
(24) Noodleman, L.; Peng, C. Y.; Case, D. A.; Mouesca, J. M. *Coord. Chem. Rev*. **1995**, *144*, 199-244.
(25) Noodleman, L.; Davidson, E. R. *Chem. Phys*. **1986**, *109*, 131-143.
(26) Bencini, A.; Totti, F.; Daul, C. A.; Doclo, K.; Fantucci, P.; Barone, V. *Inorg. Chem*. **1997**, *36*, 5022-5030.
(27) Bencini, A.; Gatteschi, D.; Totti, F.; Sanz, D. N.; McClevrty, J. A.; Ward, M. D. *J. Phys. Chem. A* **1998**, *102*, 10545.
(28) Ruiz, E.; Cano, J.; Alvarez, S.; Alemany, P. *J. Comput. Chem*. **1999**, *20*, 1391-1400.
(29) Yamaguchi, K.; Takahara, Y.; Fueno, T.; Nasu, K. *Jpn. J. Appl. Phys*. **1987**, *26*, L1362.
(30) Ali, Md. E.; Datta, S. N. *J. Phys. Chem. A* **2006**, *110*, 2776-2784.
(31) Ali, Md. E.; Datta, S. N. *J. Phys. Chem. A* **2006,** *110***,** 13232-13237**.**
(32) Polo, V.; Alberola, A.; Andres, J.; Anthony, J.; Pilkington, M. Phys. Chem. Chem. Phys. ***2008***, 10, *857-864.*
(33) Bhattacharya, D.; Misra, A. *J. Phys. Chem. A* **2009,** *113*, 5470-5475**.**
(34) Paul, S.; Misra, A. *THEOCHEM* **2009**, *907*, 35-40.
(35) Paul, S.; Misra, A. *THEOCHEM* **2009**, *895*, 156-160,
(36) Ashcroft, N.W.; Mermin, N.D, Solid *State Physics,* Holt, Rinehart and Winston, New York, 1976.
(37) F. Pauly, J. K. Viljas, J. C. Cuevas, G. Schön, *Phys. Rev. B,* 2008**,** ***77***, 155312.
(38) Stuyver, T.; Fias, S.; Proft, De F.; Geerlings, P, *Chem. Phys. Lett.* **2015**, *630*, 51-56.
(39) Kim, W. Y.; Kim, K. S. *Acc. Chem. Res*. **2010**, *43*, 111-120.
(40) Choi, Y. C.; Kim, W. Y.; Park, K. –S.; Tarakeshwar, P.; Kim, K. S.; Kim, T. –S.; Lee, J. Y. *J. Chem. Phys*. **2005**, *122*, 094706 (1-6).
(41) Shil, S.; Misra, A. *RSC Adv.* **2013**, *3*, 14352-14362.
(42) Trindle, C.; Datta, S. N. *Int. J. Quantum Chem.* **1996**, *57*, 781-799.
(43) Stasiw, D. E.; Zhang, J.; Wang, G.; Dangi, R.; Stein, B. W.; Shultz, D.A.; Kirk, M.L.; Wojtas, L.; Sommer, R. D. *J. Am. Chem.Soc*. **2015**, *137*, 9222-9225.

CHAPTER 4

(1) Nguyen, L. A.; He, H.; Pham-Huy, C. *Int. J. Biomed. Sci*. **2006**, ***2***, 85–100.
(2) Stephens, P. J.; Devlin, F. J.; Pan, J.-J. *Chirality.* **2008**, *20*, 643–663.
(3) Galán-Mascarós, J. R.; Coronado, E.; Goddard, P. A.; Singleton, J.; Coldea, A. I.; Wallis, J. D.; Coles, S. J.; Alberola, A. *J. Am. Chem. Soc*. **2010**, *132*, 9271.
(4) Pappas, C. *Physics* **2012**, *5*, 28.
(5) Train, C.; Gheorghe, R.; Krstic, V.; Chamoreau, L.-M.; Ovanesyan, N.S.; Rikken, G.L.J.A.; Gruselle, M.; Verdaguer, M. *nat. mater*. **2008**, *7*, 729-734.
(6) Togawa, Y.; Koyama, T.; Takayanagi, K.; Mori, S.; Kousaka, Y.; Akimitsu, J.; Nishihara, S.; Inoue, K.; Ovchinnikov, A. S.; Kishine, J. *Phys. Rev. Lett*. **2012**, *108*, 107202.
(7) Wagnière, G. H. *Chem Phys.***1999**, *245*,165–173.
(8) Bordács, S.; Kézsmárki, I.; Szaller, D.; Demko, L.; Kida, N.; Murakawa, H.; Onose, Y.; Shimano, R.; Rõõm, T.; Nagel, U.; Miyahara, S.; Furukawa, N.; Tokura, Y. *Nat. Phys*. **2012**, *8*, 734.
(9) Minguet, M.; Luneau, D.; Paulsen, C.; Lhotel, E.; Gorski, A.; Waluk, J.; Amabilino, D.B.; Veciana, J.; *Polyhedron* **2003**, *22*, 2349-2354.
(10) (a) Ishikawa, I.; Tajima, K. *Solid State Commun.* **1976**, *19*, 525-528.
(b) Yu, X. Z.; Onose, Y.; Kanazawa, N.; Park, J.H.; Han, J.H.; Matsui, Y.; Nagaosa, N.; Tokura, Y. *Nature* **2010,** *465*, 901-904.
(11) Kahn, O. Molecular Magnetism, VCH, New York, 1993.
(12) Coronado E, Delhae` P, Gatteschi D, Molecular magnetism: from molecular assemblies to devices; Miller J. S. (Eds); NATO ASI Series E321, vol 321, Kluwer, Dordrecht, 1996.
(13) Benelli, C.;Gatteschi, D. *Chem.Rev.* **2002**, *102*, 2369-2387.
(14) Lahti, P. M. Magnetic Properties of Organic Materials, Marcel Dekker, New York, 1999.
(15) (a) Kobayashi , H.; Kobayashi , A.; Cassoux, P.; *Chem. Soc. Rev*.**2000**, *29*, 325–333. (b) Uji, S.; Shinagawa, H.; Terashima, T.; Yakabe, T.; Terai , Y.; Tokumoto, M.; Kobayashi, A.; Tanaka, H.; Kobayashi, H. *Nature.***2001**, *410*, 908–910.
(16) (a) Prinz ,G. A. *Science*, **1998**, *282*, 1660–1663. (b) Emberly, E. G.; Kirczenow, G. *Chem. Phys*. **2002**, *281*, 311–324.
(17) (a) Matsuda, K.; Matsuo, M.; Irie, M. *J. Org. Chem.***2001**, *66*, 8799–8803. (b) Tanifuji, N.; Irie, M.; Matsuda, K. *J. Am. Chem. Soc*.**2005**, *127*, 13344–13353.
(18) (a) Bhattacharya, D.; Misra, A. *J. Phys. Chem. A*, **2009**, *113*, 5470–5475. (b) Bhattacharya, D.**;** Shil, S.; Misra, A.; Klein, D. J. *Theor. Chem. Acc*., **2010**, *127*, 57–67. (c) Bhattacharya, D.; Shil, S.; Panda, A.; Misra, A. *J. Phys. Chem. A*, **2010**, *114*, 11833–11841.
(19) Ali, Md. E.; Dutta, S.N. *J. Phys. Chem. A* **2006**, *110*, 2776-2784.
(20) (a) Tobe, Y.; Wakabayashi, T.; in *Acetylene Chemistry: Chemistry, Biology, and Material Science* (Eds.: F. Diederich, P. J. Stang, R. R. Tykwinski), Wiley-VCH, Weinheim,**2005**, pp. 387 – 426. (b) Chalifoux, W. A.; Tykwinski, R. R. *Chem. Rec*.**2006**, *6*, 169 –182. c) Shi Shun, A. L. K.; Tykwinski, R. R. *Angew. Chem. Int.*

*Ed.***2006,** *45*, 1034 – 1057. (d) Raton, B. Polyynes: Synthesis, Properties, and Applications; Cataldo, F. (Eds); Taylor & Francis, **2005**.
(21) Taylor, D. R. *Chem. Rev.***1967**, *67*, 317.
(22) Hendon, C.H.; Tiana, D.; Murray, A.T.; Carbery, D.R.; Walsh, A. *Chem. Sci*., **2013**, *4*, 4278–4284.
(23) Skibar, W.; Kopacka, H.; Wurst, K.; Salzmann, C.; Ongania, K.H.; Biani, F.F.D.; Zanello.P.; Bildstein, B. *Organometallics* **2004**,*23*,1024-1041.
(24) (a)Januszewski, J.A.; Tykwinski, R.R.; *Chem. Soc. Rev.* **2014**, *43*, 3184-3203.
(b) Januszewski, J.A.; Wendinger, D.; Methfessel, C.D.; Hampel, F.; Tykwinski, R.R.; *Angew. Chem. Int. Ed.***2013**, *52*, 1817 –1821.
(25) Gu, X.; Kaiser, R.I.; Mebel, A.M. *Chem. Phys. Chem.* **2008**, *9*, 350–369.
(26) Prasongkit, J.; Grigoriev, A.; Wendin. G.; Ahuja, R. *Phys. Rev. B* **2010**, *81*, 115404.
(27) Noodleman, L. *J. Chem. Phys.***1981**, *74*, 5737−5743.
(28) Noodleman, L.; Baerends, E. J. *J. Am. Chem. Soc.***1984**, *106*, 2316−2327.
(29) Noodleman, L.; Davidson, E. R. *Chem. Phys.***1986**, *109*, 131−143.
(30) Noodleman, L.; Peng, C. Y.; Case, D. A.; Mouesca, J. -M. *Coord. Chem. Rev.***1995**, *144*, 199−244.
(31) Yamaguchi, K.; Fukui, H.; Fueno, T. *Chem.Lett.***1986**, *15*, 625−628.
(32) Yamaguchi, K.; Takahara, Y.; Fueno, T.; Nasu, K. *Jpn. J. Appl. Phys.***1987**, *26*, L1362−L1364.
(33) Yamaguchi, K.; Jensen, F.;Dorigo, A.; Houk, K. N. *Chem.Phys. Lett.* **1988**, *149*, 537−542.
(34) Yamaguchi, K.; Takahara, Y.; Fueno, T.; Houk, K. N. *Theor. Chim.Acta* **1988**, *73*, 337−364.
(35) Frisch, M. J.; Trucks, G. W.; Schlegel, H. B.; Scuseria, G. E.; Robb, M. A.; Cheeseman, J. R.; Scalmani, G.; Barone, V.; Mennucci, B.; Petersson, G. A.; Nakatsuji, H.; Caricato, M.; Li, X.; Hratchian, H. P.; Izmaylov, A. F.; Bloino, J.; Zheng, G.; Sonnenberg, J. L.; Hada, M.; Ehara, M.; Toyota, K.; Fukuda, R.; Hasegawa, J.; Ishida, M.; Nakajima, T.; Honda, Y.; Kitao, O.; Nakai, H.; Vreven, T.; Montgomery, J. A., Jr.; Peralta, J. E.; Ogliaro, F.; Bearpark, M.; Heyd, J. J.; Brothers, E.; Kudin, K. N.; Staroverov, V. N.; Kobayashi, R.; Normand, J.; Raghavachari, K.; Rendell, A.; Burant, J. C.; Iyengar, S. S.; Tomasi, J.; Cossi, M.; Rega, N.; Millam, M. J.; Klene, M.; Knox, J. E.; Cross, J. B.; Bakken, V.; Adamo, C.; Jaramillo, J.; Gomperts, R.; Stratmann, R. E.; Yazyev, O.; Austin, A. J.; Cammi, R.; Pomelli, C.; Ochterski, J. W.; Martin, R. L.; Morokuma, K.; Zakrzewski, V. G.; Voth, G. A.; Salvador, P.; Dannenberg, J. J.; Dapprich, S.; Daniels, A. D.; Farkas, Ö.; Foresman, J. B.; Ortiz, J. V.; Cioslowski, J.; Fox, D. J. Gaussian, Inc., Wallingford CT, **2009**.
(36) Trindle, C.; Datta, S. N. *Int. J. Quantum Chem.***1996**, *57*, 781-799.
(37) Trindle, C.; Datta, S. N.; Mallik, B. *J. Am. Chem. Soc.***1997**, *119*, 12947-12951.
(38) Hermann, C.; Neugebauer, J.; Gladysz, J. A.; Reiher, M. *Inorg. Chem.* **2005**, *44*, 6174-6182.
(39) Shil, S.; Herrmann, C. *Inorg. Chem.* 2015, *54*, 11733–11740.
(40) Browne, W. R.; Hage, R.; Vos, J. G. *Coord.Chem. Rev.***2006**, *250*, 1653–1668.

(41) Borden, W.T.; Davidson, E.R. *J. Am. Chem. Soc.* **1977**, *99*, 4587–4594.
(42) Borden, W.T.; Davidson, E.R. *Acc. Chem. Res*. **1981**, *14*, 69–76.
(43) Constantinides, C. P.;Koutentis, P. A.; Schatz, J. *J. Am.Chem. Soc*. **2004**, *126*, 16232–16241.
(44) Zhang,G.; Li,S.; Jiang,Y.*J. Phys. Chem. A*. **2003**, *107*, 5573–5582.
(45) Shil, S.; Roy, M.; Misra, A. *RSC Adv*.**2015**, *5*, 105574–105582.
(46) Bhattacharya, D.; Shil, S.; Misra, A.; Bytautas, L.; Klein, D. J. *Phys. chem. Chem. Phys.* **2015**, ***17***, 14223-14237.
(47) Aoki, Y.; Imamura, A. *J. Chem. Phys*.**1995**, *103*, 9726.
(48) Imamura, A.; Aoki, Y. *Int. J. of Quantum Chem*. **2006**, *106*, 1924 –1933.
(49) Imamura, A.; Aoki, Y. *Int. J. of Quantum Chem*. **2013**, *113*, 423 –427.

CHAPTER 5

(1) Kahn, O. Molecular Magnetism. VCH, New York, **1993**.
(2) Lahti, P. M. Magnetic Properties of Organic Materials, Marcel Dekker, New York, **1999**.
(3) Kobayashi, H.; Kobayashi, A.; Cassoux, P. *Chem. Soc. Rev*. **2000**, *29*, 325.
(4) Uji, S.; Shinagawa, H.; Terashima, T.; Yakabe, T.; Terai, Y.; Tokumoto, M.; Kobayashi, A.; Tanaka, H.; Kobayashi, H. *Nature,* **2001**, *410*, 908.
(5) Matsuda, K.; Matsuo, M.; Irie. M. *J. Org. Chem.,* **2001**, *66*, 8799.
(6) Tanifuji, N.; Irie, M.; Matsuda. K. *J. Am. Chem. Soc*.**2005**, *127*, 13344.
(7) Prinz, G. A. *Science,* **1998**, ***282***, 1660.
(8) Emberly, E. G.; Kirczenow, G. *Chem. Phys*. **2002**, *281*, 311.
(9) Wang, F.; Vardeny. Z. V. *J. Mater. Chem.* **2009**, *19*, 1685.
(10) Michelfeit, M.; Schmidt, G.; Geurts, J.; Molenkamp, L. W. *Phys. Status Solidi*, **2008**, *205*, 656.
(11) Nguyen, T. D.; Ehrenfreund, E.; Vardeny, Z. V. *Science,* **2012**, *337*, 204.
(12) Yoo, J. W.; Chen, C. Y.; Jang, H. W.; Bark, C. W.; Prigodin, V. N.; Eom, C. B.; Epstein, A. J. *Nat. Mater.* **2010**, *9*, 638.
(13) Herrmann, C.; Elmisz, J. *Chem. Commun.* **2013**, *49*, 10456.
(14) Eng, M. P.; Albinsson, B. *Angew. Chem., Int. Ed.* **2006**, *45*, 5626.
(15) Wenger. O. S. *Acc. Chem. Res.,* **2011**, *44*, 25.
(16) Nitzan, A.; Ratner, M. A. *Science,* **2003**, *300*, 1384.
(17) Tao, N. J. *Nat. Nanotechnol.,* **2006**, *1*, 173.
(18) Park, B. G.; Wunderlich, J.; Martí, X.; Holý, V.; Kurosaki, Y.; Yamada, M.; Yamamoto, H.; Nishide, A.; Hayakawa, J.; Takahashi, H.; Shick, A. B.; Jungwirth, T. A. *Nat. Mater.,* **2011**, *10*, 347.
(19) Tour, J. M. *Acc. Chem. Res.,* **2000**, *33*, 791.
(20) Winkler, J. R.; Gray, H. B. *J. Am. Chem., Soc*. **2014**, *136*, 2930.
(21) Liu, H.; Wang, N.; Zhao, J.; Guo, Y.; Yin, X.; Boey, F. Y.C.; Zhang, H. *Chem. Phys. Chem*., **2008**, *9*, 1416.

(22) Khoo, K. H.; Chen, Y.; Li, S.; Quek, S. Y. *Phys. Chem. Chem. Phys.*, **2015**, *17*, 77.
(23) Zhao, X. L.; Ando, Y.; Liu, Y.; Jinno, M.; Suzuki, T. *Phys. Rev. Lett.* **2003,** *90*, 187401.
(24) Muramatsu, H.; Hayashi, T.; Kim, Y. A.; Shimamoto, D.; Endo, M.; Terrones, M.; Dresselhaus, M.S. *Nano. Lett*. **2008**, *8*, 237.
(25) Kitaura, R.; Nakanishi, R.; Saito, T.; Yoshikawa, H.; Awaga, K.; Shinohara, H. *Angew. Chem., Int. Ed.*, **2009**, *48*, 8298.
(26) Tobe, Y.; Wakabayashi, T. in *Acetylene Chemistry: Chemistry, Biology, and Material Science* (Eds.: F. Diederich, P. J. Stang, R. R. Tykwinski), Wiley-VCH, Weinheim, **2005**, pp. 387.
(27) Chalifoux, W. A.; Tykwinski, R. R. *Chem. Rec.*, **2006**, *6*, 169.
(28) Shi Shun, A. L. K.; Tykwinski, R. R. *Angew. Chem. Int,. Ed.* **2006**, *45*, 1034.
(29) Raton, B. Polyynes: Synthesis, Properties, and Applications; Cataldo, F. (Eds); Taylor & Francis, **2005.**
(30) Ma, S. *Acc. Chem. Res*. **2009**, *42*, 1679.
(31) Smadja. W. *Chem. Rev*. **1983**, *83*, 263.
(32) Zhang, Y.; Su, Y.; Wang, L.; Kong, E. S.-W.; Chen, X.; Zhang, Y. A. *Nanoscale Research Letters*, **2011**, *6*, 577.
(33) Gu, X.; Kaiser,R. I.; Mebel, A. M. *Chem. Phys. Chem.*, **2008**, *9*, 350.
(34) Weimer, M.; Hieringer, W.; Sala, F. D.; Gçrling, A. *Phys.*, **2005**, *309*, 77.
(35) Skibar, W.; Kopacka, H.; Wurst, K.; Salzmann, C.; Ongania, K. H.; Biani, F. F. D. ; Zanello, P. ; Bildstein, B. *Organometallics*, **2004**, *23*, 1024.
(36) Januszewski, J. A. ; Tykwinski, R.R. *Chem. Soc. Rev.*, **2014**, *43*, 3184.
(37) Januszewski, J. A. ; Wendinger, D.; Methfessel, C. D.; Hampel, F.; Tykwinski, R. R. *Angew. Chem. Int. Ed.*, **2013**, *52*, 1817.
(38) Bhattacharya, D.; Misra, A. *J. Phys. Chem. A*. **2009**, *113*, 5470.
(39) Bhattacharya, D.; Shil, S.; Misra, A.; Klein, D. J. *Theor. Chem. Acc*., **2010**, *127*, 57.
(40) Shil, S.; Sarbadhikary, P.; Misra, A. *RSC Adv*., **2016**, 6, 99467.
(41) Paul, S.; Misra, A. *J. Chem. Theory Comput.* **2012**, *8*, 843.
(42) Paul,S.; Misra, A. *J. Phys. Chem. A.***2010**, *114*, 6641.
(43) Ali, Md. E.; Datta, S. N. *J. Phys. Chem. A.* **2006**, *110*, 2776.
(44) Ko, K. C.; Cho, D.; Lee, J. Y. *J. Phys. Chem. A.* **2013**, *117*, 3561.
(45) Cho, D.; Ko, K.C.; Ikabata, Y.; Wakayama, K.; Yoshikawa, T.; Nakai, H.; Lee, J. Y. *J. Chem. Phys.* **2015**, *142*, 024318.
(46) Nam,Y.; Cho, D.; Lee, J. Y. *J. Phys. Chem. C* **2016**, *120*, 11237.
(47) Cho, D.; Ko, K. C.; Park, H.; Lee, J. Y. *J. Phys. Chem. C* **2015**, *119*, 10109.
(48) Cho, D.; Ko, K. C.; Lee,J. Y. *Int. J. Quant. Chem.* **2016**, *116*, 578.
(49) Ko, K. C.; Cho, D.; Lee, J. Y. *J. Phys. Chem. A* **2012**, *116*, 6837.
(50) Ko, K. C.; Son, S. U.; Lee, S. ; Lee, J. Y. *J. Phys. Chem. B* **2011**, *115*, 8401.
(51) Cho, D.; Ko, K. C.; Lee, J. Y. *J. Phys. Chem. A* **2014**, *118*, 5112.
(52) Ko, K. C.; Park, Y. G.; Cho, D.; Lee, J. Y. *J. Phys. Chem. A* **2014,** *118*, 9596.
(53) Song, M.; Song, X.; Bu, Y. *Chem. Phys. Chem.*, **2017**, *18*, 2487.

(54) Song, M.; Song, X.; Bu, Y. *J. Phys. Chem. C* **2017**, *121*, 21231.
(55) Sarbadhikary, P.; Shil, S.; Panda, A.; Misra, A. *J. Org. Chem*, **2016**, *81*, 5623.
(56) Tamura, M. ; Nakazawa, Y.; Shiomi, D.; Nozawa, K.; Hosokoshi, Y. ; Ishikawa, M.; Takahashi, M. ; Kinosita, M. *Chem. Phys. Lett.*, **1991**, *186***,** 401.
(57) Noodleman, L. *J. Chem. Phys.*, **1981**, *74*, 5737.
(58) Noodleman, L.; Baerends, E. *J. Am. Chem. Soc.*, **1984**, *106*, 2316.
(59) Noodleman, L.; Davidson, E. R. *Chem. Phys.***1986**, *109*, 131.
(60) Noodleman, L.; Peng, C. Y.; Case, D. A.; Mouesca, J. M. *Coord. Chem. Rev.*, **1995**, *144*, 199.
(61) Yamaguchi, K.; Fukui, H.; Fueno, T.*Chem. Lett.* **1986**, *15*, 625.
(62) Yamaguchi, K.; Takahara, Y.; Fueno, T.; Nasu, K. *Jpn. J. Appl. Phys.*, **1987**, *26*, L1362.
(63) Yamaguchi, K.; Jensen, F.; Dorigo, A.; Houk, K. N. *Chem. Phys. Lett.*, **1988**, *149*, 537.
(64) Yamaguchi, K.; Takahara, Y.; Fueno, T.; Houk, K. N. *Theor. Chim. Acta*, **1988**, *73*, 337.
(65) Frisch, M. J.; Trucks, G. W.; Schlegel, H. B.; Scuseria, G. E.; Robb, M. A.; Cheeseman, J. R.; Scalmani, G.; Barone, V.; Mennucci, B.; Petersson, G. A.; Nakatsuji, H.; Caricato, M.; Li, X.; Hratchian, H. P.; Izmaylov, A. F.; Bloino, J.; Zheng, G.; Sonnenberg, J. L.; Hada, M.; Ehara, M.; Toyota, K.; Fukuda, R.; Hasegawa, J.; Ishida, M.; Nakajima, T.; Honda, Y.; Kitao, O.; Nakai, H.; Vreven, T.; Montgomery, J. A., Jr.; Peralta, J. E.; Ogliaro, F.; Bearpark, M.; Heyd, J. J.; Brothers, E.; Kudin, K. N.; Staroverov, V. N.; Kobayashi, R.; Normand, J.; Raghavachari, K.; Rendell, A.; Burant, J. C.; Iyengar, S. S.; Tomasi, J.; Cossi, M.; Rega, N.; Millam, M. J.; Klene, M.; Knox, J. E.; Cross, J. B.; Bakken, V.; Adamo, C.; Jaramillo, J.; Gomperts, R.; Stratmann, R. E.; Yazyev, O.; Austin, A. J.; Cammi, R.; Pomelli, C.; Ochterski, J. W.; Martin, R. L.; Morokuma, K.; Zakrzewski, V. G.; Voth, G. A.; Salvador, P.; Dannenberg, J. J.; Dapprich, S.; Daniels, A. D.; Farkas, Ö.; Foresman, J. B.; Ortiz, J. V.; Cioslowski, J.; Fox, D. J. Gaussian, Inc., Wallingford CT, **2009**.
(66) Büttiker, M.; Imry, Y.; Landauer, R.; Pinhas, S. *Phys. Rev. B*, **1985**, *31*, 6207.
(67) Herrmann, C.; Solomon, G. C.; Subotnik, J. E.; Mujica, V.; Ratner, M. A. *J. Chem. Phys.***2010**, *132*, 024103 (1-17).
(68) Herrmann, C.; Solomon, G. C.; Ratner, M. A. *J. Am. Chem. Soc.*, **2010**, *132*, 3682.
(69) Latif, I. A.; Singh, V. P.; Bhattacharjee, U.; Panda, A.; Datta, S. N. *J. Phys. Chem. A*, **2010**, *114*, 6648–6656.
(70) Herring, C. Magnetism IIB, Direct exchange between well-separated atoms, 5, Eds. G.T. Rado and H. Suhl (**1966**) Academic Press, New York.
(71) Polo, V.; Alberola, A.; Andres, J.; Anthony, J.; Pilkington, M. *Phys. Chem. Chem. Phys*., **2008**, *10*, 857.
(72) Shil, S.; Roy, M.; Misra, A. *RSC Adv*., **2015**, *5*, 105574.
(73) Hermann, C.; Neugebauer, J.; Gladysz, J. A.; Reiher, M. *Inorg. Chem.* **2005**, *44*, 6174.

(74) Prasongkit, J. ; Grigoriev, A.; Wendin, G. ; Ahuja, R. *Phys. Rev. B,***2010**, *81*, 115404.
(75) Kondo, M.; Tada, T. ; Yoshizawa, K. *J. Phys. Chem. A* **2004**, *108*, 9143.
(76) Stuyver, T.; Fias, S. ; Proft, F. De. ; Geerlings, P. *J. Phys. Chem. C*, **2015**, *119*, 26390.
(77) Aravena, D.; Ruiz, E. *J. Am. Chem. Soc*. **2012**, *134*, 777.
(78) Herrmann, C.; Solomon, G. C.; Ratner, M. A. *J. Am. Chem. Soc.,* **2010**, *132*, 3682.
(79) Ashcroft, N. W.; Mermin, N. D. Solid *State Physics*, Holt, Rinehart and Winston, New York, **1976**.
(80) Pauly, F.; Viljas, J. K. ; Cuevas, J. C. ; Schön, G. *Phys. Rev. B,* **2008,** *77*, 155312.
(81) Tour, J. M.; Kozaki, M.; Seminario, J. M. *J. Am. Chem. Soc.,* **1998**,*120*, 8486.
(82) Modelli, A.; Venuti, M.; Scagnolari, F.; Contento, M.; Jones, D. *J. Phys. Chem. A,* **2001**,*105*, 219.
(83) Distefano, G.; Jones, D. ; Guerra, M. ; Favaretto, L. ; Modelli, A. ; Mengoli, G. *J. Phys. Chem.* **1991**, *95*, 9746.
(84) Colle, M. D.; Cova, C.; Distefano, G. ; Jones, D. ; Modelli, A. ; Comisso, N. *J. Phys. Chem. A.* **1999**,*103*, 2828.
(85) Brédas, J. L. ; Thémans, B.; Fripiat, J. G. ; André, J. M. ; Chance, R. R. *Phys. Rev. B,* **1984**,*29*, 6761.
(86) Schlicke, H.; Herrmann, C. *Chem. Phys. Chem.,* **2014**, *15*, 4011.
(87) Proppe, J.; Herrman, C. *J. Comput. Chem.* **2015**, *36*, 201.
(88) Choi, Y. C. ; Kim, W. Y. ; Park, K. S. ; Tarakeshwar, P.; Kim, K. S. ; Kim, T. S. ; Lee, J. Y. *Chem. Phys.,* **2005**, *122*, 094706.
(89) Hermann, C.; Neugebauer, J.; Gladysz, J. A.; Reiher. M. *Inorg. Chem.* **2005**, *44*, 6174.
(90) Chumak, A. V. ; Vasyuchka, V. I. ; Serga, A. A. ; Hillebrands, B. *Nat. Phys*., **2015**, *11*,453.

CHAPTER 6

(1) Taylor, D. R. *Chem. Rev.* **1967**, *67*, 317-359.
(2) Hendon, C.H.; Tiana, D.; Murray, A.T.; Carbery, D.R.; Walsh, A. *Chem. Sci*. **2013**, *4*, 4278–4284.
(3) Eliel, L. E.; Wilen, S. H. Stereochemistry of organic compounds; John Wiley & Sons: New York, **1994**; Chapter 9, p 539.
(4) Skibar, W.; Kopacka, H.; Wurst, K.; Salzmann, C.; Ongania, K.H.; Biani, F.F.D.; Zanello. P.; Bildstein, B. *Organometallics* **2004**, *23*, 1024-1041.
(5) Januszewski, J.A.; Tykwinski, R.R. *Chem. Soc. Rev.* **2014**, *43*, 3184-3203.
(6) Januszewski, J.A.; Wendinger, D.; Methfessel, C.D.; Hampel, F.; Tykwinski, *Angew. Chem. Int. Ed.* **2013**, *52*, 1817 –1821.
(7) Wendinger, D.; Tykwinski, R.R. *Acc. Chem. Res.* **2017**, *50*, 1468−1479.

(8) Shil, S.; Misra, A. *J. Phys. Chem. A* **2010**, *114*, 2022-2027.
(9) Bhattacharya, D.; Shil, S.; Misra, A. *J. Photochem. Photobiol., A* **2011**, *217*, 402−410.
(10) Zhang, F.; Song, X.; Bu, Y. *J. Phys. Chem. C* **2015**, *119*, 27930-27937.
(11) Saha, A.; Latif, I. A.; Datta, S.N. *J. Phys. Chem. A* **2011**, *115*, 1371-1379.
(12) Ali, Md. E.; Staemmler, V.; Illas, F.; Oppeneer, P.M. *J. Comput. Theory Chem.* **2013**, *9*, 5216-5220.
(13) Bhattacharya, D.; Misra, A. *J. Phys. Chem. A*, **2009**, *113*, 5470–5475.
(14) Shil, S.; Sarbadhikary, P.; Misra, A. *RSC Adv*., **2016**, *6*, 99467.
(15) Paul, S.; Misra, A. *J. Phys. Chem. A.* **2010**, *114*, 6641.
(16) Coey, J. M. D. Magnetism and magnetic materials, Cambridge University Press, Cambridge, U.K., **2010**, ISBN 13: 9780521816144.
(17) Latif, I. A.; Singh, V. P.; Bhattacharjee, U.; Panda, A.; Datta, S. N. *J. Phys. Chem. A* **2010**, *114*, 6648–6656.
(18) Ali, Md. E.; Datta, S.N. *J. Phys. Chem. A* **2006**, *110*, 2776-2784.
(19) Cho, D.; Ko, K. C.; Ikabata, Y.; Wakayama, K.; Yoshikawa, T.; Nakai, H.; Lee, J.Y. *J. Chem. Phys.* **2015**, *142*, 024318.
(20) Kolanji, K.; Postulka, L.; Wolf, B.; Lang, M.; Schollmeyer, D.; Baumgarten. M. *J. Org. Chem.* **2019**, *84*, 140−149.
(21) Song, M.; Song, X.; Bu, Y. *Chem. Phys. Chem.* **2017**, *18*, 2487-2498.
(22) Chen, D.; Deng, T.; Yang, L.; Bu, Y. *J. Phys. Chem. C* **2019**, *123*, 14152−14163.
(23) Sarbadhikary, P.; Shil, S.; Panda, A.; Misra, A. *J. Org. Chem*, **2016**, *81*, 5623.
(24) Sarbadhikary, P.; Shil, S.; Misra, A. *Phys. Chem. Chem. Phys.* **2018**, *20*, 9364-9375.
(25) Garner, M. H.; Hoffmann, R.; Rettrup, S.; Solomon, G.C. *ACS Cent. Sci.***2018**, *4*, 688-700.
(26) Garner, M. H.; Jensen, A.; Hyllested, L.; Solomon, G. C. *Chem. Sci.* **2019**, ***10***, 4598-4608.
(27) Aoki, Y.; Orimoto, Y.; Imamura, A. *ACS Cent. Sci.* **2018**, 4, 664-665.
(28) Appel, R. Multiple Bonds and Low Coordination in Phosphorus Chemistry, Georg Thieme Verlag: Stuttgart, Germany, **1990**; p 157.
(29) Escudié, J.; Ranaivonjatovo, H.; Rigon, L. *Chem. Rev*. **2000**, *100*, 3639-3696.
(30) Eichler, B.; West, R. *Adv. Organomet. Chem.* **2000**, *46*, 1-46.
(31) Escudié, J.; Ranaivonjatovo, H.; Bouslikhane, M.; Harouch, Y. E; Baiget, L.; Nemes, G.C. *Russ. Chem. Bull., Int. Ed.* **2004**, *53*, 1020-1033.
(32) Escudié, J.; Ranaivonjatovo, H. *Organometallics* **2007,** *26*, 1542-1559.
(33) Märkl, G.; Sejpka, H.; Dietl, S.; Nuber, B.; Ziegler, M. L. *Angew. Chem., Int. Ed. Engl*. **1986**, *25*, 1003-1004.
(34) Bouslikhane, M.; Gornitzka, H.; Ranaivonjatovo, H.; Escudié, J. *Organometallics* **2002**, *21*, 1531-1533.
(35) Rancurel, C.; Heise, H.; Köhler, F. H.; Schatzschneider, U.; Rentschler, E.; Vidal-Gancedo, J.; Veciana, J.; Sutter, J. –P. *J. Phys. Chem. A* **2004**, *108*, 5903-5914.
(36) Polo, V.; Alberola, A.; Andres, J.; Anthony, J.; Pilkington, M. *Phys. Chem. Chem. Phys.* **2008**, *10*, 857–864.

(37) Bhattacharya, D.; Shil, S.; Panda, A.; Misra, A. *J. Phys. Chem. A* **2010**, *114*, 11833–11841.
(38) Tamura, M.; Nakazawa, Y.; Shiomi, D.; Nozawa, K.; Hosokoshi, Y.; Ishikawa, M.; Takahashi, M.; Kinoshita, M. *Chem. Phys. Lett.* **1991**, *186*, 401-404.
(39) Ziessel, R.; Stroh, C.; Heise, H.; Köhler, F. H.; Turek, P.; Claiser, N.; Souhassou, M.; Lecomte, C. *J. Am. Chem. Soc.* **2004**, *126*, 12604-12613.
(40) Hicks, R. G.; Lemaire, M. T.; Öhrström, L.; Richardson, J. F.; Thompson, L. K.; Xu, Z. *J. Am. Chem. Soc*. **2001**, *123*, 7154-7159.
(41) Wautelet, P.; Catala, L.; Bieber, A.; Turek, P.; André, J.-J. *Polyhedron* **2001**, *20*, 1571-1576.
(42) Gomberg, M. *J. Am. Chem. Soc*. **1900**, *22*, 757-771.
(43) Gomberg, M. *Chem. Rev*. **1924**, *1*, 91-141.
(44) Kanno, F.; Inoue, K.; Koga, N.; Iwamura, H. *J. Am. Chem. Soc.***1993**, *115*, 847-850.
(45) Calder, A,; Forester, A. R.; James, P. *G.;* Luckhurst, G. R. *J. Am. Chem. Soc.* **1969**, *91*, 3724-3727.
(46) Fang, S.; Lee, M. –S.; Hrovat, D.A.; Borden, W.T. *J. Am. Chem. Soc.* **1995,** *117***,** 6727-6731.
(47) Jung, M.; Sharma, A.; Hinderberger, D.; Braun, S.; Schatzschneider, U.; Rentschler, E. *Inorg. Chem.* **2009**, *48*, 7244–7250.
(48) Oniciu, D. C.; Matsuda, K.; Iwamura, H. *J. Chem. Soc., Perkin Trans.* **1996**, *2*, 907-913.
(49) Inoue, K.; Iwamura, H. *J. Am. Chem. Soc.***1994,** *116***,** 3173-3174.
(50) Noodleman, L. *J. Chem. Phys.***1981**, *74*, 5737−5743.
(51) Noodleman, L.; Baerends, E. J. *J. Am. Chem. Soc.* **1984**, *106*, 2316−2327.
(52) Noodleman, L.; Davidson, E. R. *Chem. Phys.***1986**, *109*, 131−143.
(53) Noodleman, L.; Peng, C. Y.; Case, D. A.; Mouesca, J. -M. *Coord. Chem. Rev.***1995**, *144*, 199−244.
(54) Martin, R. L.; Illas, F. *Phys. Rev. Lett.* **1997**, *79*, 1539-1542.
(55) Caballol, R.; O. Castell, O.; Illas, F.; Moreira, I. de P. R.; Malrieu, J. P. *J. Phys. Chem. A* **1997**, *101*, 7860-7866.
(56) Paul, S.; Misra, A. *J. Chem. Theory Comput.* **2012**, *8*, 843−853.
(57)Yamaguchi, K.; Fukui, H.; Fueno, T. *Chem. Lett.***1986**, *15*, 625−628.
(58) Yamaguchi, K.; Takahara, Y.; Fueno, T.; Nasu, K. *Jpn. J. Appl. Phys.***1987**, *26*, L1362−L1364.
(59) Yamaguchi, K.; Jensen, F.;Dorigo, A.; Houk, K. N. *Chem. Phys. Lett.* **1988**, *149*, 537−542.
(60) Yamaguchi, K.; Takahara, Y.; Fueno, T.; Houk, K. N. *Theor. Chim. Acta.* **1988**, *73*, 337−364.
(61) Frisch, M. J.; Trucks, G. W.; Schlegel, H. B.; Scuseria, G. E.; Robb, M. A.; Cheeseman, J. R.; Scalmani, G.; Barone, V.; Mennucci, B.; Petersson, G. A.; Nakatsuji, H.; Caricato, M.; Li, X.; Hratchian, H. P.; Izmaylov, A. F.; Bloino, J.; Zheng, G.; Sonnenberg, J. L.; Hada, M.; Ehara, M.; Toyota, K.; Fukuda, R.; Hasegawa, J.; Ishida, M.; Nakajima, T.; Honda, Y.; Kitao, O.; Nakai, H.; Vreven, T.;

Montgomery, J. A., Jr.; Peralta, J. E.; Ogliaro, F.; Bearpark, M.; Heyd, J. J.; Brothers, E.; Kudin, K. N.; Staroverov, V. N.; Kobayashi, R.; Normand, J.; Raghavachari, K.; Rendell, A.; Burant, J. C.; Iyengar, S. S.; Tomasi, J.; Cossi, M.; Rega, N.; Millam, M. J.; Klene, M.; Knox, J. E.; Cross, J. B.; Bakken, V.; Adamo, C.; Jaramillo, J.; Gomperts, R.; Stratmann, R. E.; Yazyev, O.; Austin, A. J.; Cammi, R.; Pomelli, C.; Ochterski, J. W.; Martin, R. L.; Morokuma, K.; Zakrzewski, V. G.; Voth, G. A.; Salvador, P.; Dannenberg, J. J.; Dapprich, S.; Daniels, A. D.; Farkas, Ö.; Foresman, J. B.; Ortiz, J. V.; Cioslowski, J.; Fox, D. J. Gaussian, Inc., Wallingford CT, **2009**.

(62) Shil, S.; Herrmann, C. *Inorg. Chem.* **2015**, *54*, 11733–11740.

(63) Ali, M. E.; Roy, A. S.; Datta, S. N. *J. Phys. Chem. A* **2007**, *111*, 5523–5527.

(64) Polo, V.; Alberola, A.; Andres, J.; Anthony, J.; Pilkington, M. *Phys. Chem. Chem. Phys*. **2008**, *10*, 857-864.

(65) Shil, S.; Roy, M.; Misra, A. *RSC Adv*. **2015**, *5*, 105574-105582.

(66) Herring, C. in Magnetism IIB, Direct exchange between well-separated atoms, ed. G.T. Rado and H. Suhl, Academic Press, New York, **1966**, vol. 5.

(67) Trindle, C.; Datta, S. N. *Int. J. Quantum Chem.***1996**, *57*, 781-799.

(68) Schatzschneider, U.; Rentschler, E. *J. Mol. Struct. (Theochem)* **2003**, 638, 163–168.

(69) Hoffmann, R.; Zeiss, G. D.; Dine, G. W. V. *J. Am. Chem. Soc*. **1968**, *90*, 1485.

(70) Zhang, G.; Li, S.; Jiang, Y. *J. Phys. Chem. A* **2003**, *107*, 5573-5582.

INDEX

A
ARTAIOS, 31
Antiferromagnetic, 27

B
Broken symmetry approach, 28
Bencini, 28

C
Chiral magnet, 49
Cumulene based diradicals, 50

D
Density Functional Theory, 25
Dihedral angle, 82
DTDA, 6
Davidson, 28

E
Enantiomers, 52

F
Fermi energy, 38
Frontier molecular orbitals, 60

G
Gaussian09W, 36
GMR, 9
Giensberg, 28

H
Heteroallenes, 99

I
Imino nitroxides, 5

L
Landauer approach, 29

M
Molecule-based magnetism, 3
Magnetic Exchange Coupling Constant, 28
Molecular wire, 34
Moore's law, 8

N
NEGF, 30
Noodleman, 28

O
Organic radicals, 5

P
Polyradicals, 7

R
Regression analysis, 78
Ruitz, 28

S
Single Molecule Magnet, 3
Spintronics, 8
Spin density, 43

T
Transport property, 10
Transmission spectra, 38
TMR, 9

V
VCD spectra, 51
Verdazyl radicals, 6

Y
Yamaguchi, 29

REPRINTS OF PUBLISHED PAPERS IN CONNECTION TO THIS THESIS

1. Shil, S.; **Sarbadhikary, P**.; Misra, A. Effect of length on the transport and magnetic properties of diradical substituted molecular wires. *RSC Adv.* **2016**, *6*, 99467-99474. (**Chapter 3**)

2. Sarbadhikary, P.; Shil, S.; Misra, A. A Perspective on Designing Chiral Organic Magnetic Molecules with Unusual Behavior in Magnetic Exchange Coupling. *J. Org. Chem.* **2016**, *81*, 5623-5630. (**Chapter 4**)

3. Sarbadhikary, P.; Shil, S.; Misra, A. Magnetic and Transport Properties of Conjugated and Cumulated Molecules: the π-System Enlightens Part of the Story. *Phys. Chem. Chem. Phys.* **2018**, *20*, 9364-9375. (**Chapter 5**)

RSC Advances

PAPER

View Article Online
View Journal | View Issue

CrossMark click for updates

Cite this: *RSC Adv.*, 2016, **6**, 99467

Effect of length on the transport and magnetic properties of diradical substituted molecular wires†

Suranjan Shil,[a] Prodipta Sarbadhikary[b] and Anirban Misra*[b]

Extended π-conjugated molecules are known to have interesting applications as conducting nanowires, memory devices, and diodes. In the present work, we investigate the effect of the length of unsaturated organic molecular wires and radical substituted wires on the conduction properties of hybrid devices. At the same time, we also study the effect of the length of unsaturated radical substituted organic molecular wires on the magnetic properties. It was found that the value of magnetic exchange coupling constant (*J*) depends on the distance between spin centers. In order to measure the transmission characteristics of these conjugated molecular wires, we have designed a molecular bridge structure where the phenyl based molecular system containing conjugated multiple bonds of varying length is used as a bridging fragment between two semi-infinitely widened Au_9 fcc clusters along the Au(111) direction. A state of the art non-equilibrium Green's function (NEGF) method coupled with density functional theory (DFT) based approach has been applied on this two-probe molecular bridge system to understand its electrical transport characteristics. It was observed that the molecular wires with smaller length show higher transmission. The transmission spectra of the ferromagnetically coupled diradical based molecular wires show similar behavior to those of the wires without any substitution. Hence, there is no effect of radical substitution on transport properties for ferromagnetically coupled diradical based molecular wires, whereas for antiferromagnetically coupled systems, the scenario is different.

Received 16th September 2016
Accepted 11th October 2016

DOI: 10.1039/c6ra23147k

www.rsc.org/advances

Published on 11 October 2016. Downloaded by University of Waterloo on 08/11/2016 15:46:06.

Introduction

The term molecular wire is usually employed in molecular electronics to signify molecular scale objects that conduct electrical current with a highly preferential axis for conduction. The electrical conduction properties of molecular wires have been the focus of many studies in recent years.[1–4] Individual molecular wires are divided into two categories.[1] The first category is based on *n*-alkane chains [CH_3–$(CH_2)_{n-1}$], which have a large (~6 eV or greater) band gap separating their highest occupied molecular orbital (HOMO) and their lowest unoccupied molecular orbital (LUMO) and are relatively insulating.[5,6] The second category is based on conjugated molecules that have a small (2–4 eV) HOMO–LUMO gap and behave like ordinary semiconductors.[7–9] This second category of molecules are rigid and possess delocalized π-electrons. Jalili *et al.* investigated the effect of the length of the molecular wire on the conduction spectra of organic nanowires,[3] where the *I–V* curve for thiophenthiol based systems is non-ohmic in nature. Recently, a hybrid device was designed where gold nano particles are connected by saturated organic molecules of different lengths (alkanedithiol chains)[2] and it was observed that the conductivity increases with the length of the molecule. Electron tunneling through a molecular wire has also been studied as a function of the length and chemical structure of the molecule by Magoga *et al.*[4] They found that the tunneling phenomenon through a molecular wire relies on the damping factor and the contact conductance. The effect of bond length alternation on transport behavior has also been experimentally and theoretically demonstrated.[10] A study of charge and spin transport through *para*-phenylene oligomers reveals that the oligomeric *para*-phenylene bridge can act as a molecular wire for the charge recombination reaction. The rate of charge transport through such molecules decreases exponentially when the super-exchange mechanism dominates.[11] The decay constants (β) of diradical substituted conjugated molecular wires have been studied by Nishizawa *et al.* and they found that β is well correlated with the electronic transmission.[12]

In this work we investigate the transport property of two molecular wires of different lengths (Fig. 1) to show the effect of the length of the wire on the electrical transport properties. In this context, we designed six diradicals (Fig. 2) by substituting a methylene radical at different positions in molecular wire 1 to generate series 1 and similarly ten diradicals based on molecular wire 2 to generate the systems of series 2 (Fig. 3) to study the effect of spin polarization on the transport properties and the dependence of magnetic coupling on the distance between the radical centers. The wires we have studied here are addition polymers,

[a]*Institute for Inorganic and Applied Chemistry, University of Hamburg, Martin-Luther-King-Platz 6, 20146 Hamburg, Germany*

[b]*Department of Chemistry, University of North Bengal, Dist-Darjeeling 734013, India. E-mail: anirbanmisra@yahoo.com; Tel: +91-9434228745*

† Electronic supplementary information (ESI) available: Orbital coefficient values of wire 1 and wire 2, optimized *XYZ* coordinates of the molecular wire, molecular wire with S–H bonds and the actual molecular setup *i.e.*, the Au–molecule–Au junction are available. See DOI: 10.1039/c6ra23147k

Published on 11 October 2016. Downloaded by University of Waterloo on 08/11/2016 15:46:06.

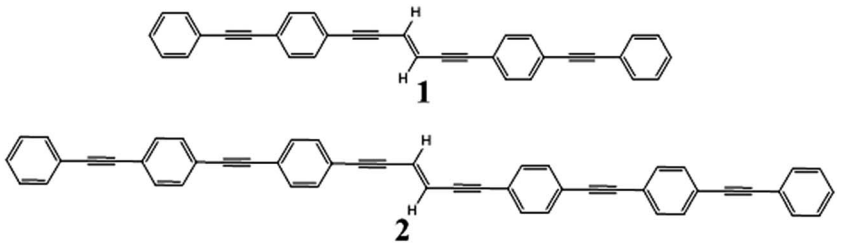

Fig. 1 Two molecular wires (1 and 2) on which transport calculations have been carried out.

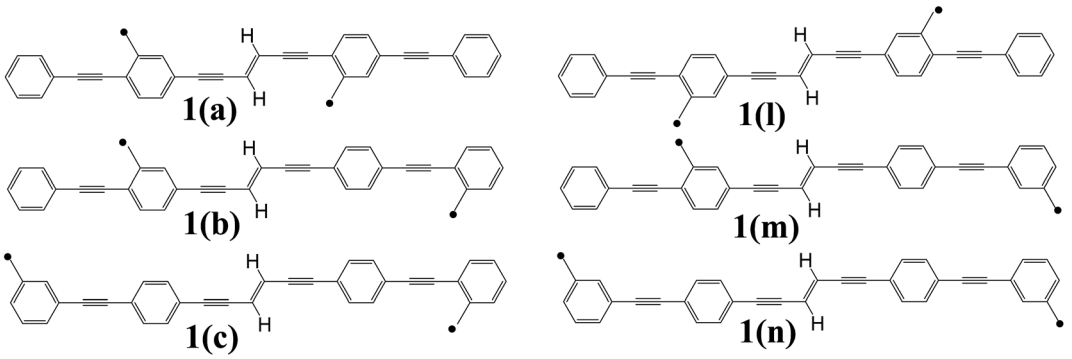

Fig. 2 Designed diradical based molecular wire 1.

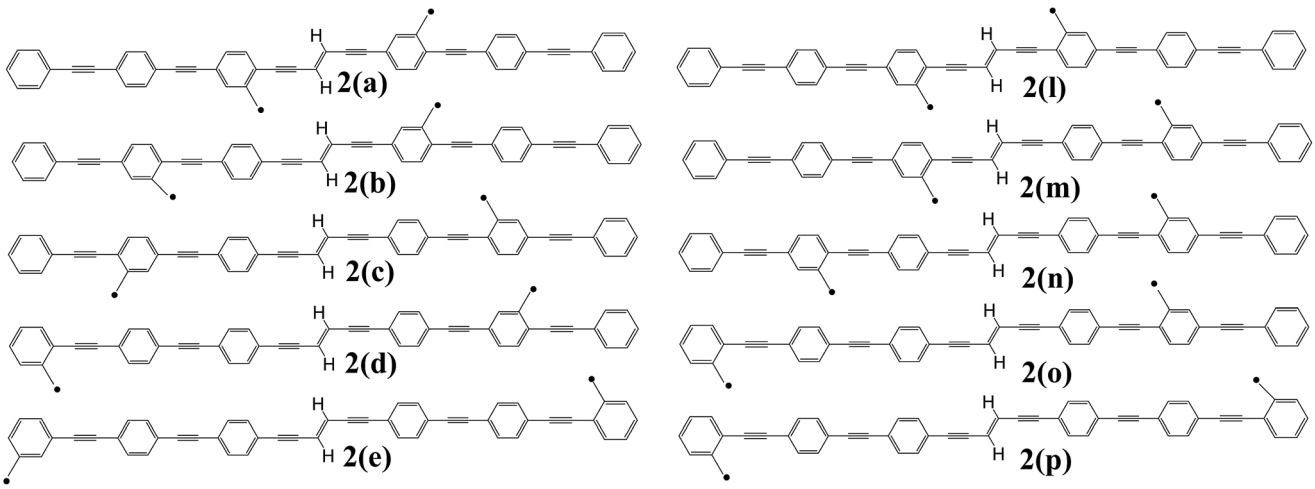

Fig. 3 Designed diradical based molecular wire 2.

and such polymers are important for application in the electronic industry.[13] The effects of entropy, the amount of molecules and their root-mean-square end-to-end distance on the physical properties of polymers are very important issues and these points were properly discussed by Lu *et al.*[14,15]

Theoretical and computational methodology

In order to determine the transport properties of the system, we need to describe the finite left electrode–molecular region–right electrode part of the infinite system. For this purpose, the gold-cluster–dithiolate–gold-cluster system has been divided into three sub systems: left gold cluster, central dithiolate, and right gold cluster, as illustrated in Fig. 4. Wires with radical substitutions are also treated in a similar manner. The magnetic properties of the diradicals are calculated on the structures without –SH and gold cluster.[16]

We calculated the transmission property using ARTAIOS code developed by Herrmann *et al.*[16,17] In this approach the dithiol molecule has been optimized in the unrestricted DFT framework with B3LYP functional and 6-31G(d,p) basis set using the Gaussian 09 quantum chemical package[18] and then the hydrogen atoms are stripped off and the resulting neutral dithiolate is

 This journal is © The Royal Society of Chemistry 2016

Published on 11 October 2016. Downloaded by University of Waterloo on 08/11/2016 15:46:06.

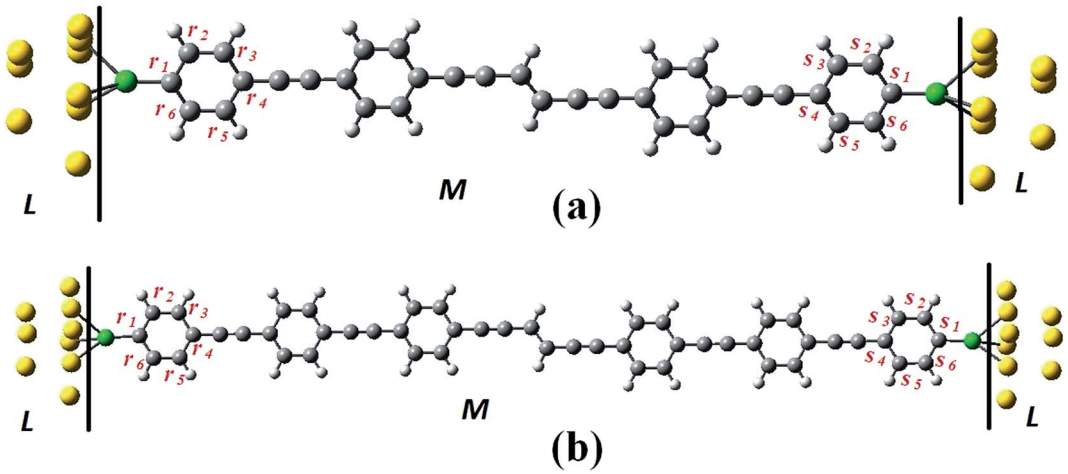

Fig. 4 (a) and (b) are the Au–molecule–Au two probe structures designed primarily for the transport calculation. The gray, white, yellow and green colors represent carbon, hydrogen, gold and sulfur atoms, respectively (L stands for lead and M stands for molecule).

placed between two Au_9 fcc clusters. The bond length between sulfur and the Au(111) surface has been chosen to be 2.48 Å with Au–Au distances of 2.88 Å as in extended gold crystals.[16] Fock and overlap matrices required for the transport calculation are obtained by single point calculation in the Gaussian 09W program package. For the transport calculation, we employed the B3LYP functional and the LANL2DZ basis set to avoid ghost transmission.[14] The transmission function is calculated within the Landauer approximation based on a Green's function approach using the post processing tool ARTAIOS.

Yoshizawa and coworkers developed an orbital rule to predict the right connections between the molecule and the electrodes.[19,20] The rule is: (1) the sign of the product of the orbital coefficients at sites r and s in the HOMO should be different from the sign of the product of the orbital coefficients at sites r and s in the LUMO, and (2) sites r and s should have the large amplitude of HOMO and LUMO. We computed the coefficients of the HOMO and LUMO of the connecting C atoms (Table 1) following Yoshizawa's rule.[19,20] The detailed list of orbital coefficient values of both the wires is given in the ESI (Table S1†).

The interaction between two magnetic sites 1 and 2 is generally expressed by Heisenberg spin Hamiltonian:

$$\hat{H} = -2J\hat{S}_1 \times \hat{S}_2 \quad (1)$$

Where $\hat{S}_1$ and $\hat{S}_2$ are the respective spin angular momentum operators and J is the exchange coupling constant. A positive value of J indicates the ferromagnetic interaction while a negative value indicates the antiferromagnetic interaction between two magnetic sites. For a diradical containing one unpaired electron on each site, J can be represented as:

$$E_{(S=1)} - E_{(S=0)} = -2J. \quad (2)$$

Many researchers[21–28] have developed different formalisms to evaluate J using an unrestricted spin polarized broken symmetry (BS) solution, depending on the extent of magnetic interaction between two magnetic sites. The equation for evaluating J proposed by Ginsberg,[23] Noodleman[24] and Davidson[25] is applicable when the interaction between two magnetic orbitals is small. On the other hand, the expression proposed by Bencini[26,27] and coworkers and Ruiz *et al.*[28] is applicable for large interaction. Nevertheless, the well-known expression given by Yamaguchi[29] is applicable for both strong and weak overlap limits. Following the well established[30,31] and widely applied method,[30–35] we use the Yamaguchi[29] formula for evaluation of J in this work, which is given by:

$$J = \frac{(E_{BS} - E_{HS})}{\langle S^2 \rangle_{HS} - \langle S^2 \rangle_{BS}} \quad (3)$$

Table 1 Orbital coefficients of connecting C atoms within molecular wires 1 and 2 (without radical substitution)

		Molecular wire 1		Molecular wire 2	
Site	Orbital	HOMO	LUMO	HOMO	LUMO
r_1	$2p_Z$	−0.0863	−0.0823	0.0560	0.0464
s_1	$2p_Z$	−0.0863	0.0823	0.0572	−0.0465

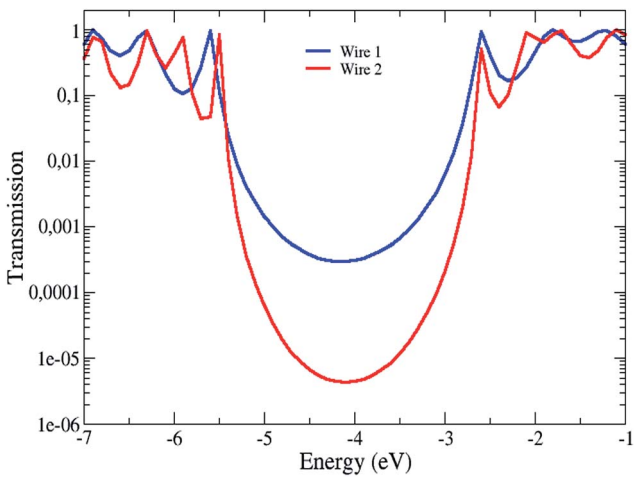

Fig. 5 Transmission spectra of molecular wire 1 and molecular wire 2 at zero bias.

Published on 11 October 2016. Downloaded by University of Waterloo on 08/11/2016 15:46:06.

Where E_{BS}, E_{HS} and $\langle S^2\rangle_{BS}$, $\langle S^2\rangle_{HS}$ are the energy and average spin square values for corresponding BS and high spin states, respectively.

Results and discussion

Transport properties of molecular wires 1 and 2

The zero bias transmission spectra of the molecular wires are given in Fig. 5. The horizontal axis corresponds to the electron energy E incident from the electrode. The proper choice of the electrode's Fermi energy is not entirely clear, so for this reason we compared different values (−2.5 eV to −5.5 eV), whereas the Fermi energy of bulk gold is −5.53 eV.[36]

We can see from Fig. 5 that molecular wire 1 has higher transmission near the Fermi level compared to molecular wire 2, which implies that the smaller wire is more efficient for electrical transport.[2]

Now from the structures of the two molecular wires one may expect that the conductivity of a system increases with increasing the number of π electrons, but organic molecules are not usually very rigid. The flexing and bending of bonds changes the overlap between different orbitals. If all the benzene rings in the molecule are in the same plane, the p orbitals have the maximum overlap, which leads to the lowest resistance. On the other hand, complete misalignment between the rings leads to the highest resistance. The decrease in transmission with the increase in the length of the wire can also be explained by Pauling's bond order,[37] which is proportional to the transmission. According to this concept, with increasing phenyl ring in a molecular wire, Pauling's bond order decreases exponentially and hence the transmission is also decreased.

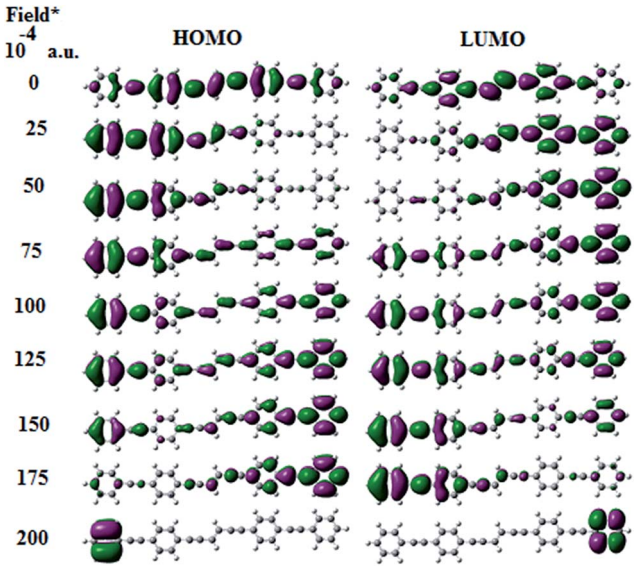

Fig. 6 Molecular orbitals of wire 1 under different electric fields.

Molecular orbitals of wire 1 and 2

Molecular orbitals contain all the quantum mechanical information about the electronic structures of a molecule. To understand the transport property through a molecule it is necessary to study the molecular orbitals because they offer spatial conduction channels for electron transport.[38] Localization of orbitals can significantly change the transport properties. An external electric field is an appropriate stimulus to tune the MOs of a molecule. It has been shown that the MOs of a molecule with and without electrode atoms at their end have similar characteristics under an external electric field.[39]

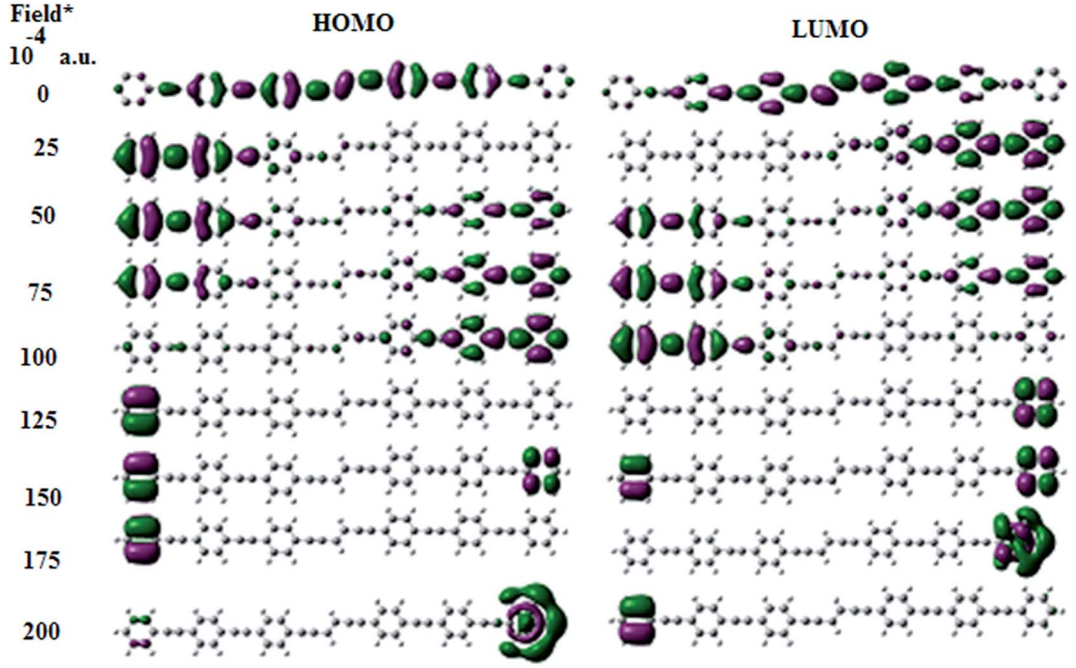

Fig. 7 Molecular orbitals of wire 2 under different electric fields.

 This journal is © The Royal Society of Chemistry 2016

Published on 11 October 2016. Downloaded by University of Waterloo on 08/11/2016 15:46:06.

Following this analogy and following one of our recent works,[40] we applied an electric field (parallel to the molecule) taking the optimized geometry (without thiol groups and lead atoms at their ends) to study the change of molecular orbital under an external electric field.

We can see from Fig. 6 and 7 that at zero external electric field the HOMO and LUMO spread over the entire molecule. After the application of the external electric field, the MOs are squeezed to a few atoms for both the wires. If we closely look at the MOs of wire 1, we can see that the HOMO and the LUMO are always collectively spread over all the molecules (except field 0.02 a.u.). However, for wire 2, the HOMO and LUMO cannot cover the whole molecule even jointly. Thus with the application of an external electric field there is a large separation in the spatial distribution of the HOMO–LUMO for molecular wire 2 as compared to wire 1.

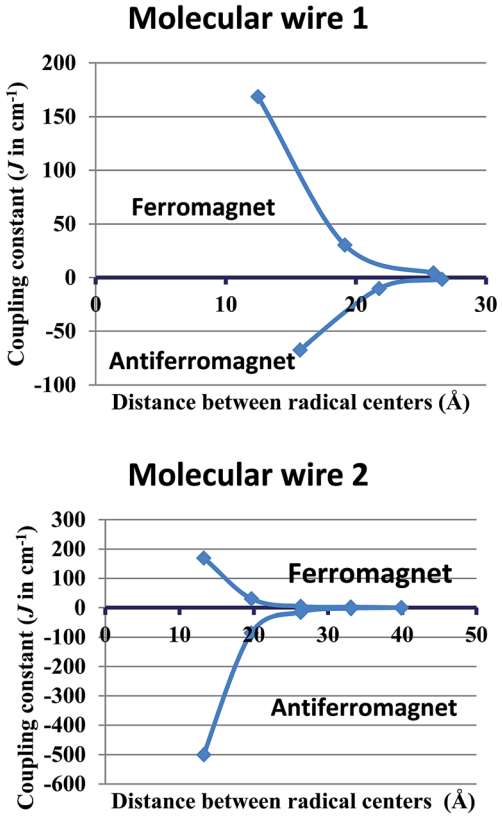

Fig. 8 Plot of magnetic exchange coupling constants as a function of distance between the radical centers.

Magnetic exchange coupling constant of the diradical substituted molecular wire

We substituted the molecular wires with two methylene radicals such that the diradical shows ferromagnetic and antiferromagnetic interaction according to the spin alternation rule[41] and we changed the position of the radicals to vary the distance between the radical centers. We plotted the magnetic exchange coupling constant as a function of the distance between radical centers (Fig. 8). The calculated magnetic exchange coupling constants of the diradical are also given in ESI Tables S2 and S3.† We can see that with increasing the distance between radical centers, the magnetic exchange coupling constant value decreases. The distance-dependent exchange coupling constant of π-conjugated molecular wires has been studied by Nishizawa *et al.* and they found similar results.[12]

Spin density distribution between diradical centers

The spin density from the DFT based approach can give us an insight about the spin polarization mechanism in the molecule for magnetic exchange. The spin densities of the high-spin states of the diradical are represented in Fig. 9 and 10. It is clear that with increasing distance between the radical centers, the spin polarization decreases; hence the coupling constant also decreases. Therefore, it is obvious that beyond certain distances between two spin centers, spin polarization is no longer effective although the molecule has a strong π-network. Another important thing is that the magnetic exchange between two spin centers depends only on the environment in between them, not on the outside substitution.

Transport property of the diradical substituted molecular wires

We studied the transport property of the diradical substituted molecular wires (in Fig. 11 and 12) to see the effect of radical

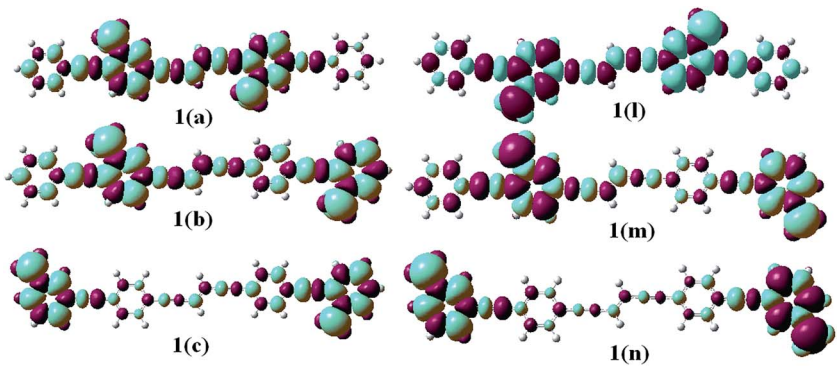

Fig. 9 Spin density distribution of the ferromagnetically coupled diradicals (high spin state) and antiferromagnetically coupled diradicals (BS state) based on molecular wire 1.

Published on 11 October 2016. Downloaded by University of Waterloo on 08/11/2016 15:46:06.

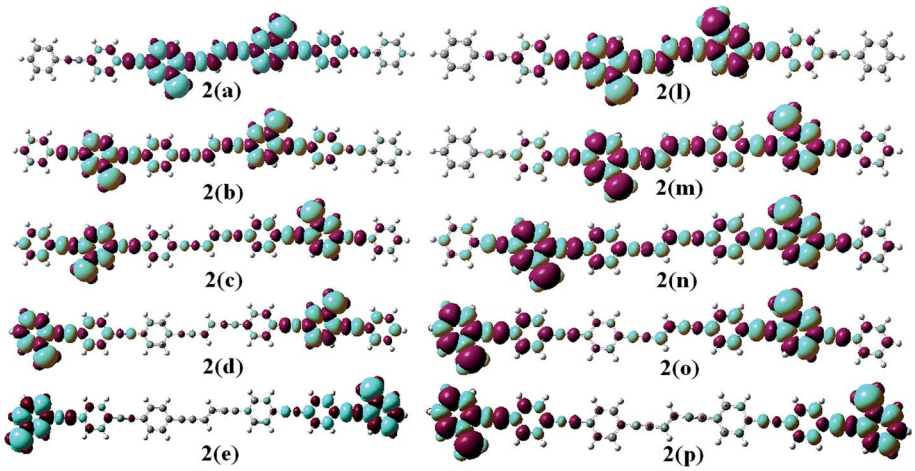

Fig. 10 Spin density distribution of the ferromagnetically coupled diradicals (high spin state) and antiferromagnetically coupled diradicals (BS state) based on molecular wire 2.

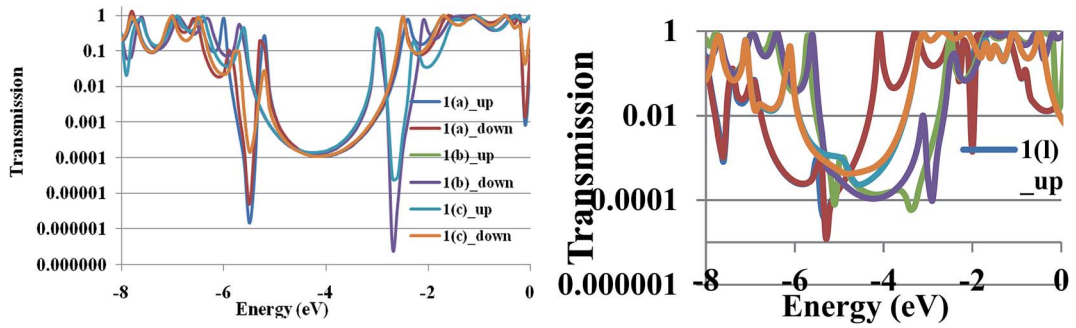

Fig. 11 The transmission spectra of the diradical substituted molecular wire 1 [1(a)–1(c) high spin state; 1(l)–1(n) BS state].

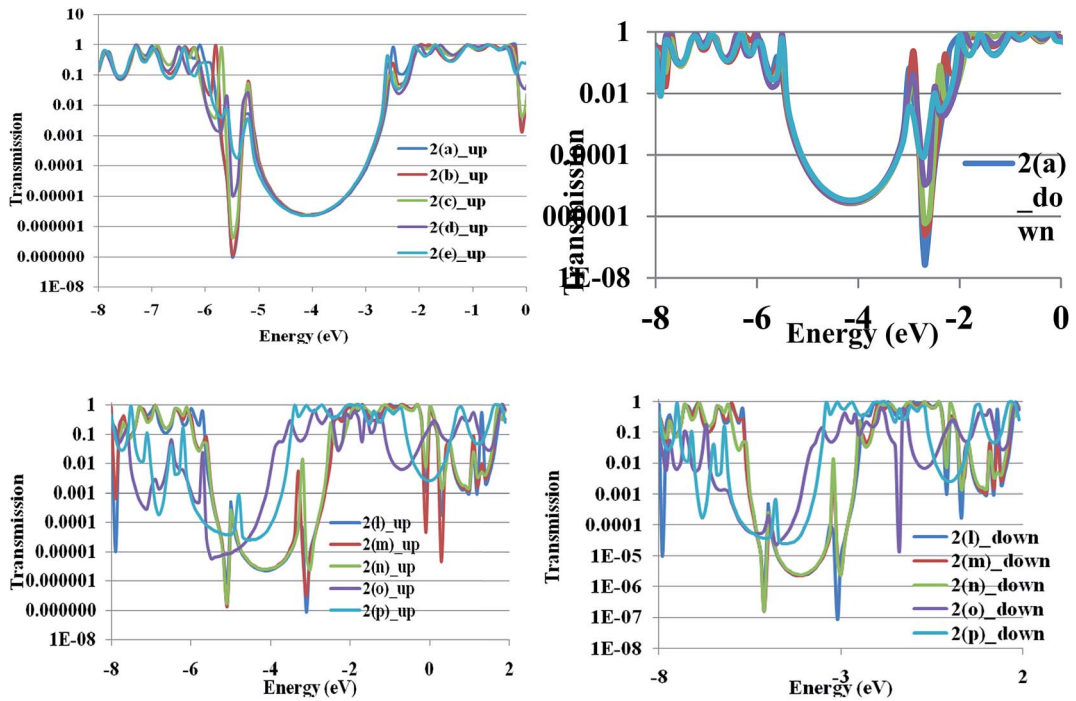

Fig. 12 The transmission spectra of the diradical substituted molecular wire 2 [2(a)–2(e) high spin state; 2(l)–2(p) BS state].

This journal is © The Royal Society of Chemistry 2016

Published on 11 October 2016. Downloaded by University of Waterloo on 08/11/2016 15:46:06.

substitution on the transport behavior of the molecular wires. We can see from the figures that the molecular wires belonging to the same series show almost similar transmission, but series 1 exhibits higher transmission than series 2. Again comparing the transmission for the molecular wire without radical substitution (Fig. 5), we observe the same result as that for the ferromagnetically coupled diradicals (Fig. 11 and 12). However, the transmission characteristics are affected by the antiferromagnetically coupled diradicals. Stasiw *et al.* showed that for donor–bridge–acceptor systems there is a large variation in magnetic exchange coupling and electronic coupling as a function of bridge conformation.[42] For our designed molecular wires (consisting of several aromatic phenyl rings along with radical substitution on the rings), when transmission occurs through the wire, possibly only local transmission of the aromatic rings appears on the Fermi level of the electrode and the radicals do not participate in the transmission of that region, which may be the reason for the same transmission after radical substitution in the ferromagnetic diradicals, but for antiferromagnetic diradicals, there is a small variation in transmission characteristics between radical substituted molecular wires.

Conclusions

To summarize, we studied the effect of the length of molecular wires on the electrical transport properties. We found that the molecular wires (addition polymer) with smaller length show higher transmission, *i.e.*, higher conduction. Another important point is that the magnetic exchange coupling constant of the radical substituted molecular wire depends only on the distance between the spin centers, not on the outsider substitution. The transmission of the molecular wire without radical substitution shows similar observations as that of the wire with radical substitution for ferromagnetically coupled diradicals; however, the transmission characteristics are slightly affected by the antiferromagnetic diradicals.

Acknowledgements

We are thankful to Prof. Dr Carmen Herrmann for giving us the permission to use her transport code ARTAIOS. AM is thankful to DST, India for financial support. SS is thankful to Sonderforschungsbereich 668, University of Hamburg for a postdoctoral fellowship.

References

1 W. Tian, S. Datta, S. Hong, R. Reifenberger, J. I. Henderson and C. P. Kubiak, *J. Chem. Phys.*, 1998, **109**, 2874–2882.
2 S. Kober, G. Gotesman and R. Naaman, *J. Phys. Chem. Lett.*, 2013, **4**, 2041–2045.
3 S. Jalili and H. Rafi-Tabar, *Phys. Rev. B: Condens. Matter Mater. Phys.*, 2005, **71**, 165410.
4 M. Magoga and C. Joachim, *Phys. Rev. B: Condens. Matter Mater. Phys.*, 1997, **56**, 4722–4729.
5 U. Durig, O. Zuger, B. Michel, L. Haussling and H. Ringsdorf, *Phys. Rev. B: Condens. Matter Mater. Phys.*, 1993, **48**, 1711–1717.
6 C. Boulas, J. V. Davidovits, F. Rondelez and D. Vuillaume, *Phys. Rev. Lett.*, 1996, **76**, 4797–4800.
7 L. A. Bumm, J. J. Arnold, M. T. Cygan, T. D. Dunbar, T. P. Burgin, L. Jones II, D. L. Allara, J. M. Tour and P. S. Weiss, *Science*, 1996, **271**, 1705–1707.
8 R. P. Andres, T. Bein, M. Dorogi, S. Feng, J. I. Henderson, C. P. Kubiak, W. Mahoney, R. G. Osifchin and R. G. Reifenberger, *Science*, 1996, **272**, 1323–1325.
9 M. A. Reed, C. Zhou, C. J. Muller, T. P. Burgin and J. M. Tour, *Science*, 1997, **278**, 252–254.
10 J. G. Kushmerick, D. B. Holt, S. K. Pollack, M. A. Ratner, J. C. Yang, T. L. Schull, J. Naciri, M. H. Moore and R. Shashidhar, *J. Am. Chem. Soc.*, 2002, **124**, 10654–10655.
11 E. A. Weiss, M. J. Ahrens, L. E. Sinks, A. V. Gusev, M. A. Ratner and M. R. Wasielewski, *J. Am. Chem. Soc.*, 2004, **126**, 5577–5584.
12 S. Nishizawa, J.-y. Hasegawa and K. Matsuda, *J. Phys. Chem. C*, 2013, **117**, 26280–26286.
13 I. D. W. Samuel, *Philos. Trans. R. Soc., A*, 2000, **358**, 193–210.
14 H. Lu, J. Leng and S. Du, *Soft Matter*, 2013, **9**, 3851–3858.
15 H. Lu and S. Du, *Polym. Chem.*, 2014, **5**, 1155–1162.
16 C. Herrmann, G. C. Solomon and M. A. Ratner, *J. Am. Chem. Soc.*, 2010, **132**, 3682–3684.
17 C. Herrmann, G. C. Solomon, J. E. Subotnik, V. Mujica and M. A. Ratner, *J. Chem. Phys.*, 2010, **132**, 024103.
18 M. J. Frisch, G. W. Trucks, H. B. Schlegel, G. E. Scuseria, M. A. Robb, J. R. Cheeseman, G. Scalmani, V. Barone, B. Mennucci and G. A. Petersson, *et al.*, *Gaussian09*, Gaussian, Inc., Wallingford, CT, 2009.
19 K. Yoshizawa, *Acc. Chem. Res.*, 2012, **45**, 1612–1621.
20 K. Yoshizawa, T. Tada and A. Staykov, *J. Am. Chem. Soc.*, 2008, **130**, 9406–9413.
21 L. Noodleman, *J. Chem. Phys.*, 1981, **74**, 5737.
22 L. Noodleman and E. J. Baerends, *J. Am. Chem. Soc.*, 1984, **106**, 2316–2327.
23 A. P. Ginsberg, *J. Am. Chem. Soc.*, 1980, **102**, 111–117.
24 L. Noodleman, C. Y. Peng, D. A. Case and J. M. Mouesca, *Coord. Chem. Rev.*, 1995, **144**, 199–244.
25 L. Noodleman and E. R. Davidson, *Chem. Phys.*, 1986, **109**, 131–143.
26 A. Bencini, F. Totti, C. A. Daul, K. Doclo, P. Fantucci and V. Barone, *Inorg. Chem.*, 1997, **36**, 5022–5030.
27 A. Bencini, D. Gatteschi, F. Totti, D. N. Sanz, J. A. McClevrty and M. D. Ward, *J. Phys. Chem. A*, 1998, **102**, 10545.
28 E. Ruiz, J. Cano, S. Alvarez and P. Alemany, *J. Comput. Chem.*, 1999, **20**, 1391–1400.
29 K. Yamaguchi, Y. Takahara, T. Fueno and K. Nasu, *Jpn. J. Appl. Phys.*, 1987, **26**, L1362.
30 Md. E. Ali and S. N. Datta, *J. Phys. Chem. A*, 2006, **110**, 2776–2784.
31 Md. E. Ali and S. N. Datta, *J. Phys. Chem. A*, 2006, **110**, 13232–13237.
32 V. Polo, A. Alberola, J. Andres, J. Anthony and M. Pilkington, *Phys. Chem. Chem. Phys.*, 2008, **10**, 857–864.

Published on 11 October 2016. Downloaded by University of Waterloo on 08/11/2016 15:46:06.

33 D. Bhattacharya and A. Misra, *J. Phys. Chem. A*, 2009, **113**, 5470–5475.
34 S. Paul and A. Misra, *J. Mol. Struct.: THEOCHEM*, 2009, **907**, 35–40.
35 S. Paul and A. Misra, *J. Mol. Struct.: THEOCHEM*, 2009, **895**, 156–160.
36 N. W. Ashcroft and N. D. Mermin, *Solid State Physics*, Holt, Rinehart and Winston, New York, 1976.
37 T. Stuyver, S. Fias, De F. Proft and P. Geerlings, *Chem. Phys. Lett.*, 2015, **630**, 51–56.
38 W. Y. Kim and K. S. Kim, *Acc. Chem. Res.*, 2010, **43**, 111–120.
39 Y. C. Choi, W. Y. Kim, K.-S. Park, P. Tarakeshwar, K. S. Kim, T.-S. Kim and J. Y. Lee, *J. Chem. Phys.*, 2005, **122**, 094706.
40 S. Shil and A. Misra, *RSC Adv.*, 2013, **3**, 14352–14362.
41 C. Trindle and S. N. Dutta, *Int. J. Quantum Chem.*, 1996, **57**, 781–799.
42 D. E. Stasiw, J. Zhang, G. Wang, R. Dangi, B. W. Stein, D. A. Shultz, M. L. Kirk, L. Wojtas and R. D. Sommer, *J. Am. Chem. Soc.*, 2015, **137**, 9222–9225.

This journal is © The Royal Society of Chemistry 2016

JOC The Journal of Organic Chemistry

Article

pubs.acs.org/joc

A Perspective on Designing Chiral Organic Magnetic Molecules with Unusual Behavior in Magnetic Exchange Coupling

Prodipta Sarbadhikary,[†] Suranjan Shil,[‡] Anirban Panda,[§] and Anirban Misra*[,†]

[†]Department of Chemistry, University of North Bengal, Dist-Darjeeling 734013, India

[‡]Institute for Inorganic and Applied Chemistry, University of Hamburg, Martin-Luther-King-Platz 6, 20146 Hamburg, Germany

[§]Department of Chemistry, J. K. College, Purulia PIN-723101, West Bengal, India

Supporting Information

ABSTRACT: A total of nine diradical-based organic chiral magnetic molecules with allene and cumulene couplers have been theoretically designed, and subsequently, their magnetic property has been studied by density functional theory. It is found that with an increase in length of the coupler, a remarkable increase in spin density within the coupler takes place. An increase in the length of the coupler reduces the energy of LUMO, and a smaller HOMO−LUMO gap facilitates stronger magnetic coupling and thereby a higher magnetic exchange coupling constant (J). This observation is supported by the occupation number of natural orbitals.

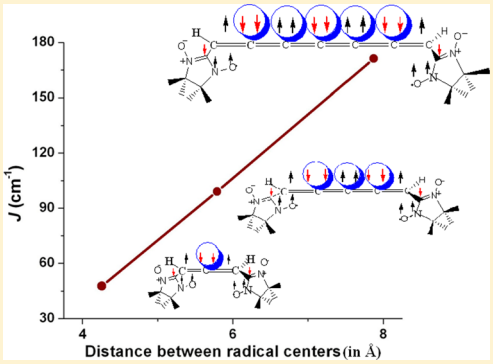

1. INTRODUCTION

Chirality is of utmost importance as it plays a key role not only in life forms but also in pharmaceutical, agricultural, and other chemical industries.[1] At present, chiral organic molecules are of great interest to organic chemists as well as pharmaceutical chemists.[2] Galán-Mascarós et al. have synthesized molecular materials with ferromagnetism, metal-like conductivity, and chirality.[3] When chirality appears in the structure of atoms in a solid that has unpaired electrons, the chiral lattice favors a screwlike arrangement of the magnetic moments of unpaired electrons, but they must compete with ferromagnetic exchange, which attempts to align all the magnetic moments in the same direction. These chiral lattices are known as chiral magnets.[4] On the other hand, chiral magnetic molecules with ferromagnetic interaction can also be regarded as chiral magnets.[5] Stable chiral magnets are important ingredients for future data storage, spintronic devices,[6] and other applications for their fascinating properties.[4] The most important phenomena shown by chiral magnets are the magneto-chiral effects that occur in chiral media in the presence of a magnetic field.[7] The synthesized chiral magnets are mainly inorganic or metallo-organic in nature.[8,9] It is observed that chiral magnets, in particular manganese silicide (MnSi), a cubic intermetallic compound that has no inversion symmetry, i.e., with a noncentrosymmetric crystal structure,[10] have attracted interest over the past few years, and they may one day reach a degree of functionality similar to that of chiral liquid crystals.[4] However, in the past few decades, the search for new ferromagnetic materials based on organic diradicals has generated tremendous interest.[11−13] Organic radicals[11] have been widely studied because of their versatile applicability in the field of magnetism[14] and their superconductivity,[15] spintronic properties,[16] photomagnetic behavior,[17] etc. In the case of organic diradicals, the magnetic interaction between two radical centers normally depends on the couplers that connect the radical centers.[18] A series of nitronylnitroxide (NN) diradicals with linear conjugated couplers have been studied by Ali and Datta, and they reported that the magnetic exchange coupling constant value decreases gradually with increasing coupler conjugation length.[19] It has been found that chains containing sp-hybridized carbon atoms are fascinating because of their unique linear structure and interesting physical properties.[20] Allenes (1,2-propadiene derivatives) make up an important class of compounds and have attracted a growing level of attention as interesting building blocks in synthetic organic chemistry.[21] Cumulenes with an odd number of carbon atoms have π-systems that are spatially orthogonal with each other; therefore, these systems contain a chiral axis, and their two pairs of substituents are in two perpendicular planes, giving rise to enantiomers.[22] Skibar et al. have synthesized cumulenes containing seven carbon atoms.[23] Januszewski et al. also have synthesized and predicted the properties of long cumulenes containing up to 10 carbon atoms.[24] Cumulenes are extensively used in molecular machines (nanomechanics), molecular wires (nanoelectronics), nonlinear optics, and molecular sensors because of their unique electronic structures.[25] It is found that among all conjugated oligomers, cumulene wires with an odd number of carbon atoms show the highest conductance with metallic-like ballistic transport behavior.[26]

Received: April 26, 2016
Published: June 10, 2016

ACS Publications © 2016 American Chemical Society

DOI: 10.1021/acs.joc.6b00943
J. Org. Chem. 2016, 81, 5623−5630

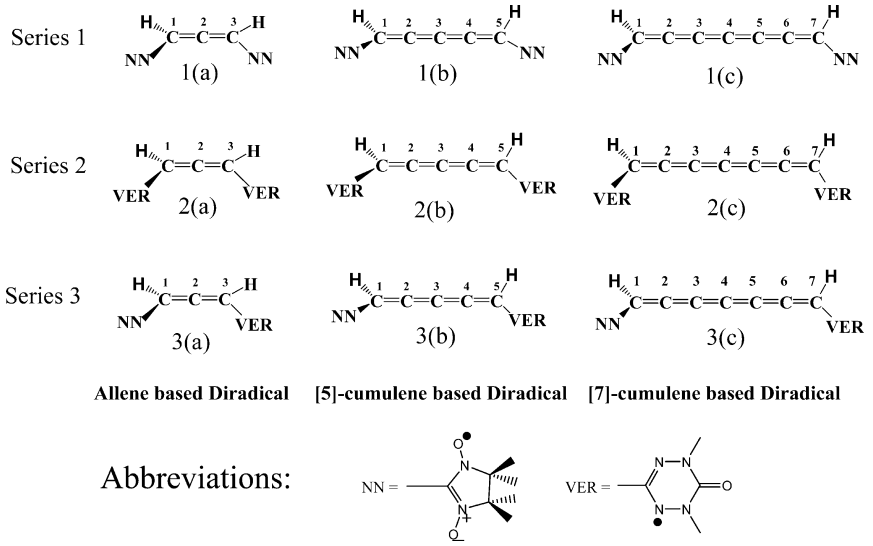

Figure 1. Allene- and cumulene-based diradicals. [5] and [7] indicate the number of carbon atoms in a coupler.

We have designed allene-based and cumulene-based (containing an odd number of carbon atoms) organic diradical systems that are shown in Figure 1 and have studied the magnetic properties of these diradicals in detail as an estimation of the intramolecular exchange coupling constant is necessary before a successful magnetic material based on organic diradicals or transition metal complexes can be synthesized. These designed molecules may be used as molecular building blocks for organic chiral magnetic solids.

2. THEORETICAL BACKGROUND

The magnetic exchange interaction between two magnetic sites 1 and 2 is generally expressed by the Heisenberg spin Hamiltonian $\hat{H} = -2J\hat{S}_1\hat{S}_2$, where $\hat{S}_1$ and $\hat{S}_2$ are the respective spin angular momentum operators and J is the exchange coupling constant between two magnetic centers. When J is positive, the high-spin state is lower in energy and the coupling is said to be ferromagnetic. A negative value of J is representative of antiferromagnetic interaction in the diradical, and a low-spin state is the ground state. For a diradical containing a single unpaired electron on each site, J can be represented as $E_{(S=1)} - E_{(S=0)} = -2J$.

Multiconfiguration approaches are suitable for describing pure spin states in an appropriate manner, but these methods are resource intensive and were not used in this work. To circumvent this issue, the broken symmetry (BS) approach by Noodleman et al.[27−30] in the density functional theory (DFT) framework is a more useful alternative for evaluating J that can eventually lead to an estimate of the energy of the diradical singlet. The ideal BS state is a weighted average of the singlet and the triplet and has an M_S equal to zero. The ideal triplet (T) state has $\langle S^2\rangle = 2$, whereas $\langle S^2\rangle = 1$ in the ideal BS state, which results in $E(\mathrm{BS}) - E(\mathrm{T}) = J$. However, in the actual calculation, approximate $\langle S^2\rangle$ values are obtained, and hence, the BS solution is often found to be spin-contaminated. Therefore, a correction is needed to calculate the coupling constant.

The spin-projected formula given by Yamaguchi[31−34] for the evaluation of the magnetic exchange coupling constant (J) is free from such spin contamination and applicable for both low and high overlap between magnetic orbitals, which can be written as $J = (E_{\mathrm{BS}} - E_{\mathrm{HS}})/(\langle S^2\rangle_{\mathrm{HS}} - \langle S^2\rangle_{\mathrm{BS}})$, where E_{BS}, E_{HS}, $\langle S^2\rangle_{\mathrm{BS}}$, and $\langle S^2\rangle_{\mathrm{HS}}$ are the energies and average spin square values for the BS and high-spin states, respectively.

3. COMPUTATIONAL STRATEGY

The molecular structures of all the diradicals have been fully optimized in each spin state by hybrid exchange-correlation functionals B3LYP and M06 in combination with the 6-311++G(d,p) basis set within the unrestricted formalism using the Gaussian09 quantum chemical package.[35] A broken symmetry (BS) singlet solution has been performed for mixing of the HOMO and the LUMO. The magnetic exchange coupling constant (J) value for each molecule has been estimated from the energies of triplet and BS states at the same level of theory using the spin-projected formula given by Yamaguchi.[31−34] To confirm the enantiomeric nature of our designed systems, we analyze the vibrational circular dichroism (VCD) spectra. Detailed analyses of geometrical parameters, the spin density distribution, and molecular orbital and natural orbital occupancies have been calculated with the optimized geometry. Details of the computational procedure are discussed in the Supporting Information.

4. RESULTS AND DISCUSSION

It is well-known that the two enantiomers of a chiral compound show optical rotation values of the same angles but in opposite directions in the presence of plane-polarized light. The absolute configuration of a chiral molecule can be determined from its VCD spectrum as the VCD spectra of the two enantiomers of a chiral molecule are equal in magnitude and opposite in sign.[2] Here we have tried to verify the enantiomeric relationship between our designed chiral molecules. For series 2 diradicals (Figure S1), calculated VCD spectra (Figure S2) confirm the stereochemistry as well as the enantiomeric relationship between them. The other diradicals (series 1 and series 3) have similar couplers; therefore, it is obvious that they will follow the same trend as series 2. The point here is that the form of the Hamiltonian guarantees the magnetic exchange coupling constant of the diradical-based chiral enantiomers to be equal in magnitude.

Magnetic Exchange Coupling Constant. The calculated magnetic exchange coupling constants of all the diradicals are listed in Table 1. The consistency of magnetic exchange coupling constant values has been confirmed using two different exchange-correlation functionals (B3LYP and M06). It is observed that although the values of coupling constants are different for different methods, they follow similar trends. From Table 1, it is

DOI: 10.1021/acs.joc.6b00943
J. Org. Chem. 2016, 81, 5623−5630

Table 1. Intramolecular Magnetic Exchange Coupling Constants (J) of Designed Diradicals

system	J (cm^{-1}) [B3LYP/6-311++G(d,p)]	J (cm^{-1}) [M06/6-311++G(d,p)]
1(a)	47.66	63.17
1(b)	99.09	146.28
1(c)	171.28	244.31
2(a)	15.30	22.96
2(b)	30.36	45.00
2(c)	53.17	86.95
3(a)	28.33	39.14
3(b)	55.84	78.62
3(c)	95.42	147.65

observed that with the increase in the chain length of the coupler from the allene-based diradical to the [5]-cumulene-based diradical, the magnetic exchange coupling constant increases almost 2-fold, and again upon the transition from the [5]-cumulene-based diradical to the [7]-cumulene-based diradical, the coupling constant further increases by approximately 2-fold, which contradicts the fact that the level of magnetic exchange decreases with an increase in the length of conjugated systems.[19] Therefore, it can be argued that there must be a major contribution of the coupler in the magnetic exchange pathway, and this observation demands a detailed investigation of the electronic structure of these couplers. If we compare the coupling constants of the same coupler with different radicals, we can see that the NN-based diradicals have highest coupling constant and VER-based diradicals have the lowest; a combination of two radicals NN and VER gives the coupling constant in between. Thus, we can conclude that the nitronyl nitroxide radical is more suitable for obtaining a coupling constant higher than that of verdazyl radical with allene and cumulene couplers. We have calculated the absolute energy values of the diradicals as $^1/_2(E^T_{NN} + E^T_{VER})$ and for mixed radical systems (see Table S3) and found that for allene-based diradicals the energy difference is as small as 0.00036 au and for longer cumulene there is no energy difference at all, which suggests that the interaction between radicals at the two ends of the molecules is not radical specific and decreases with an increase in the length of the carbon chain.

Spin Density Distribution. The spin density of the DFT-based approach can give us insight into the spin polarization mechanism for magnetic exchange coupling within the molecule. The exchange coupling constant between two magnetic sites largely depends on the delocalization of π-electron densities between them. Hence, to understand the anomalous increase in the magnitude of J, we have conducted spin density distribution analysis. Hund's rule-based spin density alternation rule[36,37] helps to predict the nature of magnetic interaction for diradicals with different couplers. Ferromagnetic exchange coupling takes place between two spin centers when they are connected by an even number of conjugated bonds, and antiferromagnetism occurs for an odd number of bonds.[36,37] The spin density distribution of the diradicals in their high-spin states (Figure S3) confirms that all these diradicals exhibit intramolecular ferromagnetic coupling.

The spin density on different atoms of a coupler and also the total spin density of a coupler in designed diradicals are listed in Table 2. Hermann et al. have proposed that cumulene-based systems with an even number of carbon centers, spin delocalization onto the chain increases as the length of the chain increases.[38] For our designed systems, it is also found that with an increase in the chain length of the coupler, the spin density on different atoms of the coupler and the total spin density on the coupler increase, which is quite contradictory from the concept that with an increase in the chain length of conjugated systems the spin density on the coupler decreases.[19] Hence, as argued in the previous subsection, there must be some special reason that facilitates spin polarization in such systems.

Spin Polarization. Chiral allene and cumulene couplers contain an even number of π-bonds in perpendicular planes; therefore, the two end π-bonds are perpendicular to each other. A close inspection of the spin density plot in Figure 2 for series 1

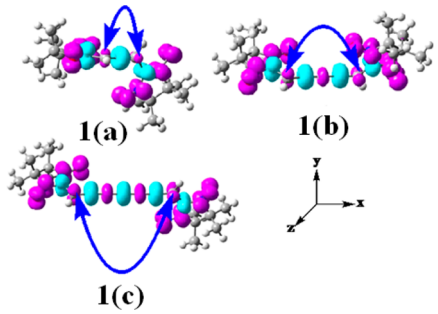

Figure 2. Spin density plot for the diradicals of series 1 in their triplet states [B3LYP/6-311++G(d,p)] (iso value of 0.004), in which magenta and sky colors represent the α and β spins, respectively. The blue arrow represents two end carbons of the coupler.

diradicals points to the fact that the spin density distributions of π-electrons of two end carbon atoms of the coupler are individually directed along two Cartesian axes (y and z directions), but for rest of the carbon atoms within the coupler, spin polarization of π-electrons is along both the y and z directions collectively, causing a

Table 2. Spin Density Distribution on Each Atom of the Coupler and Total Spin Density of the Coupler in Designed Diradicals in Their Triplet State [B3LYP/6-311++G(d,p)]

	spin density on different atoms of the coupler							
system	C1	C2	C3	C4	C5	C6	C7	total spin density
1(a)	0.0768	−0.2655	0.0768	–	–	–	–	−0.1120
1(b)	0.1072	−0.2664	0.1572	−0.2665	0.1071	–	–	−0.1614
1(c)	0.1501	−0.3004	0.2041	−0.3196	0.2041	−0.3004	0.1501	−0.2120
2(a)	0.0616	−0.141	0.0616	–	–	–	–	−0.0177
2(b)	0.0831	−0.1341	0.0652	−0.1341	0.0831	–	–	−0.0366
2(c)	0.1223	−0.1659	0.0899	−0.1396	0.0899	−0.1659	0.1223	−0.0470
3(a)	0.0638	−0.1862	0.0683	–	–	–	–	−0.0541
3(b)	0.1025	−0.2095	0.114	−0.1969	0.0953	–	–	−0.0946
3(c)	0.1437	−0.2437	0.1711	−0.2488	0.1469	−0.2316	0.1362	−0.1262

DOI: 10.1021/acs.joc.6b00943
J. Org. Chem. 2016, 81, 5623−5630

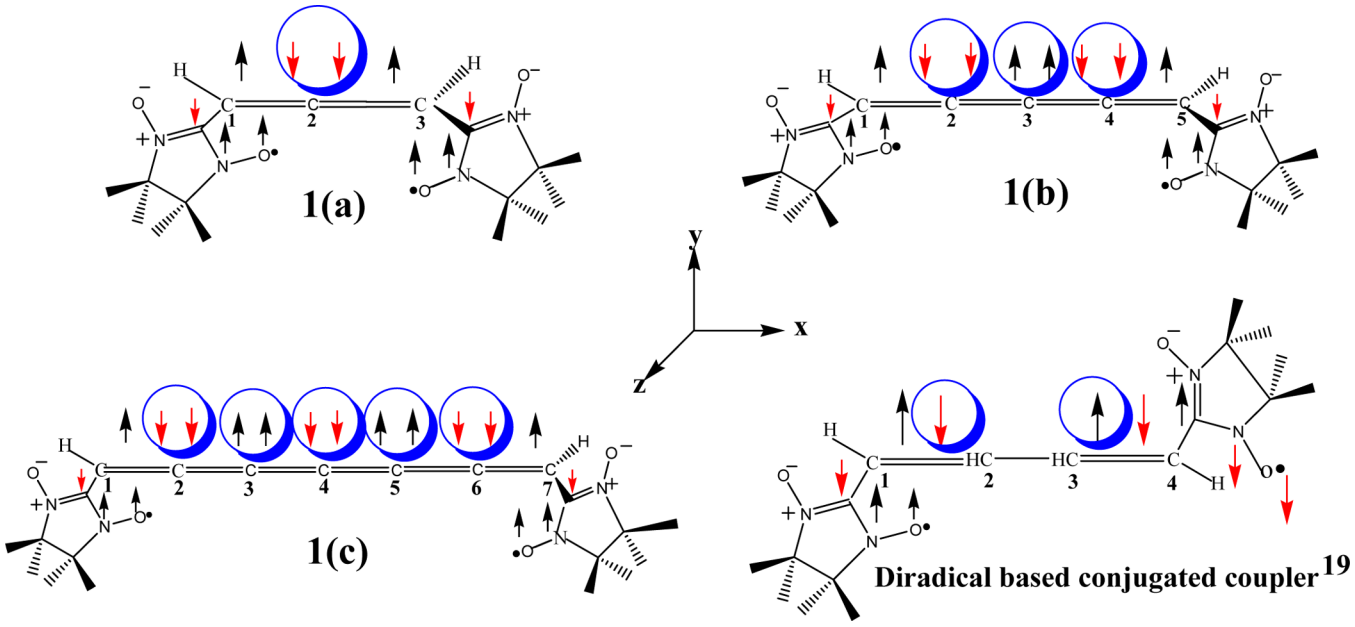

Figure 3. Spin polarization of π-electrons within the coupler (for series 1).

high level of accumulation of spin density for the middle carbons of the coupler chain. A plausible mechanistic pathway of spin polarization within the coupler is shown in Figure 3.

To explain the increase in spin density upon addition of a carbon center within the coupler, and simultaneously to explain the contradictory behavior of spin polarization in cumulenes compared to that of conjugated systems (i.e., alternating σ- and π-bonds), a detailed investigation of the mechanistic pathway of spin polarization was conducted. Figure 3 shows that the two end carbons in the allene-based diradical contain one π-bonding electron on each of them, but the central carbon contains two π-bonding electrons in two different p orbitals at a time. Therefore, for allene-based diradicals, spin polarization is greater in the middle carbon than in the end carbons. Now upon comparison of the allene-based diradical with the [5]-cumulene-based diradical, we find that the former contains only one carbon with two π-electrons in the central region of the coupler but later contains three carbons with two π-electrons on each. As a result, the [5]-cumulene-based diradical has higher level of accumulation of spin density on each carbon of the coupler compared to that of the allene-based diradical. A similar trend in the [7]-cumulene-based diradical is also observed. Thus, one can surmise that spin polarization increases considerably with an increase in the number of carbon centers of the coupler in cumulene systems.

Upon comparison of the spin density of cumulene with that of the conjugated coupler, it is found that for conjugated coupler-based diradicals, each carbon atom of the coupler contains one π-electron on each and no such enhancement of spin polarization occurs; moreover, a decrease in spin density with an increase in the chain length of the coupler is observed as the distance between the radical centers increases. Figure 4 is a plot of the coupling constant versus the distance between the radical centers that clearly shows the variation of the coupling constant with distance.

Therefore, a high level of accumulation of spin density within the coupler overcomes the distance factor between the radical centers in the case of cumulene-based diradicals, and higher magnetic exchange coupling results from the increase in the length of the coupler.

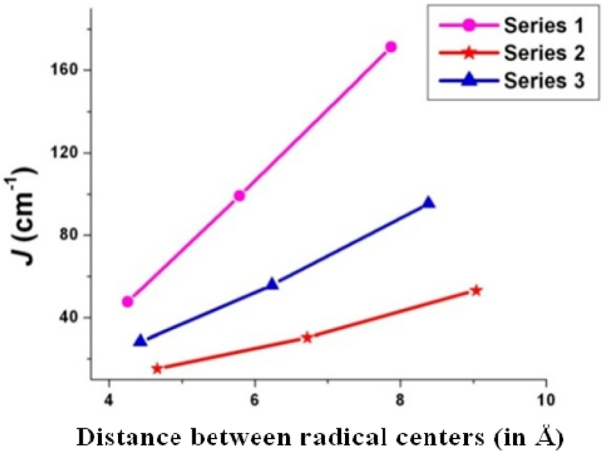

Figure 4. Plot of the magnetic exchange coupling constant vs distance between the radical centers [B3LYP/6-311++G(d,p)].

Molecular Structures. A small change in molecular structure can lead to a drastic change in the magnetic coupling constant.[39] Therefore, it is important to study the molecular structure of the allene- and cumulene-based diradicals to understand their magnetic behavior. The optimized geometrical parameters of our designed diradicals are reported in Tables 3 and 4.

The most important structural aspect is the bond distance alteration of the cumulene moiety. Our calculations predict a distinct alternation of adjacent C═C bonds, and the first and last bond lengths for all the diradicals are approximately close to the double bond length in ethylene (132 pm). The central double bond distance in [5]-cumulene-based diradicals is approximately 127 pm, and their values are between the double bond length in ethylene (132 pm) and the triple bond length in acetylene (121.2 pm). The central bond distances for [7]-cumulene are also approximately 128 pm, and double bond lengths elsewhere in the bridge chain equal 126 pm and their values between the double bond length in ethylene (132 pm) and the triple bond length in acetylene (121.2 pm). When two different groups are included, all the double bond lengths become unequal (see series 3). These

DOI: 10.1021/acs.joc.6b00943
J. Org. Chem. 2016, 81, 5623−5630

Table 3. Bond Distances between Two Atoms and Average Bond Distances of the Couplers for the Designed Diradicals in their Triplet State [B3LYP/6-311++G(d,p)][a]

	bond distance										
system	C1═C2	C2═C3	C3═C4	C4═C5	C5═C6	C6═C7	average bond distance of coupler	distance between C1 and L	distance between C3 and R	distance between C5 and R	distance between C7 and R
1(a)	131.1	131.1	–	–	–	–	131.1	143.8	143.8	–	–
1(b)	132.6	127.0	127.0	132.6	–	–	129.8	142.8	–	142.8	–
1(c)	133.3	126.4	128.1	128.1	126.4	133.3	129.3	142.3	–	–	142.3
2(a)	130.7	130.7	–	–	–	–	130.7	147.3	147.3	–	–
2(b)	131.9	127.2	127.2	131.9	–	–	129.5	146.6	–	146.6	–
2(c)	132.3	126.7	128.0	128.0	126.7	132.3	129.0	146.2	–	–	146.2
3(a)	131.3	130.5	–	–	–	–	130.1	144.0	147.2	–	–
3(b)	132.6	126.9	127.3	131.8	–	–	129.7	142.9	–	146.5	–
3(c)	133.3	126.3	128.3	127.9	126.8	132.4	129.2	142.3	–	–	146.2

[a]All bonds are in picometers. L is the connecting atom of the left radical center and R the connecting atom of the right radical center.

Table 4. Bond Angles (degrees) for the Couplers in the Diradicals in Series 1−3 in Their Triplet State [B3LYP/6-311++G(d,p)]

system	∠c1−c2−c3	∠c2−c3−c4	∠c3−c4−c5	∠c4−c5−c6	∠c5−c6−c7
1(a)	173.87	–	–	–	–
1(b)	174.35	177.97	174.35	–	–
1(c)	174.33	178.42	179.8	178.41	174.33
2(a)	177.92	–	–	–	–
2(b)	178.12	179.76	178.11	–	–
2(c)	178.13	179.88	179.95	179.87	178.14
3(a)	175.75	–	–	–	–
3(b)	174.54	178.49	178.23	–	–
3(c)	174.44	178.59	179.76	179.83	178.11

different bond lengths are indicative of electronically different bonding situations.

Another important point is that the average C−C bond length tends to decrease with an increase in cumulene chain length in a particular series, as for series 1 the values are 131.1, 129.8, and 129.3 pm for systems 1(a)−1(c), respectively, and this is closer to a double bond distance, as expected. It is observed that with a decrease in the average bond length in each series, there is the possibility of increasing the s-character of the coupler. The higher the s-character, the greater the electronegativity of that atom and the greater the likelihood of localizing the spin density on that atom, which facilitates the higher spin densities on the coupler with an increase in length. From Table 3, it is also clear that with an increase in the length of the coupler the distance between the carbon atoms of the coupler and the radical centers decreases in each series; therefore, the level of conjugation between the coupler and the radical center increases. Thus, ultimately, a better π-interaction results with an increase in the chain length of the coupler.

The computed bond angles between the carbon atoms in the coupler are listed in Table 4. It is confirmed that the bond angle of the coupler deviates from the exact angle of allene (180°); hence, they are the systems with a nonlinear C═C═C framework and are characterized by slightly deviated orthogonal π-bonds. This bending is greater in the case of allene-based diradicals than in the case of cumulene-based diradicals. For this, the allene π-system is significantly disturbed, and the central carbon atom is no longer sp-hybridized as in typical all-carbon allenes. Now, via comparison of diradical-substituted allene with their higher homologue, it is found that with an increase in the chain length the middle allene counterpart goes nearly 180° [e.g, for 1(a), ∠c1−c2−c3 = 173.87°; for 1(b), ∠c2−c3−c4 = 177.97°; for 1(c), ∠c3−c4−c5 = 179.8°]. Hence, there is relatively strong π-interaction with increasing chain length in each series, and the coupling constant increases accordingly.

Molecular Orbital Analysis. The shape of molecular orbitals plays a major role in determining the magnetic properties of the diradicals, electronic transport, etc.[40] Frontier molecular orbitals (FMOs) of all the axially chiral allene- and cumulene-based diradicals are presented in Figure 5. According to Borden and co-workers when the nonbonding molecular orbitals of a diradical have no atoms in common, i.e., disjointed in nature, the diradicals favor the antiferromagnetic state as the ground state. The nondisjointed SOMOs favor the ferromagnetic ground state. From Figure 5, one can see that α-SOMOs of diradicals in series 1 and 2 are nondisjointed and α-SOMOs of diradicals in series 3 are disjointed, although all the diradicals are ferromagnetic in nature. We have conducted molecular orbital analysis of diradicals 1 and 2 with varying geometries to check the stability of the nondisjointed nature of the SOMOs and found that the SOMOs are unaltered upon structural changes (Figure S4). Thus, Borden's analogy,[41,42] which is derived for alternant hydrocarbons, does not fit for the disjointed diradicals in series 3. Thus, it may be surmised that Borden's analogy, which is derived for alternant hydrocarbons, does not fit for these diradicals, and such systems follow a different mechanism for magnetic interaction.

The molecular orbital analysis of the BS determinant of an allene-based diradical (see Figure S5) shows that for 1(a) and 2(a) diradicals, the α-HOMO and β-HOMO are on the two individual radical centers. However, α-SOMOs of the triplet state for those diradicals are distributed collectively on two radical centers, but for series 3 diradicals [(a)], the shape of the α-HOMO and β-HOMO of the BS determinant and α-SOMOs of the triplet state are the same. Therefore, the SOMOs of the BS determinant and triplet state are not exactly the same for all the diradicals but are distributed only over radical centers.

Mechanism of Magnetic Interaction. Molecular orbitals play an important role in understanding the magnetic coupling between two radical centers. It is known that the SOMOs are mainly responsible for magnetic interaction in diradicals through itinerant exchange[41−44] and the small SOMO−SOMO gap or degenerate SOMOs produce a strong magnetic exchange coupling constant. The SOMO−SOMO energy gap and the HOMO−LUMO energy gap for the designed diradicals are listed in Table 5. The energy of FMOs is given in Table S4. We observe

DOI: 10.1021/acs.joc.6b00943
J. Org. Chem. 2016, 81, 5623−5630

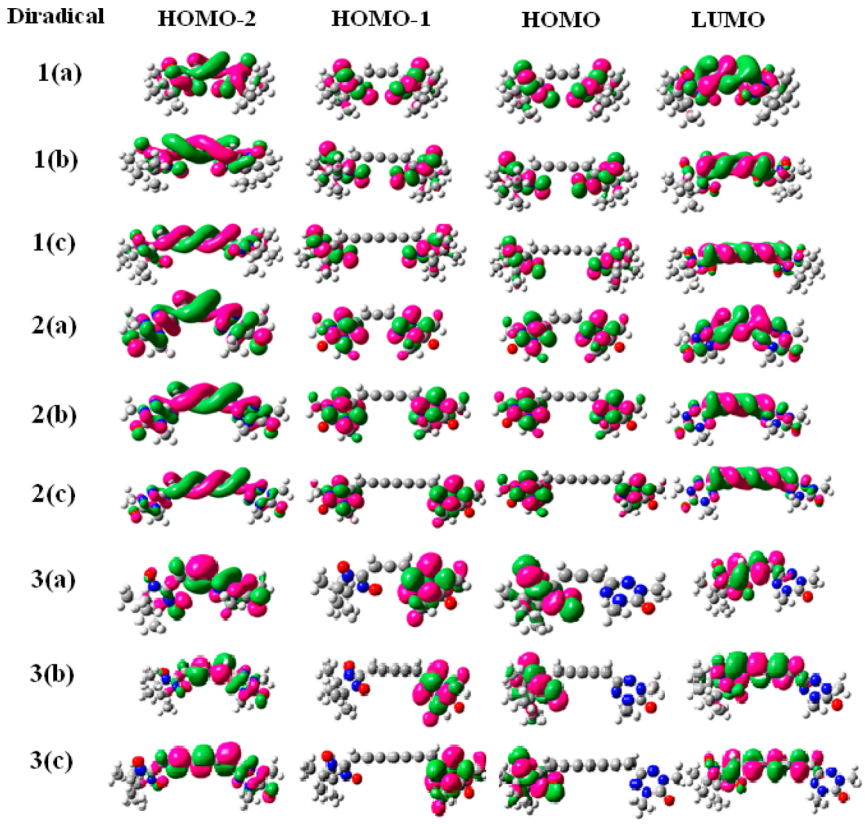

Figure 5. Spatial distribution of molecular orbitals of all the diradicals in their triplet states [B3LYP/6-311++G(d,p)] (iso value of 0.02), in which green and pink colors represent the different phase of the orbital coefficients.

Table 5. Energy Differences between SOMO1 $(HOMO)_\alpha$–SOMO2 $(HOMO-1)_\alpha$ (ΔE_{SS}) and $HOMO_\alpha$–$LUMO_\alpha$ (ΔE_{HL}) and Magnetic Exchange Coupling Constants (J) in Their Triplet State [B3LYP/6-311++G(d,p)]

system	ΔE_{SS} (eV)	ΔE_{HL} (eV)	J (cm^{-1})
1(a)	0.01	3.71	47.66
1(b)	0.00	3.03	99.09
1(c)	0.00	2.64	171.28
2(a)	0.02	4.14	15.30
2(b)	0.00	3.35	30.36
2(c)	0.00	2.85	53.17
3(a)	0.13	3.72	28.33
3(b)	0.13	3.00	55.84
3(c)	0.09	2.79	95.42

from the values listed in Table 5 that for series 1 and 2, the two SOMOs are almost degenerate, although they have different J values in each series. Another interesting point is that for diradicals 3(a) and 3(b) the SOMO–SOMO gap is largest and equal in magnitude but shows different J values. Therefore, the SOMO–SOMO gap is not the only guiding factor in determining the extent of magnetic interaction; there must be some other factor that guides magnetic exchange. In a couple of our recent works, we have found that the SOMO–SOMO gap is not responsible for the strength of magnetic coupling but rather that the HOMO–LUMO gap plays a more important role.[39,45,46] If we focus on the difference in energy between the HOMO and LUMO in this study, it has been found that upon going from the allene-based diradical to its higher homologue ([5]- and [7]-cumulene) in each series, there is a smooth decrease in the HOMO–LUMO energy gap. Hermann et al. also have shown that the α-HOMO–α-LUMO gap decreases with an increase in the carbon chain lengths of cumulene-based systems containing an even number of carbon centers.[38] Therefore, we can conclude that diradicals with a small HOMO–LUMO gap facilitate a strong magnetic coupling constant, and diradicals based on allene and cumulene couplers with a small HOMO–LUMO gap will be promising candidates for designing chiral organic magnetic molecules.

Our designed diradicals based on allene and [5]- and [7]-cumulene couplers (containing an odd number of carbon atoms) have two π-conjugations that are mutually perpendicular to each other. Imamura and Aoki have proposed that polyyne has two π-conjugated systems mutually perpendicular to each other and both the π-conjugations have a tendency to follow a bond alternation that is the origin of a competition between them.[47−49] With an increase in the length of the polyyne chain, a remarkable transition in the molecular structure takes place from an almost equidistant bond structure to an intensely alternating bond structure, which causes an increase in the HOMO level and a decrease in the LUMO level. As a result, there is a sudden decrease in the HOMO–LUMO gap with an increase in the length of the polyyne chains. The orbital phases of two mutually perpendicular π-conjugations for our designed diradicals are shown in Figure 6.

For our designed diradicals, $HOMO_\alpha$ and $(HOMO-1)_\alpha$ are the nonbonding molecular orbitals; therefore, the energy of LUMO decreases and the energy of HOMO−2 increases remarkably (shown in Figure 7), which satisfies the proposal of Imamura et al.[47−49] As a result, there is a decrease in the $HOMO_\alpha$–$LUMO_\alpha$ and $(HOMO-2)_\alpha$–$(HOMO-1)_\alpha$ energy gaps.

DOI: 10.1021/acs.joc.6b00943
J. Org. Chem. 2016, 81, 5623−5630

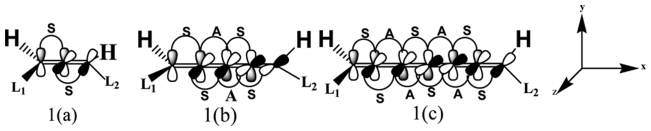

Figure 6. Structure of allene-based diradical and cumulene-based diradical with phases of HOMO−2. S indicates symmetric and A antisymmetric in the phase of MO. L_1 and L_2 are the left and right radical centers, respectively.

To determine the role of LUMO in the magnetic exchange coupling constant, we have computed the electron occupation in LUMO and HOMO−2 and SOMOs (Table 6).

From Table 6, we can see that LUMOs have a considerable amount of occupation. Therefore, we can assume that the LUMO takes part in the exchange mechanism. Here, we can see that in case of diradicals (c) in all series 1−3, the LUMO has the highest level of occupation in their respective series. The higher level of occupation in the LUMO favors strong intramolecular magnetic exchange coupling between the radical centers. Therefore, there is a correlation between the LUMO occupation and magnetic exchange coupling constant.

5. CONCLUSION

All the designed diradicals have ferromagnetic interaction that is strengthened upon addition of chiral centers within the coupler. Spin density distribution analysis shows that with an increase in the length of the coupler, enhancement of spin polarization along the coupler takes place and the probability of localizing the spin density on each chiral center increases. Addition of chiral centers within the coupler lowers the energy of LUMO; a smaller HOMO−LUMO gap facilitates a stronger magnetic coupling, and a higher magnetic exchange coupling constant (J) results. From natural orbital occupancies, we found that with an increase in the chain length of the chiral coupler the occupancy of LUMO increases. Furthermore, nonapplicability of Borden's rule indicates that a good way of predicting the ground state of the diradical systems having allene and [n]-cumulene coupler should be by Hund's rule-based spin density alternation. A close inspection of J values shows that NN stands for a better choice of radical center over VER and mixed radicals. Thereby, we expect that this trend might inspire synthetic chemists to synthesize NN-based chiral magnetic molecules with strong ferromagnetic interaction. The diradicals with an [n]-cumulene coupler with n being an even number will show antiferromagnetic behavior according to the spin alternation rule. These antiferromagnetic diradicals will be discussed elsewhere.

Table 6. Natural Orbital Occupation of the Diradicals in the Triplet State [B3LYP/6-311++G(d,p)]

system	HOMO−2	HOMO−1	HOMO	LUMO
1(a)	1.968	1.0	1.0	0.032
1(b)	1.952	1.0	1.0	0.048
1(c)	1.924	1.0	1.0	0.073
2(a)	1.990	1.0	1.0	0.009
2(b)	1.986	1.0	1.0	0.014
2(c)	1.980	1.0	1.0	0.020
3(a)	1.969	1.0	1.0	0.031
3(b)	1.954	1.0	1.0	0.046
3(c)	1.931	1.0	1.0	0.069

■ ASSOCIATED CONTENT

Supporting Information

The Supporting Information is available free of charge on the ACS Publications website at DOI: 10.1021/acs.joc.6b00943.

R and *S* configurations and VCD spectra of series 2 diradicals, exchange coupling constants of the enantiomers, energy and *J* values of the diradicals using different functionals (B3LYP and M06), spin density distribution using B3LYP, spatial distribution of molecular orbitals of the diradicals with varying geometries, molecular orbital of the diradicals in their broken symmetry state, energies of FMOs of all diradicals, and coordinates of the optimized geometries (PDF)

■ AUTHOR INFORMATION

Corresponding Author

*Phone: +91-9434228745. E-mail: anirbanmisra@yahoo.com.

Notes

The authors declare no competing financial interest.

■ ACKNOWLEDGMENTS

This work is supported by DST, India. S.S. is thankful to Sonderforschungsbereich 668, University of Hamburg, for a

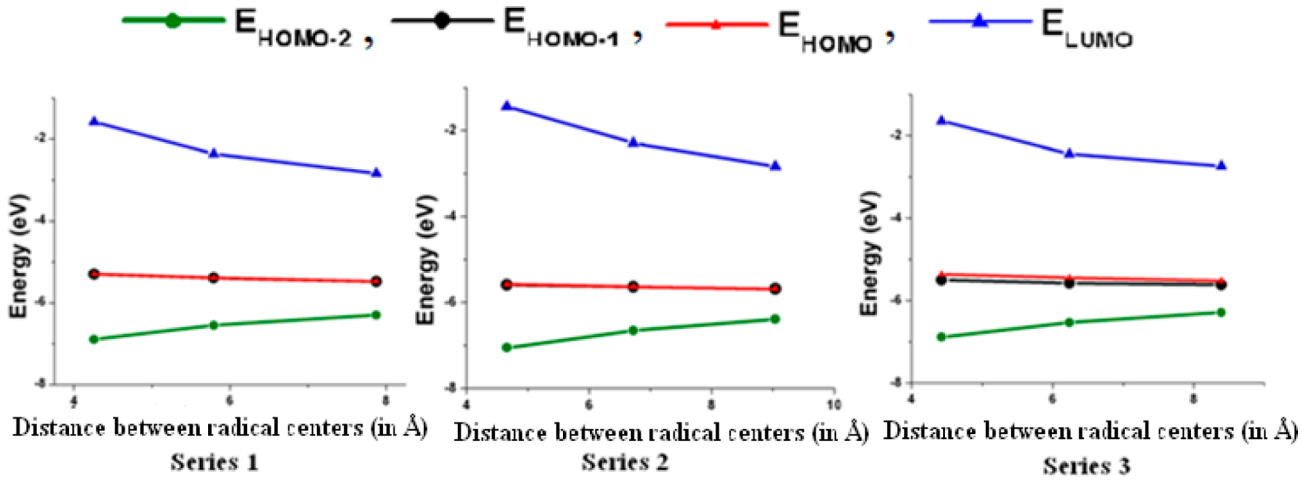

Figure 7. Plot of energy vs distance between radical centers for series 1−3 in their triplet state [B3LYP/6-311++g(d,p)].

DOI: 10.1021/acs.joc.6b00943
J. Org. Chem. 2016, 81, 5623−5630

postdoctoral fellowship. We are also thankful to the Hamburg regional computing center (RRZ) for computational resources.

REFERENCES

(1) Nguyen, L. A.; He, H.; Pham-Huy, C. *Int. J. Biomed. Sci.* **2006**, *2*, 85−100.
(2) Stephens, P. J.; Devlin, F. J.; Pan, J.-J. *Chirality* **2008**, *20*, 643−663.
(3) Galán-Mascarós, J. R.; Coronado, E.; Goddard, P. A.; Singleton, J.; Coldea, A. I.; Wallis, J. D.; Coles, S. J.; Alberola, A. *J. Am. Chem. Soc.* **2010**, *132*, 9271.
(4) Pappas, C. *Physics* **2012**, *5*, 28.
(5) Train, C.; Gheorghe, R.; Krstic, V.; Chamoreau, L.-M.; Ovanesyan, N. S.; Rikken, G. L. J. A.; Gruselle, M.; Verdaguer, M. *Nat. Mater.* **2008**, *7*, 729−734.
(6) Togawa, Y.; Koyama, T.; Takayanagi, K.; Mori, S.; Kousaka, Y.; Akimitsu, J.; Nishihara, S.; Inoue, K.; Ovchinnikov, A. S.; Kishine, J. *Phys. Rev. Lett.* **2012**, *108*, 107202.
(7) Wagnière, G. H. *Chem. Phys.* **1999**, *245*, 165−173.
(8) Bordács, S.; Kézsmárki, I.; Szaller, D.; Demko, L.; Kida, N.; Murakawa, H.; Onose, Y.; Shimano, R.; Rõõm, T.; Nagel, U.; Miyahara, S.; Furukawa, N.; Tokura, Y. *Nat. Phys.* **2012**, *8*, 734.
(9) Minguet, M.; Luneau, D.; Paulsen, C.; Lhotel, E.; Gorski, A.; Waluk, J.; Amabilino, D. B.; Veciana, J. *Polyhedron* **2003**, *22*, 2349−2354.
(10) (a) Ishikawa, I.; Tajima, K.; Bloch, D.; Roth, M. *Solid State Commun.* **1976**, *19*, 525−528. (b) Yu, X. Z.; Onose, Y.; Kanazawa, N.; Park, J. H.; Han, J. H.; Matsui, Y.; Nagaosa, N.; Tokura, Y. *Nature* **2010**, *465*, 901−904.
(11) Kahn, O. *Molecular Magnetism*; VCH: New York, 1993.
(12) Coronado, E.; Delhaè, P.; Gatteschi, D. *Molecular magnetism: From molecular assemblies to devices*; Miller, J. S., Ed.; NATO ASI Series E321; Kluwer: Dordrecht, The Netherlands, 1996; Vol. *321*.
(13) Benelli, C.; Gatteschi, D. *Chem. Rev.* **2002**, *102*, 2369−2387.
(14) Lahti, P. M. *Magnetic Properties of Organic Materials*; Marcel Dekker: New York, 1999.
(15) (a) Kobayashi, H.; Kobayashi, A.; Cassoux, P. *Chem. Soc. Rev.* **2000**, *29*, 325−333. (b) Uji, S.; Shinagawa, H.; Terashima, T.; Yakabe, T.; Terai, Y.; Tokumoto, M.; Kobayashi, A.; Tanaka, H.; Kobayashi, H. *Nature* **2001**, *410*, 908−910.
(16) (a) Prinz, G. A. *Science* **1998**, *282*, 1660−1663. (b) Emberly, E. G.; Kirczenow, G. *Chem. Phys.* **2002**, *281*, 311−324.
(17) (a) Matsuda, K.; Matsuo, M.; Irie, M. *J. Org. Chem.* **2001**, *66*, 8799−8803. (b) Tanifuji, N.; Irie, M.; Matsuda, K. *J. Am. Chem. Soc.* **2005**, *127*, 13344−13353.
(18) (a) Bhattacharya, D.; Misra, A. *J. Phys. Chem. A* **2009**, *113*, 5470−5475. (b) Bhattacharya, D.; Shil, S.; Misra, A.; Klein, D. J. *Theor. Chem. Acc.* **2010**, *127*, 57−67. (c) Bhattacharya, D.; Shil, S.; Panda, A.; Misra, A. *J. Phys. Chem. A* **2010**, *114*, 11833−11841.
(19) Ali, Md. E.; Datta, S. N. *J. Phys. Chem. A* **2006**, *110*, 2776−2784.
(20) (a) Tobe, Y.; Wakabayashi, T. In *Acetylene Chemistry: Chemistry, Biology, and Material Science*; Diederich, F., Stang, P. J., Tykwinski, R. R., Eds.; Wiley-VCH: Weinheim, Germany, 2005; pp 387−426. (b) Chalifoux, W. A.; Tykwinski, R. R. *Chem. Rec.* **2006**, *6*, 169−182. (c) Shi Shun, A. L. K.; Tykwinski, R. R. *Angew. Chem., Int. Ed.* **2006**, *45*, 1034−1057. (d) Raton, B. *Polyynes: Synthesis, Properties, and Applications*; Cataldo, F., Ed.; Taylor & Francis: Boca Raton, FL, 2005.
(21) Taylor, D. R. *Chem. Rev.* **1967**, *67*, 317.
(22) Hendon, C. H.; Tiana, D.; Murray, A. T.; Carbery, D. R.; Walsh, A. *Chem. Sci.* **2013**, *4*, 4278−4284.
(23) Skibar, W.; Kopacka, H.; Wurst, K.; Salzmann, C.; Ongania, K. H.; Fabrizi de Biani, F.; Zanello, P.; Bildstein, B. *Organometallics* **2004**, *23*, 1024−1041.
(24) (a) Januszewski, J. A.; Tykwinski, R. R. *Chem. Soc. Rev.* **2014**, *43*, 3184−3203. (b) Januszewski, J. A.; Wendinger, D.; Methfessel, C. D.; Hampel, F.; Tykwinski, R. R. *Angew. Chem., Int. Ed.* **2013**, *52*, 1817−1821.
(25) Gu, X.; Kaiser, R. I.; Mebel, A. M. *ChemPhysChem* **2008**, *9*, 350−369.
(26) Prasongkit, J.; Grigoriev, A.; Wendin, G.; Ahuja, R. *Phys. Rev. B: Condens. Matter Mater. Phys.* **2010**, *81*, 115404.
(27) Noodleman, L. *J. Chem. Phys.* **1981**, *74*, 5737−5743.
(28) Noodleman, L.; Baerends, E. J. *J. Am. Chem. Soc.* **1984**, *106*, 2316−2327.
(29) Noodleman, L.; Davidson, E. R. *Chem. Phys.* **1986**, *109*, 131−143.
(30) Noodleman, L.; Peng, C. Y.; Case, D. A.; Mouesca, J.-M. *Coord. Chem. Rev.* **1995**, *144*, 199−244.
(31) Yamaguchi, K.; Fukui, H.; Fueno, T. *Chem. Lett.* **1986**, *15*, 625−628.
(32) Yamaguchi, K.; Takahara, Y.; Fueno, T.; Nasu, K. *Jpn. J. Appl. Phys.* **1987**, *26*, L1362−L1364.
(33) Yamaguchi, K.; Jensen, F.; Dorigo, A.; Houk, K. N. *Chem. Phys. Lett.* **1988**, *149*, 537−542.
(34) Yamaguchi, K.; Takahara, Y.; Fueno, T.; Houk, K. N. *Theor. Chim.Acta* **1988**, *73*, 337−364.
(35) Frisch, M. J.; Trucks, G. W.; Schlegel, H. B.; Scuseria, G. E.; Robb, M. A.; Cheeseman, J. R.; Scalmani, G.; Barone, V.; Mennucci, B.; Petersson, G. A.; Nakatsuji, H.; Caricato, M.; Li, X.; Hratchian, H. P.; Izmaylov, A. F.; Bloino, J.; Zheng, G.; Sonnenberg, J. L.; Hada, M.; Ehara, M.; Toyota, K.; Fukuda, R.; Hasegawa, J.; Ishida, M.; Nakajima, T.; Honda, Y.; Kitao, O.; Nakai, H.; Vreven, T.; Montgomery, J. A., Jr.; Peralta, J. E.; Ogliaro, F.; Bearpark, M.; Heyd, J. J.; Brothers, E.; Kudin, K. N.; Staroverov, V. N.; Kobayashi, R.; Normand, J.; Raghavachari, K.; Rendell, A.; Burant, J. C.; Iyengar, S. S.; Tomasi, J.; Cossi, M.; Rega, N.; Millam, M. J.; Klene, M.; Knox, J. E.; Cross, J. B.; Bakken, V.; Adamo, C.; Jaramillo, J.; Gomperts, R.; Stratmann, R. E.; Yazyev, O.; Austin, A. J.; Cammi, R.; Pomelli, C.; Ochterski, J. W.; Martin, R. L.; Morokuma, K.; Zakrzewski, V. G.; Voth, G. A.; Salvador, P.; Dannenberg, J. J.; Dapprich, S.; Daniels, A. D.; Farkas, Ö.; Foresman, J. B.; Ortiz, J. V.; Cioslowski, J.; Fox, D. J. *Gaussian09*; Gaussian, Inc.: Wallingford, CT, 2009.
(36) Trindle, C.; Nath Datta, S. N. *Int. J. Quantum Chem.* **1996**, *57*, 781−799.
(37) Trindle, C.; Datta, S. N.; Mallik, B. *J. Am. Chem. Soc.* **1997**, *119*, 12947−12951.
(38) Herrmann, C.; Neugebauer, J.; Gladysz, J. A.; Reiher, M. *Inorg. Chem.* **2005**, *44*, 6174−6182.
(39) Shil, S.; Herrmann, C. *Inorg. Chem.* **2015**, *54*, 11733−11740.
(40) Browne, W. R.; Hage, R.; Vos, J. G. *Coord. Chem. Rev.* **2006**, *250*, 1653−1668.
(41) Borden, W. T.; Davidson, E. R. *J. Am. Chem. Soc.* **1977**, *99*, 4587−4594.
(42) Borden, W. T.; Davidson, E. R. *Acc. Chem. Res.* **1981**, *14*, 69−76.
(43) Constantinides, C. P.; Koutentis, P. A.; Schatz, J. *J. Am. Chem. Soc.* **2004**, *126*, 16232−16241.
(44) Zhang, G.; Li, S.; Jiang, Y. *J. Phys. Chem. A* **2003**, *107*, 5573−5582.
(45) Shil, S.; Roy, M.; Misra, A. *RSC Adv.* **2015**, *5*, 105574−105582.
(46) Bhattacharya, D.; Shil, S.; Misra, A.; Bytautas, L.; Klein, D. J. *Phys. Chem. Chem. Phys.* **2015**, *17*, 14223−14237.
(47) Aoki, Y.; Imamura, A. *J. Chem. Phys.* **1995**, *103*, 9726.
(48) Imamura, A.; Aoki, Y. *Int. J. Quantum Chem.* **2006**, *106*, 1924−1933.
(49) Imamura, A.; Aoki, Y. *Int. J. Quantum Chem.* **2013**, *113*, 423−427.

DOI: 10.1021/acs.joc.6b00943
J. Org. Chem. 2016, 81, 5623−5630

PCCP

PAPER

View Article Online
View Journal | View Issue

Check for updates

Cite this: *Phys. Chem. Chem. Phys.*, 2018, **20**, 9364

Magnetic and transport properties of conjugated and cumulated molecules: the π-system enlightens part of the story†

Prodipta Sarbadhikary,[a] Suranjan Shil [b] and Anirban Misra *[a]

Received 7th September 2017,
Accepted 2nd March 2018

DOI: 10.1039/c7cp06113g

rsc.li/pccp

We have investigated the intramolecular magnetic exchange coupling constants (*J*) for a series of nitronyl nitroxide diradicals connected by a range of linear conjugated and cumulene couplers focusing on the unusual π-interaction properties within the couplers. Distance between radical centers, spin density within the couplers, as well as the dihedral angles between the radical centers and the plane of the coupler influence the strength of magnetic coupling. We also establish that with the increase in the length of the coupler, the strength of magnetic interaction in conjugated and cumulated systems varies in a different way. Transport calculations show that with the increase in chain length, diradicals based on cumulene containing an even number of carbon atoms act as better conductors than cumulenes with an odd number of carbon atoms. It is also observed that with the increase in the length of the conjugated coupler based diradicals, transmission does not vary in a sequential way.

Published on 06 March 2018. Downloaded by University of North Bengal on 10/30/2019 8:59:40 AM.

1. Introduction

The magnetic interactions of organic radicals[1] and methods of controlling their magnetic properties have been widely investigated for their potential applications in the field of magnetism,[2] superconductivity,[3,4] photomagnetism,[5,6] spintronics[7,8] including their use in spin field effect transistors, magnetic semiconductors, spin-polarized light-emitting diodes, spin valves, and so on.[9–12] On the other hand, tunable molecular wires that reconcile electronic communication,[13] energy transfer,[14] electron transfer,[15] charge transport,[16] *etc.* have been sparkles in the eye of theoreticians and experimentalists.[17]

Spintronic elements whose transport properties are governed by antiferromagnetic interactions are also known.[18] Much efforts have been devoted over the past decades to the design and synthesis of π-conjugated molecular wires[19] (containing delocalized electrons) and it is a persistent challenge in molecular electronics to control the conductance and current flow through such systems. Getting high conductance is also of interest in the distance-dependent attenuation of electron transfer and transport.[20–22]

Among all carbon nanostructures, linear chains of carbon atoms have been predicted to have excellent properties for various transport related applications.[23–25] It is found that chains containing sp-hybridized carbon atoms are fascinating due to their unique linear structure and interesting physical properties.[26–29] Recently allenes have acquired major attraction as their reactivity and selectivity can be simply tuned by varying their electronic and steric effects with appropriate substituents.[30,31] Zhang *et al.* have shown that cumulenes act as semiconductors and polyynes as metallic monatomic chains by their rigidity, and these properties make them promising for applications in nanotechnology.[32] Cumulenes and their substituted counterparts have also been used as elements for nonlinear optics, molecular sensors,[33] molecular machines (nanomechanics),[34] and molecular wires (nano-electronics, which is an emerging field in structural chemistry). Skibar *et al.*[35] and Januszewski *et al.*[36,37] have synthesized and predicted the properties of long cumulene systems.

The magnetic interaction between two radical centers generally depends on the distance and the nature of the couplers.[38–42] The π-interaction as well as the spin-polarization through the coupler plays a major role in controlling the magnitude and sign of the coupling constant.[43] An estimation of the exchange coupling constant is necessary before synthesizing a successful organic magnetic material based on organic diradicals.

[a] *Department of Chemistry, University of North Bengal, Dist-Darjeeling 734013, India. E-mail: anirbanmisra@yahoo.com; Tel: +91-9434228745*
[b] *Center for Atomic-scale Materials Design (CAMD), Department of Physics, Technical University of Denmark, Fysikvej, Bld. 307, 2800 Kgs, Lyngby, Denmark*

† Electronic supplementary information (ESI) available: The exchange coupling constant and the energy of the diradicals using B3LYP, B3LYP-D, CAM-B3LYP, singlet and triplet weightings, bond angle for the couplers, spin density distribution on coupler using B3LYP, Transmission spectra of all the diradical based molecular wires (for β spin), energy of FMOs of all diradicals, bond distance between two neighboring atoms of all the molecular wires used in transport calculations, the coordinates of the optimized geometries and the coordinates of the molecular wires used for transport calculations are available. See DOI: 10.1039/c7cp06113g

This journal is © the Owner Societies 2018

Published on 06 March 2018. Downloaded by University of North Bengal on 10/30/2019 8:59:40 AM.

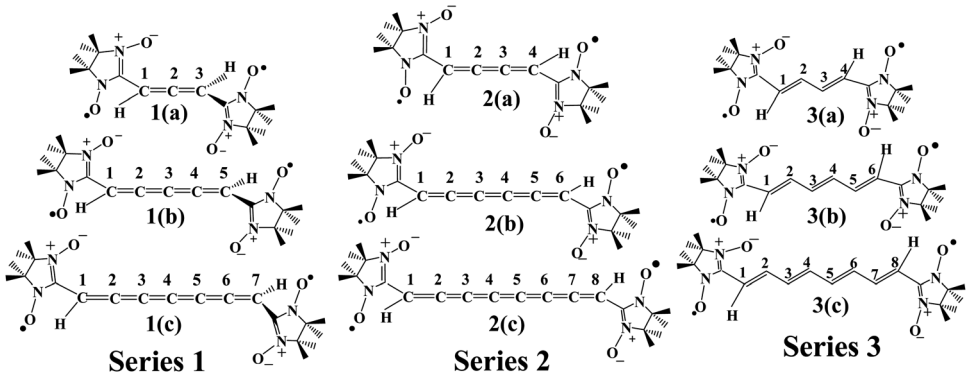

Fig. 1 Designed diradicals based on allene, cumulene and the conjugated couplers. Series 1 represents allene and cumulene based diradicals containing an odd number of carbon atoms, series 2 represents cumulene based diradicals containing an even number of carbon atoms, and series 3 represents diradicals based on conjugated systems.

There are many systematic studies on the intramolecular magnetic coupling constants for organic diradicals linking with various couplers.[44–54] Recently we have studied the anomalous magnetic property of diradicals based on chiral allene and cumulene couplers (containing an odd number of carbon atoms) where the π-orbitals at both ends of the coupler are perpendicular to each other and may be used as building blocks for chiral magnets.[55] For cumulenes containing an even number of carbon atoms, the π-orbitals at both ends of the cumulene chain are parallel to each other and hence have a different electronic structure compared to that of odd cumulenes. On the other hand, conjugated systems have alternating double bonds. Therefore, as a continuation of our previous work,[55] we are motivated to investigate the effect of unusual π-interaction of cumulene based diradicals containing an even number of carbon atoms as well as diradicals based on conjugated systems (shown in Fig. 1) on the magnetic properties, as this will provide completeness to this study. We use nitronyl nitroxide radicals as radical sources where the unpaired spin comes from the –NO group of the nitronyl nitroxide moiety.[56] In addition to that we also study the coherent electronic transport characteristics of cumulene based diradicals (with both odd and even number of carbon atoms) and the conjugated couplers.

2. Theoretical background and computational strategy

The magnetic exchange interaction between two magnetic sites 1 and 2 is normally expressed by the Heisenberg spin Hamiltonian $\hat{H} = -2J\hat{S}\cdot\hat{S}_2$, where $\hat{S}_1$ and $\hat{S}_2$ are the respective spin angular momentum operators and J is the effective exchange coupling constant between two magnetic sites. The positive sign of J means the coupling is ferromagnetic and the high-spin state is the lower energy state. A negative value of J is representative of antiferromagnetic interaction in the diradical and a low-spin state is the ground state. For a diradical having a single unpaired electron on each site, J can be represented as $E_{(S=1)} - E_{(S=0)} = -2J$.

Multi-configuration approaches are appropriate to describe pure spin states in a proper manner, but these methods are resource intensive and are not used in this work. To circumvent this issue, the Broken symmetry (BS) approach proposed by Noodleman *et al.*[57–60] in the DFT framework is a more useful alternative to evaluate J which can ultimately lead to an estimation of the energy of diradical singlets. The limiting form of the BS state is a weighted average of the singlet and the triplet, and has $M_S = 0$. The ideal triplet (T) state has an $\langle S^2\rangle = 2$, whereas $\langle S^2\rangle = 1$ in the ideal BS state and that results in $E(\mathrm{BS}) - E(\mathrm{T}) = J$. However in the actual calculation approximate $\langle S^2\rangle$ values are obtained, and hence BS solution is often found to be spin contaminated. Therefore, a correction is needed to calculate the coupling constant. The spin projected formula given by Yamaguchi[61–64] for the estimation of the magnetic exchange coupling constant (J) is capable of taking such spin contamination into account and is applicable for both low and high overlaps between magnetic orbitals, and it can be written as $J = (E_{\mathrm{BS}} - E_{\mathrm{HS}})/(\langle S^2\rangle_{\mathrm{HS}} - \langle S^2\rangle_{\mathrm{BS}})$, where E_{BS}, E_{HS} and $\langle S^2\rangle_{\mathrm{BS}}$, $\langle S^2\rangle_{\mathrm{HS}}$ are the energy and average spin square values for the corresponding BS and high-spin states.

All calculations related to magnetic properties have been done using the Gaussian09 package.[65] The popular B3LYP exchange–correlation potential was used in combination with the 6-311++G(d,p) basis set within the unrestricted formalism for all geometry optimizations. The frequency calculation gives positive values for all these systems which confirms that the geometries are in local minima. To obtain open shell broken symmetry (BS) singlet solution ''guess = (read, mix)'' keyword is used for mixing of the HOMO and the LUMO. The magnetic exchange coupling constant (J) value for each molecule has been estimated from the energies of triplet and BS states at the same level of theory using the spin projected formula given by Yamaguchi.

B3LYP is a well-tested and widely used functional but it lacks dispersion correction and long range correction. We therefore compute the magnetic exchange coupling constant of our designed systems with dispersion corrected B3LYP (B3LYP-D) (given in Tables S1, S4, and S7, ESI†) and to include long range correction we use CAM-B3LYP (given in Tables S2, S5, and S8, ESI†).

Published on 06 March 2018. Downloaded by University of North Bengal on 10/30/2019 8:59:40 AM.

We found that there is no qualitative change of the magnetic exchange coupling constant due to dispersion correction and long range correction in the functional. All the functionals give qualitatively consistent results except the CAM-B3LYP functional which gives average spin square values far from 1 to the BS solution. Considering all these facts, we stick to the B3LYP functional for rest of the calculations.

In the coherent tunnelling regime the finite bias current ($I_s(V)$) conduction of electron spins through a gold–molecule–gold junction can be calculated by the following equation:

$$I_s(V) = \frac{e}{h}\int_{E_F-eV/2}^{E_F+eV/2} dE T_S(E, V) \quad (1)$$

where V is the finite bias voltage, E_F is the Fermi energy, E is the energy and $T_S(E,V)$ is the transmission function. In the Landauer–Imry–Büttiker approximation,[66] the zero voltage conductance, *i.e.*, $(dI/dV)_{V=0}$, is proportional to $T(E_F)$. Therefore, it is reasonable to take integration over $E_F - \frac{eV}{2}$ to $E_F + \frac{eV}{2}$. The T_s can be calculated from the retarded ($\Gamma_{L/R,s}$) and advanced ($G_{C,sr/a}$) Green's function of the electrode–molecule–electrode system as

$$T_s(E,V) = \mathrm{tr}(\Gamma_{R,s} G^r_{L,s} \Gamma_{L,s} G^a_{C,s}) \quad (2)$$

The detailed theoretical approach we use here can be found in ref. 67 and 68.

In order to obtain the transport properties of all the designed systems, instead of simply considering the prototypical diradical based on cumulene and conjugated couplers, we add a polyacetylene chain (spacer groups, containing 4 carbon atoms), ensuring that there is no considerable interaction between the electrodes and any atom of the radical sites. The dithiol (obtained by replacing two end hydrogen atoms of the polyyne chain by a –SH group) molecule has been optimized and then the hydrogen atoms are stripped off and the resulting neutral dithiolate is placed between two electrodes (shown in Fig. 2). Each electrode consists of nine gold atoms that are organized as a six-atom triangular fcc-gold (111)-surface connected to the molecule, with a second layer having three gold atoms. The bond length between sulfur and Au(111) surface has been chosen to be 2.48 Å and the Au–Au distance as 2.88 Å as in

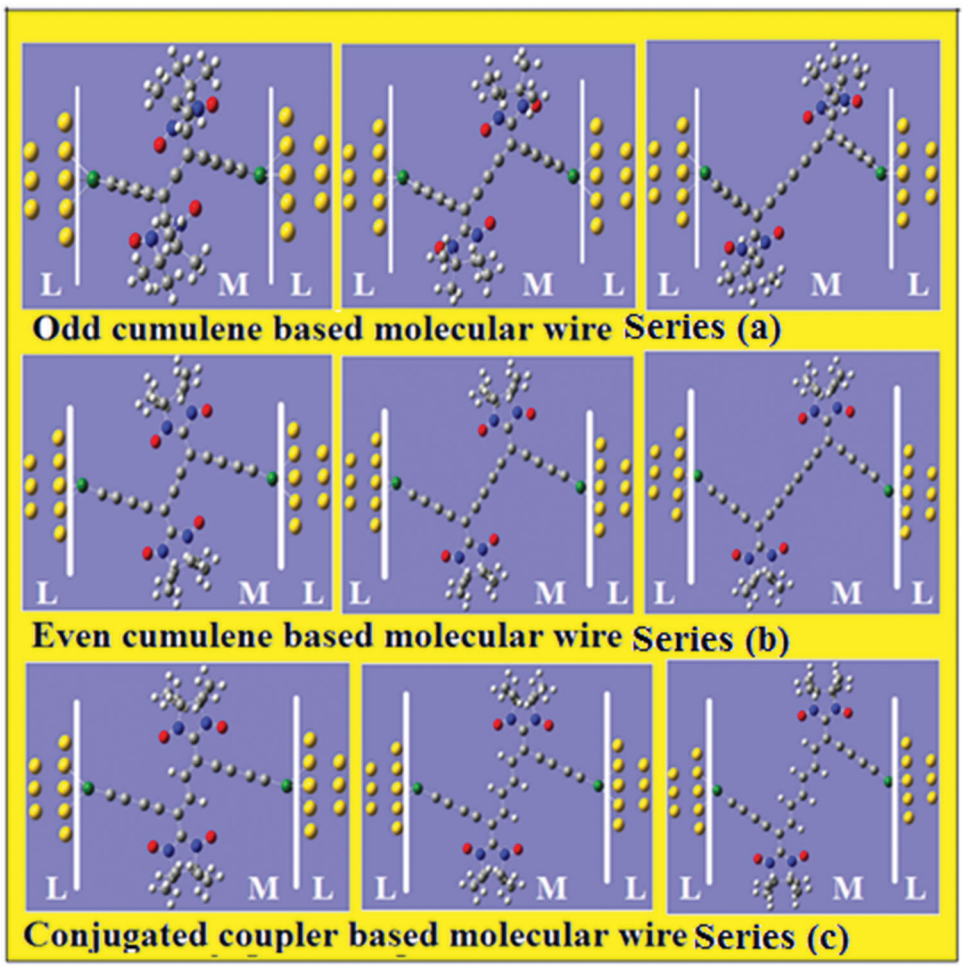

Fig. 2 Designed diradical based systems on which transport calculations have been carried out (L stands for lead and M stands for molecule; grey, white, red, blue, yellow and green colors represent carbon, hydrogen, oxygen, nitrogen, gold and sulfur atoms respectively). Part (a) represents odd cumulene based molecular wires, part (b) represents even cumulene based molecular wires and part (c) represents conjugated coupler based molecular wires.

 This journal is © the Owner Societies 2018

Published on 06 March 2018. Downloaded by University of North Bengal on 10/30/2019 8:59:40 AM.

extended gold crystals. Fock and overlap matrices required for the transport calculations are achieved by a single point calculation in the GAUSSIAN09 program package.[65] For the transport calculation we employ the B3LYP functional and the LANL2DZ basis set to avoid ghost transmission.[67] Basis sets of triple-zeta quality or higher sometimes give artificially high transmission and possibly may give wrong conclusions about chemical trends. In such cases, transport persists when molecular atoms are substituted by basis functions alone (called "ghost atoms"). It is tested that the basis set of double zeta quality without polarization functions (*e.g.* Lanl2dz) gives negligible ghost transmission. This observation has been systematically studied by Herrmann and co-workers given in ref. 67.

In order to obtain the transport properties, the designed systems have been divided into three subsystems: gold-cluster–dithiolate–gold-cluster as illustrated in Fig. 2. We have calculated the transmission property using the ARTAIOS code developed by Herrmann *et al.*[67,68]

3. Results and discussion

Magnetic exchange coupling constant

The calculation of J yields ferromagnetic interaction for linkers with an odd number of carbon atoms,[55] while antiferromagnetic coupling is predicted for diradicals connected by linkers with an even number of carbon atoms (Fig. 3; see Tables S1–S8, ESI†). The net weights of singlet and triplet components in the BS solution are given in Tables S9–S11, ESI†. Fig. 3 shows that an increase in the number of carbon atoms from an odd cumulene connector to an even cumulene connector causes a great contrast in magnitude as well as a change in the sign of the magnetic exchange coupling constant values. It is observed that with the increase in the number of carbon atoms of the coupler, the magnitude of J increases for both the series of odd and even cumulene based diradicals [the increase of J through the odd cumulene based diradical series is almost twice from 1(a) to 1(b) and from 1(b) to 1(c)],[55] while for conjugated couplers, the magnitude of the J value decreases gradually. Therefore cumulenes with an even number of carbon atoms show an increase in the coupling constant value with the increase in the distance between two radical centers, though an opposite result is normally expected keeping parity with the conjugated systems. Thus together with the previous work[55] it provides completeness to this particular study. Therefore, it can be argued that there must be a major contribution of the π-interaction of the couplers in magnetic exchange pathways and this observation demands a detailed investigation of the electronic structure of these couplers.

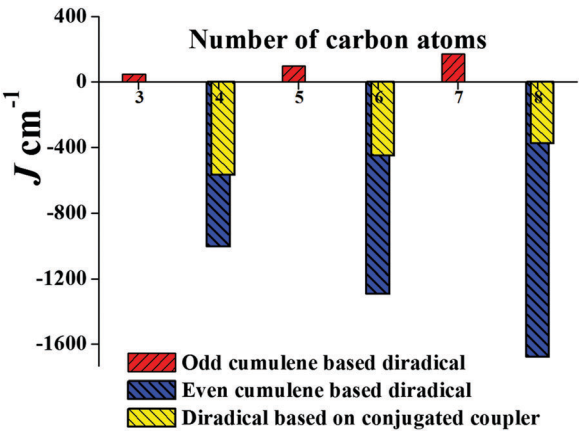

Fig. 3 Plot of magnetic exchange coupling constant J (in cm^{-1}) *vs.* number of carbon atoms within the coupler (using B3LYP/6-311++G(d,p)). The red color represents the coupling constant for the odd cumulene based diradical (series 1), the blue color represents the even cumulene based diradical (series 2), and the yellow color represents the diradical based on a conjugated coupler (series 3).

Factors affecting magnetic exchange coupling

The magnetic interaction depends on the distance r between the magnetic centers as $\exp(-r)$;[69] therefore for our designed systems one may expect a decrease in the coupling constant value with the increase in the number of carbon atoms within the coupler (as the distance between radical centers also increases as given in Table 1). But for the odd-numbered cumulene series (1(a), 1(b), and 1(c)), the coupling constant is positive and increases in magnitude with the increase in the number of carbon atoms in the cumulene chain (shown in Fig. 4). The relation is almost perfectly linear (R^2 = 0.99, from regression analysis).

For even numbered cumulenes (2(a), (b), and (c)) the coupling constant shows a linear relationship with the increase in the number of carbon atoms in the cumulene chain (shown in Fig. 5), but is negative and larger in magnitude. For the even cumulene series, the relation is almost perfectly linear ($R^2 > 0.99$ from regression analysis).

Polo *et al.* have shown that the magnitude of J depends strongly on the planarity of the molecular structure of the diradical as more effective orbital overlap between the π-systems can thus be reached.[70] Shil *et al.* have also shown that when the coupler and the radical centers are in different planes, coupling between them decreases.[71] We have previously reported[55] that the delocalization of the π-electrons affects the spin density which controls the exchange coupling constant for odd cumulene based diradicals. Therefore, there are different factors (such as the distance between radical centers, spin polarization pathways, and the planarity of the molecular structure of the diradical), which controls the values of J and make it difficult to predict the value and nature of J.

(i) Distance between radical centers r (in Å). From Table 1 it is clear that continuing from the smaller coupler to its higher homologues in each series, the distance between radical centers increases as expected. Therefore there should be a decrease in J values from smaller to the larger coupler as discussed earlier.[69] This trend is observed in the conjugated systems of series 3, but for cumulene couplers of series 1 and series 2, an opposite result is found. This result clearly indicates that the magnitude of the coupling constant values not only depends on the distance between the radical centers but also depends on other factors which are discussed under subsequent points.

Published on 06 March 2018. Downloaded by University of North Bengal on 10/30/2019 8:59:40 AM.

Table 1 Distance between radical centers r (in Å) (using B3LYP/6-311++G(d,p))

System	r (in Å)	Coupling constant (J cm^{-1})	System	R (in Å)	Coupling constant (J cm^{-1})	System	r (in Å)	Coupling constant (J cm^{-1})
1(a)	4.256	47.66	2(a)	6.407	−1003.86	3(a)	6.989	−565.03
1(b)	5.790	99.09	2(b)	7.869	−1291.24	3(b)	9.263	−450.12
1(c)	7.873	171.28	2(c)	9.815	−1678.7	3(c)	11.391	−373.53

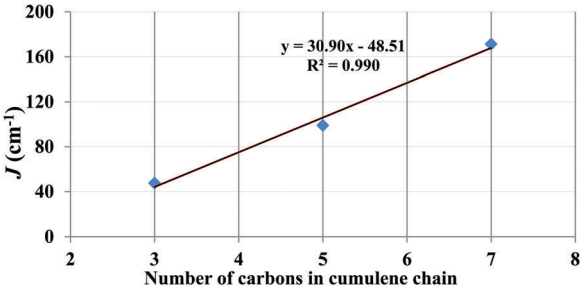

Fig. 4 Plot of J (cm^{-1}) *vs.* number of carbon atoms in the cumulene chain (regression analysis) for the odd cumulene series (1(a), 1(b), and 1(c)) (using B3LYP/6-311++G(d,p)).

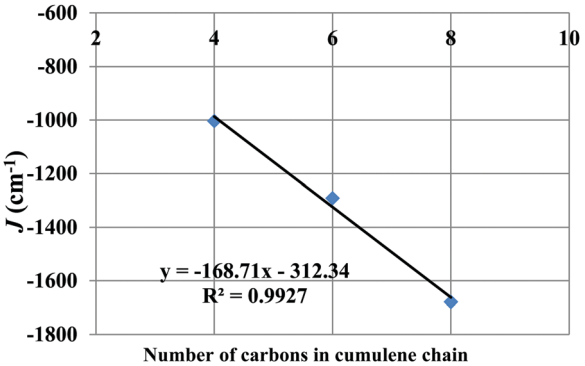

Fig. 5 Plot of J (cm^{-1}) *vs.* number of carbon atoms in the cumulene chain (regression analysis) for the even cumulene series (2(a), (b), and (c)) (using B3LYP/6-311++G(d,p)).

(ii) Spin density distribution on the coupler. The spin density of the DFT based approach gives us an insight into the spin polarization mechanism for magnetic exchange coupling within the molecule. Hermann *et al.* have proposed that for cumulene systems (with an even number of carbon centers), the spin delocalization onto the chain increases as the length of the chain gets longer.[72] From the spin density distribution plot of Fig. 6 it is observed that for even cumulene based diradicals there is an accumulation of excess spin density on all the middle carbon atoms of the coupler, *i.e.*, along the y and z direction collectively (represented by the red arrow). From Table 2 it is clear that the spin density on each carbon of the coupler and the average spin density increase with the increase in the length of the coupler. In our previous work we have shown that for odd cumulene based diradicals, a large accumulation of spin density within the coupler occurs due to the presence of two π-electrons at a time on each sp-carbon atom of the coupler,[55] and this also occurs for even cumulene based diradicals.

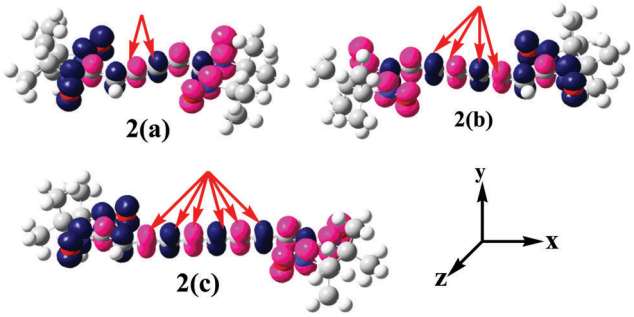

Fig. 6 Spin density plot for the even cumulene based diradicals (series 2) in their BS states (B3LYP/6-311++G(d,p)) (iso value 0.004); magenta and blue colors represent the α and β spins respectively. The red arrow represents the carbons with excess spin density.

But in the case of conjugated systems the spin density of the coupler is distributed in one direction only *i.e.*, along the y direction only (shown in Fig. 7), and with the increase in the length of the coupler, a decrease in average spin density is observed from Table 3. Therefore, spin density is one of the major factors that results in an ultimate increase in J values for diradicals based on cumulene systems and in a decrease for diradicals based on conjugated couplers with the increase in the number of carbon atoms of the coupler.

(iii) Dihedral angle. The cumulenes – (C_n) – (where n is either an even or odd number of carbon atoms) have two orthogonal π-systems, while the conjugated systems – $(HC{=}CH)_k$ – have only one π-orbital (with k taking values 2, 3, and 4). For cumulene systems with nitronyl nitroxide end groups, the two types of perpendicular π-interactions are represented by red and blue arrows (Fig. 8(a) and (b)), whereas for conjugated systems only one π-interaction is shown by the blue arrow (Fig. 8(c)). In odd cumulene based diradicals (Fig. 8(a)), the extent of π-interaction between the cumulene chain and the radical end groups is lower compared to the π-interaction in even cumulene based diradicals (Fig. 8(b)). This is because for odd cumulenes, each type of π-interaction (represented by red/blue arrows in Fig. 8(a)) can conjugate with one radical site at a time but not with both radical end groups (as the two radical centers are not in the same plane). But for even cumulene systems (Fig. 8(b)), among the two π-interactions of the cumulene chain, one π-system (the π-interaction is represented by the blue arrow) extends the length of the cumulene skeleton and can conjugate with both sides of end groups (Fig. 8(b), where the two radical centers are in the same plane).[36] Therefore for odd cumulene based diradicals, the perpendicular plane between two radical centers causes a small magnitude of coupling constant, but for even cumulene based diradicals, the planarity of two radical centers causes large magnitude of coupling constant values.

 This journal is © the Owner Societies 2018

Published on 06 March 2018. Downloaded by University of North Bengal on 10/30/2019 8:59:40 AM.

Table 2 Spin density distribution on each atom of the coupler of even cumulene-based diradicals in their BS state (B3LYP/6-311++G(d,p))

	Spin density on different atoms of the coupler								
Systems	C1	C2	C3	C4	C5	C6	C7	C8	Average spin density on each atom of the coupler
2(a)	0.2260	−0.2082	0.2082	−0.2260	—	—	—	—	0.2171
2(b)	0.2407	−0.2274	0.2484	−0.2484	0.2274	−0.2407	—	—	0.2388
2(c)	0.2630	−0.2510	0.2620	−0.2123	0.2123	−0.2619	0.2510	−0.2630	0.2471

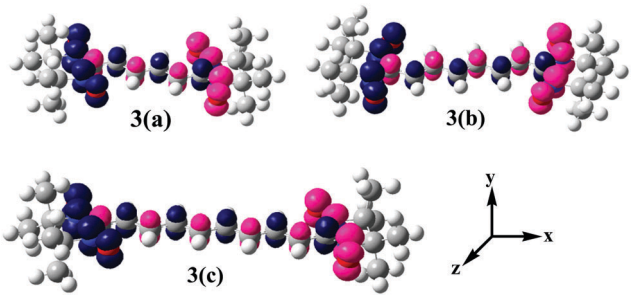

Fig. 7 Spin density plot for the diradical based conjugated systems (series 3) in their BS states (B3LYP/6-311++G(d,p)) (iso value 0.004); magenta and blue colors represent the α and β spins respectively.

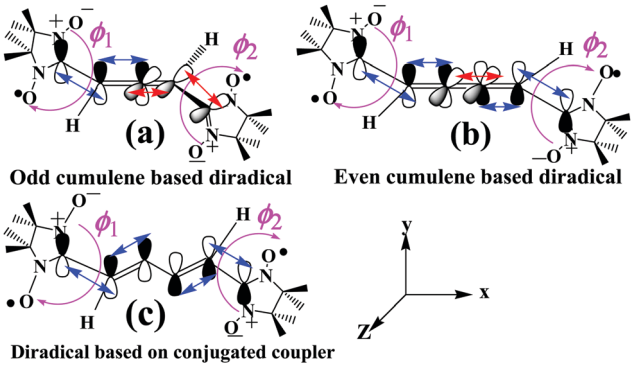

Fig. 8 π-interaction of diradicals based on cumulene and conjugated couplers. φ_1 and φ_2 denote the dihedral angle between the plane of the coupler and that of the nitronyl nitroxide radicals (the blue arrow represents one π-interaction (*i.e.*, overlap between p_y–p_y orbitals) and the red arrow represents another π-interaction (*i.e.*, p_z–p_z orbitals)). We have taken a representative figure from each series. Part (a) represents π-interaction of odd cumulene based diradicals, part (b) represents π-interaction of even cumulene based diradicals, and part (c) represents π-interaction of diradicals based on conjugated systems.

For even cumulene couplers, as the distance between radical sites increases the interaction may be expected to decline. However the increase in average spin density within the cumulene connector enhances the interaction. The net effect is small. For diradicals based on conjugated couplers, there is only one π-interaction that can conjugate with both sets of end groups (shown in Fig. 8(c)), but the increase in the distance as well as the decrease in spin density within the coupler causes an overall decrease in the *J* value with the increase in the chain length of the coupler. Therefore, as a whole the π-interaction is the enlightening factor that controls the magnetic property of our designed systems.

Coherent electron transport through diradicals

Cumulene wires are known to be the potential candidates in nanoelectronic applications.[73] Prasongkit *et al.* theoretically studied the conductivity of cumulene based molecular wires and showed that all cumulenes yield higher conductance compared to other conjugated polymers, and for the odd-cumulene wires the conductance is still higher than that of even-cumulene wires as well as polyynes.[73] They also showed that the conductance of odd-cumulenes does not exhibit any marked dependence on the molecular length. However, Kondo *et al.* showed an exponential decrease of transmission for oligo (*p*-phenylene) dithiolate wires with the increase in the distance between two leads.[74] Apart from polyyne and cumulene systems, the polyene systems have a series of alternating single and double bonds through which transmission is possible.[75]

Magnetic molecules have wide applications in the field of spintronics.[76] In recent times organic radicals capable of constructing spintronic devices like spin valves, spin filters, *etc.* are reported.[77] In order to design a diradical based electronic device it is important to understand the transport properties of the diradicals. Though much study has been made over the conductivity of cumulenes, in this section we try to understand the qualitative trend of the transport property of the chiral cumulene based diradicals from our previous work[55] and the diradicals based on achiral cumulene and conjugated systems studied here. Schematic representations of the systems on which the transport properties have been studied are given in Fig. 9. Our comparison is based on the relative positions of the transmission spectra with respect to each other, rather than on their absolute positions with respect to the Fermi level of the gold cluster. Therefore the addition of the polyacetylene chain (spacer groups, containing 4 carbon atoms) at both ends of the cumulene and conjugated systems does not affect the transport property of the molecules under investigation because the

Table 3 Spin density distribution on each atom of the coupler of diradicals based on conjugated systems in their BS state (B3LYP/6-311++G(d,p))

	Spin density on different atoms of the coupler								
Systems	C1	C2	C3	C4	C5	C6	C7	C8	Average spin density on each atom of the coupler
3(a)	0.1845	−0.1637	0.1637	−0.1845	—	—	—	—	0.1741
3(b)	0.1607	−0.1596	0.1342	−0.1342	0.1596	−0.1607	—	—	0.1515
3(c)	0.1704	−0.1639	0.1278	−0.1335	0.1335	−0.1278	0.1651	−0.1706	0.1491

Published on 06 March 2018. Downloaded by University of North Bengal on 10/30/2019 8:59:40 AM.

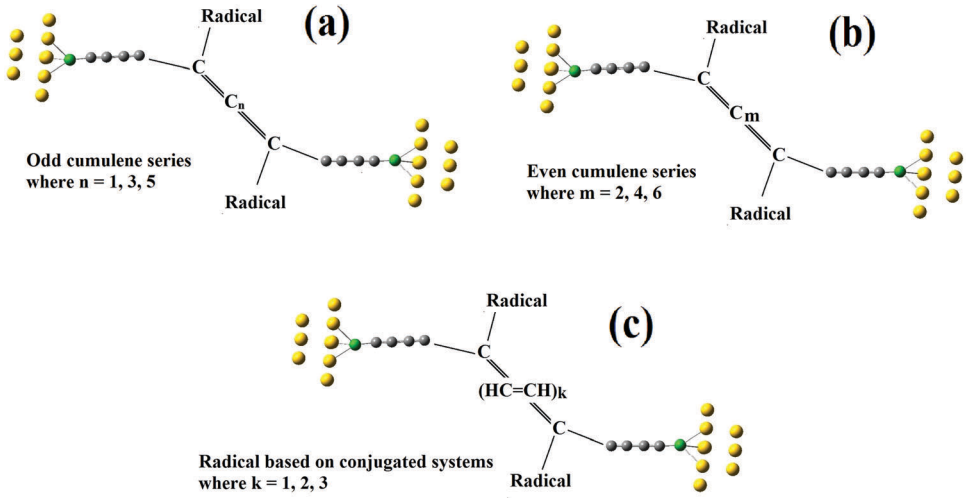

Fig. 9 Schematic representation of the radical based systems on which the transport properties have been studied.

acetylenic chains are conducting (also the relative positions of the transmission spectra are not affected by the atom number of the electrode).

For our designed systems (Fig. 9), the zero bias transmission spectra of the diradicals are given in Fig. 10 (for α spin only). Usually the Fermi energy of bulk gold (−5.5 eV) is assumed,[78] but a Fermi energy of −5.0 eV is taken from DFT calculations.[79] For our calculation the Fermi energy is chosen to be −5.0 eV and marked with a dashed line in Fig. 10 (therefore, when we compare the transmission spectra of our designed molecules,

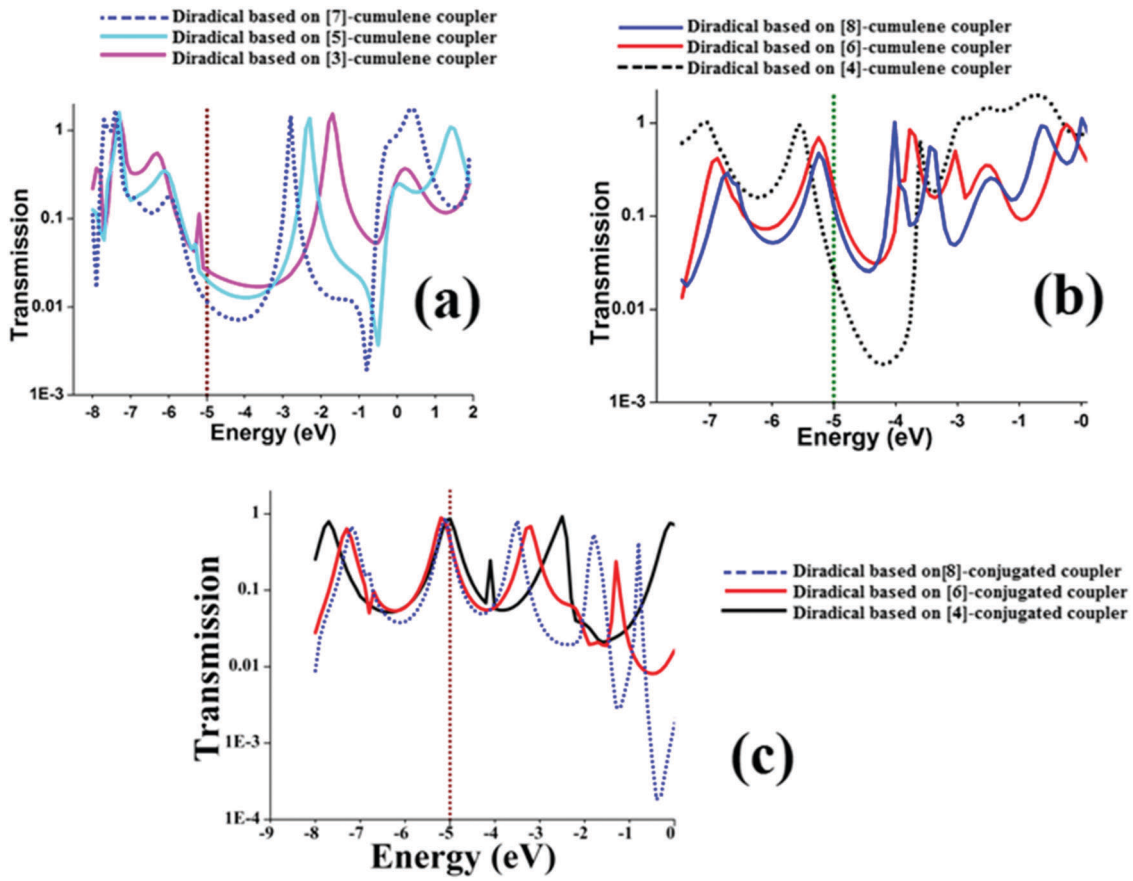

Fig. 10 Transmission spectra of all the designed diradical based molecular wires (for α spin). (The transmission is expressed using a log scale.) Part (a) represents the transmission spectra of odd cumulene based diradicals, part (b) represents the transmission spectra of even cumulene based diradicals, and part (c) represents the transmission spectra of diradicals based on conjugated systems.

 This journal is © the Owner Societies 2018

Published on 06 March 2018. Downloaded by University of North Bengal on 10/30/2019 8:59:40 AM.

the shift in Fermi energy should be the same for all the molecules with respect to the Fermi level of the gold cluster (−5 eV) and thus does not affect qualitative comparisons based on the relative positions of the transmission spectra of all the molecules with respect to each other). It is clear from Fig. 10 that with the increase in the length of the odd cumulene chains from [3]- to [5]-cumulene based diradicals and from [5]- to [7]-cumulene based diradicals (the number within the bracket represents the number of carbon atoms of the couplers within the two radical centers) the transmission decreases at the Fermi level (Fig. 10(a)), but for even cumulene based diradicals from [4]- to [6]-cumulenes, the transmission increases and after that (from [6]- to [8]-cumulene based diradicals) the transmission value remains almost constant at the Fermi level (Fig. 10(b)). Therefore, diradicals based on odd and even cumulene couplers show different characteristics of transmission. Moreover, Prasongkit *et al.* have shown that cumulene wire with an odd number of carbon atoms gives higher transmission than that of the even one,[73] which results from the high density of states of odd cumulene chains in the lowest unoccupied molecular orbital levels which spans through the Fermi level of the electrodes. But our calculation of cumulene based diradicals shows the opposite trend (*i.e.*, with the increase in the length of the cumulene chain, even cumulene based diradicals have higher transmission compared to that of odd cumulene based diradicals). This is possibly due to the addition of radicals within the cumulene systems. On the other hand the transmission remains almost constant for diradicals based on conjugated systems at the Fermi level marked with a dashed line at −5.0 eV (Fig. 10(c)). For all of our designed systems, there is no difference between α (Fig. 10) and β spin transmission (Fig. S1, in ESI†); therefore they have no spin filtering ability.

In order to understand the role of radical substitution in the transport property qualitatively, we have calculated the zero bias transmission spectra of cumulene and conjugated systems without radical centers shown in Fig. 11.

For our designed systems without radical centers (Fig. 11), the zero bias transmission spectra are given in Fig. 12.

When we compare the results of diradical based systems (Fig. 10(a) and (b)) with that of bare systems (Fig. 12(a) and (b)), it is observed that, there is a variation in transmission with the increase in the length of the odd and even cumulene based diradicals (Fig. 10(a) and (b)), but for systems without radical centers (Fig. 12(a) and (b)), the transmission remains constant at the Fermi level. Comparing the transmission value for diradicals based on conjugated systems with that of bare systems, it is found that for each set of molecules there is no variation of transmission values with the increase in the chain length of the coupler. However, a higher transmission value is observed in the case of radical based systems (Fig. 10(c)) compared to bare systems (Fig. 12(c)) at the Fermi level marked with a dashed line at −5.0 eV. Therefore, there is a contribution of radical substitution in the transport property.

Factors affecting the transmission in radical substituted systems

(i) HOMO–LUMO energy gap. It is well known that the highest occupied molecular orbital (HOMO) and the lowest unoccupied molecular orbital (LUMO) play central roles in the transport properties[80–84] and the Fermi levels reside somewhere in between the HOMO and the LUMO. Schlicke *et al.* have proposed that if two radical centers are perpendicular to each other and also to the coupler, there is a loss of conjugation in between them, and this is reflected as an increase of the HOMO–LUMO gap, which further contributes to the low conductance.[85] Proppe *et al.* have suggested that in the case of polyene systems the transmission increases at the Fermi level if there is a closer proximity of the HOMO energy and the Fermi energy.[86] Choi *et al.* showed that the molecular orbitals of a molecule with electrode atoms as well as without electrode atoms have similar orbital characteristics.[87] Therefore the transmission properties of a molecule between two electrodes can be manipulated by using our designed diradical systems (Fig. 1) without the gold electrodes. Hermann *et al.* also have shown that for cumulene based systems containing an even

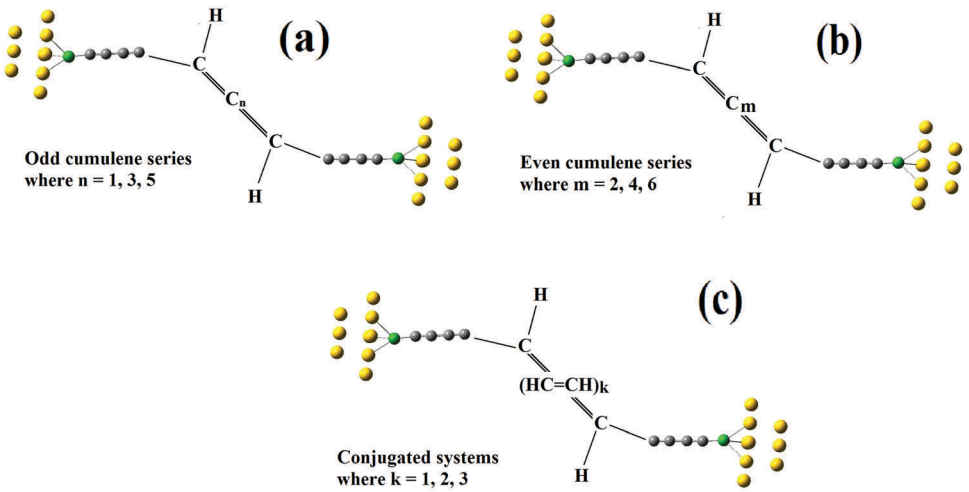

Fig. 11 Schematic representation of the systems without radical centers on which the transport properties have been studied.

Published on 06 March 2018. Downloaded by University of North Bengal on 10/30/2019 8:59:40 AM.

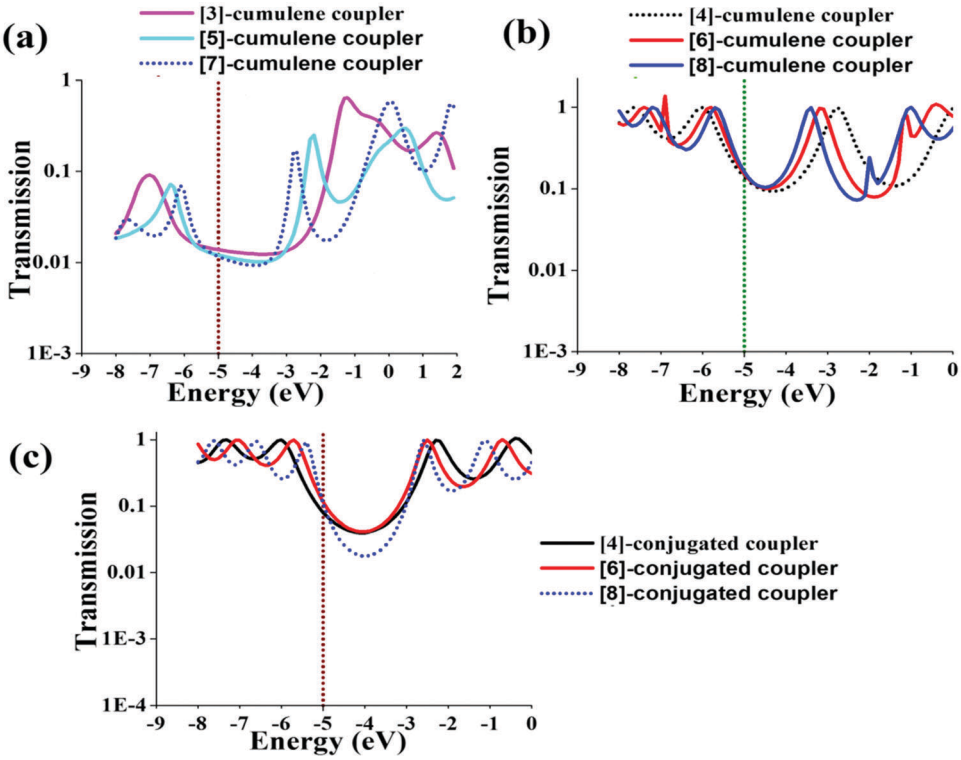

Fig. 12 Transmission spectra of all the designed molecular wires without radical centers. (The transmission is expressed using a log scale.) Part (a) represents the transmission spectra of bare odd cumulene systems, part (b) represents the transmission spectra of bare even cumulene systems, and part (c) represents the transmission spectra of bare conjugated systems.

Table 4 Energy difference between $HOMO_\alpha$ and $LUMO_\alpha$ (ΔE_{HL} in eV) for all the systems (B3LYP/6-311++G(d,p))

Systems	ΔE_{HL} (eV)	Systems	ΔE_{HL} (eV)	Systems	ΔE_{HL} (eV)
1(a)	3.71	2(a)	2.71	3(a)	2.99
1(b)	3.03	2(b)	2.45	3(b)	2.82
1(c)	2.64	2(c)	2.28	3(c)	2.70

number of carbon centers, the α-HOMO–α-LUMO gap decreases with the increase in carbon chain length.[88] For our designed systems the frontier orbital energy splitting is shown in Table 4 (also in Tables S14 and S15, ESI†). It is evident that, with the increase in the number of carbon atoms of the couplers in each series, frontier orbital energy splitting decreases gradually. Therefore an increase in transmission with the increase in the number of carbon atoms in each series is expected. But from the transmission curve (Fig. 10) it is clear that although the transmission characteristics show a predictable result to some extent for diradicals based on the even cumulene series, for diradicals based on odd cumulenes and diradicals based on conjugated systems the scenario is different. Hence, there must be some other factors guiding the situation.

(ii) Distance between leads (considering the distance between sulfur atoms). In order to study the transmission characteristics, the sulfur atoms may be provided to connect the diradical based molecular wires into the close proximity of the gold electrode, so that the molecular wire can electronically couple to the electrode providing an electrode–sulfur—molecular wire–sulfur–electrode tunneling pathway. Therefore if the distance between two electrodes is small, a better transmission should be expected. For our designed systems the distances between two leads (*i.e.* between the sulfur atoms) is given in Table 5. It is found that, for both odd and even cumulene based diradicals as well as for diradicals based on conjugated couplers, with the increase in the number of carbon atoms, the distance between two sulfur atoms increases gradually. As a result, there should be a decrease in the transmission value with the increase in the distance between two electrodes for each series. But the transmission value shows different characteristics for each series. Therefore two different factors (distance between two leads and the HOMO–LUMO energy gap) affect the transmission. For radicals based on conjugated systems the two factors counterbalance each other and ultimately a constant transmission value results (Fig. 10(c)).

If the conjugation between the lead and the molecular region is better, higher transmission should be expected. At the same time, greater the distance between S and the rest of the molecular region, lower should be the transmission due to the lower possibility of tunneling of electrons from the gold lead to the molecular region and *vice versa*. For this reason the distance between S and the nearest C has been considered. Fig. S2 (in ESI†) shows that for [3]-cumulene based diradicals as well as for [5]-cumulene based diradicals, the distance between S and C is 1.69 Å, *i.e.*, it is unaltered, but for [7]-cumulene based

 This journal is © the Owner Societies 2018

Published on 06 March 2018. Downloaded by University of North Bengal on 10/30/2019 8:59:40 AM.

Table 5 Distance between two leads (in Å) (considering the distance between two sulfur atoms)

Systems	Distance between two leads (in Å)	Systems	Distance between two leads (in Å)	Systems	Distance between two leads (in Å)
1(a)	11.33	2(a)	15.53	3(a)	14.82
1(b)	13.32	2(b)	16.97	3(b)	15.72
1(c)	14.52	2(c)	18.56	3(c)	16.59

diradicals the distance between S and C is 1.74 Å, hence there should be a decrease in transmission, which satisfies the transmission characteristics, *i.e.*, a decrease in transmission in [7]- cumulene based diradical systems (Fig. 10(a)).

(iii) Spin density distribution within the coupler and radical centers. The spin density distributions of the molecular wires attached to the leads are given in Fig. 13–15. Fig. 14 presents some interesting observation that needs further discussion. There seems to be no spin amplitude in the [4]-cumulene fragment in Fig. 14(a) but there is substantial amplitude along the chains of the length [6]- and [8]-cumulene connector (Fig. 14(b) and (c)). The spin alternation rule predicts that the alpha spin at a radical site will induce beta spin at a neighboring C, alpha at the next and so forth. If two alternating-spin patterns emanating from distinct sites interfere constructively, then there will be strong amplitude along the connecting path, and if the interference is destructive then there would be no amplitude. As a result of overall destructive interference in Fig. 14(a) a diamagnetic situation arises, whereas in other cases constructive interference occurs and high spin amplitude is observed in an antiferromagnetic situation (in Fig. 14(b) and (c)). Such systems can be exploited as logic gates in spintronic applications.[89] Therefore for the system

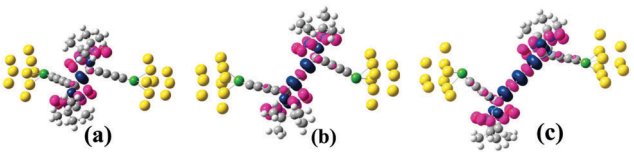

Fig. 13 Spin polarization pathways within the odd cumulene based molecular wires (iso value 0.004). Part (a) represents the spin density distribution within the allene based molecular wire, part (b) represents the spin density distribution within the cumulene (containing 5 carbon atoms) based molecular wire, and part (c) represents the spin density distribution within the cumulene (containing 7 carbon atoms) based molecular wire.

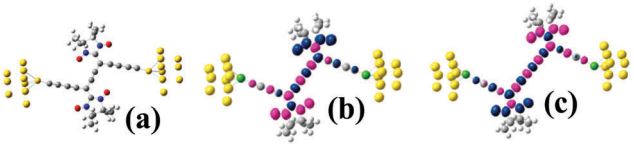

Fig. 14 Spin polarization pathways within the even cumulene based molecular wires (iso value 0.004). Part (a) represents the spin density distribution within the cumulene (containing 4 carbon atoms) based molecular wire, part (b) represents the spin density distribution within the cumulene (containing 6 carbon atoms) based molecular wire, and part (c) represents the spin density distribution within the cumulene (containing 8 carbon atoms) based molecular wire.

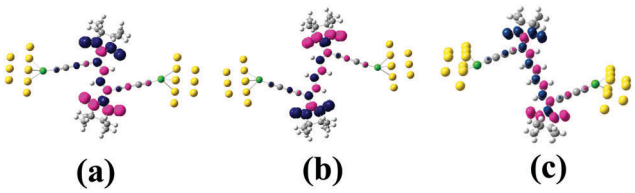

Fig. 15 Spin polarization pathways within the molecular wires based on conjugated couplers (iso value 0.004). Part (a) represents the spin density distribution within the conjugated system (containing 4 carbon atoms) based molecular wire, part (b) represents the spin density distribution within the conjugated system (containing 6 carbon atoms) based molecular wire, and part (c) represents the spin density distribution within the conjugated system (containing 8 carbon atoms) based molecular wire.

represented in Fig. 14(a) there occurs spin quenching when such systems are attached to the leads. Thus, an ultimate decrease in transmission in [4]-cumulene based diradicals is observed and a correlation of spin polarization and the transmission characteristics of our designed systems can be intuited.

So, it can be surmised that there are different guiding factors such as the HOMO–LUMO energy gap, distance between two leads as well as the spin polarization that contribute to the ultimate transmission characteristics in molecular junction transport. The preference of one factor over other causes an increase or decrease in transmission. Finally the origin of all the factors is the unusual π-interaction within the couplers that produces different transmission characteristics of our designed systems.

4. Conclusion

To sum up, there is a variation in J values for diradicals based on the odd cumulene series, diradicals based on the even cumulene series and diradicals based on conjugated couplers. It has been found that the existence of a distinctive spin polarization pathway in cumulene systems (compared to conjugated systems), distance between two radical centers (that may possibly interrupt the spin polarization pathway) and a planar structure, which allows better orbital overlap between π-systems compared to a non-planar one, control the magnetic exchange coupling constant values. Largely speaking, the unusual π-interaction within the coupler is the enlightening factor that controls the magnetic properties of our designed systems. It is also found that the frontier energy splitting, distance between two electrodes and the spin polarization pathways play a major role in determining the transmission characteristics of our designed systems.

Published on 06 March 2018. Downloaded by University of North Bengal on 10/30/2019 8:59:40 AM.

Conflicts of interest

The authors declare no competing financial interest.

Acknowledgements

This work is supported by DST, India. The authors are thankful to Prof. Dr Carmen Herrmann for giving permission to use the transport code ARTAIOS.

References

1 O. Kahn, *Molecular Magnetism*, VCH, New York, 1993.
2 P. M. Lahti, *Magnetic Properties of Organic Materials*, Marcel Dekker, New York, 1999.
3 H. Kobayashi, A. Kobayashi and P. Cassoux, *Chem. Soc. Rev.*, 2000, **29**, 325.
4 S. Uji, H. Shinagawa, T. Terashima, T. Yakabe, Y. Terai, M. Tokumoto, A. Kobayashi, H. Tanaka and H. Kobayashi, *Nature*, 2001, **410**, 908.
5 K. Matsuda, M. Matsuo and M. Irie, *J. Org. Chem.*, 2001, **66**, 8799.
6 N. Tanifuji, M. Irie and K. Matsuda, *J. Am. Chem. Soc.*, 2005, **127**, 13344.
7 G. A. Prinz, *Science*, 1998, **282**, 1660.
8 E. G. Emberly and G. Kirczenow, *Chem. Phys.*, 2002, **281**, 311.
9 F. Wang and Z. V. Vardeny, *J. Mater. Chem.*, 2009, **19**, 1685.
10 M. Michelfeit, G. Schmidt, J. Geurts and L. W. Molenkamp, *Phys. Status Solidi*, 2008, **205**, 656.
11 T. D. Nguyen, E. Ehrenfreund and Z. V. Vardeny, *Science*, 2012, **337**, 204.
12 J. W. Yoo, C. Y. Chen, H. W. Jang, C. W. Bark, V. N. Prigodin, C. B. Eom and A. J. Epstein, *Nat. Mater.*, 2010, **9**, 638.
13 C. Herrmann and J. Elmisz, *Chem. Commun.*, 2013, **49**, 10456.
14 M. P. Eng and B. Albinsson, *Angew. Chem., Int. Ed.*, 2006, **45**, 5626.
15 O. S. Wenger, *Acc. Chem. Res.*, 2011, **44**, 25.
16 A. Nitzan and M. A. Ratner, *Science*, 2003, **300**, 1384.
17 N. J. Tao, *Nat. Nanotechnol.*, 2006, **1**, 173.
18 B. G. Park, J. Wunderlich, X. Martí, V. Holý, Y. Kurosaki, M. Yamada, H. Yamamoto, A. Nishide, J. Hayakawa, H. Takahashi, A. B. Shick and T. A. Jungwirth, *Nat. Mater.*, 2011, **10**, 347.
19 J. M. Tour, *Acc. Chem. Res.*, 2000, **33**, 791.
20 J. R. Winkler and H. B. Gray, *J. Am. Chem. Soc.*, 2014, **136**, 2930.
21 H. Liu, N. Wang, J. Zhao, Y. Guo, X. Yin, F. Y. C. Boey and H. Zhang, *Chem. Phys. Chem.*, 2008, **9**, 1416.
22 K. H. Khoo, Y. Chen, S. Li and S. Y. Quek, *Phys. Chem. Chem. Phys.*, 2015, **17**, 77.
23 X. L. Zhao, Y. Ando, Y. Liu, M. Jinno and T. Suzuki, *Phys. Rev. Lett.*, 2003, **90**, 187401.
24 H. Muramatsu, T. Hayashi, Y. A. Kim, D. Shimamoto, M. Endo, M. Terrones and M. S. Dresselhaus, *Nano Lett.*, 2008, **8**, 237.
25 R. Kitaura, R. Nakanishi, T. Saito, H. Yoshikawa, K. Awaga and H. Shinohara, *Angew. Chem., Int. Ed.*, 2009, **48**, 8298.
26 Y. Tobe and T. Wakabayashi, in *Acetylene Chemistry: Chemistry, Biology, and Material Science*, ed. F. Diederich, P. J. Stang and R. R. Tykwinski, Wiley-VCH, Weinheim, 2005, p. 387.
27 W. A. Chalifoux and R. R. Tykwinski, *Chem. Rec.*, 2006, **6**, 169.
28 A. L. K. Shi Shun and R. R. Tykwinski, *Angew. Chem., Int. Ed.*, 2006, **45**, 1034.
29 B. Raton, in *Polyynes: Synthesis, Properties, and Applications*, ed. F. Cataldo, Taylor & Francis, 2005.
30 S. Ma, *Acc. Chem. Res.*, 2009, **42**, 1679.
31 W. Smadja, *Chem. Rev.*, 1983, **83**, 263.
32 Y. Zhang, Y. Su, L. Wang, E. S.-W. Kong, X. Chen and Y. A. Zhang, *Nanoscale Res. Lett.*, 2011, **6**, 577.
33 X. Gu, R. I. Kaiser and A. M. Mebel, *Chem. Phys. Chem.*, 2008, **9**, 350.
34 M. Weimer, W. Hieringer, F. D. Sala and A. Gçrling, *Chem. Phys.*, 2005, **309**, 77.
35 W. Skibar, H. Kopacka, K. Wurst, C. Salzmann, K. H. Ongania, F. F. D. Biani, P. Zanello and B. Bildstein, *Organometallics*, 2004, **23**, 1024.
36 J. A. Januszewski and R. R. Tykwinski, *Chem. Soc. Rev.*, 2014, **43**, 3184.
37 J. A. Januszewski, D. Wendinger, C. D. Methfessel, F. Hampel and R. R. Tykwinski, *Angew. Chem., Int. Ed.*, 2013, **52**, 1817.
38 D. Bhattacharya and A. Misra, *J. Phys. Chem. A*, 2009, **113**, 5470.
39 D. Bhattacharya, S. Shil, A. Misra and D. J. Klein, *Theor. Chem. Acc.*, 2010, **127**, 57.
40 S. Shil, P. Sarbadhikary and A. Misra, *RSC Adv.*, 2016, **6**, 99467.
41 S. Paul and A. Misra, *J. Chem. Theory Comput.*, 2012, **8**, 843.
42 S. Paul and A. Misra, *J. Phys. Chem. A*, 2010, **114**, 6641.
43 Md. E. Ali and S. N. Datta, *J. Phys. Chem. A*, 2006, **110**, 2776.
44 K. C. Ko, D. Cho and J. Y. Lee, *J. Phys. Chem. A*, 2013, **117**, 3561.
45 D. Cho, K. C. Ko, Y. Ikabata, K. Wakayama, T. Yoshikawa, H. Nakai and J. Y. Lee, *J. Chem. Phys.*, 2015, **142**, 024318.
46 Y. Nam, D. Cho and J. Y. Lee, *J. Phys. Chem. C*, 2016, **120**, 11237.
47 D. Cho, K. C. Ko, H. Park and J. Y. Lee, *J. Phys. Chem. C*, 2015, **119**, 10109.
48 D. Cho, K. C. Ko and J. Y. Lee, *Int. J. Quantum Chem.*, 2016, **116**, 578.
49 K. C. Ko, D. Cho and J. Y. Lee, *J. Phys. Chem. A*, 2012, **116**, 6837.
50 K. C. Ko, S. U. Son, S. Lee and J. Y. Lee, *J. Phys. Chem. B*, 2011, **115**, 8401.
51 D. Cho, K. C. Ko and J. Y. Lee, *J. Phys. Chem. A*, 2014, **118**, 5112.
52 K. C. Ko, Y. G. Park, D. Cho and J. Y. Lee, *J. Phys. Chem. A*, 2014, **118**, 9596.
53 M. Song, X. Song and Y. Bu, *Chem. Phys. Chem.*, 2017, **18**, 2487.
54 M. Song, X. Song and Y. Bu, *J. Phys. Chem. C*, 2017, **121**, 21231.

 This journal is © the Owner Societies 2018

Published on 06 March 2018. Downloaded by University of North Bengal on 10/30/2019 8:59:40 AM.

55 P. Sarbadhikary, S. Shil, A. Panda and A. Misra, *J. Org. Chem.*, 2016, **81**, 5623.
56 M. Tamura, Y. Nakazawa, D. Shiomi, K. Nozawa, Y. Hosokoshi, M. Ishikawa, M. Takahashi and M. Kinosita, *Chem. Phys. Lett.*, 1991, **186**, 401.
57 L. Noodleman, *J. Chem. Phys.*, 1981, **74**, 5737.
58 L. Noodleman and E. Baerends, *J. Am. Chem. Soc.*, 1984, **106**, 2316.
59 L. Noodleman and E. R. Davidson, *Chem. Phys.*, 1986, **109**, 131.
60 L. Noodleman, C. Y. Peng, D. A. Case and J. M. Mouesca, *Coord. Chem. Rev.*, 1995, **144**, 199.
61 K. Yamaguchi, H. Fukui and T. Fueno, *Chem. Lett.*, 1986, 625.
62 K. Yamaguchi, Y. Takahara, T. Fueno and K. Nasu, *Jpn. J. Appl. Phys.*, 1987, **26**, L1362.
63 K. Yamaguchi, F. Jensen, A. Dorigo and K. N. Houk, *Chem. Phys. Lett.*, 1988, **149**, 537.
64 K. Yamaguchi, Y. Takahara, T. Fueno and K. N. Houk, *Theor. Chim. Acta*, 1988, **73**, 337.
65 M. J. Frisch, G. W. Trucks, H. B. Schlegel, G. E. Scuseria, M. A. Robb, J. R. Cheeseman, G. Scalmani, V. Barone, B. Mennucci, G. A. Petersson, H. Nakatsuji, M. Caricato, X. Li, H. P. Hratchian, A. F. Izmaylov, J. Bloino, G. Zheng, J. L. Sonnenberg, M. Hada, M. Ehara, K. Toyota, R. Fukuda, J. Hasegawa, M. Ishida, T. Nakajima, Y. Honda, O. Kitao, H. Nakai, T. Vreven, J. A. Montgomery, Jr., J. E. Peralta, F. Ogliaro, M. Bearpark, J. J. Heyd, E. Brothers, K. N. Kudin, V. N. Staroverov, R. Kobayashi, J. Normand, K. Raghavachari, A. Rendell, J. C. Burant, S. S. Iyengar, J. Tomasi, M. Cossi, N. Rega, M. J. Millam, M. Klene, J. E. Knox, J. B. Cross, V. Bakken, C. Adamo, J. Jaramillo, R. Gomperts, R. E. Stratmann, O. Yazyev, A. J. Austin, R. Cammi, C. Pomelli, J. W. Ochterski, R. L. Martin, K. Morokuma, V. G. Zakrzewski, G. A. Voth, P. Salvador, J. J. Dannenberg, S. Dapprich, A. D. Daniels, Ö. Farkas, J. B. Foresman, J. V. Ortiz, J. Cioslowski and D. J. Fox, *Gaussian 09, revision D.01*, Gaussian, Inc., Wallingford CT, 2009.
66 M. Büttiker, Y. Imry, R. Landauer and S. Pinhas, *Phys. Rev. B: Condens. Matter Mater. Phys.*, 1985, **31**, 6207.
67 C. Herrmann, G. C. Solomon, J. E. Subotnik, V. Mujica and M. A. Ratner, *J. Chem. Phys.*, 2010, **132**(024103), 1–17.
68 C. Herrmann, G. C. Solomon and M. A. Ratner, *J. Am. Chem. Soc.*, 2010, **132**, 3682.
69 C. Herring, in *Magnetism IIB, Direct exchange between well-separated atoms*, ed. G.T. Rado and H. Suhl, Academic Press, New York, 1966, vol. 5.
70 V. Polo, A. Alberola, J. Andres, J. Anthony and M. Pilkington, *Phys. Chem. Chem. Phys.*, 2008, **10**, 857.
71 S. Shil, M. Roy and A. Misra, *RSC Adv.*, 2015, **5**, 105574.
72 C. Hermann, J. Neugebauer, J. A. Gladysz and M. Reiher, *Inorg. Chem.*, 2005, **44**, 6174.
73 J. Prasongkit, A. Grigoriev, G. Wendin and R. Ahuja, *Phys. Rev. B: Condens. Matter Mater. Phys.*, 2010, **81**, 115404.
74 M. Kondo, T. Tada and K. Yoshizawa, *J. Phys. Chem. A*, 2004, **108**, 9143.
75 T. Stuyver, S. Fias, F. De. Proft and P. Geerlings, *J. Phys. Chem. C*, 2015, **119**, 26390.
76 D. Aravena and E. Ruiz, *J. Am. Chem. Soc.*, 2012, **134**, 777.
77 C. Herrmann, G. C. Solomon and M. A. Ratner, *J. Am. Chem. Soc.*, 2010, **132**, 3682.
78 N. W. Ashcroft and N. D. Mermin, *Solid State Physics*, Holt, Rinehart and Winston, New York, 1976.
79 F. Pauly, J. K. Viljas, J. C. Cuevas and G. Schön, *Phys. Rev. B: Condens. Matter Mater. Phys.*, 2008, **77**, 155312.
80 J. M. Tour, M. Kozaki and J. M. Seminario, *J. Am. Chem. Soc.*, 1998, **120**, 8486.
81 A. Modelli, M. Venuti, F. Scagnolari, M. Contento and D. Jones, *J. Phys. Chem. A*, 2001, **105**, 219.
82 G. Distefano, D. Jones, M. Guerra, L. Favaretto, A. Modelli and G. Mengoli, *J. Phys. Chem.*, 1991, **95**, 9746.
83 M. D. Colle, C. Cova, G. Distefano, D. Jones, A. Modelli and N. Comisso, *J. Phys. Chem. A*, 1999, **103**, 2828.
84 J. L. Brédas, B. Thémans, J. G. Fripiat, J. M. André and R. R. Chance, *Phys. Rev. B: Condens. Matter Mater. Phys.*, 1984, **29**, 6761.
85 H. Schlicke and C. Herrmann, *Chem. Phys. Chem.*, 2014, **15**, 4011.
86 J. Proppe and C. Herrman, *J. Comput. Chem.*, 2015, **36**, 201.
87 Y. C. Choi, W. Y. Kim, K. S. Park, P. Tarakeshwar, K. S. Kim, T. S. Kim and J. Y. Lee, *Chem. Phys.*, 2005, **122**, 094706.
88 C. Hermann, J. Neugebauer, J. A. Gladysz and M. Reiher, *Inorg. Chem.*, 2005, **44**, 6174.
89 A. V. Chumak, V. I. Vasyuchka, A. A. Serga and B. Hillebrands, *Nat. Phys.*, 2015, **11**, 453.